Ministry for Primary Industries
Manatū Ahu Matua

Characterisation and a length-based assessment model for scampi (*Metanephrops challengeri*) at the Auckland Islands (SCI 6A)

I.D. Tuck

October 2017

New Zealand Government

Growing and Protecting New Zealand

TABLE OF CONTENTS

EXECUTIVE SUMMARY

A stock assessment of the Auckland Islands (SCI 6A) scampi stock has been undertaken through MPI project DEE201612. This work has further modified and developed an existing model for this stock, which is based on previous assessment models for other scampi stocks. Considerable progress was made with the model, with developments also relevant to other scampi assessments, and the assessment was accepted by the SFAWG. This provides the first accepted assessment for SCI 6A.

A fishery characterisation was undertaken, and a CPUE index was estimated for the stock, incorporating spatial and temporal components in the fishery. The earliest model for this stock incorporated considerable spatial structure, but following preliminary investigations, the SFAWG recommended the development of a single area model for each scampi stock, including the fitting an annual CPUE index, along with photographic and trawl survey indices. Sensitivity to natural mortality, and to the CV on the YCS prior were investigated as part of this model, for which MCMCs were generated with M fixed at 0.2 and 0.25. All models provided broadly consistent stock trajectories and current stock status estimates, with median estimates of SSB_{2016}/SSB_0 ranging from 67 – 72%. While overall patterns of YCS were similar between models, the range of variability was sensitive to the assumed CV on the YCS prior. All models estimated a series of above average YCSs in recent years, but models with higher CV values estimated the most recent year to have the highest YCS in the series. Projections out to 2020 suggested that SSB would remain well above 40% SSB_0 with future catches up to the TACC.

1.   INTRODUCTION

This report undertakes a fishery characterisation for the Auckland Islands (SCI 6A) scampi stock, and applies a previously developed Bayesian, length-based, two-sex population model to this stock. The first attempt at developing a length-based population model for any scampi stock was conducted for SCI 1 (Cryer et al. 2005), which was implemented using the general-purpose stock assessment program CASAL v2.06 (September 2004). This model for SCI 1 was developed further and the same model structure was also applied to SCI 2 in a later project (Tuck & Dunn 2006). This model was first applied to the SCI 6A stock in 2011 (Tuck & Dunn 2012), and then subsequently in 2014 (Tuck 2015) although neither of these assessments were accepted. The current study used CASAL v 2.22 (Bull et al. 2008) which included a slightly modified selectivity option. Developments in the model implementation and structure have been largely based on suggestions raised at the MFish funded Scampi Assessment Workshop (Tuck & Dunn 2009), and subsequently at Shellfish Fisheries Assessment Working Group (SFAWG) meetings. Assessments for SCI 1, SCI 2 and SCI 3 using this model were accepted in 2011, 2013, 2015 and 2016 (Tuck 2014, Tuck 2016a, Tuck 2016b, Tuck & Dunn 2012).

We describe the available data and how they were used, the parameterisation of the model, and model fits and sensitivities. This report fulfils Ministry for Primary Industries project DEE2016-12 "*Stock assessment of scampi*", undertaking an assessment of SCI 6A. The objective of this project was to conduct a stock assessment, including estimating yield for SCI 6A in 2015–16.

1.1 The Auckland Islands (SCI 6A) scampi fishery

Scampi is fished all around New Zealand, in nine fishery management areas (Figure 1). The SCI 6A fishery is one of New Zealand's four main scampi fisheries (the others being SCI 1, SCI 2 and SCI 3), and over the last 5 years (2011–12 to 2015–16) has contributed an average of 156 tonnes annually, having declined from the previous 5 years (2006–07 to 2010–11 average 239 tonnes), and 283 tonnes in the five years before that. The landings in 2015–2016 (263 tonnes) show a considerable increase on recent years however (Figure 2). The TACC for SCI 6A is 306 tonnes, and the total TACC for all management areas is 1224 tonnes.

The spatial distribution of targeted scampi fishing within SCI 6A is focussed to the east of the Auckland Islands in water depths from 350 – 550 m. (Figure 3). This fishery extends slightly deeper than other scampi fisheries around New Zealand. Scampi surveys conducted in the area have focussed on the main area of the fishery, and survey strata coverage is illustrated in Figure 3.

The history of scampi management in New Zealand has been complex, and subject to legal scrutiny (Carter 2003). The first reported domestic catches of scampi were in the 1987–88 fishing year, when special section 63 and section 64 permits were issued for investigative fishing and the use of small mesh trawl nets. Interpretation of the requirements for fishing under the Fisheries Act 1983 varied between regional offices of the Ministry of Fisheries, but the fishery expanded rapidly, and by the start of the 1990–91 fishing year, 14 commercial fishing permits had been granted and 39 applications for special permits had been received.

The Ministry recognised that it needed to control the rapid expansion of the fishery, to prevent overfishing, and adopted a national approach, with a species specific prohibition on the taking of scampi imposed on 1st October 1990 under section 65 of the Fisheries Act 1983, with rules and criteria established for granting exemptions to the prohibition. These criteria included recognition of previous access to the fishery, or a demonstration of a commitment to the fishery.

Prior to the 1991–92 fishing year, there were no limits on scampi catches for any area. In the 1991–92 fishing year, Individual Quotas (IQs) were introduced for SCI 1 and SCI 2 (allocated on the basis of the permit holder's catch in 1990–91), with competitive catch limits introduced for all other areas. The IQs were maintained for SCI 1 & 2 in 1992–93, and introduced for SCI 4 & 6A (allocated on the basis of

the permit holder's catch in 1991–92), with competitive catch limits maintained for other areas. This management system (with IQs for SCI 1, 2, 4 & 6A, and competitive limits for other stocks) was maintained with the introduction of Individual Catch Entitlement (ICE) regulations in 1999, and continued until the Court of Appeal ruled that the scampi ICE regulations were unlawful in October 2001, after which all scampi stocks were managed under competitive catch limits. Scampi was introduced into the QMS on 1st October 2004 with a Total Allowable Commercial Catch of 306 tonnes for SCI 6A, and this limit has been unchanged to date.

Coincident with the introduction of scampi to the QMS, management area boundaries were revised for SCI 3 and SCI 4, SCI 6A and SCI 6B (Figure 4), on the basis of examination of patterns in catch distribution and composition (Cryer 2000). This changed the SCI 6A area from a "bubble" encompassing the area within 50 nautical miles of the Auckland Islands to a larger box which included all the scampi fishing activity in the area.

Previous fishery characterisations have been undertaken for this area by Cryer & Coburn (2000), Tuck (2009, 2016a) and (Tuck & Dunn 2012).
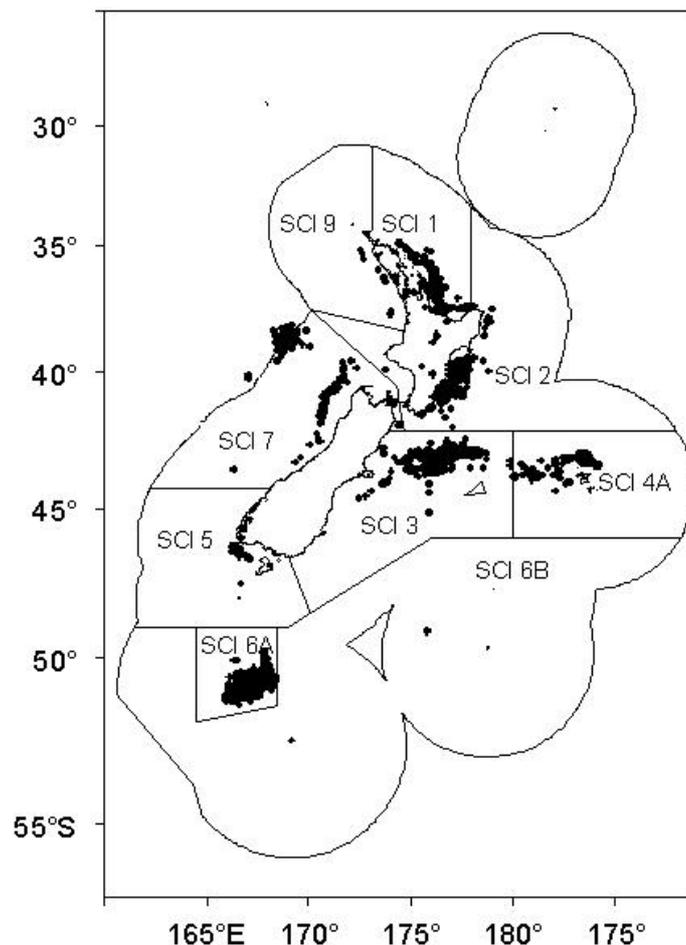
Figure 1: Spatial distribution of the scampi fishery since 1988–89. Each dot shows the midpoint of one or more tows recorded on TCEPR with scampi as the target species.
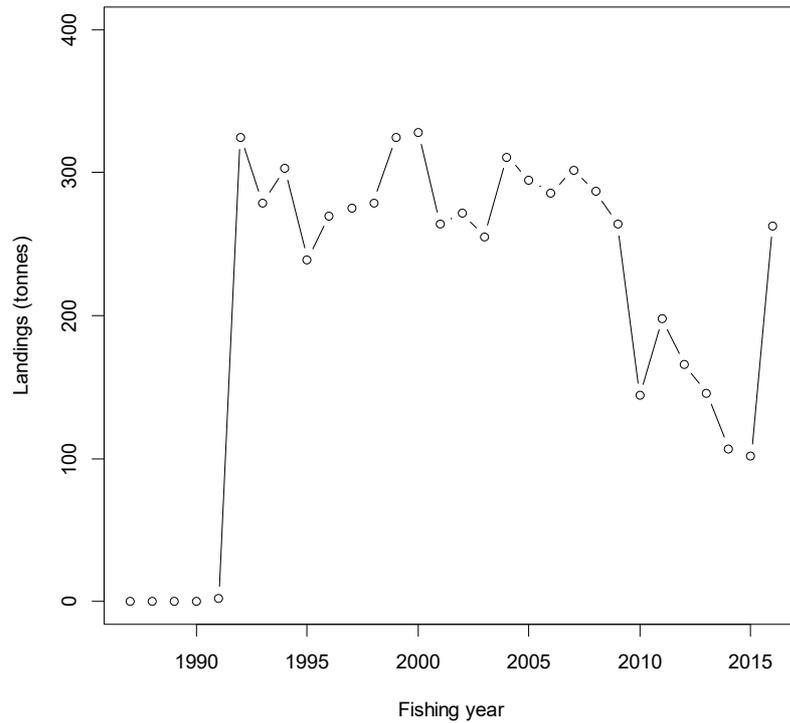
Figure 2: Time series of scampi landings from SCI 6A by fishing year (MHR data).
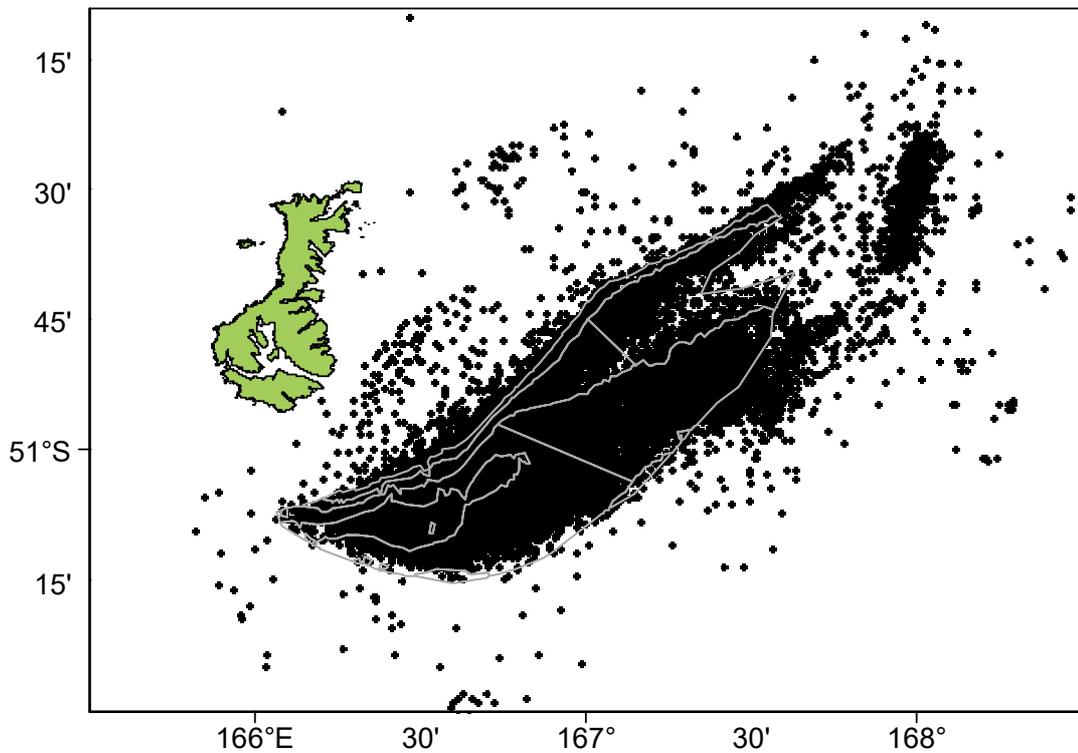
**Figure 3: Spatial distribution of the scampi fishery within management area SCI 6A since 1988–89. Each dot shows the midpoint of one or more tows recorded on TCEPR with scampi as the target species. The boundaries of the scampi survey strata are shown in grey.**
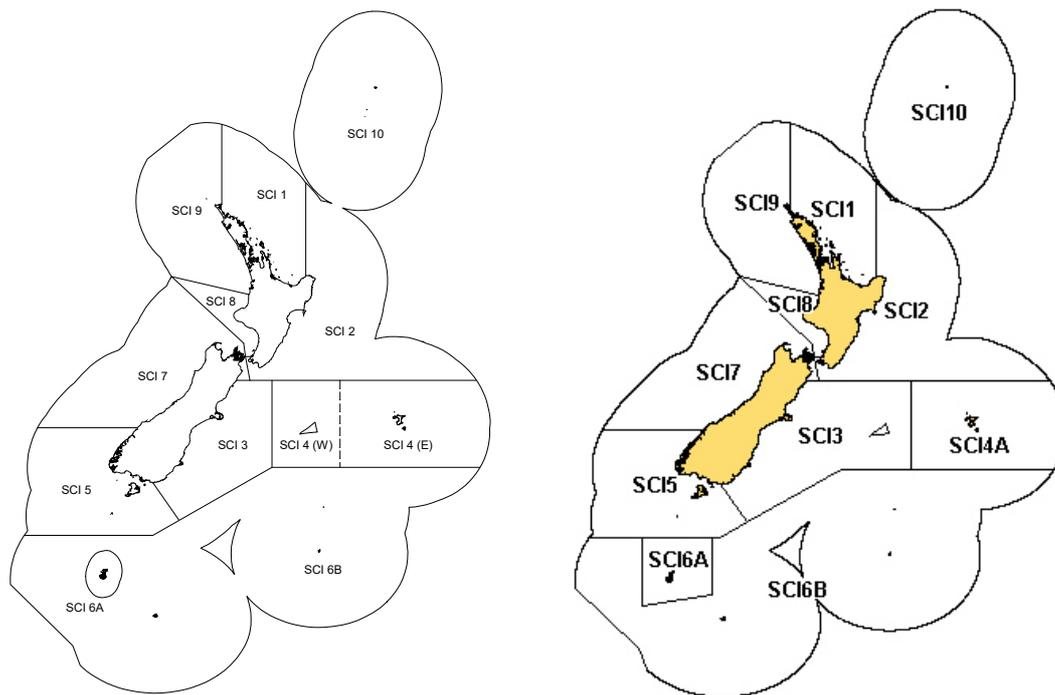
Figure 4: Left - Scampi fishery management areas, prior to 2004–05 fishing year. Right - Scampi fishery management areas, as revised at the start of the 2004–05 fishing year, when the boundaries between SCI 3 and SCI 4A, and SCI 6A and SCI 6B were changed.

2. FISHERY CHARACTERISATION AND DATA

2.1 Commercial catch and effort data

Scampi fishers have consistently reported catches on the Trawl Catch, Effort, and Processing Returns (TCEPR) form since its introduction in 1989–90, providing a very valuable record of catch and effort on a tow-by-tow basis.

Data were extracted from the MPI TCEPR database (extract 10884), requesting all tows where scampi (SCI) was the nominated target species, or was reported in the catch. Errors in TCEPR records are reducing in frequency, but do occur, and the raw records were groomed in the following manner. For each record, the reported data were used to estimate the duration of the trawl shot, the distance between the start and finish locations, and the mid point between the start and finish locations. Tows with zero scampi catch were excluded. All tows that recorded zero hours tow duration (but some scampi catch) were reset to the median tow duration for the trip. All tows with a tow distance greater than 100 km were reset to the median of the midpoint of tows on the same day, adjacent days, or the trip, depending on available data. The SCI 6A data were then extracted from this full data set on the basis of latitude and longitude. All analysis was conducted on the basis of the current management area boundaries.

Subsequent analyses were conducted on this "groomed" version of the data set (30 906 records), representing over 95% of all scampi landings taken from SCI 6A. This data set is considered to be the most appropriate to investigate patterns in the fishery, as it represents the targeted scampi fishery, and latitude and longitude data are available for spatial aspects of the analysis. Characterisations prior to Tuck (2015) have used a slightly different grooming approach (to that discussed above), details of which are provided in Tuck (2009). Comparisons of unstandardized CPUE data for the earlier and revised grooming approaches have previously been examined (Tuck 2014). The revised grooming slightly

reduces the estimated CPUE prior to 2003 (due to rounding of the haul duration data), but the medians of the annual values appear identical after this.

Total annual landings for the fishery, and the percentage by the target scampi fishery, are presented in Table 1, and the distribution of fishing activity within the SCI 6A area over time is presented in Figure 5 and Figure 6. The area over which the assessment model is applied is defined as the survey strata (350–550 m depth range in the main area of the fishery) (Figure 3), where over 90% of the reported targeted scampi catch from SCI 6A has been taken in most years (Table 1). The fishery initially developed in the shallower and western areas of the grounds, closest to the Auckland Islands, extending out to the full extent of the core area by the late 1990s. This area has been consistently fished since the late 1990s, with smaller isolated patches (to the east) fished up until 2004. These more easterly patches were outside of the gazetted SCI 6A management area at the time (see Figure 4), and as such were subject to different catch constraints. The core (modelled) area has accounted for over 97% of scampi targeted catch in all years. A box plot of the unstandardized CPUE (Figure 7) shows that catch rates initially declined from very high values in the early 1990s, fluctuated without trend until the late 2000s, remained at the lower end of the observed range between 2011 and 2014, and have since increased to more mid-range levels in the most recent years.

Table 1: Reported commercial landings (tonnes) from the 1986–87 to 2015–16 fishing years for SCI 6A, catch estimated from scampi target fishery, and estimated catch from modelled area (survey strata).

Fishing year	Landings (MHR)	Target catch (TCEPR)	% SCI target	Estimated catch (modelled area)	% catch (modelled area)
1990–91	2	1.90	95.00%	0.85	44.74%
1991–92	325	324.79	99.93%	314.37	96.79%
1992–93	279	253.84	90.98%	189.90	74.81%
1993–94	303	269.50	88.94%	235.64	87.44%
1994–95	239	217.11	90.84%	216.02	99.50%
1995–96	270	226.52	83.90%	220.13	97.18%
1996–97	275	276.15	100.42%	228.95	82.91%
1997–98	279	297.92	106.78%	247.65	83.13%
1998–99	325	309.71	95.30%	233.03	75.24%
1999–00	328	311.22	94.88%	260.16	83.59%
2000–01	264	283.39	107.34%	255.25	90.07%
2001–02	272	249.36	91.68%	231.24	92.73%
2002–03	255	249.31	97.77%	215.64	86.49%
2003–04	311	285.93	91.94%	241.44	84.44%
2004–05	295	280.82	95.19%	280.08	99.74%
2005–06	286	273.43	95.61%	271.36	99.24%
2006–07	302	288.34	95.48%	284.75	98.75%
2007–08	287	274.71	95.72%	272.84	99.32%
2008–09	264	249.63	94.56%	236.74	94.84%
2009–10	144	136.99	95.13%	127.20	92.85%
2010–11	198	185.03	93.45%	178.59	96.52%
2011–12	166	158.72	95.62%	155.53	97.99%
2012–13	146	137.04	93.86%	133.99	97.77%
2013–14	107	99.47	92.97%	83.05	83.49%
2014–15	102	95.00	93.14%	71.32	75.07%
2015–16	263	246.14	93.59%	236.63	96.14%

The breakdown of catch by survey depth stratum and fishing year is presented in Figure 8. As evident from the spatial pattern (Figure 5), catches were focussed in the shallower areas in the initial years of the fishery, but since the mid 1990s, the middle depth bands (400–450 m and 450–500 m) have dominated. No more than 3% of the overall catch has come from outside the 350–550 m depth range in any one year, and less than 1% in all years since 1993–94.

Monthly patterns of effort and catch are presented for SCI 6A in Figure 9 and Figure 10. Up until 1999–2000, fishing was focussed between January and May, although there was some activity throughout the year. The fishery was managed with competitive catch limits between 2001–02 and 2003–04, and during this period, effort and catches were focussed in the first few months of the fishing year. Since the introduction of scampi into the QMS (2004–05), very little trawling has taken place between January and February (or in December in more recent years), which is the period during which there is a higher incidence of post moult (soft shell) animals. Fishing effort has been relatively evenly distributed through the rest of the year.
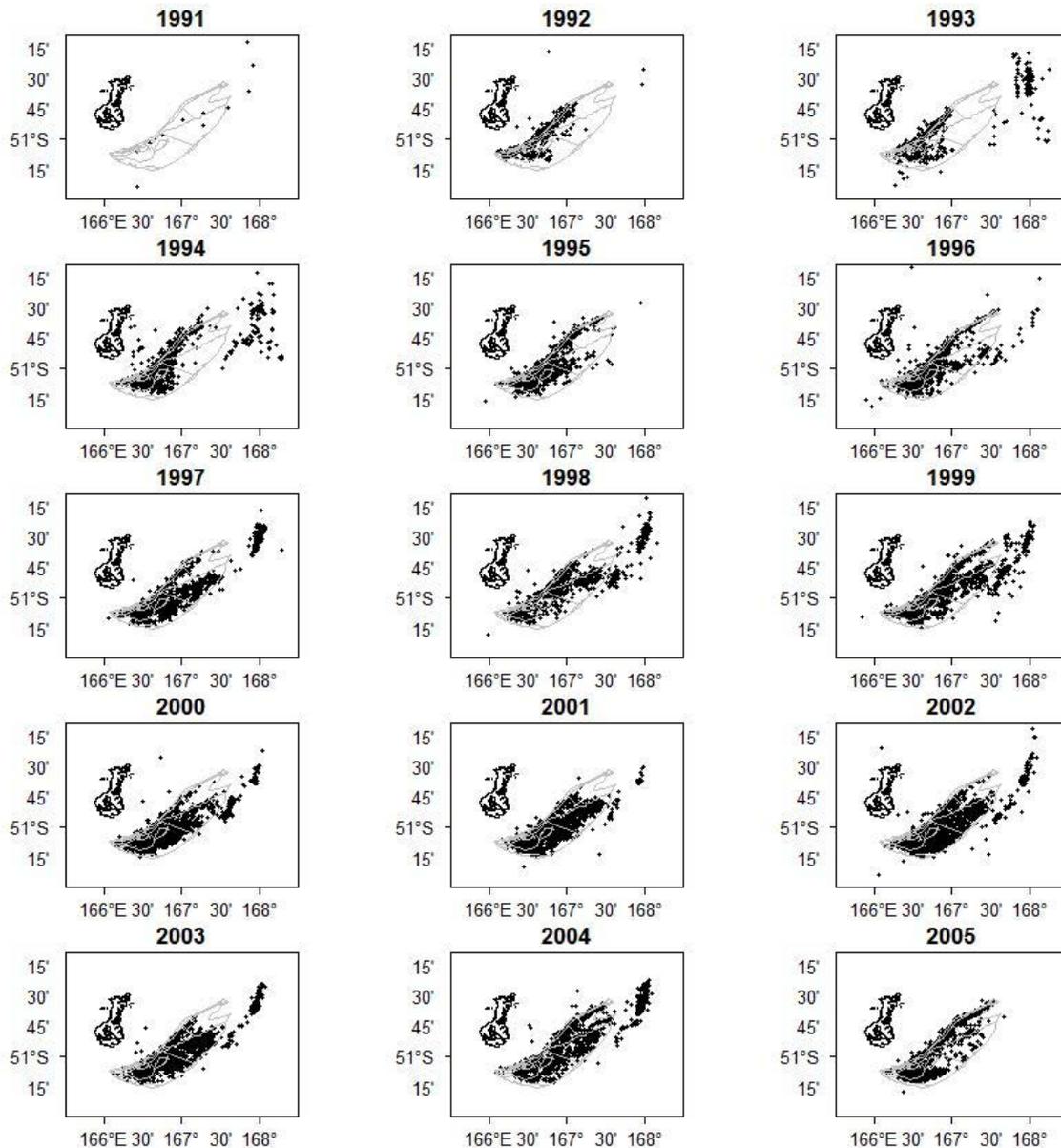

Figure 5: Spatial distribution of the main area of the SCI 6A scampi trawl fishery from 1990–91 to 2004–05. Each dot represents the midpoint of one or more tows reported on TCEPR. The general area covered by the plots is indicated within Figure 6.
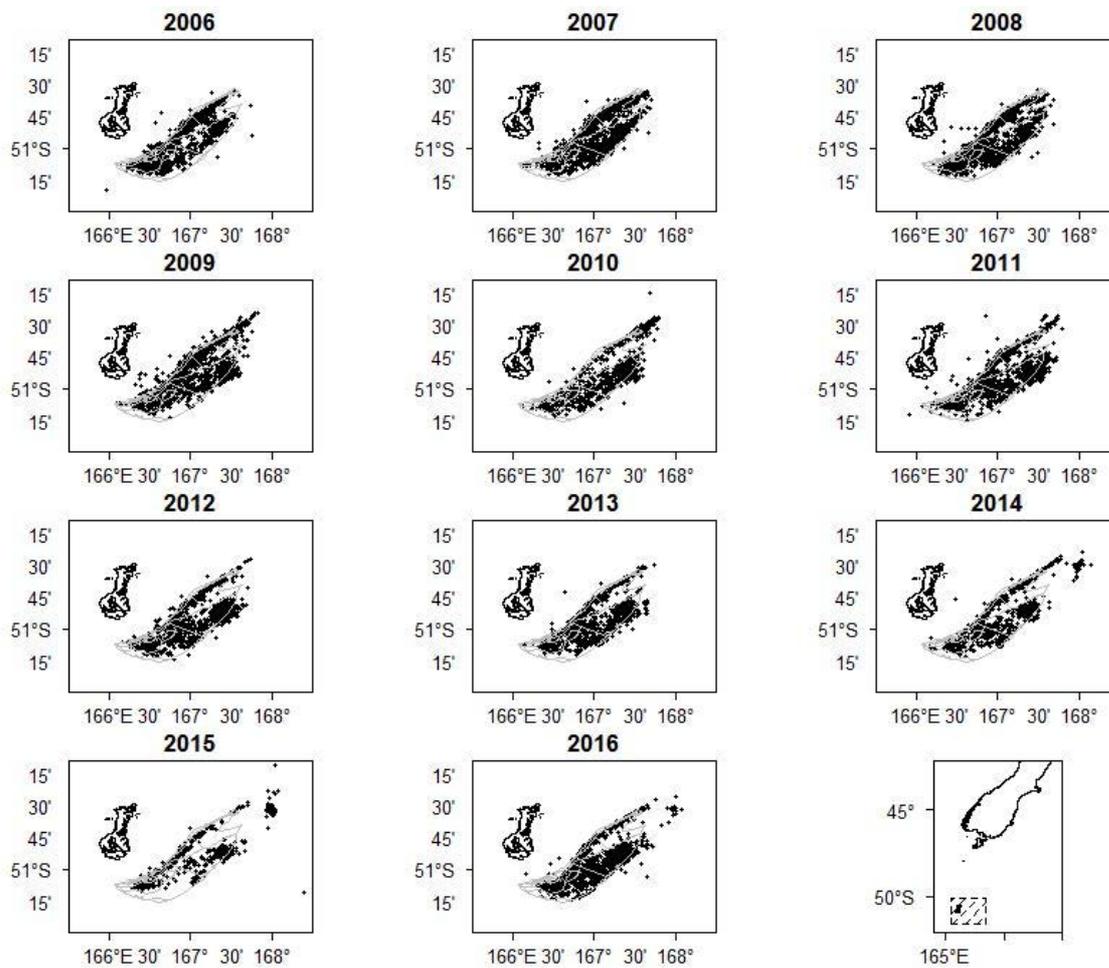
Figure 6: Spatial distribution of the main area of the SCI 6A scampi trawl fishery from 2002–03 to 2012–13. Each dot represents the midpoint of one or more tows reported on TCEPR. The general area covered by the plots is indicated by the shaded box in bottom right plot.

SCI 6A
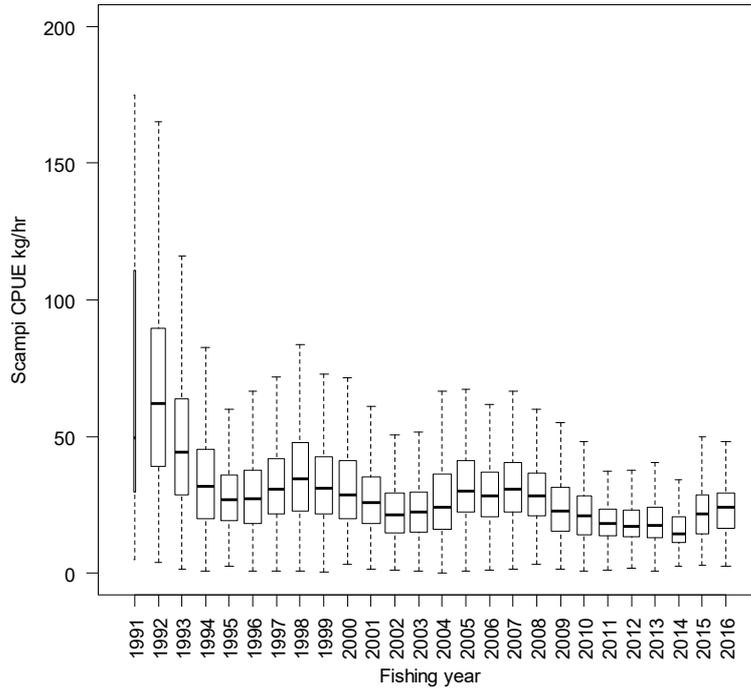
Figure 7: Box plots (with outliers removed) of unstandardized catch rate distributions (catch (kg) divided by tow effort (hours)) with tows of zero scampi catch excluded, by fishing year for the SCI 6A fishery. Box widths are proportional to square root of number of observations in each fishing year.

Catches by depth range

Largest circle represents 229 tonnes
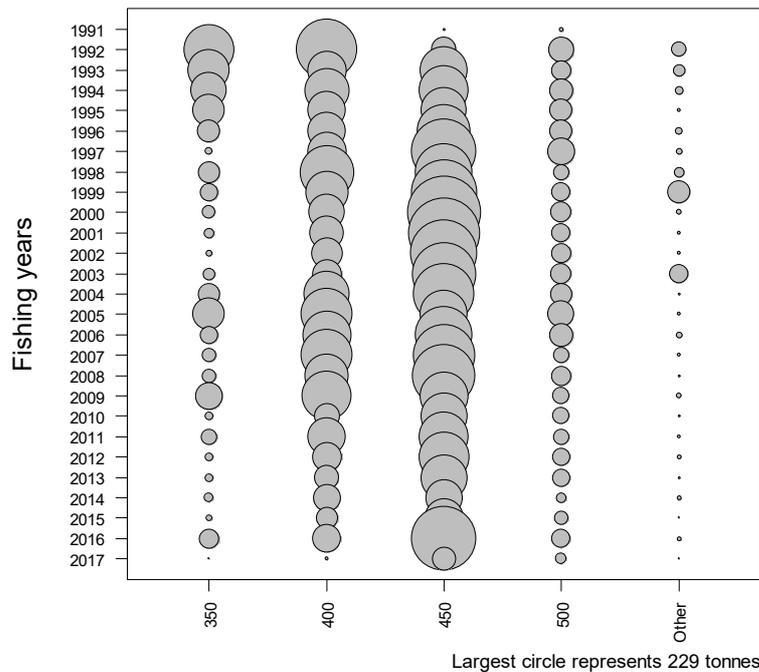
Figure 8: Annual catch breakdown by survey depth strata (and outside modelled area, 'Other') and fishing year for SCI 6A. Data only extracted to end November 2016 (2016–17 fishing year). Label '350' on x-axis indicates the 350–400 m stratum, etc.

Effort by month, SCI 6A

Largest circle represents 3867 hours
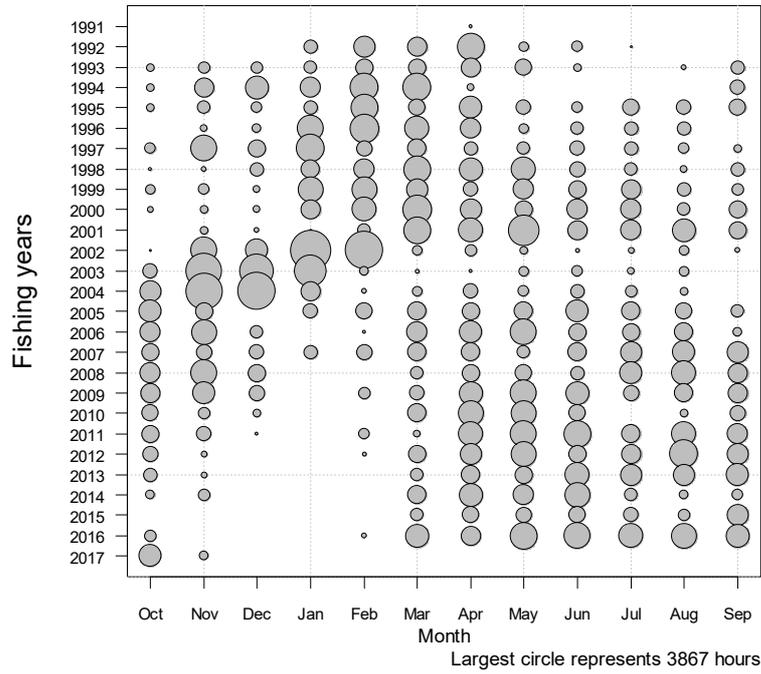
Figure 9: Monthly pattern of fishing effort in the scampi targeted fishery by fishing year for the core (modelled) area of SCI 6A. Data only extracted to end November 2016 (2016–17 fishing year).

Catch by month, SCI 6A

Largest circle represents 97.8 tonnes
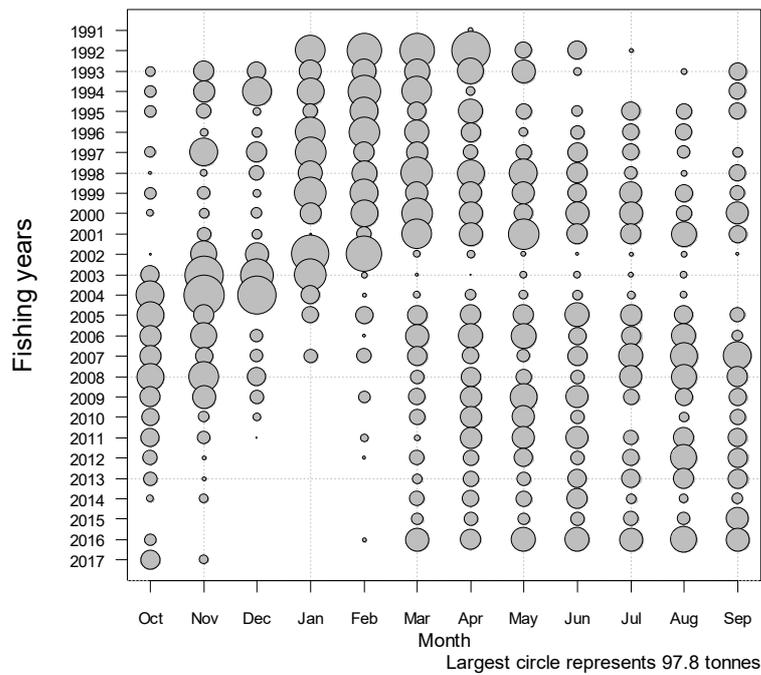
Figure 10: Monthly pattern of scampi catches in the scampi targeted fishery by fishing year for the core (modelled) area of SCI 6A. Data only extracted to end November 2016 (2015–16 fishing year ending 30 September).

2.2 Seasonal patterns in scampi biology

Previous development of the length based model for scampi has shown that determination of appropriate time steps for the model is important in fitting to length and sex ratio data in particular (Tuck & Dunn 2006, Tuck & Dunn 2009, Tuck & Dunn 2012). Scampi inhabit burrows, and are not usually vulnerable to trawling when they withdraw to their burrow. Catchability varies between the sexes on a seasonal basis as a result of sex specific moulting and reproductive behaviour, which leads to seasonal changes in the sex ratio of catches.

Current knowledge of the timing of scampi biological processes in SCI 6A is summarised in Table 2 (revised from Tuck 2010, Tuck & Dunn 2012). From patterns in the proportion of soft (post moult) animals (Figure 11), ovigerous females (Figure 12), and egg stage observed in commercial catches (Figure 13), mature female moulting appears to start in September and to be focussed around October and November, just after the hatching period (July – August). Hatching has been recorded at various times through the year, and appears to vary between stocks (Wear 1976; K. Heasman, Cawthron, pers. com.). Mating occurs after the females have moulted, while the shell is still soft, and new eggs are spawned onto the pleopods in December – January. The main male moulting period occurs between December and March.

The combination of different biological processes for males and females leads to different relative availabilities of the two sexes through the year, resulting in the pattern of sex ratio (displayed as proportion males) shown in Figure 14. This figure has been plotted on a half monthly basis, as some months appear to include a clear shift in sex ratio. Males are markedly less abundant than females in catches between December and March (male catches being reduced during their moulting period), the ratio of the sexes in the catches is roughly equal between April and June, and also in November, with males dominating from July to October.

On the basis of our understanding of the timing of biological processes for scampi in this area, and the seasonal pattern in sex ratios, we have defined the modelled year as running from mid-November, with three time steps, mid-November to mid-April (when females dominate in catches), mid-April to June (when the sex ratio is about equal), and July to mid-November (when males dominate in catches). (Table 3).

Table 2: Summary of scampi biological processes for SCI 6A. Revised from Tuck (2010) and Tuck & Dunn (2012).

	Jan	Feb	Mar	Apr	May	Jun	Jul	Aug	Sep	Oct	Nov	Dec
Male moult	X	X	X									X
Female moult									X	X	X	
Mating									X	X		
Eggs spawn	X											X
Eggs hatch							X	X				

Table 3: Annual cycle of the population model for SCI 6A, showing the processes taking place at each time step, their sequence in each time step, and the available observations. Fishing and natural mortality that occur within a time step occur after all other processes, with 50% of the natural mortality for that time step occurring before and 50% after the fishing mortality.

| Step	Period	Process	Proportion in time step
1	Mid Nov – Mid Apr	Maturation	1.0
		Growth (both sexes)	
		Natural mortality	0.42
		Fishing mortality	From TCEPR
2	Mid Apr – Jun	Recruitment	1.0
		Natural mortality	0.21
		Fishing mortality	From TCEPR
3	Jul – Mid Nov	Natural mortality	0.37
		Fishing mortality	From TCEPR
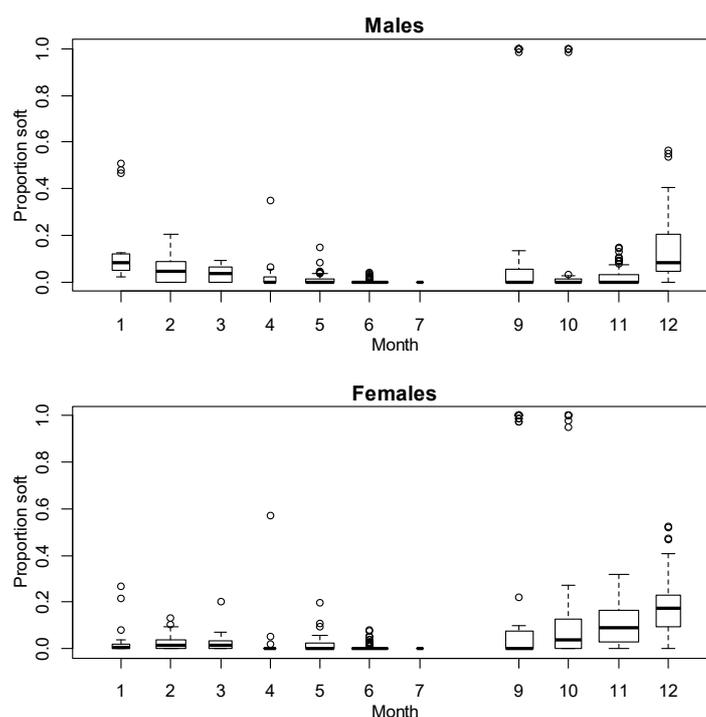
Figure 11: Box plots of proportions of soft animals (post moult) by sex and month, as recorded by observers. Box widths proportional to square root of number of observations for that month. No samples available from August.
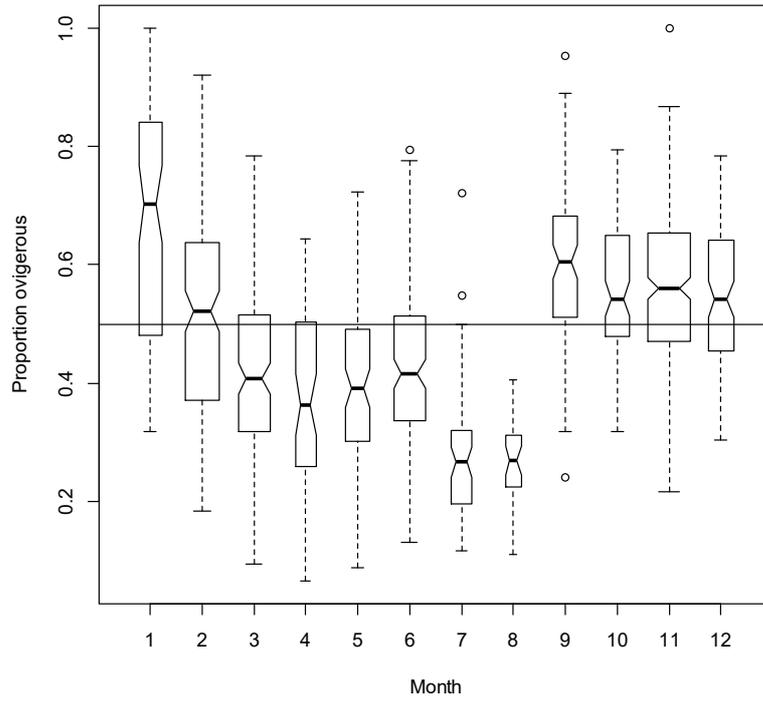
Figure 12: Box plots of proportions of ovigerous females by month, as recorded by observers. Box widths are proportional to square root of number of observations for that month.
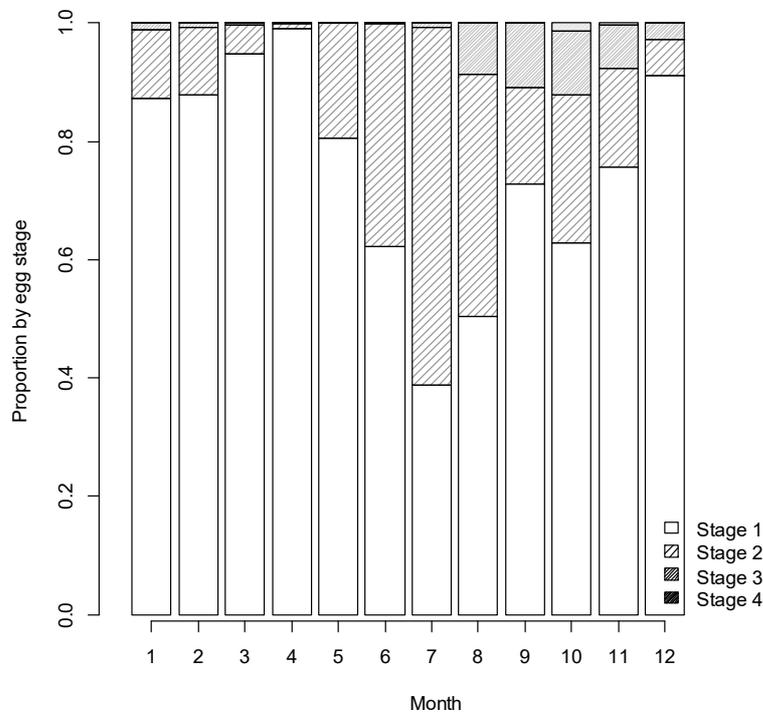

Figure 13: Bar plots of the proportion of ovigerous females by egg stage and month, from observer sampling in SCI 6A.
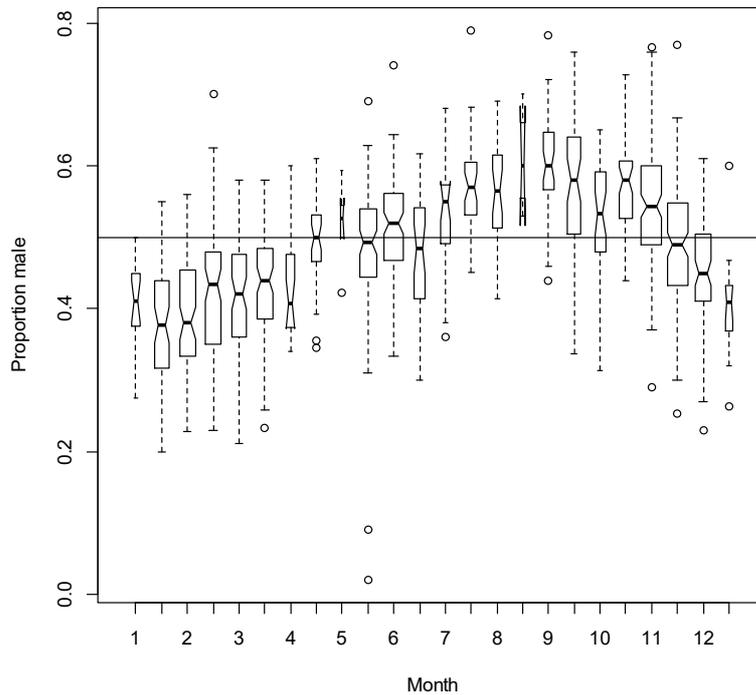
Figure 14: Box plots of proportion of males in catches by half month from observer sampling in the SCI 6A fishery. Box widths are proportional to square root of number of observations for that half month.

2.3 Standardised CPUE indices

2.3.1 Core vessels

A plot of vessel activity (number of scampi targeted tows recorded) over time is presented for SCI 6A in Figure 15. Eight vessels were active through most of the first decade of the fishery, but some of these dropped out of the fishery after 2003–04 (vessels D, G, I, N and P continuing to be active in most years), and a new vessel (S) being introduced at around this time.

Figure 16 (upper plot) shows the proportion of the total catch (over the history of the fishery) in relation to the number of years the vessels contributing that catch have been active in the fishery, and on the basis of this, a cut off of 10 years of activity has been selected to identify ten core vessels. Over the full history of the fishery, these vessels caught over 93% of the scampi targeted catch taken from SCI 6A. The lower plot of Figure 16 shows the proportion of catch accounted for in each year by vessels active for over 10 years. Similar analyses in previous characterisations (e.g., Tuck 2014) have also examined a 5 year vessel activity cut off, but for SCI 6A, this results in the same vessels being selected. Other than the 1991–92 to 1993–94 and 2002–03 to 2003–04 periods, the core vessels (active for over 10 years) have accounted for over 90% of targeted scampi catches in each year; often over 99%.

The pattern of activity for the selected core vessels is shown in Figure 17. Vessels D, G, I, and N have been active throughout the history of the fishery (albeit with some gaps for some vessels), while vessels E, and F were only active up until 2002–03. Vessel H was also active in this early period, and returned to the fishery in 2013–14, vessel P has been active since 1997–98, and vessel S was active from 2002–03 until 2012–13.
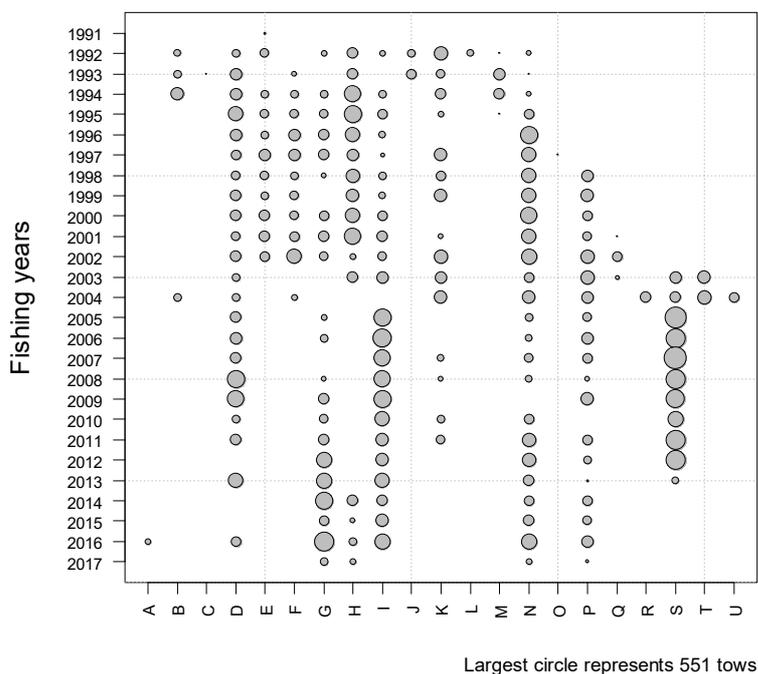
Figure 15: The temporal pattern of fishing activity by vessel and fishing year for the modelled area of SCI 6A. The area of each circle is proportional to the number of tows recorded.
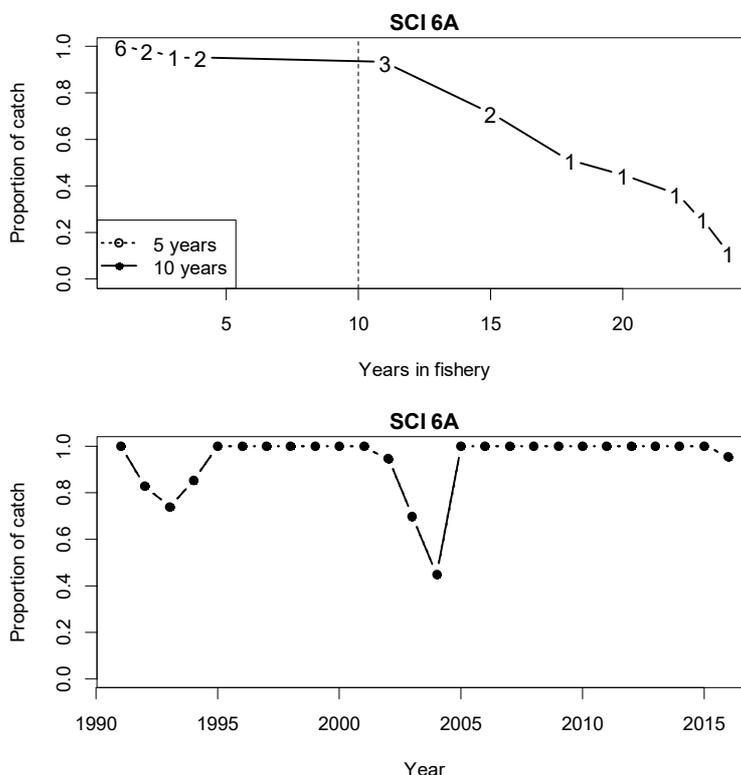

Figure 16: Catch breakdown by vessel. Upper plot - Proportion of total scampi catch (all years) plotted against the number of years the vessels reporting that catch have been active in the fishery. Numbers indicate number of vessels active for that duration. Vertical dotted line represents cut off for core vessels. Lower plot – Proportion of annual catch reported by vessels active in the fishery for 5 and 10 years, which is the same for both time periods.
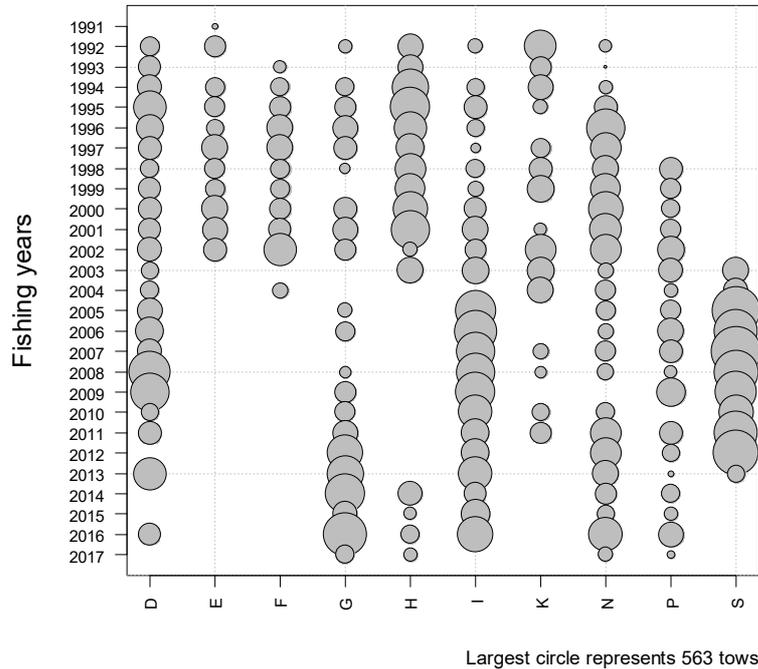
Figure 17: Core vessel pattern of fishing activity by vessel and fishing year for the modelled area of SCI 6A. The area of each circle is proportional to the number of tows recorded.

2.3.2 Exclusion of poorly sampled time periods

Following the approach developed for SCI 3 (Tuck 2013), time steps that were poorly sampled by the core vessels were excluded from the standardisation of the CPUE, on the basis that a small number of tows in an area, or at a particular time, may not provide a good index of abundance. Records were excluded from the CPUE standardisation when there were fewer than 10 tows recorded by core vessels within a time step in a year (Figure 18).
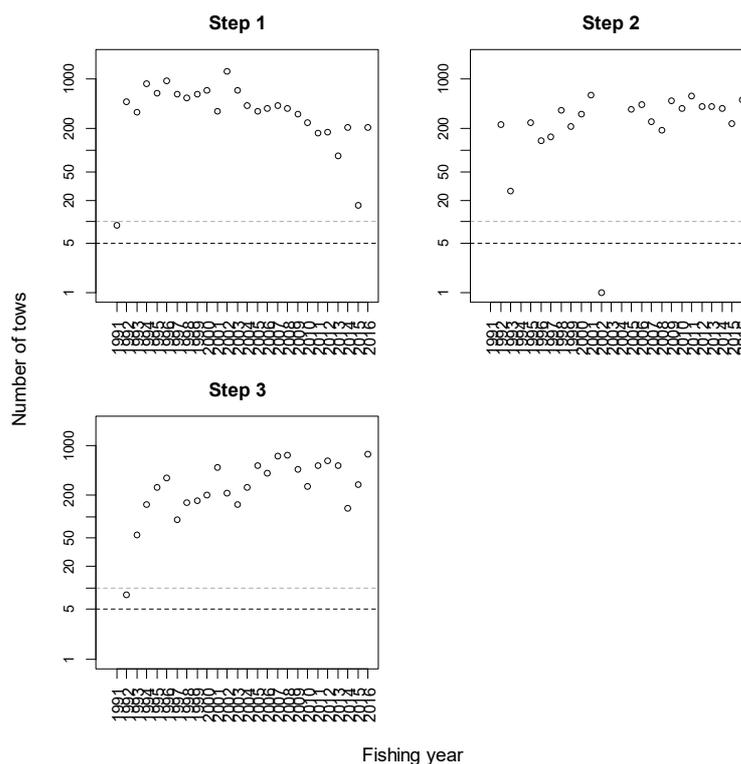
Figure 18: Numbers of commercial tows available within the core vessel dataset by time step and fishing year for SCI 6A. Dashed lines represent arbitrary cut offs at 5 and 10 tows.

2.3.3   Calculation of abundance indices

Individual event records from the ten core vessels were used to generate abundance indices (28 981 events). For the first preliminary assessment of SCI 6A, separate abundance indices were fitted for different survey strata and time steps (Tuck & Dunn 2012), but more recently the SFAWG has suggested a simplification of the model structure. Therefore, in subsequent assessments an initial model was examined allowing for the potential of model year*time_step*depth_band interactions. Scampi catch of core vessels was modelled using a year index (forced), model time step, vessel, time of day, state of moon, depth, fishing duration and trawl gear parameters.

The time of day of each tow was calculated in relation to nautical dawn and dusk (time when the sun is 12 degrees below the horizon in the morning and evening), as calculated by the *crepescule* function of the *maptools* package in R. Individual tows were characterised on the basis of whether they included dawn (shot before dawn, hauled after dawn and before dusk), day (shot after dawn, hauled before dusk), dusk (shot before dusk, hauled after dusk and before dawn) or night (shot after dusk and hauled before dawn). Longer tows including more than one period (i.e. shot before dusk and hauled after dawn) were excluded from this part of the analysis, which resulted in the exclusion of 89 records from a total of almost 29 000 tows undertaken by the core vessels fishing in SCI 6A.

Individual hauls were also categorised in terms of moon state, on the assumption that tidal current strength at the sea floor will be related to the lunar cycle. Tows were categorised by their date in relation to the lunar cycle, as Full moon (more than 26 days since full moon, or less than 3 days since full moon), Waning (4 – 11 days since full moon), New moon (12 – 18 days since full moon), and Waxing (19 – 26 days since full moon).

Within the core vessels identified, three have changed gear configuration (twin rig to triple rig) in recent years, and two have changed engine power over the history of the fishery. Engine power was fitted within the model as a third order polynomial, and gear configuration as a two level factor (twin or triple rig). Gear configuration for a particular vessel and date was determined on the basis of information provided by the fishing industry as to when vessels changed from twin to triple, and all tows after this date are defined as triple rig. It is acknowledged that vessels may change configuration within a trip depending on gear damage or fishing conditions, but it is unclear how reliably this has been recorded on TCEPR forms in the past (as effort width). Preliminary examination of the data for the core vessels suggested that the values recorded were generally realistic, and following some minor grooming, "effort width" was also offered as a third order polynomial term to the model.

In addition, examination of the data for SCI 3 (Tuck 2013) identified a distinct shift in trawl duration between 2002–03 and 2006–07 (from about 5 hours to 7 hours). This shift (in SCI 3) was fleet-wide, and associated with a modification to the top of the trawl to reduce the bycatch (John Finlayson, Sanford Ltd. pers comm.), enabling vessels to fish for longer on each tow. Box plots of tow duration over time have been examined for each of the core vessels identified for SCI 6A (Figure 19), and rather than the relatively rapid shift in trawl duration recorded by the same vessels in SCI 3 (Figure 20), within SCI 6A the increase in haul duration appears to have been more gradual, starting in the early 1990s, and stabilising at about 7 hours by the mid to late 1990s (Figure 19). This is a very similar pattern to that observed for SCI 1 and SCI 2 (Tuck 2014). Once the bycatch modification to the gear was introduced by a vessel (around 2004–05), it was used in all fisheries, but it does not appear to have had an effect on tow duration in SCI 6A (or SCI 1 and SCI 2). For each vessel, the timing of the gear modification was estimated from examination of tow durations in SCI 3, and fitted as a two level factor in the model.

Catch indices were derived using generalised linear modelling (GLM) procedures (Francis 1999, Vignaux 1994), using the statistical software R. The response variable in the GLM was the natural logarithm of scampi catch. The fishing_year (combined with any time step or depth strata for the index) was entered as a categorical covariate (explanatory) term on the right-hand side of the model. Standardised CPUE abundance indices (canonical) were derived from the exponential of the fishing-year covariate terms as described in Francis (1999).
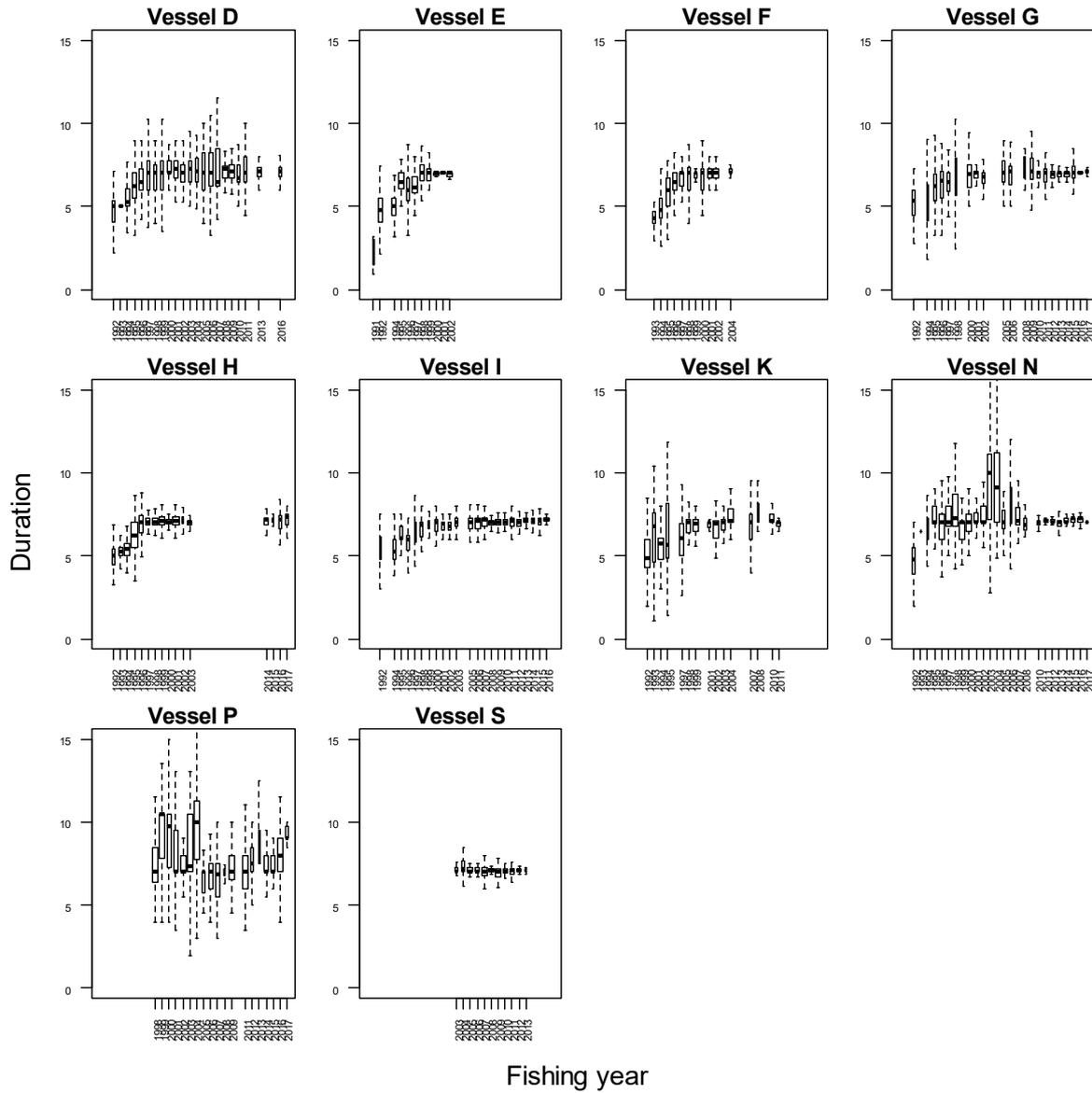
Figure 19: Box plots of tow duration (hours) for scampi targeted fishing in SCI 6A for the ten core vessels identified. Box widths are proportional to square root of number of observations.
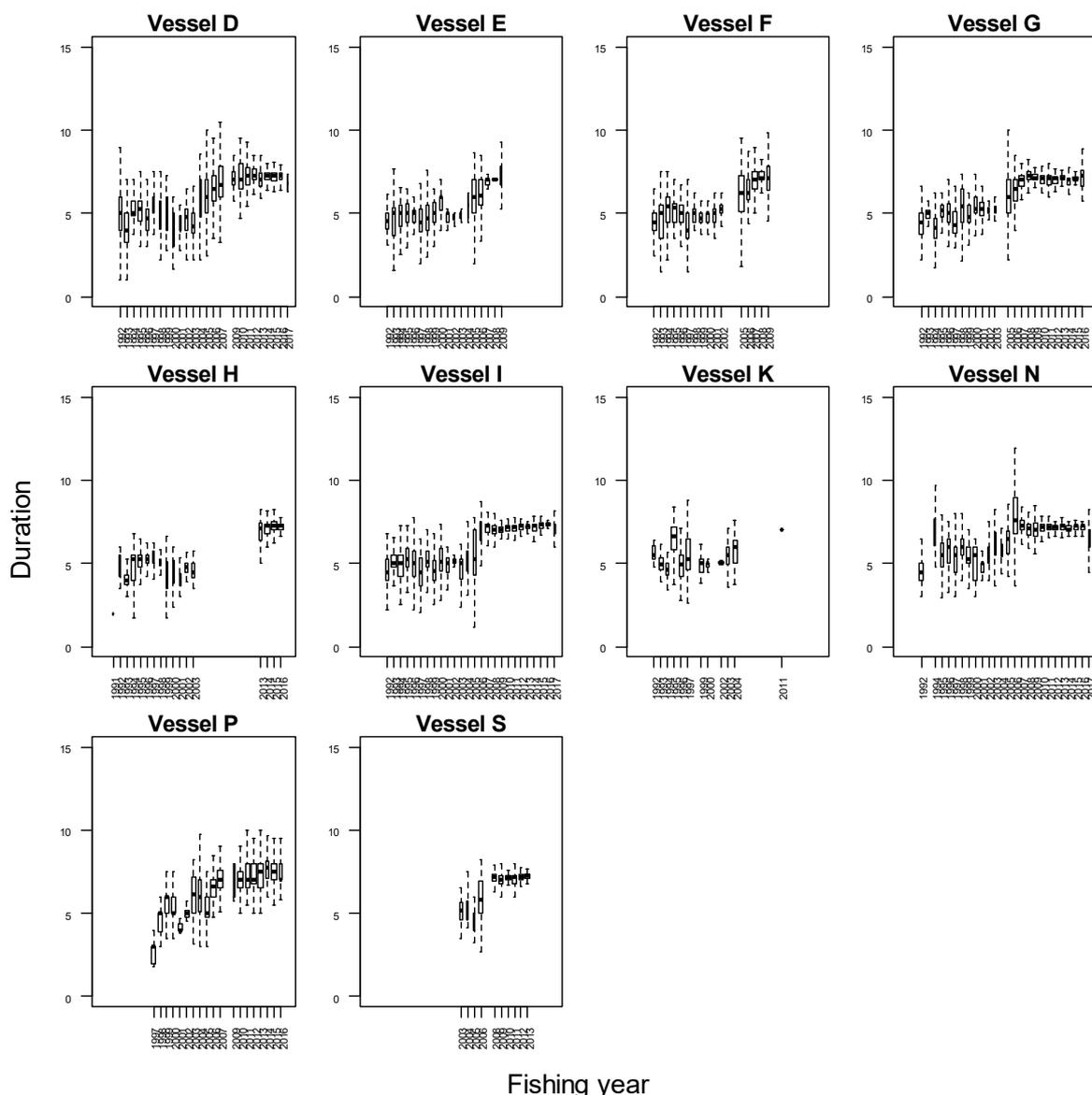
Figure 20: Box plots of tow duration (hours) for scampi targeted fishery in SCI 3 for the ten core vessels also identified for SCI 6A. Box widths are proportional to square root of number of observations.

In order to accommodate a non-linear relationship with the response variable (log catch), the continuous variables (effort, engine power, gear width) were "offered" to the GLMs as third order polynomials. Vessel, depth (binned into the 50 m survey strata), time of day, moon phase, twin or triple rig and bycatch modification were "offered" to the GLMs as factors. Some effects (e.g., gear width) were represented by more than one term, and the model was allowed to select which (if any) were retained. A forward fitting, stepwise, multiple-regression algorithm was used to fit GLMs to groomed catch, effort and characterisation data. The stepwise algorithm generates a final regression model iteratively and uses a simple model with a single predictor variable, fishing year (forced), as the initial or base model. The reduction in residual deviance relative to the null deviance is calculated for each additional term added to the base model. The term that results in the greatest reduction in residual deviance is added to the base model if this results in an improvement in residual deviance of more than 1%. The algorithm repeats this process, updating the model, until no new terms can be added. Diagnostic plots for the final models are presented in Appendix 1 (Bentley et al. 2012).

Preliminary investigations into different error distributions (comparing log normal, gamma and weibull) using a simple standardisation model

$$Log(catch) \sim fishing\_year$$

identified that the gamma distribution provided a slight improvement in the distribution of residuals, and this error distribution was used for calculation of the indices reported below. Diagnostic plots for the three compared error distributions, and for the final standardisation model, are presented in Appendix 1.

2.3.4 Final CPUE index

Stepwise regression analysis of the dataset with the full model to estimate the CPUE indices for SCI 6A resulted in an initial model with model year, time of day, fishing duration, vessel, model step, and a second order interaction between model year and model step retained (Table 4). The model explained 38% of the variation in the data. Depth was not retained within the model, either as a separate term, or as part of an interaction, suggesting that it does not contribute much to explaining the deviance in the model.

Table 4: Analysis of deviance table for initial standardisation model (including year:time step interations) selected by stepwise regression for SCI 6A.

	Df	Deviance explained	Additional deviance explained (%)
NULL			
model_year	24	1560.07	20.54
TOD	3	460.53	6.06
poly(fishing_duration, 3)	3	365.63	4.81
vessel	9	170.31	2.24
model_step	2	135.42	1.78
model_year:model_step	43	192.85	2.54

A second model was examined without the option of interactions, which explained 35.4% of the variation in the data (Table 5). Predicted CPUE (for vessel M with a 7 hour fishing duration) from the models with and without model_year:time_step interactions did not suggest that exclusion of the interaction term would have a big influence on the assessment model outputs (Figure 21), and the SFAWG agreed to use the standardised CPUE from the model excluding interactions.

Table 5: Analysis of deviance table for standardisation model (excluding year:time step interations) selected by stepwise regression for SCI 6A.

	Df	Deviance explained	Additional deviance explained (%)	Overall influence (%)[*]
NULL				
model_year	24	1560.07	20.54	
TOD	3	460.53	6.06	4.74
poly(fishing_duration, 3)	3	365.63	4.81	4.21
vessel	9	170.31	2.24	2.87
model_step	2	135.42	1.78	2.44

*- Overall influence as in table 1 of Bentley et al. (2012)

The standardised CPUE index used in the assessment model is presented along with the unstandardized CPUE data in Figure 22.
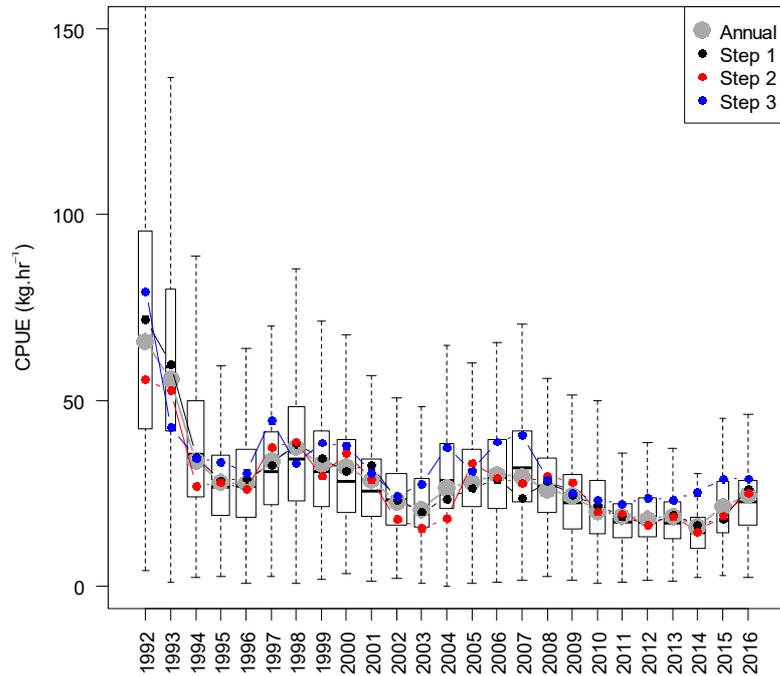
Figure 21: Predicted CPUE (for vessel M, with 7 hour tows) from the model with and without the model_year:time_step interaction. Box plots show unstandardized CPUE for each year. Box widths are proportional to square root of number of observations.
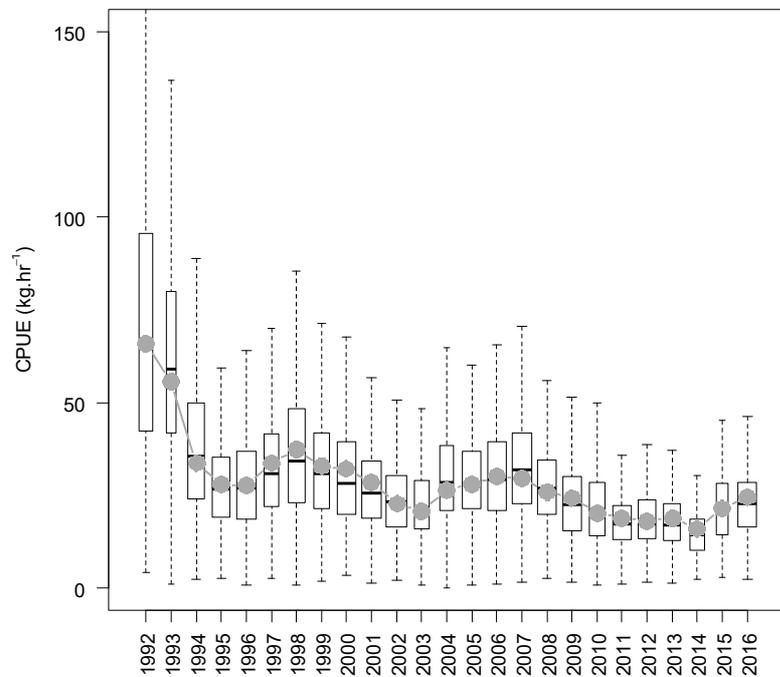

Figure 22: Annual standardised CPUE index from final model, and box plots of unstandardized CPUE. Box widths are proportional to square root of number of observations.

3. MODEL STRUCTURE

3.1 Seasonal and spatial structure, and the model partition

The model partitions the SCI 6A scampi population by sex and length class. Growth between length classes is determined by sex-specific length-based growth parameters. Individuals enter the partition by recruitment and are removed by natural mortality and fishing mortality. The model's annual cycle (starting in mid-November) is slightly offset from the fishing year to coincide with the moult cycle, and is divided into the three time-steps described above (on basis of Table 2). The choice of three time steps was based on current understanding of scampi biology and sex ratio in catches. Note that model references to "year" within this report refer to the modelled or fishing year, and are labelled as the most recent calendar year, e.g. the fishing year 1998–99 is referred to as "1999" throughout. Previous models for SCI 6A have included spatial structure (Tuck & Dunn 2012), but following the characterisation and preliminary model investigation, the SFAWG recommended a single area model for the assessment.

The model uses capped logistic length based selectivity curves for commercial fishing and research trawl surveys, which are allowed to vary with sex and time step (where necessary). While the sex ratio data suggest that the relative catchability of the sexes varies through the year (hence the model time structure adopted), there is no reason to suggest that assuming equal availability, selectivity at size would be different between the sexes. Therefore the two sex selectivity implementation developed within CASAL for previous scampi assessments (Tuck & Dunn 2012) was applied. This allows the L_{50} (size at which 50% of individuals are retained) and a_{95} ($L_{50} + a_{95}$ gives size at which 95% of individuals are retained) selectivity parameters to be estimated as single values shared by both sexes in a particular time step, but allows for different availability between the sexes through estimation of different a_{max} (maximum level of selectivity) values for each sex. The change in the depth distribution of the fishery in the early years (Figure 8), and the implication for selectivity (since mean size is larger in shallower areas) were allowed for using a shift parameter in the selectivity, related to the median depth of fishing in each year. Photographic survey abundance indices are not sex specific, and a double normal length based selectivity curve is applied, to allow for reduced availability of males (which grow to a larger size than females) at the time of the survey, related to moulting.

3.2 Biological inputs

3.2.1 Growth

Scampi growth has been investigated through field tagging exercises in SCI 6A in 2007, 2008, 2009, 2013 and 2016 (Tuck et al. 2009a, Tuck et al. 2009b, Tuck et al. 2015a, Tuck et al. 2017, Tuck et al. 2007), with recaptures reported by the fishing industry. Growth data are fitted within the model. The tag recapture data for each release event have been split into year-time step combinations, and the numbers of recaptures per event are tabulated in Table 6.

Table 6: Numbers of scampi recaptured by release and recapture time step (SCI 6A). Releases and recaptures labelled by fishing year_time step.

Release / Recapture	2007_1	2008_1	2009_1	2013_1	2016_1
2007_1	25				
2007_2	42				
2007_3	81				
2008_1	4	26			
2008_2	6	30			
2008_3	6	76			
2009_1	0	17	51		
2009_2	1	23	136		
2009_3	1	14	78		
2010_2	0	0	1		
2013_1	0	0	0	42	
2013_2	0	0	0	85	
2013_3	0	0	0	25	
2014_1	0	0	0	29	
2014_3	0	0	0	3	
2015_2	0	0	0	3	
2016_1	0	0	0	0	18
2016_2	0	0	0	1	27

For the various combinations of release and recapture, the length increment is plotted by sex against initial length for the 2007 release in Figure 23, for the 2008 and 2009 release in Figure 24, for the 2009 and 2013 release in Figure 25, and for the 2013 and 2016 release in Figure 26. Growth for both sexes is thought to occur in time step 1.
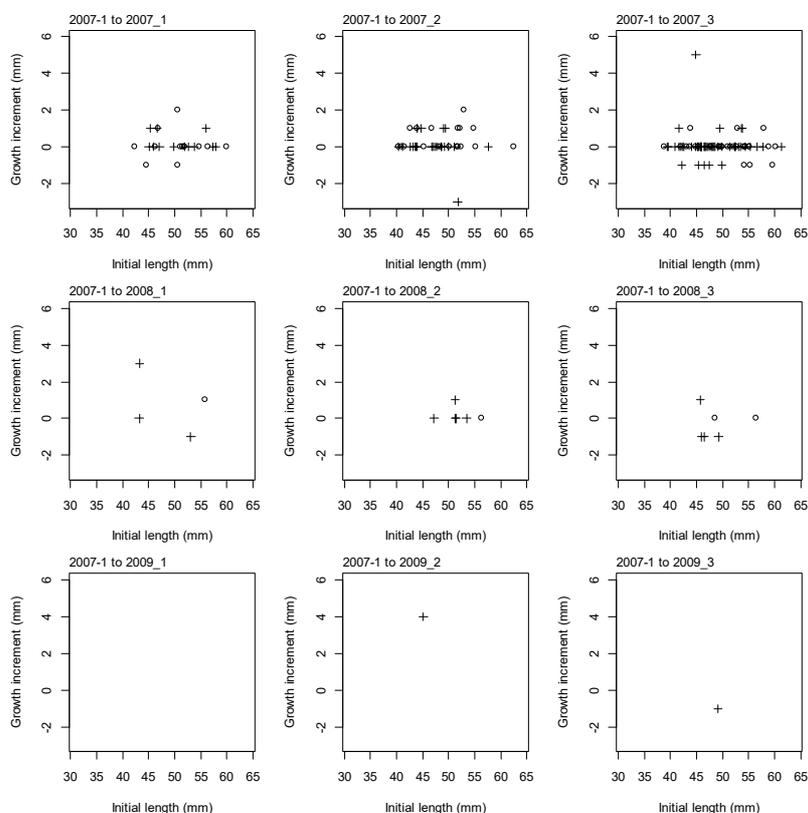
Figure 23: Plot of initial length against growth increment by combination of release and recapture time steps for 2007 releases. Males represented by hollow symbols, females represented by crosses.
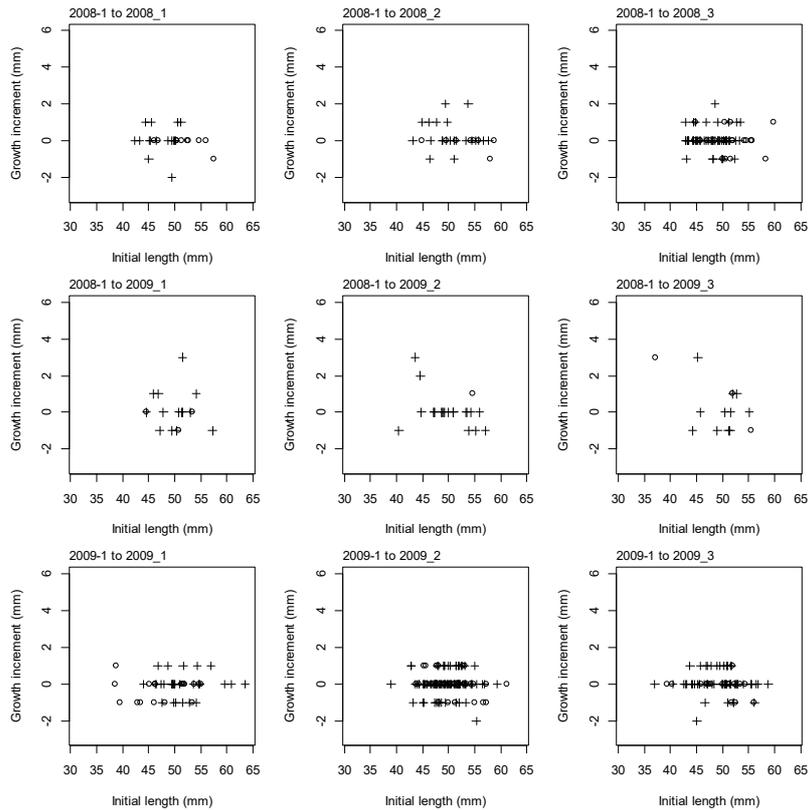
Figure 24: Plot of initial length against growth increment by combination of release and recapture time steps for 2008 and 2009 releases. Males represented by hollow symbols, females represented by crosses.

Given the overall size distribution of scampi from SCI 6A, with animals reaching larger sizes (compared to the other areas examined), it would be anticipated that the growth increment at size would be greater than in SCI 1 and SCI 2, and more comparable with SCI 3.
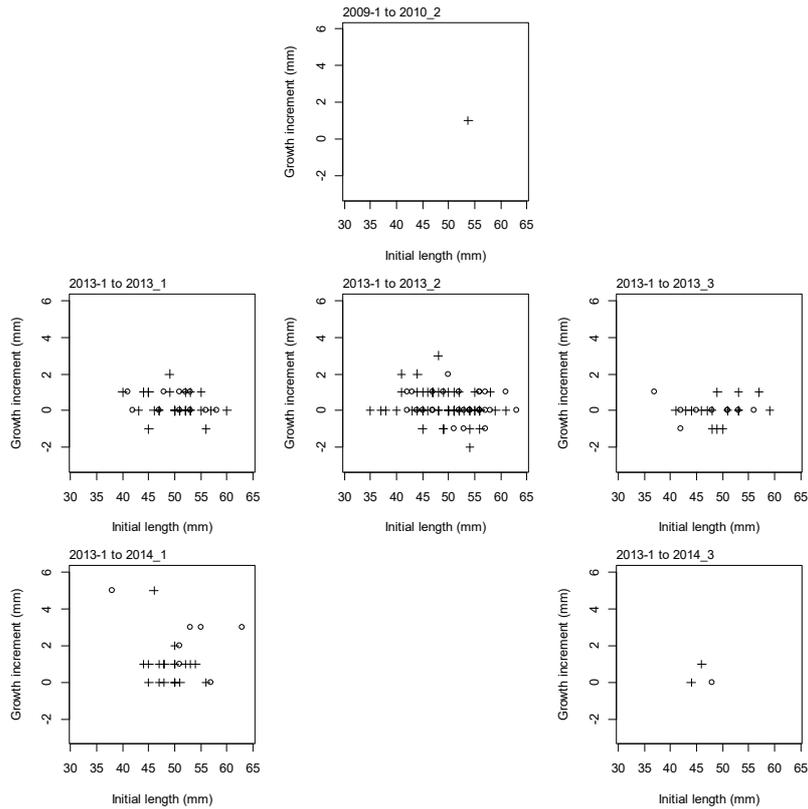
Figure 25: Plot of initial length against growth increment by combination of release and recapture time steps for 2009 (recaptured in 2010) and 2013 releases. Males represented by hollow symbols, females represented by crosses.
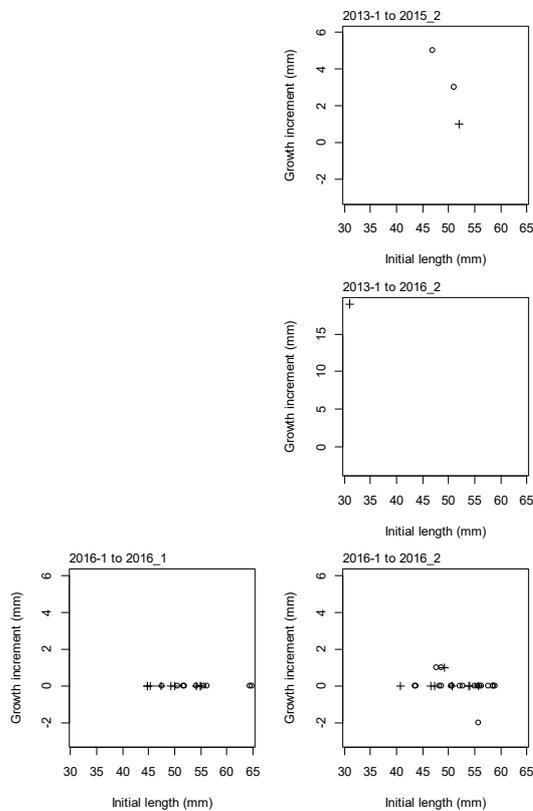
Figure 26: Plot of initial length against growth increment by combination of release and recapture time steps for 2013 (recaptured in 2015 and 2016) and 2016 releases. Males represented by hollow symbols, females represented by crosses.

3.2.2 Maturity

Female maturity can be estimated from gonad staging or the presence of eggs on the pleopods. Gonad stages are recorded from research survey catches (although only on scampi not tagged and released), while the presence and development stage of eggs on pleopods are recorded from research survey and observer sampling. No data are available for the maturity of male scampi, so their maturity ogive was assumed to be identical to that of females, although studies on *N. norvegicus* in Europe have suggested that male maturity may occur at a larger size (although possibly the same age) than females (Tuck et al. 2000). Maturity is not considered to be a part of the model partition, but the proportion of mature females in each length class were fitted within the model based on a logistic ogive with a binomial likelihood (Bull et al. 2008). Analysis of the proportion mature data, modelled as a function of length within a GLM framework, with a quasibinomial distribution of errors and a logit link (McCullagh & Nelder 1989),

$$P.mature = a + b * Length$$

which equates to the logistic model. The model was weighted by the number measured at each length. After obtaining estimates for the parameters a and b, the length at which 50% are mature (L_{50}) was calculated from:

$$L_{50} = -\frac{a}{b}$$

with selection range (SR) calculated from:

$$SR = \frac{(2.\ln(3))}{b}$$

Ovary stage at length data are presented in Figure 27. The L_{50} estimate for the SCI 6A data was 37.0 mm, with a selection range a_{25} to a_{75} of 5.8 mm.
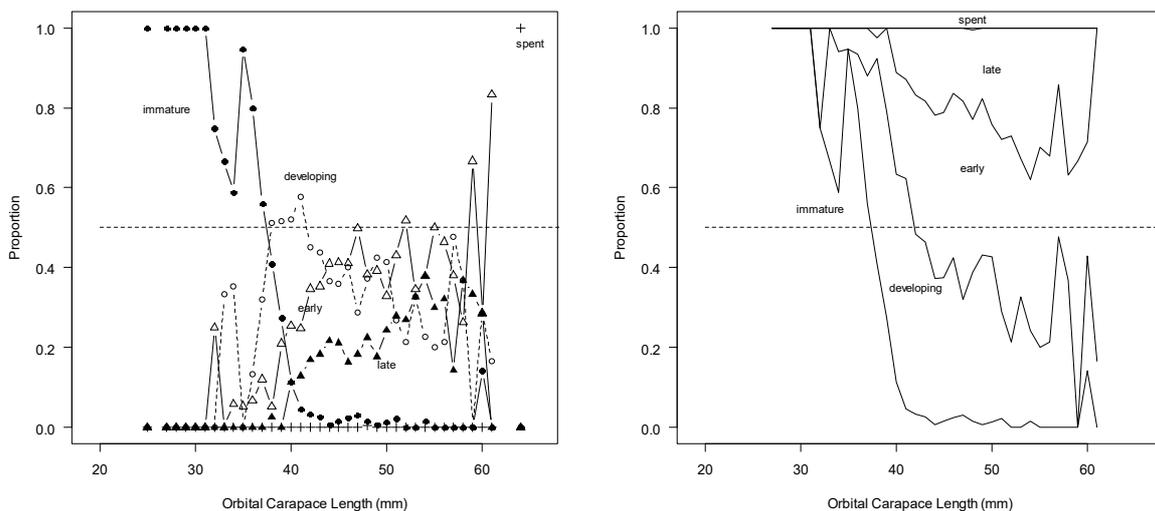

Figure 27: Proportions of female scampi having various developmental stages of internal ovaries. Left panel shows proportions of each stage separately, right panel shows combined proportions. Aggregated data from research voyages in SCI 6A, all conducted in February/March.
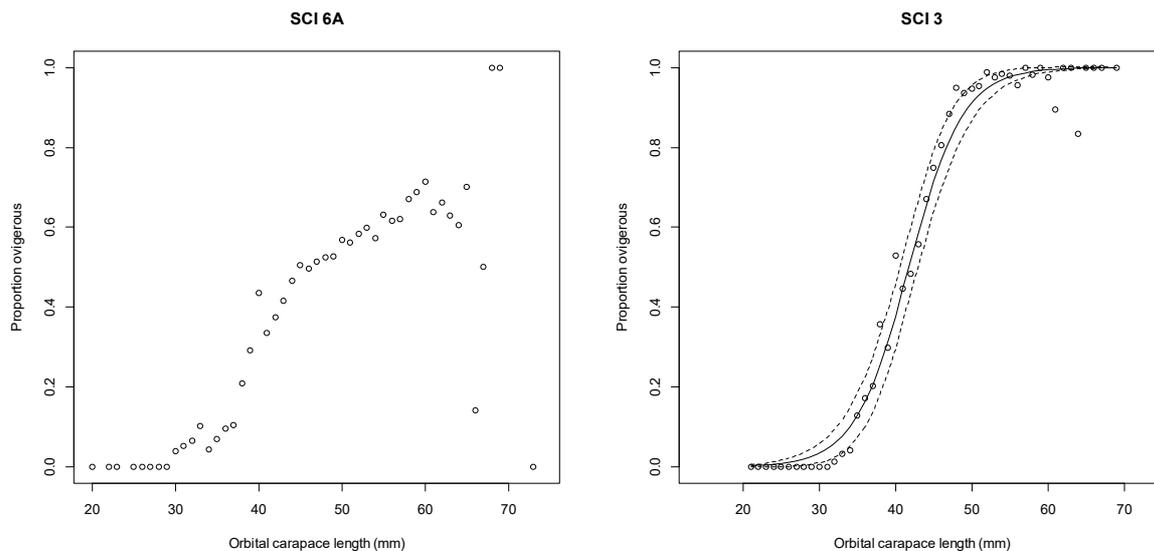
Figure 28: Left: Proportions of female scampi carrying eggs (ovigerous) at length, from observer sampling in January to March in SCI 6A, just after the spawning period. Right: Equivalent figure for SCI 3 for comparison (Tuck 2016b). Solid line represents logistic curve fitted to the data (L_{50} 41.8 mm and selection range 7.8 mm). Dashed line represents plus or minus one Standard Error.

3.2.3 Natural mortality

The instantaneous rate of natural mortality (M), has not been estimated directly for any scampi species, but estimates have been made (0.2 – 0.25) based on the estimate of the K parameter from a von Bertalanffy growth curve (Cryer & Stotter 1999) using a correlative method (Charnov et al. 1983, Pauly 1980). Morizur (1982) used length distributions from 'quasi-unexploited' *Nephrops* stocks to obtain estimates for annual *M* of 0.2–0.3. The values most commonly assumed for assessment of *Nephrops* stocks in the Atlantic is 0.3 for males and immature females, and 0.2 for mature females (assumed less vulnerable to predation during the ovigerous period) (Bell et al. 2006). For New Zealand scampi, M has previously been fixed at 0.2 (Tuck & Dunn 2012), or both 0.2 and 0.3 (Tuck 2014). Within the current assessment, preliminary models were explored where M was estimated, but the SFAWG requested to only develop models with M fixed at 0.2 and 0.25.

3.3 Catch data

Data for the model were collated over the spatial and temporal strata as defined in the model structure. Catches in the modelled area represent over 90% of scampi catches from SCI 6A. Details of catches by fishing year and time step, are provided in Table 7.

Table 7: Catch (t) breakdown by model year and time step for SCI 6A.

Model year	Step 1	Step 2	Step 3
1988	0.0	0.0	0.0
1989	0.0	0.0	0.0
1990	0.0	0.0	0.0
1991	0.89	0.00	0.00
1992	212.59	89.94	12.04
1993	126.67	46.09	35.97
1994	230.24	0.15	34.55
1995	130.22	46.39	61.19
1996	167.84	23.56	70.98
1997	149.99	45.67	32.35
1998	123.87	72.63	35.43
1999	129.65	55.02	59.86
2000	137.87	65.30	71.00
2001	73.37	85.62	78.79
2002	188.21	4.57	59.45
2003	126.62	5.34	88.59
2004	163.61	19.69	79.31
2005	81.01	87.84	125.38
2006	85.15	84.40	114.28
2007	68.83	43.69	185.70
2008	86.39	40.91	157.75
2009	62.04	106.78	81.55
2010	39.35	47.56	46.79
2011	25.79	82.39	82.93
2012	20.23	44.46	97.97
2013	10.95	49.36	82.44
2014	24.77	45.50	19.06
2015	9.37	20.67	46.53
2016	44.82	77.45	130.57

3.4 CPUE indices

The annual CPUE indices estimated within the standardisation (Figure 22) were fitted within the model as abundance indices. There has been considerable discussion on whether CPUE is proportional to abundance for scampi (Tuck 2009), with rapid increases in both CPUE and trawl survey catch rates for a number of stocks in the early to mid 1990s (and changes in sex ratio in trawl survey catches) initially being considered related to changes in catchability. Later analysis (Tuck & Dunn 2009) suggested that the observed changes in sex ratio were related to slight changes in the survey timing in relation to the moult cycle. Similar patterns in CPUE are observed over the same period for rock lobster (Starr 2009, Starr et al. 2009), and scampi in SCI 3 (Tuck 2013), which may suggest broad scale environmental drivers influencing crustacean recruitment. The CPUE patterns for SCI 1 are mirrored by trawl survey catch rates, suggesting that they do not reflect fisher learning. While not considered appropriate for use as an index in the model (Tuck 2013), a scampi abundance index generated from the middle depths (*R.V. Tangaroa*) trawl survey shows a very similar temporal pattern to the standardised CPUE indices for SCI 3, also supporting the suggestion that the increases in scampi catch rate observed during the 1990s reflect scampi abundance, rather than fisher learning.

The standardised CPUE index was fitted using the approach of Clark & Hare (2006), as recommended by Francis (2011). This approach fits lowess smoothers with different degrees of smoothing (Figure 29), and uses the residuals from each fit to estimate the CV. From visual examination of the fits, the SFAWG determined that a CV of 0.2 was appropriate for the CPUE, although sensitivity to narrower and wider CVs was also be examined in preliminary model runs.
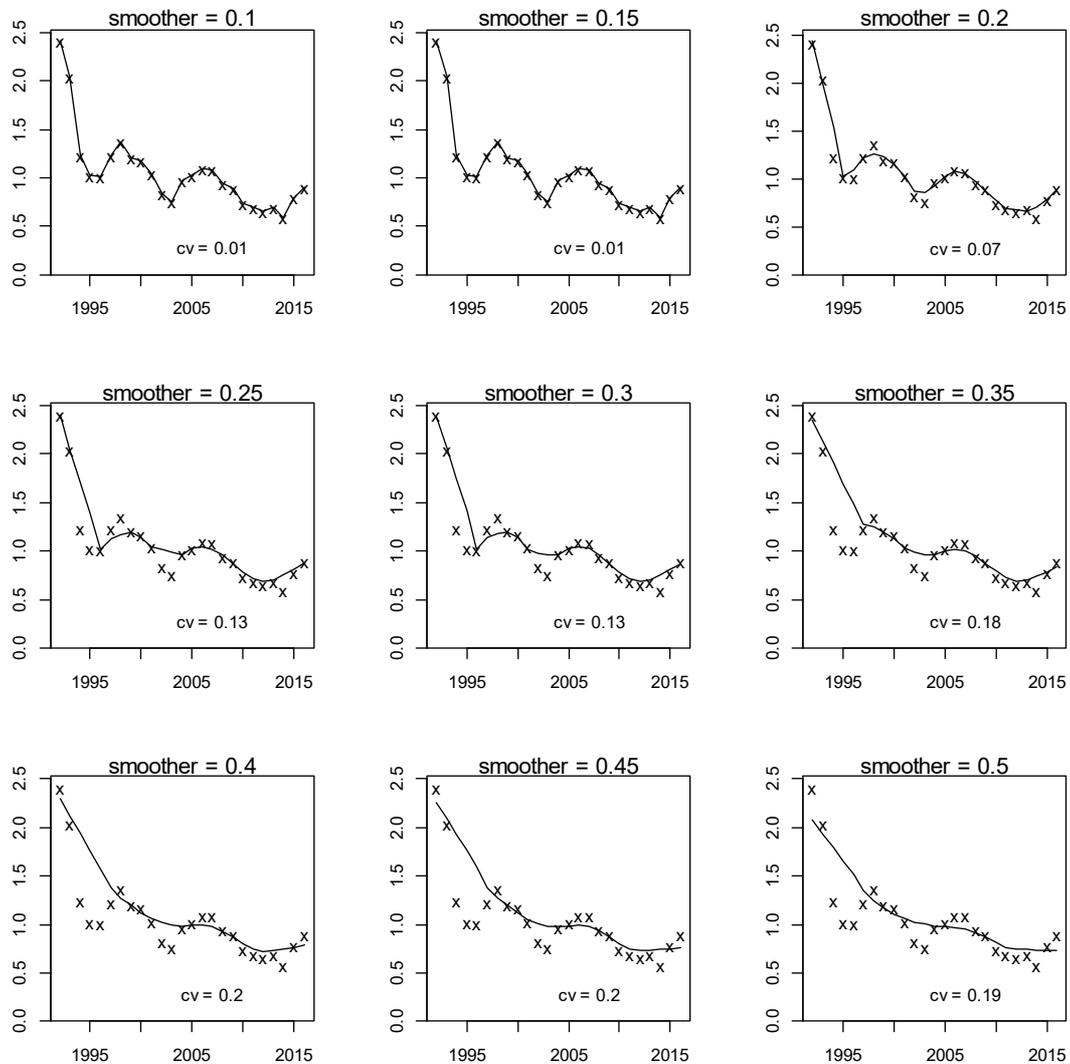

Figure 29: Fits of lowess smoothers to the standardised CPUE index.

3.5 Research survey indices

Trawl surveys were conducted annually in SCI 6A from the *F.V. San Tongariro*, between 2007 and 2009, with a fourth survey in 2013. The *F.V. San Tongariro* left the scampi fishery after 2013, and is no longer available for the survey. In 2016 the survey was conducted from the *R.V. Kaharoa*, using the standard trawl gear used on previous scampi surveys in SCI 1, SCI 2 and SCI 3. Details of the *F.V. San Tongariro* and *R.V. Kaharoa* scampi survey trawl gears are presented in Appendix 3. Each of these surveys was conducted (in conjunction with a photographic survey) between February and April.

3.5.1 Photographic surveys

Photographic surveys of SCI 6A have been conducted in 2007–09, 2013 and 2016 (Tuck et al. 2009a, Tuck et al. 2009b, Tuck et al. 2015a, Tuck et al. 2017, Tuck et al. 2007). These surveys provide two indices of scampi abundance, one based on major burrow openings, and one based on visible scampi. Both indices are subject to uncertainty, either from burrow detection and occupancy rates (for burrow based indices) or emergence patterns (for visible scampi based indices). The burrow index has been used to date within assessments for SCI 1, SCI 2 and SCI 3 (Tuck 2013, Tuck & Dunn 2012), but in SCI 6A scampi appear to spend less time in burrows, with animals frequently observed associated with "trench features" (possibly collapsed burrows) (Tuck et al. 2007), and the visible scampi index has been used (Tuck & Dunn 2012). Survey estimates are provided in Table 8. Details of the estimation of the catchability priors are provided in Section 3.7.

Table 8: Time series of photographic survey visible scampi abundance (millions) and CV for SCI 6A.

Survey	Abundance	CV
2007	60.45	0.14
2008	53.42	0.08
2009	36.59	0.14
2013	32.83	0.16
2016	48.72	0.14

3.5.2 Trawl surveys

Stratified random trawl surveys of scampi in SCI 6A, 350–550 m depth, were conducted in conjunction with photographic surveys described above. The 2007 – 2013 surveys were conducted by the same vessel, using the same trawl, but a gear loss just before the 2009 survey meant that slightly different trawl doors were used for that survey, with the catch rates scaled appropriately to account for this (Tuck et al. 2009a). The 2016 survey used a different vessel, and it is not clear how consistent the 2016 biomass estimate is with the earlier series (Tuck et al. 2017). Comparison of photographic survey (which is expected to be independent of vessel) and trawl survey abundance estimates were used to provide estimates of the relative catchability of the *San Tongariro* and *Kaharoa* scampi trawl gear (Figure 30), suggesting that the *San Tongariro* caught almost twice as much scampi as the *Kaharoa*, and the SFAWG therefore decided the 2016 trawl survey index point should be excluded from the assessment at present. Survey estimates are provided in Table 9. Details of the estimation of the catchability priors are provided in Section 3.7.
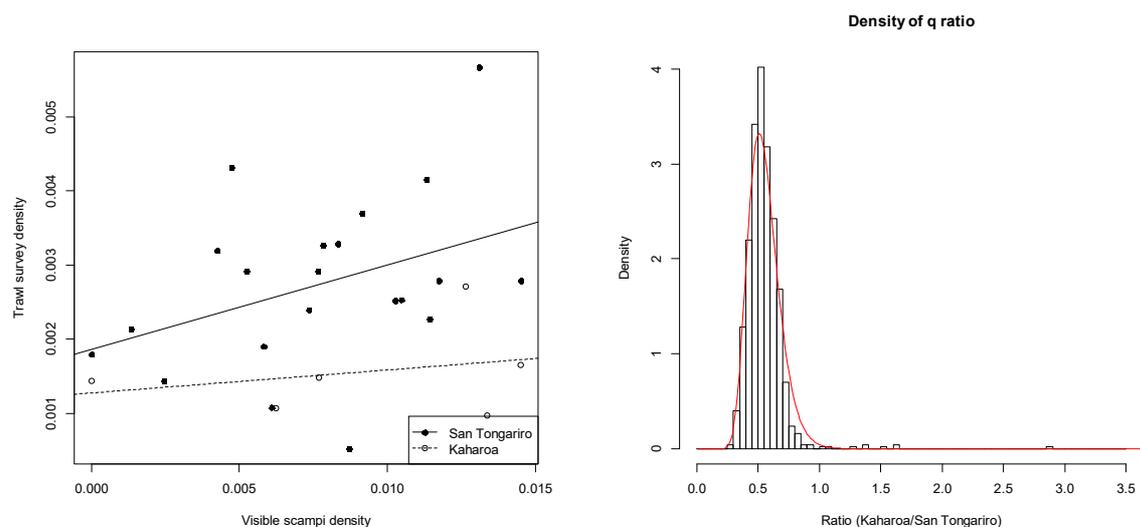

Figure 30: Plot of stratum level trawl survey scampi densities against photo survey scampi densities by vessel (left plot), and the distribution of the q-ratio (ratio between q values estimated for the two vessels for potential use as a prior). The red line represents the estimated log-normal distribution for the q-ratio prior, with mean of 0.55, and CV of 0.23.

Table 9: Time series of trawl survey scampi biomss (tonnes) and CV for SCI 6A.

Survey	Vessel	Biomass	CV
2007	*San Tongariro*	1 073.5	0.18
2008	*San Tongariro*	1 229.2	0.18
2009	*San Tongariro*	821.6	0.09
2013	*San Tongariro*	1 258.0	0.09
2016	*Kaharoa*	593.8	0.09

3.6 Length distributions

3.6.1 Commercial catch length distributions

Ministry for Primary Industries observers have collected scampi length frequency data from scampi targeted fishing on commercial vessels in SCI 6A since 1991–92. The numbers of tows for which length data are available are presented by fishing year in Table 10.

Table 10: Numbers of scampi observer length frequency samples from SCI 6A, by model year, time step and combined depth band.

	Step			Step 1		Step 2		Step 3	
Model year	1	2	3	350–450	450–550	350–450	450–550	350–450	450–550
1991	0	0	0	0	0	0	0	0	0
1992	81	0	0	78	1	0	0	0	0
1993	69+	0	13	49	19	0	0	9	4
1994	88	0	35	34	54	0	0	7	28
1995	20	0	0	5	15	0	0	0	0
1996	32	0	19	13	19	0	0	0	19
1997	24	24	58	5	19	0	24	1	57
1998	87	6	1	65	22	0	6	1	0
1999	0	0	21	0	0	0	0	2	19
2000	24	0	0	1	23	0	0	0	0
2001	0	36	11	0	0	0	36	0	11
2002	14	0	55	0	14	0	0	38	17
2003	39	0	57	10	29	0	0	26	31
2004	7	0	0	1	6	0	0	0	0
2005	0	0	24*	0	0	0	0	2	22*
2006	17*	0	0	1*	16*	0	0	0	0
2007	34	0	13	29	5	0	0	0	13
2008	13	12	25	2	11	8	4	6	19
2009	14	0	0	2	12	0	0	0	0
2010	0	30	0	0	0	4	26	0	0
2011	43	27	59	16	27	17	10	1	58
2012	0	31	0	0	0	20	11	0	0
2013	0	89	0	0	0	8	81	0	0
2014	0	56	0	0	0	25	31	0	0
2015	0	0	0	0	0	0	0	0	0
2016	0	16	84	0	0	1	15	6	78

+ - 35 tows in 1993_1 measured scampi to the centimetre, rather than millimetre, and these have been excluded from further analysis.
* - exclusion of observer trip 10242 removes 8 samples from time step 3 in 2005 (all from the 450–550 m depth range, and all 17 samples from time step 1 in 2006.

Examination of the commercial catch length distributions as part of the previous characterisation of this fishery (Tuck 2015) identified depth related spatial structure in the length composition data (larger scampi in shallower water). Patterns in the sex ratio and mean size from the scampi observer length frequency data were examined using multivariate tree regression (using the R package *mvpart*). Data were analysed for each year separately at the observed tow level, with response variables regressed on

the explanatory variables half_month and depth_bin. Pruning was conducted to determine the tree with the smallest cross-validated relative error. Depth splits were identified in over half of the years, with 450 m identified most frequently. The temporal splits identified were consistent with those already proposed for the model structure (Table 3).

On the basis of both the mean size and sex ratio (proportion males) within catches, it was considered appropriate to stratify the observer length data by depth, with separate strata for 350–450 m, and 450–550 m (combined).

Detailed examination of the length distribution data also identified some anomalous data that was excluded from further analyses. The median size of scampi in SCI 6A has generally varied between 44 mm and 55 mm, but a trip where the median size was 39 mm was removed, as the data suggest that the observer was not following measurement protocols correctly. Data from another trip where scampi were measured to the nearest whole cm (rather than mm) were also excluded.

On the basis of the observer sampling within the two depth bands (350–450 m and 450–550 m) and the three time steps within each fishing year (Table 10), the proportion of scampi catch represented by the sampling observer (having at least one observer sample from that depth in that time step) has been examined (Table 11). This ranged from 25% (1998, time step 3) to 100%, with 32 of the 39 observed year_step combinations having over 90% of the catches represented by sampling. The SFAWG considered that 90% representation was an appropriate cut-off for inclusion in the assessment model, with the other data being excluded. For the year_step combinations retained, proportional length distributions (and associated CVs) were calculated using CALA (Francis et al. 2016), using the approaches previously implemented in NIWA's *Catch-at-Age* software (Bull & Dunn 2002). Plots of the proportional length distribution are shown by year by time step in Figure 31 to Figure 36.

Table 11: Estimated scampi catch (tonnes) in the modelled area by model year and time step, and the percentage of catch represented by the observer sampling.

Model year	Estimated catch			% represented by sampling		
	Step 1	Step 2	Step 3	Step 1	Step 2	Step 3
1991	0.89	0.00	0.00			
1992	212.59	89.94	12.04	100.00		
1993	126.67	46.09	35.97	100.00		100.00
1994	230.24	0.15	34.55	100.00		100.00
1995	130.22	46.39	61.19	100.00		
1996	167.84	23.56	70.98	100.00		80.33
1997	149.99	45.67	32.35	100.00	70.45	100.00
1998	123.87	72.63	35.43	100.00	61.58	25.51
1999	129.65	55.02	59.86			100.00
2000	137.87	65.30	71.00	100.00		
2001	73.37	85.62	78.79		84.06	92.96
2002	188.21	4.57	59.45	83.84		100.00
2003	126.62	5.34	88.59	100.00		100.00
2004	163.61	19.69	79.31	100.00		
2005	81.01	87.84	125.38			100.00*
2006	85.15	84.40	114.28	100.00*		
2007	68.83	43.69	185.70	100.00		65.86
2008	86.39	40.91	157.75	100.00	100.00	100.00
2009	62.04	106.78	81.55	100.00		
2010	39.35	47.56	46.79		100.00	
2011	25.79	82.39	82.93	100.00	100.00	100.00
2012	20.23	44.46	97.97		100.00	
2013	10.95	49.36	82.44		100.00	
2014	24.77	45.50	19.06		100.00	
2015	9.37	20.67	46.53			
2016	44.82	77.45	130.57		100.00	100.00

* - exclusion of observer trip 10242 does not affect sample coverage for time step 3 in 2005 (because another trip also provides coverage), but removes all samples from time step 1 in 2006.
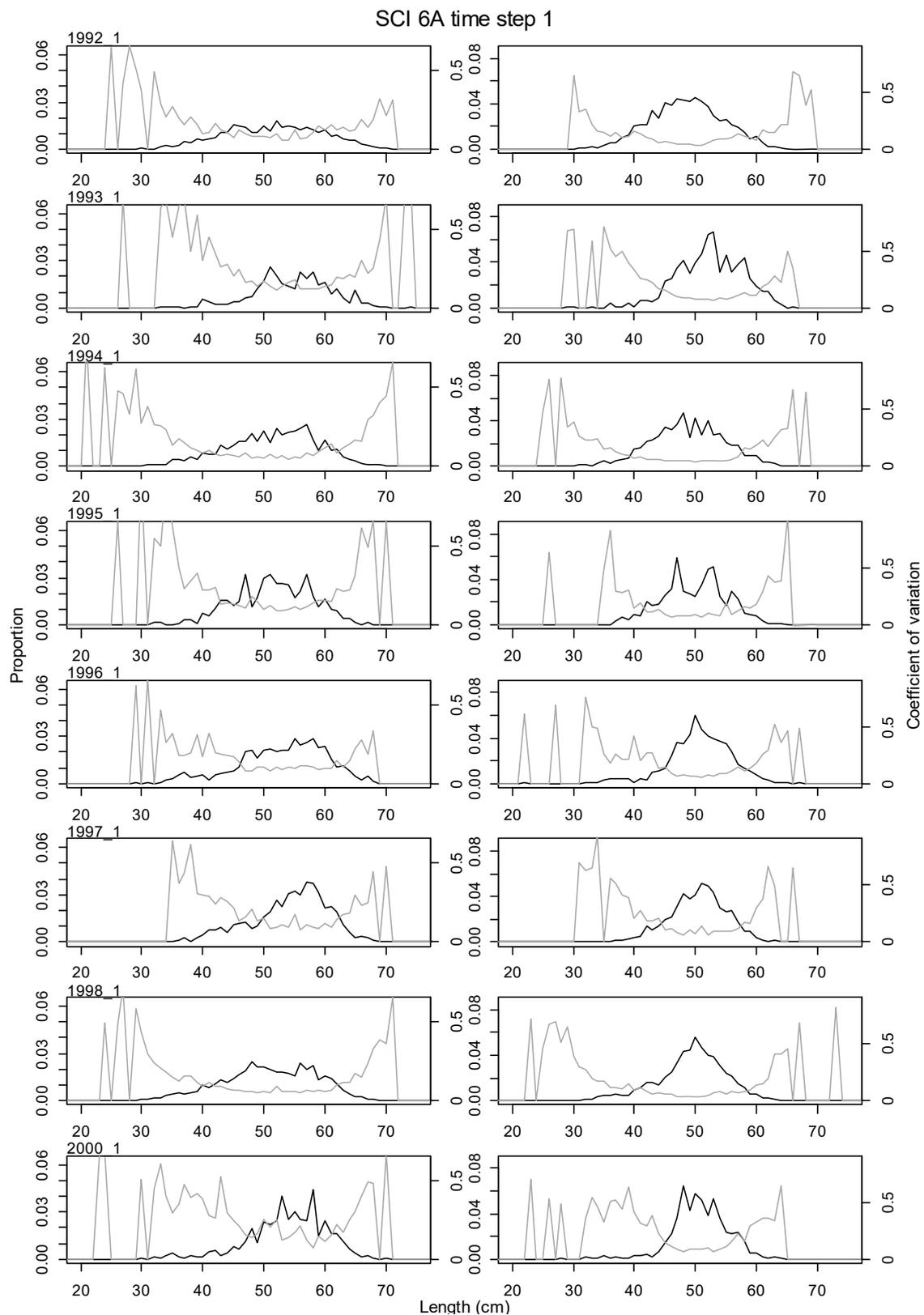
Figure 31: Proportional length frequencies (black line) and CVs (grey line) for commercial catches by model year and time step 1 for SCI 6A. Males plotted on left, females on right.
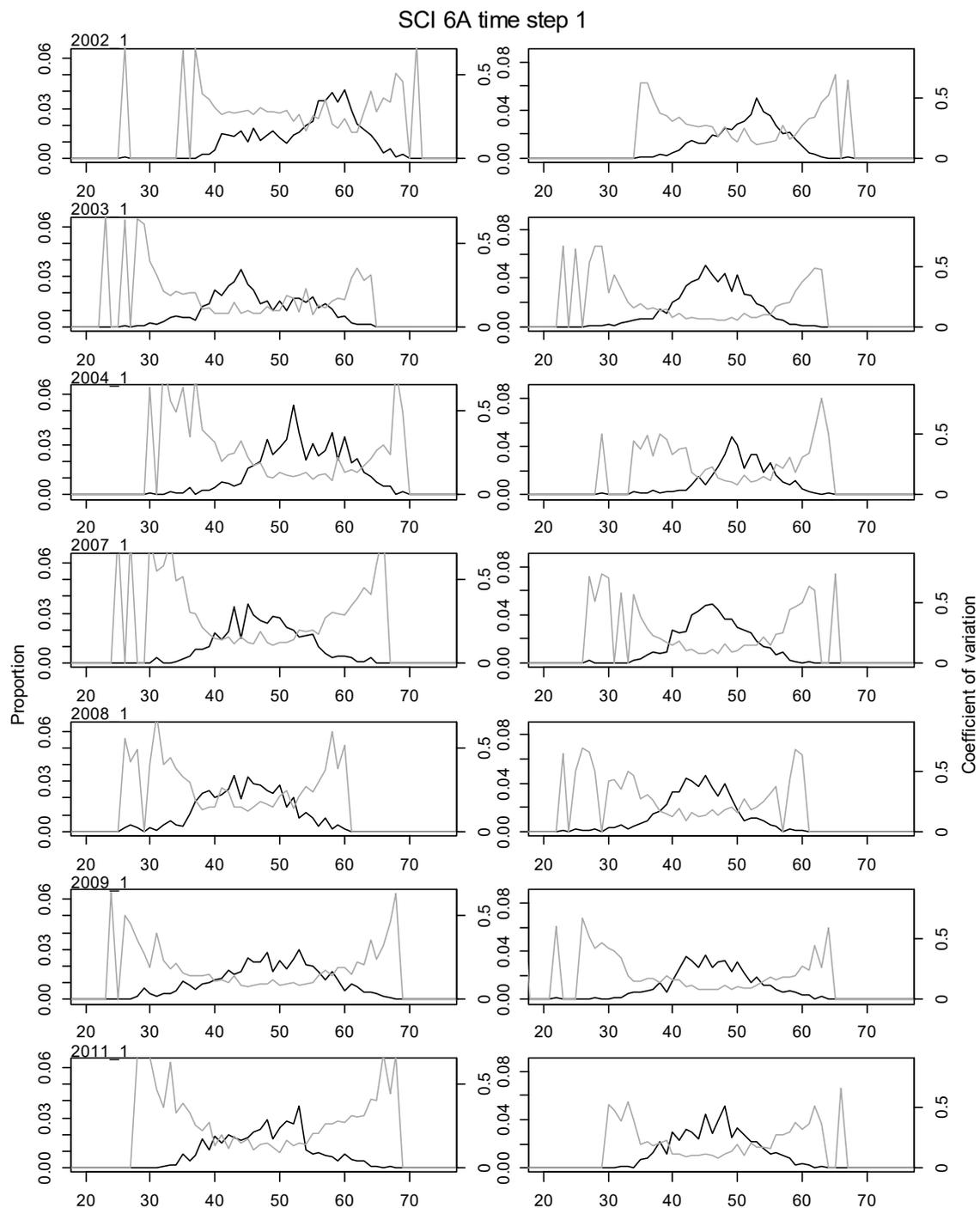
Figure 32: Proportional length frequencies (black line) and CVs (grey line) for commercial catches by model year and time step 1 (continued) for SCI 6A. Males plotted on left, females on right.
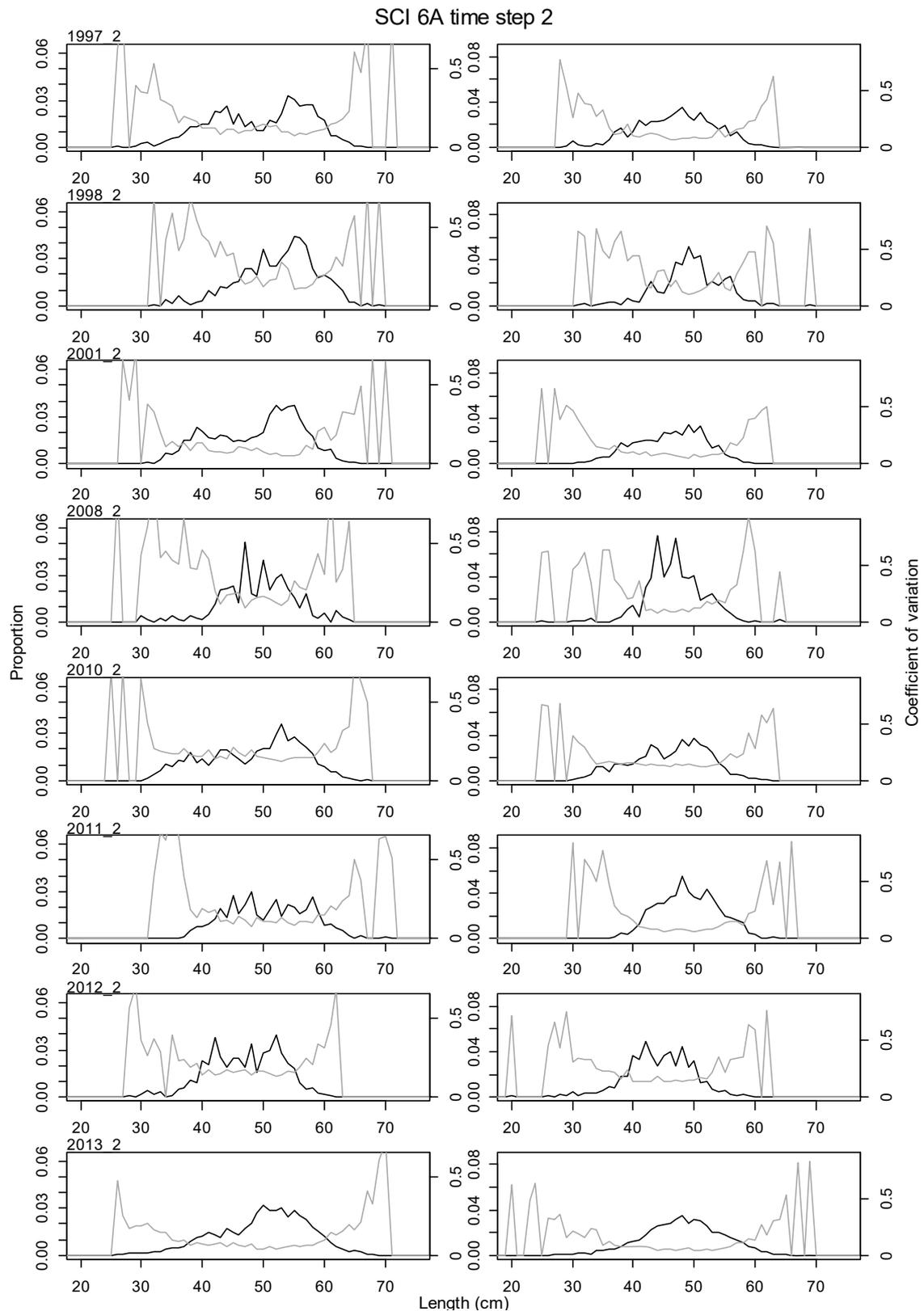
Figure 33: Proportional length frequencies (black line) and CVs (grey line) for commercial catches by model year and time step 2 for SCI 6A. Males plotted on left, females on right.
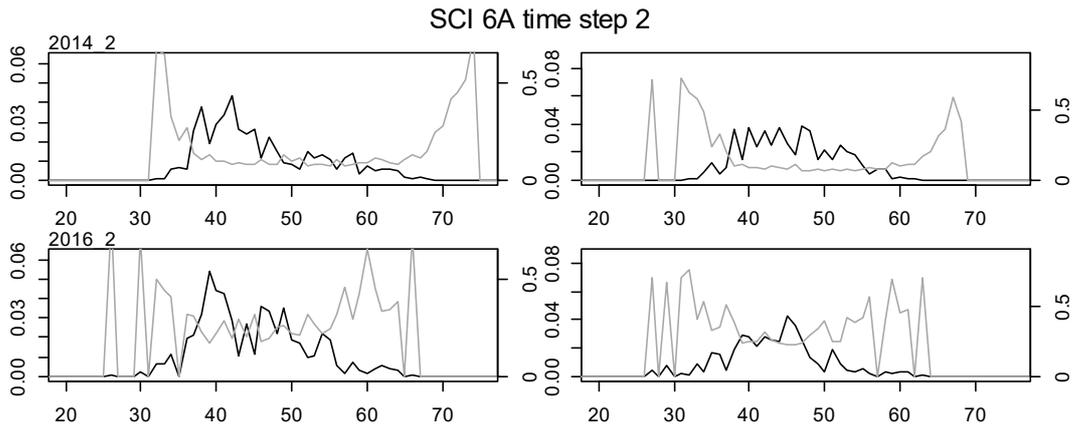
Figure 34: Proportional length frequencies (black line) and CVs (grey line) for commercial catches by model year and time step 2 for SCI 6A. Males plotted on left, females on right.
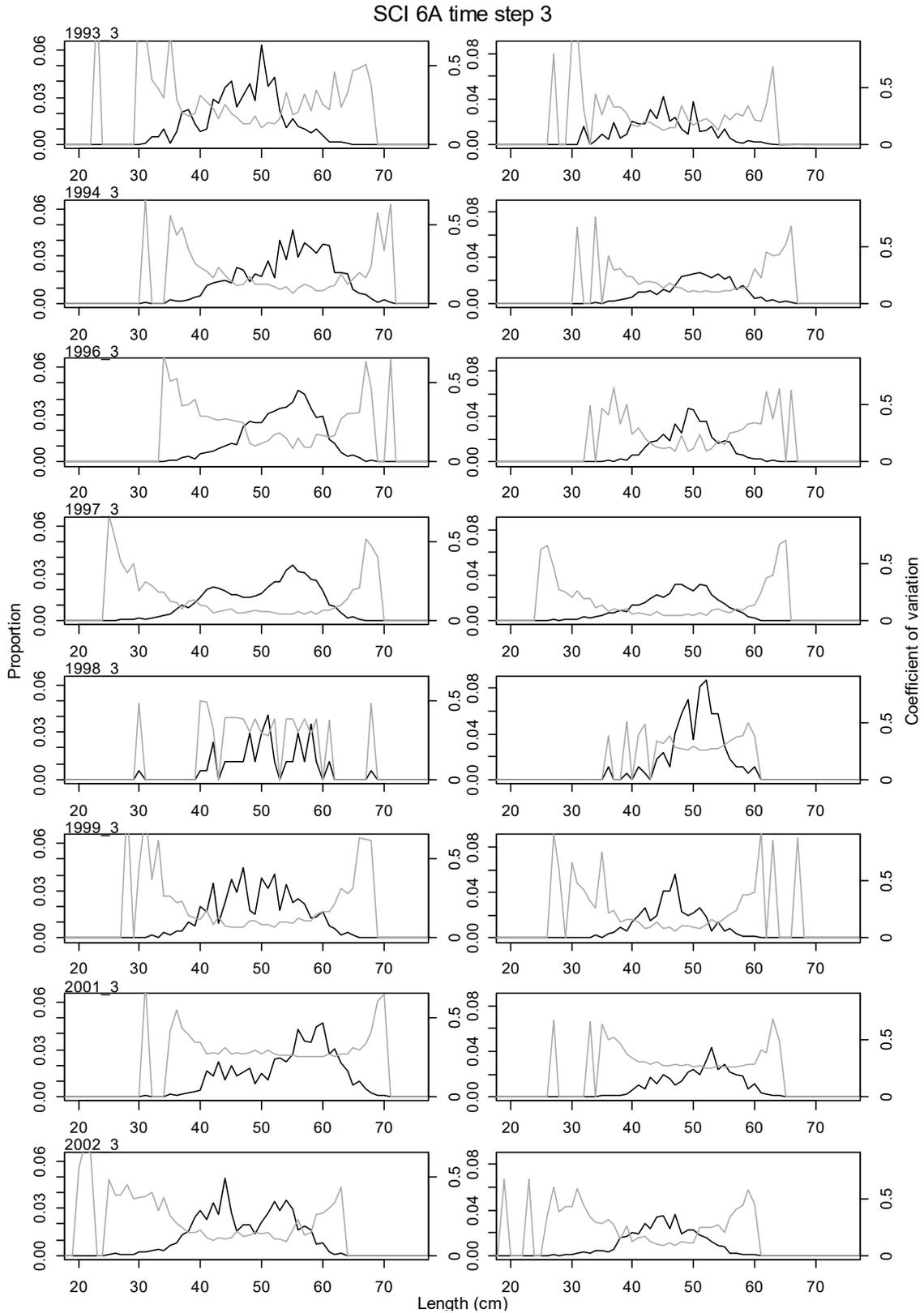
Figure 35: Proportional length frequencies (black line) and CVs (grey line) for commercial catches by model year and time step 3 for SCI 6A. Males plotted on left, females on right.
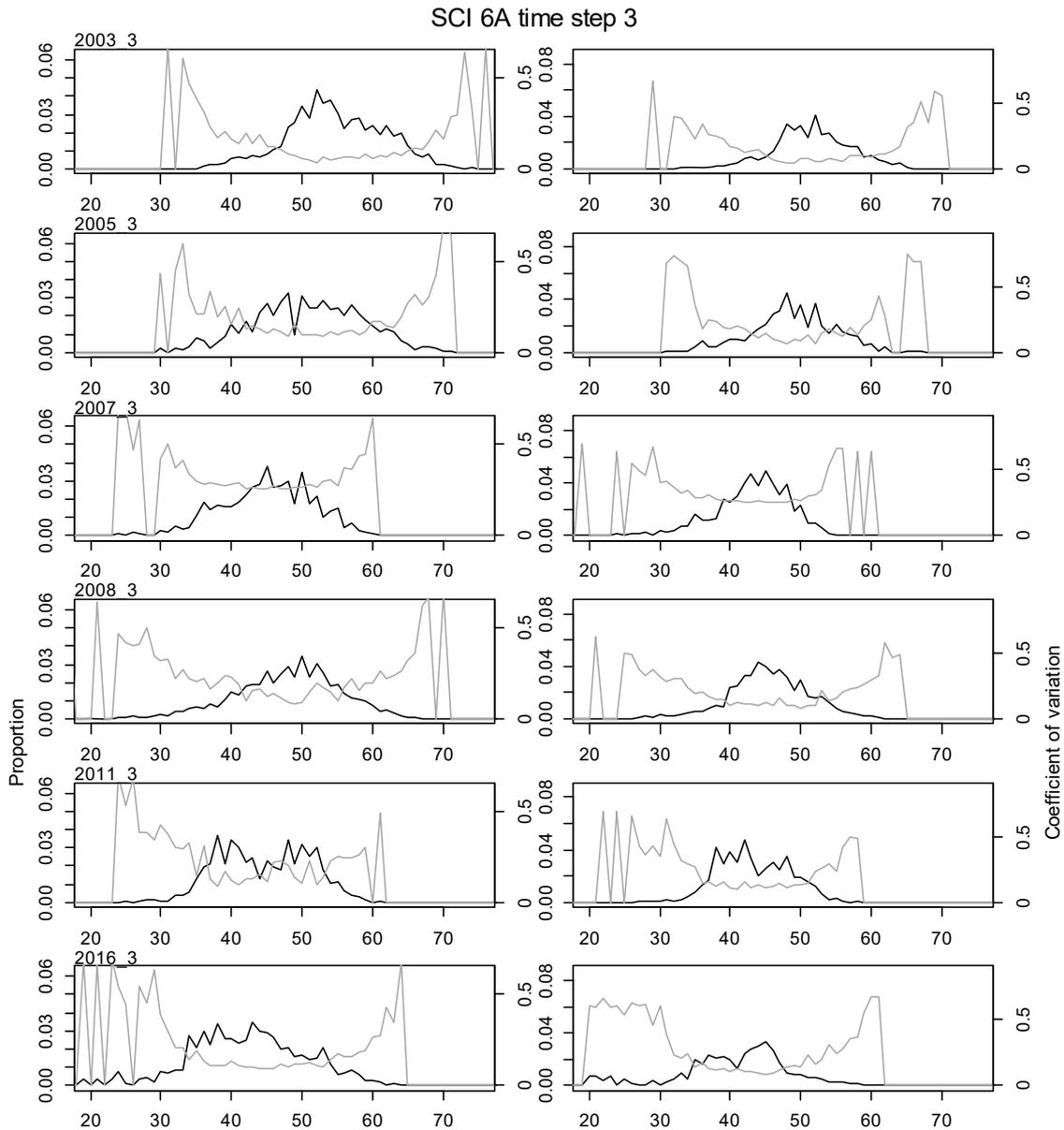
Figure 36: Proportional length frequencies (black line) and CVs (grey line) for commercial catches by model year and time step 3 (continued) for SCI 6A. Males plotted on left, females on right.

3.6.2 Trawl survey length distributions

Length frequency samples from research trawling have been taken by scientific staff on all surveys (Table 9). Estimated length frequency distributions (with associated CVs) were derived using NIWA's CALA software (Francis et al. 2016), using 1 mm OCL (Orbital Carapace Length) length classes by sex, and are presented in Figure 37.

In preliminary model runs, separate selectivity curves were estimated for commercial fishing in the three time steps, and the trawl survey (which occurred in time step 1 only). This led to L_{50} estimates that were considered to vary unrealistically between time steps and so, at the suggestion of the SFAWG, the length frequency of survey (from a commercial vessel) and commercial fishing catches were compared (Figure 38). These were considered to be similar enough to share selectivity parameters between the trawl survey and observer time step 1 data, which helped to provide more consistent L_{50} estimates.
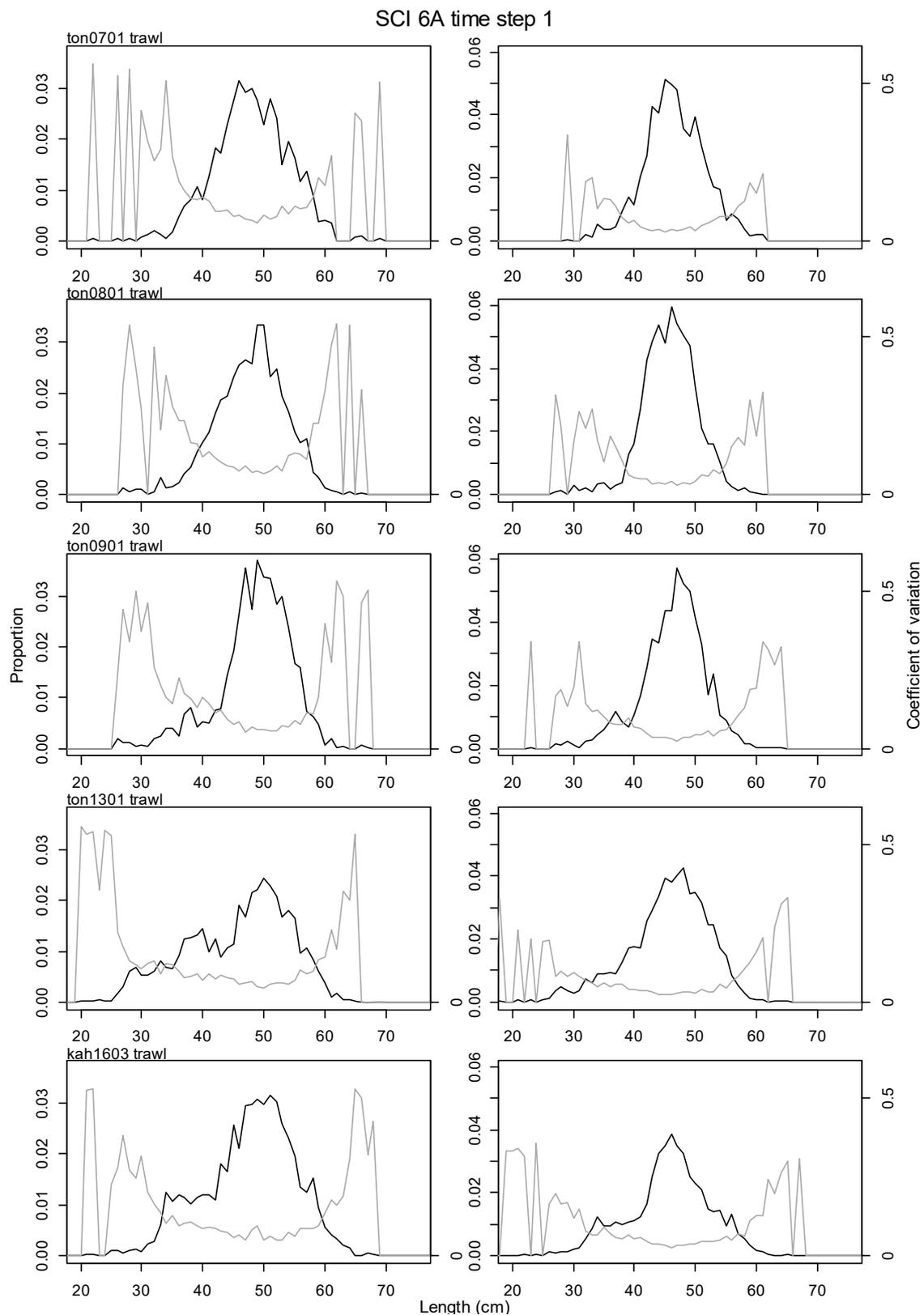
Figure 37: Proportional length frequencies (black line) and CVs (grey line) for research survey catches by model year for SCI 6A. Males plotted on left, females on right.
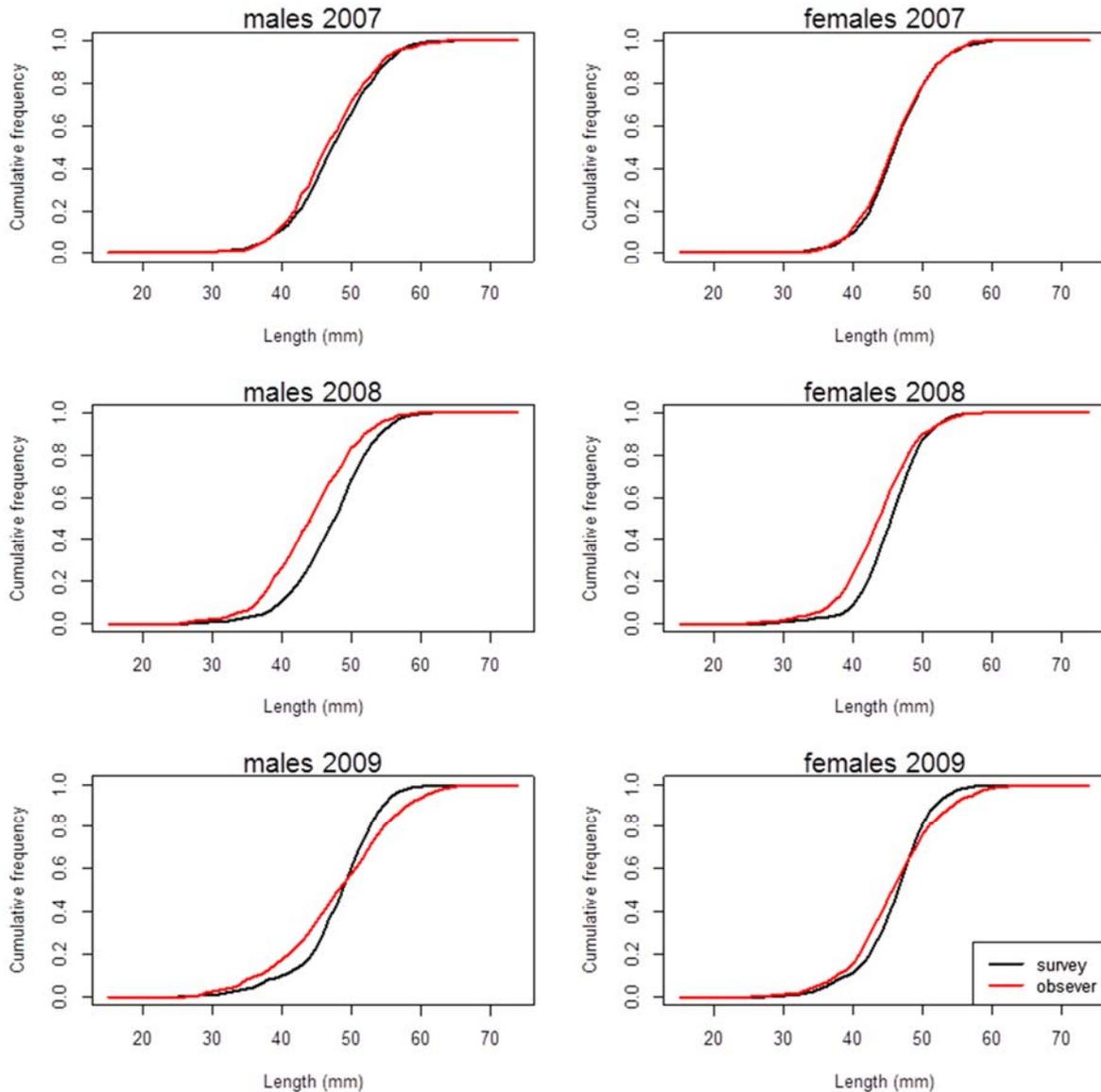
Figure 38: Cumulative frequency distributions for survey and commercial (observer) samples by sex for time step 1. No observer data were available for time step 1 in 2013.

3.6.3 Photo survey length distributions

Length frequency distributions were estimated for the relative photographic abundance series, by measuring the abdomen width of those visible animals, and converting abdomen width to orbital carapace length. Abdomen width is a measure considered to be less affected by foreshortening, when scampi are not orientated perpendicular to the plane of the camera, which is typically the case when they are viewed from above.

As with other scampi (Tuck et al. 2000), the relationship between abdomen width and carapace length changes for *Metanephrops* females at maturity, with a wider abdomen providing more space to carry eggs on the pleopods (Figure 39).
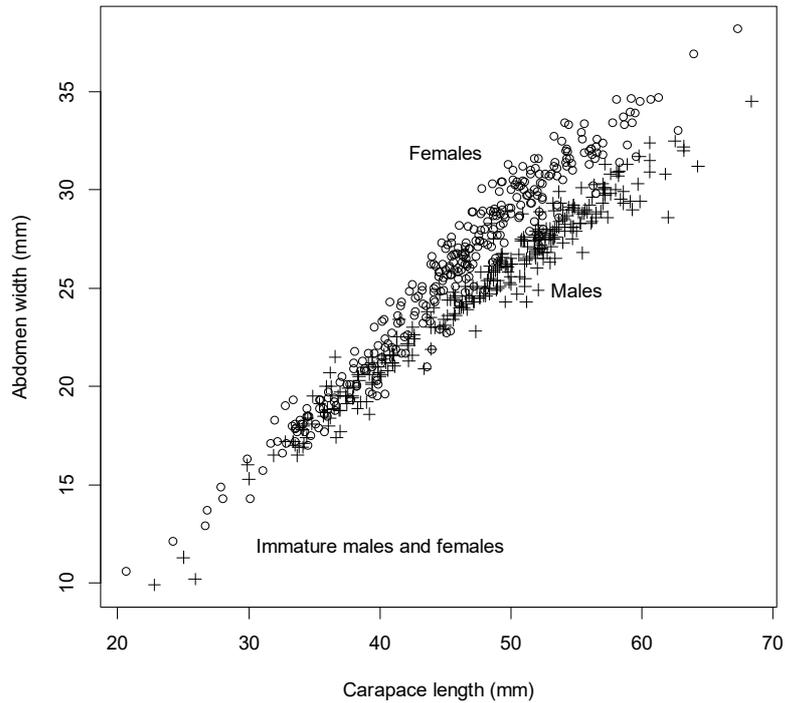
Figure 39: Relationship between abdomen width and carapace length for scampi in SCI 6A.

It is not possible to confidently determine scampi sex from the survey photographs, but the pattern in sex ratio in relation to length appears quite consistent between surveys (Figure 40). Using the data from the trawl surveys on the proportion by sex at length, and the relationship between carapace length and abdomen width for males (and immature females), maturing females, and mature females (Figure 41), the proportion of males by abdomen width increment can be estimated (Figure 42).
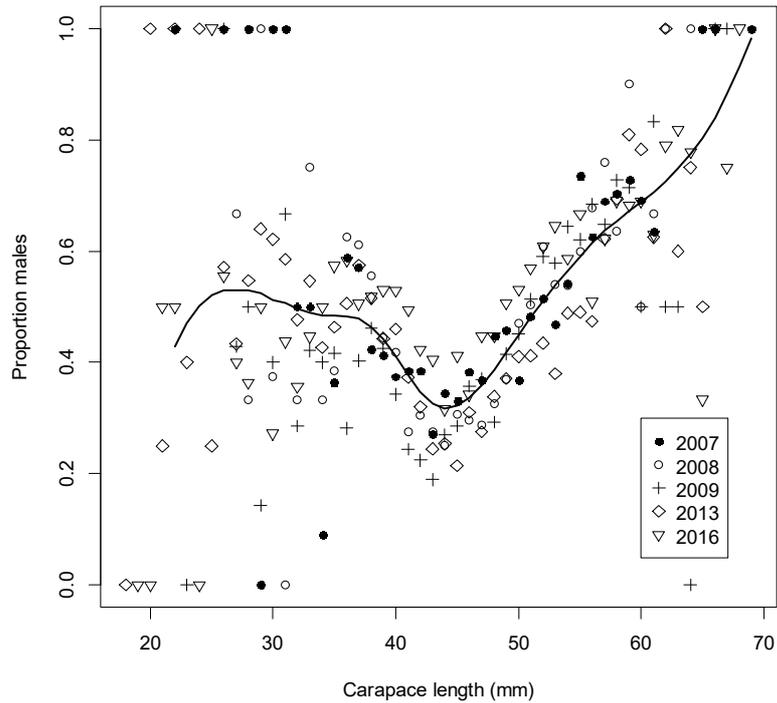
Figure 40: Plot of proportion of males in trawl survey catches against carapace length for each of the SCI 6A surveys, with an overall (lowess) smoother fitted through the data.
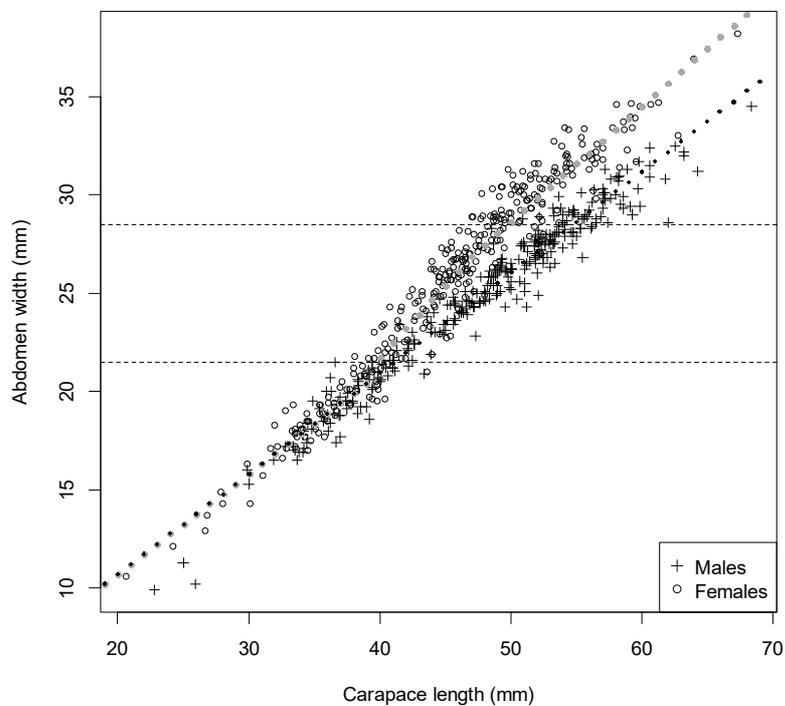
Figure 41: Relationship between abdomen width and carapace length for scampi in SCI 6A, with regression fits shown for different population components. Solid black symbols represent male regression. Solid grey symbols represent female regressions, with horizontal dashed lines representing transition range between immature and mature regressions.
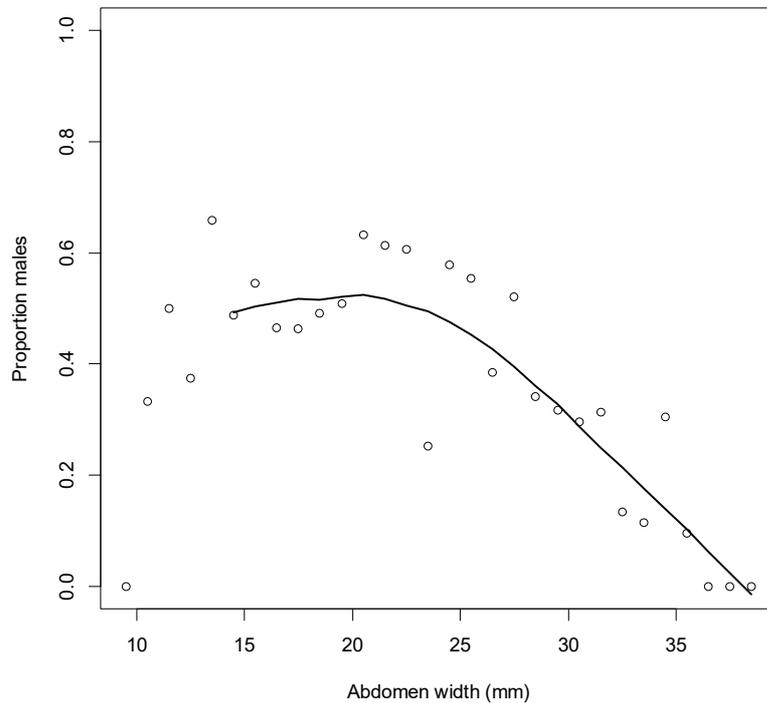
Figure 42: Overall plot of proportion of males in trawl survey catches against abdomen width for SCI 6A surveys, with an overall (lowess) smoother fitted through the data.

Each abdomen width measurement from each photographic survey was assigned a sex (on the basis of the probability observed in the trawl survey data shown in Figure 42), and then converted to a carapace length using the sex and abdomen width appropriate, abdomen width ~ carapace length relationship (Figure 41). To estimate the CVs at length for each year, we used a bootstrapping procedure, resampling with replacement from the original observations. Compared with the length frequency distributions from trawl catches, this procedure gave very large CVs, but we think this is realistic given the uncertainties involved in generating a length frequency distribution from photographs, and converting from abdomen width to carapace length. Estimates of the length frequency distributions (with associated CVs) for visible scampi are presented in Figure 43.
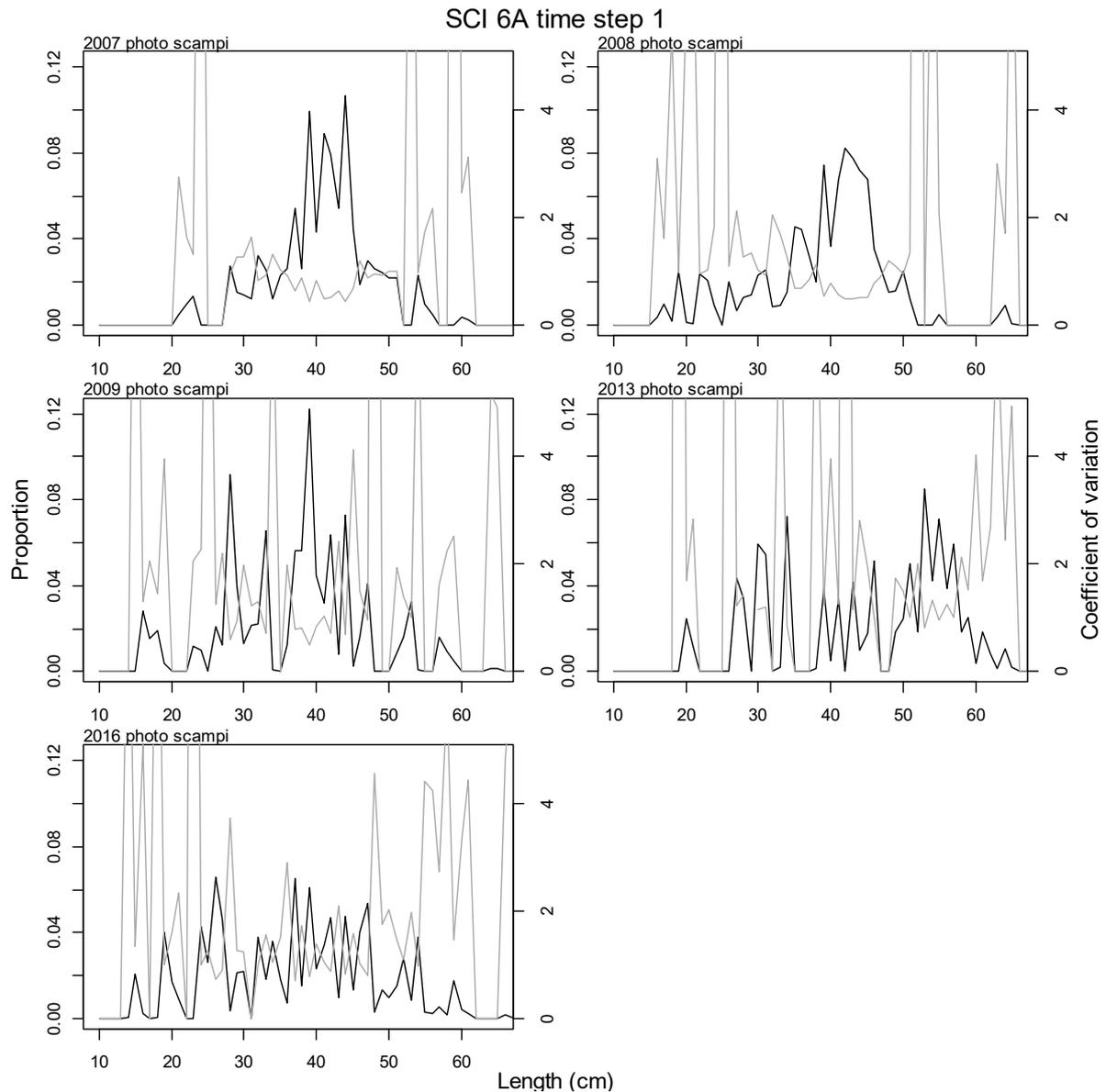
Figure 43: Proportional length frequency distributions (black line) and CVs (grey line) for photo survey observations of visible scampi by model year for SCI 6A.

3.7 Model assumptions and priors

Maximum Posterior Density (MPD) fits were found within CASAL using a quasi-Newton optimiser and the BETADIFF automatic differentiation package (Bull et al. 2008). Fitting was done inside the model except for the weighting of the abundance and length frequency data. For the length frequency data, observation-error CVs were estimated using CALA, and then converted to equivalent observation-error multinomial Ns, which were used within the model. The appropriate multinomial Ns to account for both observation and process error were then calculated from the model residuals (method TA1.8), and these final Ns were used in all models (Francis 2011). This generally resulted in small Ns for the commercial length frequency data in particular, and therefore relatively low weighting within the model. For the CPUE indices, the approach proposed by Clark & Hare (2006), and recommended by Francis (2011) was applied, estimating the appropriate CV by fitting a smoother to the index. Process error for trawl and photo survey indices were estimated within preliminary runs of the model, and then on the basis of this, fixed at 0.25 and 0.2 respectively. CASAL was also used to

generate Monte-Carlo Markov Chains (MCMC) for the base models. MPD output was analysed using the extract and plot utilities in the CASAL library running under the general analytical package R.

The initial model was based on that described previously (Tuck 2014, Tuck 2015, Tuck & Dunn 2009, Tuck & Dunn 2012). The model inputs include catch data, abundance indices (CPUE, trawl and photo surveys) and associated length frequency distributions. The parameters estimated by the base model include SSB_0 and R_0, and time series of SSB and year class strength, selectivity parameters for commercial and research trawling, and the photo survey, and associated catchability coefficients. To reduce the number of fitted parameters, the catchability coefficients (qs) for commercial fishing, research trawling, and photographic surveys have previously been assumed to be "nuisance" rather than free parameters. At the request of the SFAWG, models were also run with the qs as free parameters. The only informative priors used in the initial model were for *q-Photo*, *q-Trawl*, and the YCS vector (which constrains the variability of recruitment).

3.7.1 Scampi catchability

Previous priors for scampi catchability have been largely based on information on *Nephrops* emergence and occupancy rates from European studies conducted in far shallower waters than *Metanephrops* populations inhabit (Tuck & Dunn 2012), but the acoustic tagging study conducted at the Mernoo Bank in October 2010 offered an opportunity to estimate priors for occupancy and emergence from New Zealand data (Tuck 2013). Acoustic tagging was repeated successfully within the SCI 1 and SCI 2 surveys in 2012 (Tuck et al. 2015b), and was also conducted within the SCI 6A survey in 2013 (although less successfully). The data collected within these studies have been used to estimate catchability priors (Tuck et al. 2015a).

Acoustic tags were fitted to scampi which were released with a moored hydrophone, which recorded tag detections, and hence when animals were emerged from burrows. Data were recorded over a period of up to 21 days (Tuck et al. 2015a). Some tag detections showed distinct cyclical patterns (12.6 hour cycle), but most animals showed no clear patterns, and the proportion of scampi detectable over the duration of the studies varied from 40 to 86% (2.5th to 97.5th percentile of range), with a median detection of 66%. On the basis of shallow water trials with the acoustic tags, and scampi observations, it is assumed that these detections include scampi in burrow entrances (door keeping) and scampi walking free on the seabed (emerged) (all of which would be visible to the photographic survey).

Emergence and photographic survey data were combined to estimate catchability for major burrow opening counts, visible animal counts, and trawl catches. Using the overall proportion detectable (over the duration of the mooring deployment) as an estimate of the proportion of scampi that would be visible in photographs (emerged or door keeping) at a particular time of day, the density of visible scampi in each survey can be scaled to a population density estimate. Overall proportion detectable also provides a catchability for estimates of visible scampi. The population density estimate was used in conjunction with photographic survey estimates of scampi burrows, and emerged scampi, to provide estimates of burrow count and trawl survey catchability, respectively. Uncertainty in each component was accounted for through resampling from the original distributions (1000 iterations), and the mean and upper and lower bound (2.5th and 97.5th quantiles) of the estimated catchability distributions were fitted within a binomial GLM (probit link) to estimate the slope and intercept of the cumulative frequency distribution, which in turn were used to estimate the mean and standard deviation of the lognormal distribution of the priors for the various catchability terms used in the assessment model (Table 12).

3.7.2 Priors for *q*s

q-Photo
This is the proportion of the scampi population represented by the count of major burrow openings. The best estimate is 2.561 (major burrow openings divided by estimated scampi density). Upper and lower estimates are taken as the 2.5th and 97.5th percentiles of the distribution.

q-Trawl
This is the proportion of the scampi population represented by the trawl survey catches. The best estimate is 0.367 (scampi out of burrows divided by estimated scampi density). Upper and lower estimates are taken as the 2.5th and 97.5th percentiles of the distribution.

q-Scampi
This is the proportion of the scampi population represented by the count of visible scampi. The best estimate is 0.667 (visible scampi divided by estimated scampi density). Upper and lower estimates are taken as the 2.5th and 97.5th percentiles of the distribution.

3.7.3 Estimation of prior distributions

The bounds and best estimate were assumed to represent the 2.5th, 50th and 97.5th percentiles of the prior distribution. These values were fitted within a binomial GLM (probit link) to estimate the slope and intercept of the cumulative frequency distribution, which in turn were used to estimate the mean and standard deviation of the lognormal distribution of the prior. The distributions of the priors are presented in Figure 44. The distributions of the priors are somewhat different to those used in the SCI 1 assessment (Tuck 2014), reflecting the lower proportion of the SCI 6A scampi population that appear to be associated with burrows than in other areas (Tuck et al. 2015a).

Table 12: Component factors for estimation of priors for q-Scampi, q-Photo, and q-Trawl.

		SCI 6A		Source
	lower	best	upper	
Major opening	$0.0216\ m^{-2}$	$0.0258\ m^{-2}$	$0.0299\ m^{-2}$	Survey
Visible scampi (Emerged + door keeping)	$0.0048\ m^{-2}$	$0.0067\ m^{-2}$	$0.0086\ m^{-2}$	Survey
Emerged scampi	$0.0024\ m^{-2}$	$0.0037\ m^{-2}$	$0.0052\ m^{-2}$	Survey
Scampi as % of openings		26%		Visible/openings
% of scampi emerged		56%		Out/visible
Emergence	47%	67%	87%	Acoustic tags
Estimated scampi density	0.010	0.010	0.009	Visible/emergence
Estimated occupancy	48%	39%	33%	Est. den./major
q_Trawl	0.228	0.367	0.538	Out/Est. den.
q_scampi	0.467	0.667	0.867	Vis/Est. den.
q_photo	1.574	2.561	3.690	Major/Est. den.
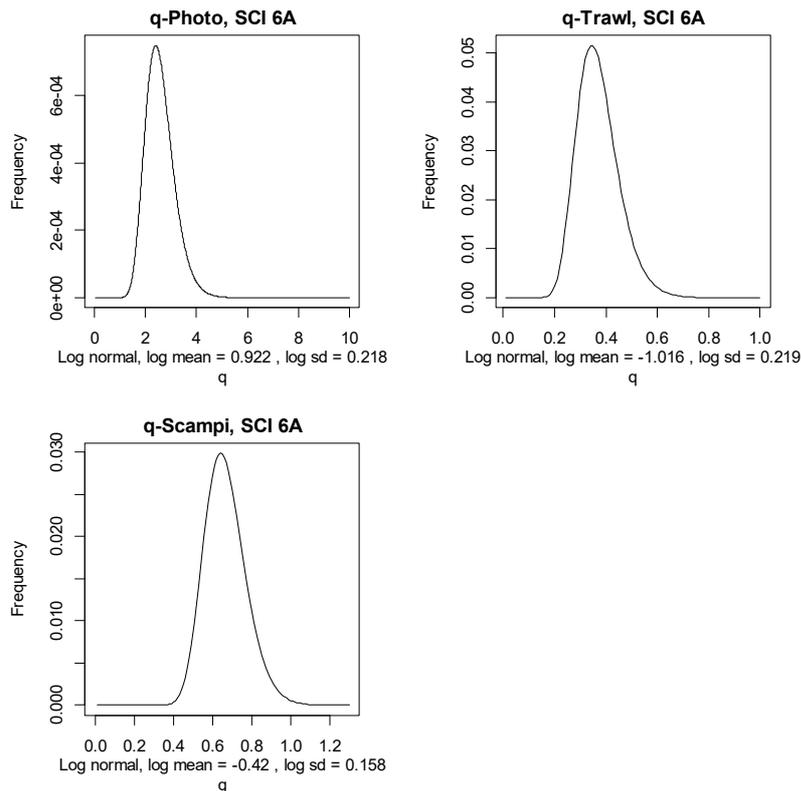
Figure 44: Estimated distribution of *q-Trawl*, *q-Scampi* and *q-Photo* for SCI 6A.

3.7.4   Recruitment

Few data are available on scampi recruitment. Relative year class strengths were fixed at 1 for the two most recent years, and were assumed to average 1.0 over all other years. In the initial model development (Cryer et al. 2005) lognormal priors on relative year class strengths were assumed, with mean 1.0 and CV of 0.2, and the sensitivity of year class strength (YCS) variation was examined in further developments (Tuck & Dunn 2006). More recent model investigations, particularly those fitting the CPUE indices, suggest that the constraint on variability in YCS may be too severe, and the SFAWG suggested increasing the CV (Tuck & Dunn 2012). In the initial implementation, lognormal priors on relative year class strengths were assumed, with mean 1.0 and CV of 1.0. The relationship between stock size and recruitment for scampi is unknown, and a Beverton Holt relationship with a steepness of 0.8 has been assumed. New Zealand scampi have very low fecundity (Fenaughty 1989, Wear 1976) (in the order of tens to hundreds of eggs carried by each female), so very successful recruitment is probably not plausible at low abundance. Recruitment enters the model partition as a year class, with a normally distributed OCL of mean 10 mm and CV of 0.4.

4.   ASSESSMENT MODEL RESULTS

4.1 Initial models

As described in Section 3.1, a single area model was applied, with an annual CPUE index, and photo and trawl survey indices. Preliminary model runs were largely based on the models successfully applied to assessments in SCI 1, 2 and 3 (Tuck 2016a, Tuck 2016b), but a number of issues/concerns were identified:

1. The model initially estimated commercial selectivity to vary considerably for L_{50} between time steps. This was not considered to be realistic. The length composition from the surveys

(conducted from a commercial vessel, using commercial trawl gear with a research codend) were considered to be sufficiently similar to the observer data that selectivity parameters could be shared for time step 1 (see 3.6.2), and this greatly improved the consistency in the estimation of L_{50}.

2. The preliminary model consistently estimated a very large year class, either at the start or end of the series. The first models examined started in 1986 (by default) although the fishery and CPUE data started in 1991. An early rapid decline in the CPUE, followed by a more stable period, despite quite consistent landings, was interpreted by the model as fishing down a very large year class from the late 1980s. Starting the model in 1991 removed this early year class issue, but then estimated a very large year class in the final estimated year of the model.

3. The data (CPUE and photo survey) provide some evidence of an increase in abundance at the end of the series (supporting above average recruitment), but not to the extreme extent (YCS greater than 5) estimated by the model. Successively excluding data from the later years, or fixing YCS in later years, consistently estimated an extreme year class strength in the final year available, suggesting that the issue was related to model structure rather than data.

Having identified that the extreme YCS values were related to model structure, the parameterisation of recruitment within the model was examined. The preliminary model, and those applied to other scampi stocks, used the Haist parameterisation of YCS (Bull et al. 2012) where

$$YCS_i = \frac{y_i}{\bar{y}}$$

with a lognormal prior on y_i with mean of 1 and CV of 1, and a small penalty to ensure that the mean of YCS does not drift away from 1 ("a YCS average to 1 penalty"). Sensitivity trials with the Haist parameterisation showed that both individually removing the penalty, and tightening the CV on the YCS prior, reduced the final YCS estimated by the model, but only removing the penalty and tightening the CV (to 0.7) generated a final YCS estimate of similar magnitude to previous good years.

On the basis of these investigations, the sensitivity to the CV on the YCS prior was investigated for models with the Haist parameterisation but no YCS average to 1 penalty, and also without the Haist parameterisation but with a YCS average to 1 penalty. For the Haist parameterisation model, the YCS in the final year was sensitive to the CV on the YCS prior, but estimates of SSB_0 and stock trajectory were relatively insensitive (Figure 45, upper row). In contrast, without the Haist parameterisation the SSB_0 and stock trajectory estimates were also sensitive to the CV on the YCS prior (Figure 45, lower row).

The SFAWG therefore agreed to proceed with a model structure implementing the Haist parameterisation, without the YCS average to 1 penalty, and with tighter CVs on the YCS prior. Preliminary examination of the implications of this parameterisation change to previously accepted stock assessment models for SCI 1 (Figure 46) and SCI 2 (Figure 47) did not suggest that perceptions of stock status would be altered, although this will be further examined as these assessments are updated.
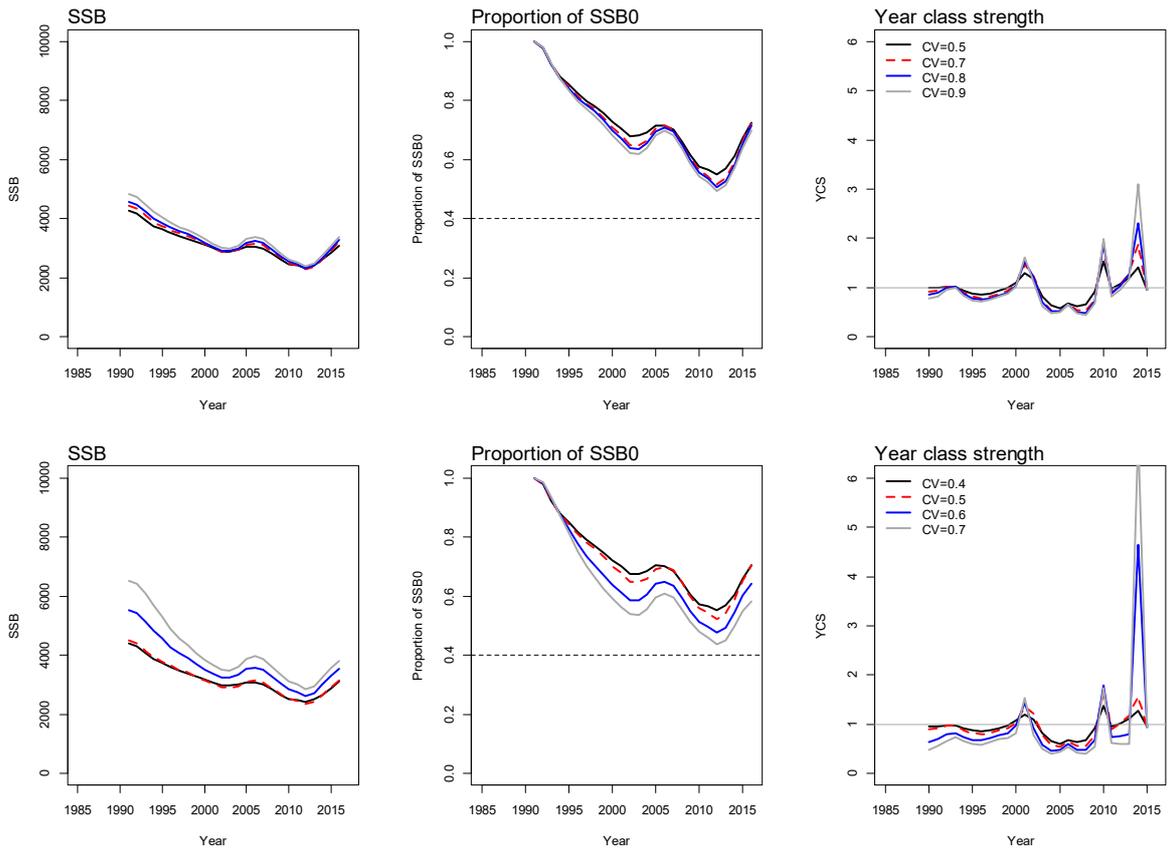
Figure 45: Model runs examining sensitivities to YCS parameterisation, showing SSB, SSB as a proportion of SSB$_0$ and YCS for a range of YCS prior CVs, for model with Haist parameterisation with no YCS average to 1 penalty (upper row), and model without Haist parameterisation with a large YCS average to 1 penalty (lower row).
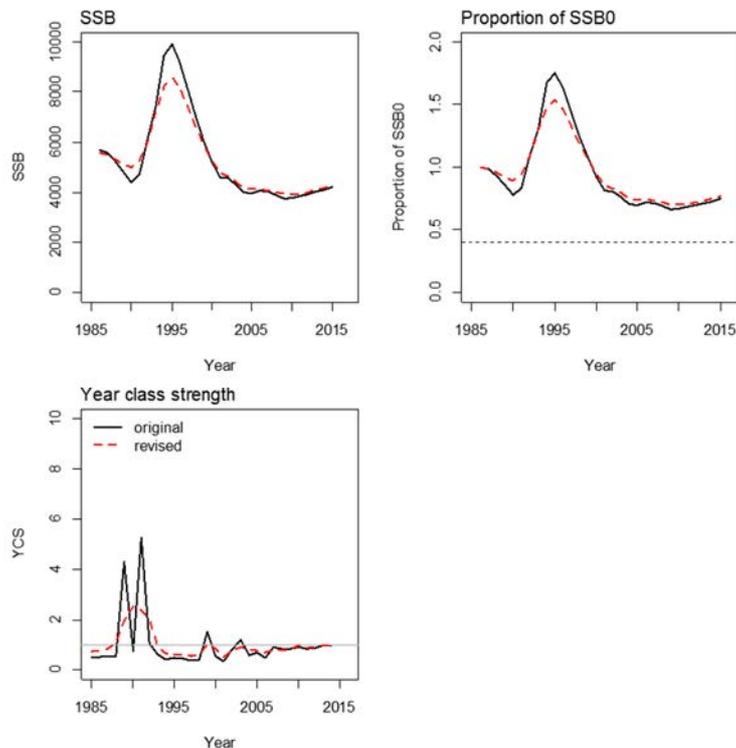
Figure 46: Sensitivity of accepted SCI 1 assessment model (Tuck 2016a) to revised recruitment parameterisation (no YCS average to 1 penalty, CV on YCS prior = 0.7).
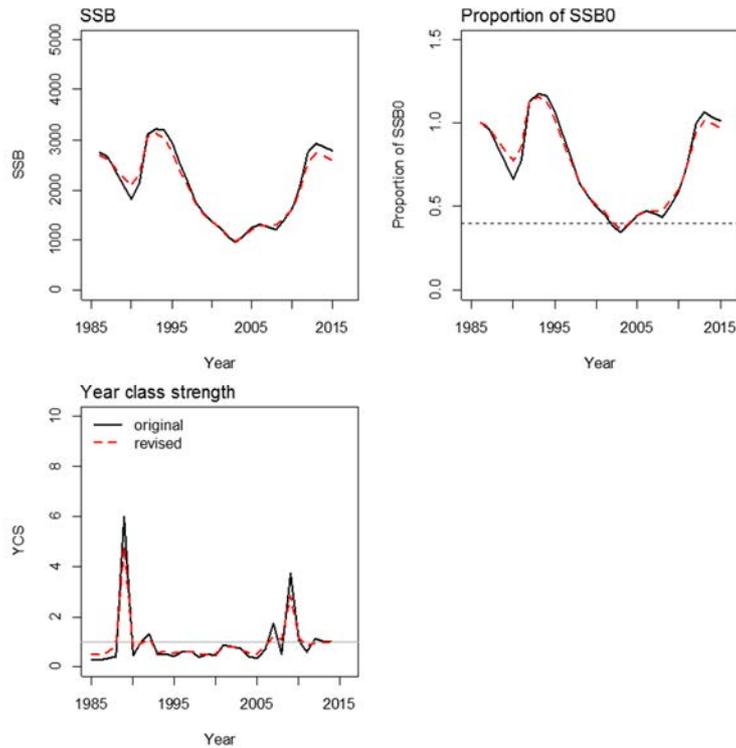
Figure 47: Sensitivity of accepted SCI 2 assessment model (Tuck 2016a) to revised recruitment parameterisation (no YCS average to 1 penalty, CV on YCS prior = 0.7).

4.2 Base models

Given the sensitivity of the estimation of YCS in the final year to the CV of the YCS prior, and the potential implications of this for projections, the SFAWG requested the base models to include sensitivity runs to both the CV on the YCS prior and M. Details of differences between models examined within the analyses are presented in Table 13. Key parameter and quantity estimates from the MPD fits for the models described in Table 14, and stock and recruitment trajectories are presented in Figure 48. Models were developed with catchabilities as nuisance and free parameters, although MPD outputs were very similar for the two versions of the same model, and so the free parameter models are only discussed in relation to MCMCs. Various model output plots and diagnostics are presented in Appendices 4 to 7 for each of the models.

Table 13: General details of models examined within sensitivity analyses for SCI 6A.

Model	M	CV of YCS prior
1	0.2	0.4
2	0.2	0.7
3	0.25	0.4
4	0.25	0.7

There was little difference between models in terms of the fits to observed data. All the models showed a steady decline in biomass until the early 2000s, followed by a slight increase, a further decline, and an increase (to levels comparable with the mid 2000s) in the most recent years (Figure 48). SSB_0 was

estimated to be slightly higher with a lower M (Table 14), and YCS showed a greater range with a larger CV on the YCS prior, but overall patterns in SSB trajectory and YCS were very similar.

Table 14: Estimated key parameters and quantities from MPD fits for SCI 6A sensitivity model runs.

		Model 1	Model 2	Model 3	Model 4
M		0.2	0.2	0.25	0.25
CV on YCS prior		0.4	0.7	0.4	0.7
CPUE-Commercialq		0.0005	0.0005	0.0005	0.0005
TrawlSurveyq		0.5214	0.5093	0.5157	0.4960
PhotoSurvey_animals_q		0.7303	0.7231	0.7236	0.7150
initialization.SSB_0		4508.83	4715.35	4172.85	4440.55
SSB_{2016}		3022.19	3141.37	2957.65	3157.9
SSB_{2016}/ SSB_0		67%	67%	71%	71%
maturity_props.all	a50	36.69	36.69	36.69	36.69
	a to 95	7.16	7.15	7.15	7.15
selectivity.shift_a		0.0119	0.0090	0.0181	0.0160
selectivity[Fishing_1]	a50	43.46	43.01	43.53	43.10
	a to 95	11.89	11.78	11.93	11.76
	amax M	0.82	0.80	0.88	0.84
selectivity[Fishing_2]	a50	41.57	40.77	41.21	40.41
	a to 95	9.98	8.87	9.75	8.71
	amax M	1.10	1.07	1.16	1.11
selectivity[Fishing_3]	a50	42.00	42.00	42.00	42.00
	a to 95	11.36	11.51	11.34	11.46
	amax M	1.56	1.52	1.68	1.61
selectivity[Scampi_out]	a1	41.94	42.09	42.04	42.40
	aL	23.00	23.12	30.00	25.39
	aR	23.79	22.95	29.16	24.01
growth[1].g_male	g20	9.12	9.52	10.39	10.71
	g45	1.34	1.40	1.60	1.63
growth[1].g_female	g20	10.75	10.81	12.69	12.63
	g45	0.00	0.00	0.00	0.00
growth[1].minsigma_male		4.06	4.08	4.54	4.56
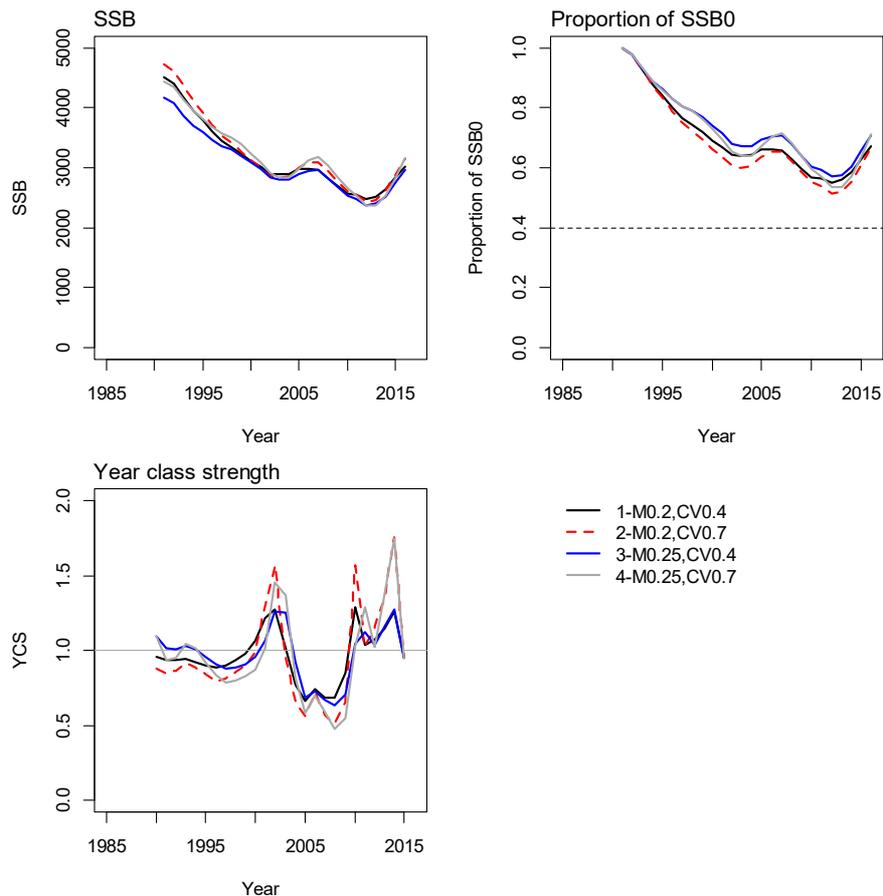
Figure 48: Plots of SSB, SSB as a proportion of SSB₀, and year class strength (YCS) for MPD fits to the SCI 6A sensitivity model runs.

4.2.1 Model 1: M fixed at 0.20, CV on YCS prior 0.4

The outputs and diagnostics for Model 1 (M = 0.20, CV on YCS prior = 0.4) are presented in Appendix 4. The estimated SSB_0 was 4508 t, with SSB_{2016} 3022 t, 67% of SSB_0. Fits to the abundance indices and normalised residuals (A4. 1), show that the model fitted the general trend in CPUE since the mid 1990s reasonably well, and matched the increase in abundance observed in the photographic survey, but simply estimated a steady decline for the trawl survey (2009–2013), and did not match the observed pattern as well. The SSB is estimated to have declined to about 2002, increased to 2007, declined further to about 2013, and then increased (A4. 2). Year class strengths were estimated to be above average between 2000 and 2003, below average from 2004 to 2009, and above average after this. Estimated selectivity curves (A4. 3) matched observed changes in sex ratio between time steps, with males less available to trawling during time step 1, and more available in time step 3. MPD estimates of trawl and photo survey catchability were within the prior distribution (A4. 4), and the residuals from the fits to growth increments did not suggest any trend (A4. 5). Individual fits to the observer length frequency distributions were variable (A4. 6 – A4. 8), with the data weighting giving observer length frequency samples low effective sample size (A4. 9 – A4. 11). There is some evidence of a pattern in the residuals from the fits to the length frequency distributions (A4. 13 – A4. 18), which may suggest a reduced availability at around 40 – 45 mm CL, rather than the logistic selectivity applied in the model, but the magnitude of the pattern is small (less than half a standard deviation). Fits to the trawl survey length frequency distributions were generally better (A4. 19), and effective sample size larger (A4. 21), but the fits showed a similar pattern in the residuals (A4. 24). Sample sizes for photo survey length

frequency distributions were low, with high CVs, but the model estimated the average shape of the length distribution reasonably well (A4. 27)

The likelihood profile when B_0 is fixed shows a minimum at around 4500 t (A4. 28), with the overall profile being quite U shaped. The priors are quite influential on the likelihood (particularly in avoiding lower SSB_0 values), while different data sets within the abundance indices and proportions at length give higher or lower SSB_0 values.

MCMC runs

Three independent MCMC chains were started a random step away from the MPD for the model, and run for 3 million simulations, with every two thousandth sample saved, giving a set of 1500 samples, from which the first 500 were excluded as a burn in. Preliminary examination of the MCMC chains from the models with qs as free parameters suggested that the individual chains had not converged (A4. 29). New chains were started using a covariance matrix recalculated from these initial chains (rather than the covariance matrix from the MPD), but no improvement in convergence diagnostics was noted. It is possible that the process of recalculating the covariance matrix may need to be repeated a number of times to provide satisfactory MCMC chains from a model with qs as free parameters. This will be investigated further in future assessments, but the SFAWG agreed that consideration of the model q with as nuisance parameters was appropriate.

The three chains from the model where qs were estimated as nuisance parameters were examined for evidence of lack of convergence (A4. 30), and concatenated and systematically thinned to produce a 3000 sample chain for projections. The three chains were very consistent (A4. 30), as were the distributions for SSB_0, SSB_{2016} and SSB_{2016}/SSB_0 providing no evidence of lack of convergence (A4. 31). Posterior distributions of trawl and photo survey catchability were within the prior distribution (A4. 32), with the MPD estimates also located within the posterior distributions. The posterior trajectory of SSB (Figure 49) suggests a decline from about 1991 to 2002, a more stable period to 2007, a further decline to 2012, and an increase after 2013. The median estimate of current status (SSB_{2016}/SSB_0) is 68% (95% CI 57.1% – 78.9%), with 0% probability that SSB_{2016} is below 40% SSB_0. The model estimates a consistent series of at or above average YCSs since 2010, with the final estimated year (2014) at a level comparable with the previous peak year (2002).
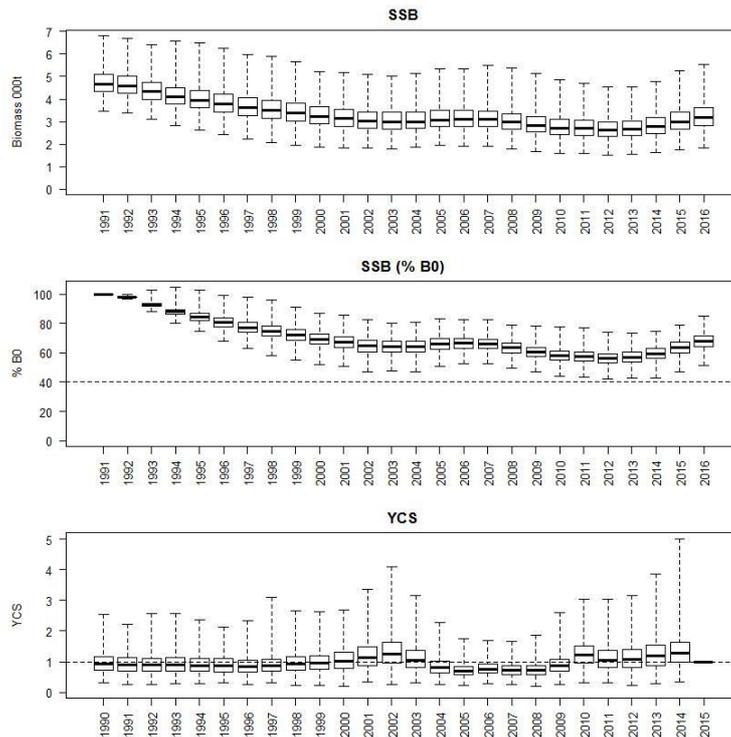
Figure 49: Posterior trajectory of SSB, SSB_{2016}/SSB_0 and YCS for Model 1.

4.2.2   Model 2: M fixed at 0.20, CV on YCS prior 0.7

The outputs and diagnostics for Model 2 (M = 0.20, CV on YCS prior = 0.7) are presented in Appendix 5. The estimated SSB_0 was 4715 t, with SSB_{2016} 3141 t, 67% of SSB_0. Fits to the abundance indices and normalised residuals (A5. 1), show that as with Model 1, the model fitted the general trend in CPUE since the mid 1990s reasonably well, and matched the increase in abundance observed in the photographic survey, but simply estimated a steady decline for the trawl survey (2009–2013), and did not match the observed pattern as well. SSB is estimated to have declined to about 2002, increased to 2007, declined further to about 2013, and then increased (A5. 2). Year class strengths were estimated to be above average between 2000 and 2002, below average from 2004 to 2009, and above average after this, and in general, followed a very similar pattern to Model 1, but over a greater range. Estimated selectivity curves (A5. 3) matched observed changes in sex ratio between time steps, with males less available to trawling during time step 1, and more available in time step 3. MPD estimates of trawl and photo survey catchability were within the prior distribution (A5. 4), and the residuals from the fits to growth increments were very similar to Model 1 and did not suggest any trend (A5. 5). Individual fits to the observer length frequency distributions were variable (A5. 6 – A5. 8), with the data weighting giving observer length frequency samples low effective sample size (A5. 9 – A5. 11). As with Model 1, there is some evidence of a pattern in the residuals from the fits to the length frequency distributions (A5. 13 – A5. 18), although the magnitude of the pattern is small (less than half a standard deviation). Fits to the trawl survey length frequency distributions were generally better (A5. 19), and effective sample size larger (A5. 21), but also showed a similar pattern in the residuals (A5. 24). Sample sizes for photo survey length frequency distributions were low, with high CVs, but the model estimated the average shape of the length distribution reasonably well (A5. 27).

The likelihood profile when B_0 is fixed shows a minimum just under 5000 t (A5. 28), with the overall profile being quite U shaped. The priors appear to be the most influential component on the likelihood (with the prior on trawl and photo survey catchability avoiding lower SSB_0 values, and the prior on YCS avoiding higher SSB_0 values), while the data sets were less influential.

MCMC runs

Three independent MCMC chains were started a random step away from the MPD for the model, and run for 3 million simulations, with every two thousandth sample saved, giving a set of 1500 samples, from which the first 500 were excluded as a burn in. As with Model 1, preliminary examination of the MCMC chains from the models with q as free parameters suggested that the individual chains had not converged, and use of a recalculated covariance matrix did not improve convergence diagnostics.

The three chains from the model q with as nuisance parameters were examined for evidence of lack of convergence (A5. 29), and concatenated and systematically thinned to produce a 3000 sample chain for projections. The three chains were very consistent (A5. 29), as were the distributions for SSB_0, SSB_{2016} and SSB_{2016}/SSB_0 providing no evidence of lack of convergence (A5. 30). Posterior distributions of trawl and photo survey catchability were within the prior distribution (A5. 31), with the MPD estimates also located within the posterior distributions. The posterior trajectory of SSB (Figure 50) is very similar to Model 1, and suggests a decline from about 1991 to 2002, a more stable period to 2007, a further decline to 2012, and an increase after 2013. The median estimate of current status (SSB_{2016}/SSB_0) is 67% (95% CI 54.9% – 79.9%), with 0% probability that SSB_{2016} is below 40% SSB_0. The model estimates a consistent series of at or above average YCSs since 2010, with the final estimated year (2014) higher than any previous years, and higher than the Model 1 estimate (1.70 compared to 1.27).
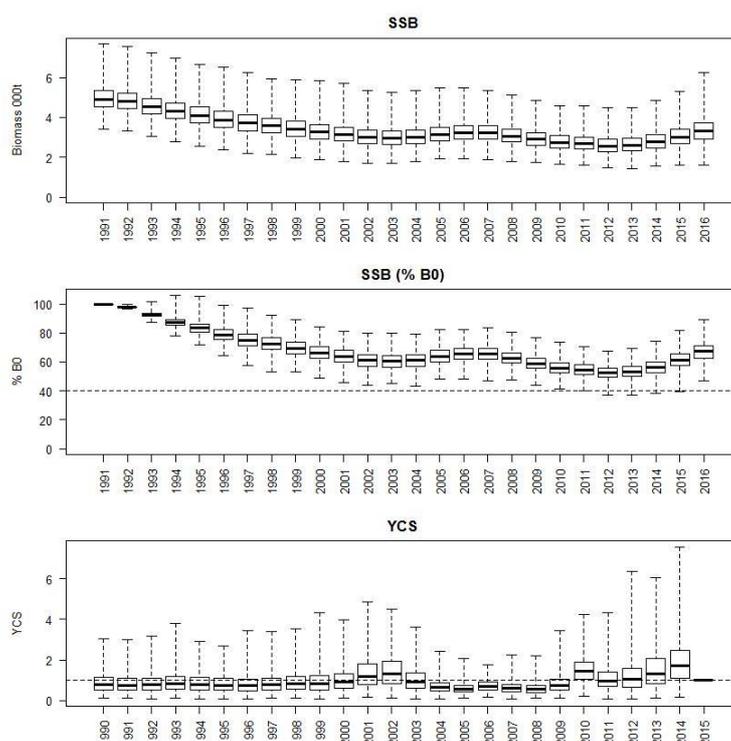
Figure 50: Posterior trajectory of SSB, SSB_{2016}/SSB_0 and YCS for Model 2.

4.2.3   Model 3: M fixed at 0.25, CV on YCS prior 0.4

The outputs and diagnostics for Model 3 (M = 0.25, CV on YCS prior = 0.4) are presented in Appendix 6. The estimated SSB_0 was 4173 t, with SSB_{2016} 2958 t, 71% of SSB_0. Fits to the abundance indices and normalised residuals (A6. 1) show that the model fitted the general trend in CPUE since the mid 1990s reasonably well, and matched the increase in abundance observed in the photographic survey, but as with the previously described models, simply estimated a steady decline for the trawl survey (2009–2013), and did not match the observed pattern as well. SSB is estimated to have declined to about 2002, increased to 2007, declined further to about 2013, and then increased (A6. 2). Year class strengths were

estimated to be above average between 2000 and 2002, below average from 2004 to 2009, and above average after this, and in general, following a very similar trend to Model 1. Estimated selectivity curves (A6. 3) matched observed changes in sex ratio between time steps, with males less available to trawling during time step 1, and more available in time step 3. MPD estimates of trawl and photo survey catchability were within the prior distribution (A6. 4), and the residuals from the fits to growth increments were very similar to Model 1 and did not suggest any trend (A6. 5). Individual fits to the observer length frequency distributions were variable (A6. 6 – A6. 8), with the data weighting giving observer length frequency samples low effective sample size (A6. 9 – A6. 11). As with the previously discussed models, there is some evidence of a pattern in the residuals from the fits to the length frequency distributions (A6. 13 – A6. 18), although the magnitude of the pattern is small (less than half a standard deviation). Fits to the trawl survey length frequency distributions were generally better (A6. 19), and effective sample size larger (A6. 21), but also showed a similar pattern in the residuals (A6. 24). Sample sizes for photo survey length frequency distributions were low, with high CVs, but the model estimated the average shape of the length distribution reasonably well (A6. 27).

The likelihood profile when B_0 is fixed shows a minimum just over 4000 t (A6. 28), with the overall profile being U shaped. The priors appear to be influential in avoiding lower SSB_0 values, while the CPUE index was influential in avoiding higher SSB_0 values. Individual data sets from the proportions at length data provided contrasting signals.

MCMC runs

Three independent MCMC chains were started a random step away from the MPD for the model, and run for 3 million simulations, with every two thousandth sample saved, giving a set of 1500 samples, from which the first 500 were excluded as a burn in. As with Model 1 and 2, preliminary examination of the MCMC chains from the models with q as free parameters suggested that the individual chains had not converged, and use of a recalculated covariance matrix did not improve convergence diagnostics.

The three chains from the model q with as nuisance parameters were examined for evidence of lack of convergence (A6. 29), and concatenated and systematically thinned to produce a 3000 sample chain for projections. The three chains were very consistent (A6. 29), as were the distributions for SSB_0, SSB_{2016} and SSB_{2016}/SSB_0 providing no evidence of lack of convergence (A6. 30). Posterior distributions of trawl and photo survey catchability were within the prior distribution (A6. 31), with the MPD estimates also located within the posterior distributions. The posterior trajectory of SSB (Figure 51) is very similar to Model 1, and suggests a decline from about 1991 to 2002, a more stable period to 2007, a further decline to 2012, and an increase after 2013. The median estimate of current status (SSB_{2016}/SSB_0) is 72% (95% CI 61.3% – 83.4%), with 0% probability that SSB_{2016} is below 40% SSB_0. The model estimates a consistent series of at or above average YCSs since 2010, with the final estimated year (2014) slightly higher than any previous years, and slightly higher than the Model 1 estimate (1.31 compared to 1.27).
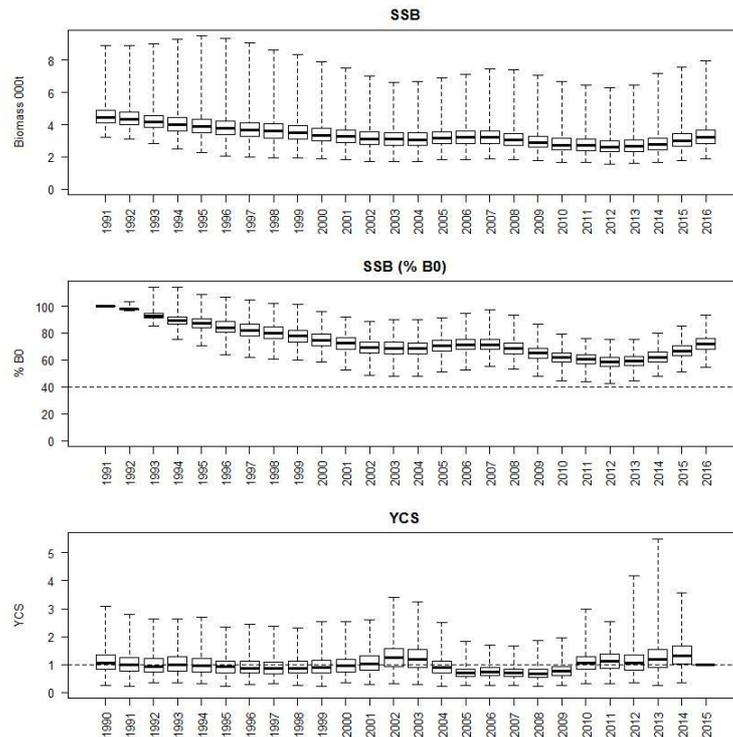
Figure 51: Posterior trajectory of SSB, SSB$_{2016}$/SSB$_0$ and YCS for Model 3.

4.2.4 Model 4: M fixed at 0.25, CV on YCS prior 0.7

The outputs and diagnostics for Model 4 (M = 0.25, CV on YCS prior = 0.7) are presented in Appendix 7. The estimated SSB$_0$ was 4441 t, with SSB$_{2016}$ 3157 t, 71% of SSB$_0$. Fits to the abundance indices and normalised residuals (A7. 1), show that as with all the models, the model fitted the general trend in CPUE since the mid 1990s reasonably well, and matched the increase in abundance observed in the photographic survey, but simply estimated a steady decline for the trawl survey (2009–2013), and did not match the observed pattern as well. SSB is estimated to have declined to about 2002, increased to 2007, declined further to about 2013, and then increased (A7. 2). Year class strengths were estimated to be above average between 2000 and 2002, below average from 2004 to 2009, and above average after this, and in general, followed a very similar pattern to the other models, and with a similar magnitude of variability as Model 2. Estimated selectivity curves (A7. 3) matched observed changes in sex ratio between time steps, with males less available to trawling during time step 1, and more available in time step 3. MPD estimates of trawl and photo survey catchability were within the prior distribution (A7. 4), and the residuals from the fits to growth increments were very similar to Model 1 and did not suggest any trend (A7. 5). Individual fits to the observer length frequency distributions were variable (A7. 6 – A7. 8), with the data weighting giving observer length frequency samples low effective sample size (A7. 9 – A7. 11). As with the other models, there is some evidence of a pattern in the residuals from the fits to the length frequency distributions (A7. 13 – A7. 18), although the magnitude of the pattern is small (less than half a standard deviation). Fits to the trawl survey length frequency distributions were generally better (A7. 19), and effective sample size larger (A7. 21), but also showed a similar pattern in the residuals (A7. 24). Sample sizes for photo survey length frequency distributions were low, with high CVs, but the model estimated the average shape of the length distribution reasonably well (A7. 27).

The likelihood profile when B$_0$ is fixed shows a minimum around 4500 t (A7. 28), with the overall profile being quite U shaped. The priors appear to be the most influential component on the likelihood

(with the prior on trawl and photo survey catchability avoiding lower SSB_0 values, and the prior on YCS avoiding higher SSB_0 values), while the data sets were less influential.

MCMC runs

Three independent MCMC chains were started a random step away from the MPD for the model, and run for 3 million simulations, with every two thousandth sample saved, giving a set of 1500 samples, from which the first 500 were excluded as a burn in. As with Model 1, preliminary examination of the MCMC chains from the models with q as free parameters suggested that the individual chains had not converged, and use of a recalculated covariance matrix did not improve convergence diagnostics.

The three chains from the model q with as nuisance parameters were examined for evidence of lack of convergence (A7. 29), and concatenated and systematically thinned to produce a 3000 sample chain for projections. The three chains were very consistent (A7. 29), as were the distributions for SSB_0, SSB_{2016} and SSB_{2016}/SSB_0 providing no evidence of lack of convergence (A7. 30). Posterior distributions of trawl and photo survey catchability were within the prior distribution (A7. 31), with the MPD estimates also located within the posterior distributions. The posterior trajectory of SSB (Figure 52) is very similar to the other models, and suggests a decline from about 1991 to 2002, a more stable period to 2007, a further decline to 2012, and an increase after 2013. The median estimate of current status (SSB_{2016}/SSB_0) is 72% (95% CI 58.5% – 86.4%), with 0% probability that SSB_{2016} is below 40% SSB_0. The model estimates a consistent series of at or above average YCSs since 2010, with the final estimated year (2014) higher than any previous years, and comparable with the Model 3 estimate.
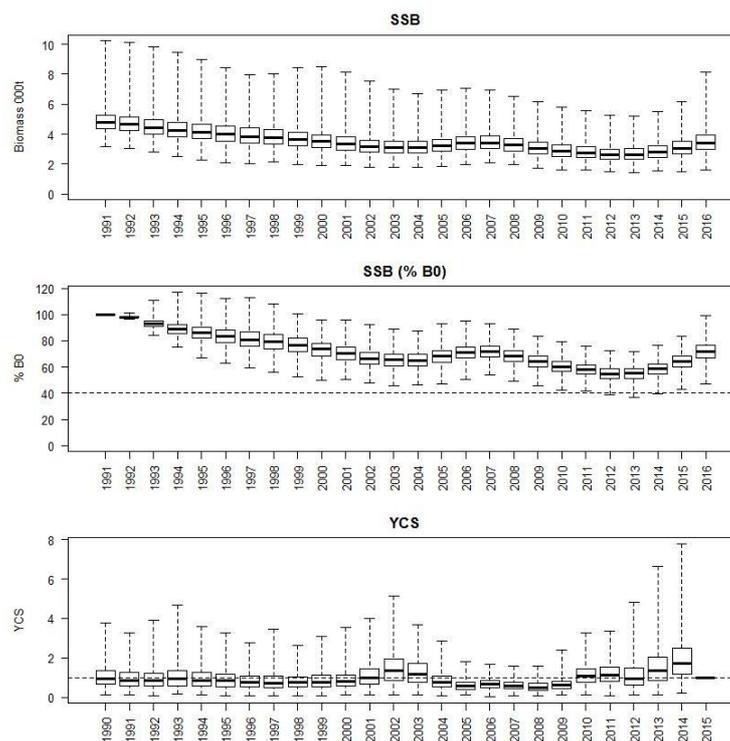
Figure 52: Posterior trajectory of SSB, SSB_{2016}/SSB_0 and YCS for Model 4.

4.3 Recent recruitment

The four models estimated very similar overall stock trajectories (SSB/SSB_0), with the only significant differences relating to the models with lower M, or higher CV on the YCS prior models producing higher estimates of SSB_0, and the models with higher CV on the YCS prior estimating greater variability in YCS (although with a very similar overall pattern), and a particularly high YCS_{2014}. These differences

have minimal effect on perceptions of stock status, but may have more important implications for projections.

Observer sampling of commercial catches has been quite patchy over the fishery (Table 10), complicating the comparison of length compositions. No data are available from time step 1 since 2011, but data from time steps 2 (Figure 34) and 3 (Figure 36) support the suggestion of increased catches of smaller scampi since 2014 (implying better than average YCS). There are insufficient data available to judge how recent YCSs compare with the previous peak YCS from 2002.

Length frequency compositions from the trawl survey series (Figure 37) also support the suggestion of a recent improvement in YCS (compared to 2007 – 2009). The proportion of smaller individuals in catches is considerably higher in 2013 than in previous years. The 2016 survey data were not included in the assessment model (SFAWG decision based on vessel change (see Section 3.5) and clear catchability differences), but given the mesh sizes used, scampi length selectivity is expected to be relatively consistent between the vessels, and the proportion of smaller individuals in catches is consistent with better YCSs than earlier years.

4.4 Grade composition data

There is little evidence of individual year class modes within the observer (Figure 31 to Figure 36) or trawl survey (Figure 37) length frequency data, and therefore recruitment patterns can only be inferred from patterns in the proportions of smaller scampi in catches. The catch composition data (particularly the observer data) has relatively little weight in the model. There is therefore a concern that the model has few data from which to estimate year class strengths, and is simply estimating strong year classes where they are required to match increases in CPUE.

While not currently used within the model, additional data are available, in the form of daily catch records by processor grade (Hartill & Tuck 2010, Tuck & Bian 2012). These data have been provided by the scampi fishing industry, and report the daily weight of scampi packaged in each of five whole animal, two tail categories, and a fishmeal (or "standard") component. In future iterations of the scampi assessment model we aim to include these data, but there are currently a number of logistical difficulties preventing this. A preliminary analysis of the data was conducted, modelling the proportion (by weight) that small scampi (meal, grade 5, and tailed categories) contribute to daily catches against year, time step and vessel, with a binomial distribution of errors. The model estimated a declining contribution of small scampi to catches from about 2006 to 2012 (Figure 53), which would be consistent with below average YCS from 2004 to 2010 (allowing for growth to fishable size), and an increase after this, supporting the recruitment pattern estimated by the model. The contribution to catches of small animals in the most recent years is comparable to that observed in the early 2000s, suggesting that YCSs may be comparable (along the lines of the CV on YCS prior of 0.4).
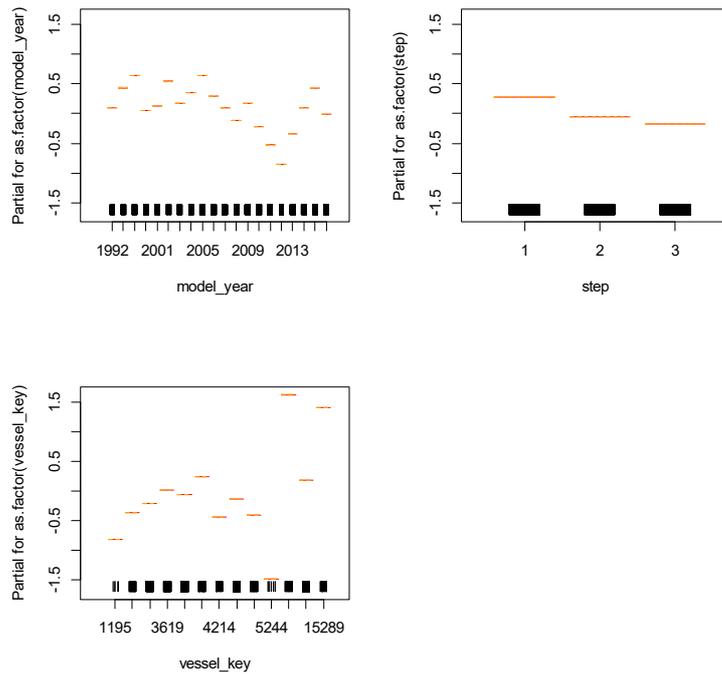
Figure 53: Termplot for model examining the proportion of the catch weight made up by small scampi, showing the effect of year time step and vessel on the proportion of small scampi in the catch, having taken into account (partialled out) the other terms.

4.5 Fishing pressure

Annual fishing intensity (equivalent annual F) and the level of fishing that, if applied forever, would result in an equilibrium biomass of 40% SSB_0 (F 40% B_0) were calculated using methods described by Cordue (2012). Estimates of annual fishing intensity and the Harvest Strategy Standard reference points were not sensitive to the choice of CV on the YCS prior, and so results are presented for Model 1 and Model 3, examining sensitivity to M (Figure 54 and Figure 55). While the F 40% B_0 level differs between M assumptions, the overall pattern of the relationship between F and SSB relative to this reference point is similar. While SSB declined with the development of the fishery, it reached a minimum in 2012, and has increased more recently. At all times through the fishery, SSB has remained well above the 40% SSB_0 target, and annual fishing intensity at its peak in 2007 was only about half the level estimated to result in an equilibrium biomass of 40% SSB_0, and thus remains well below F 40% B_0.
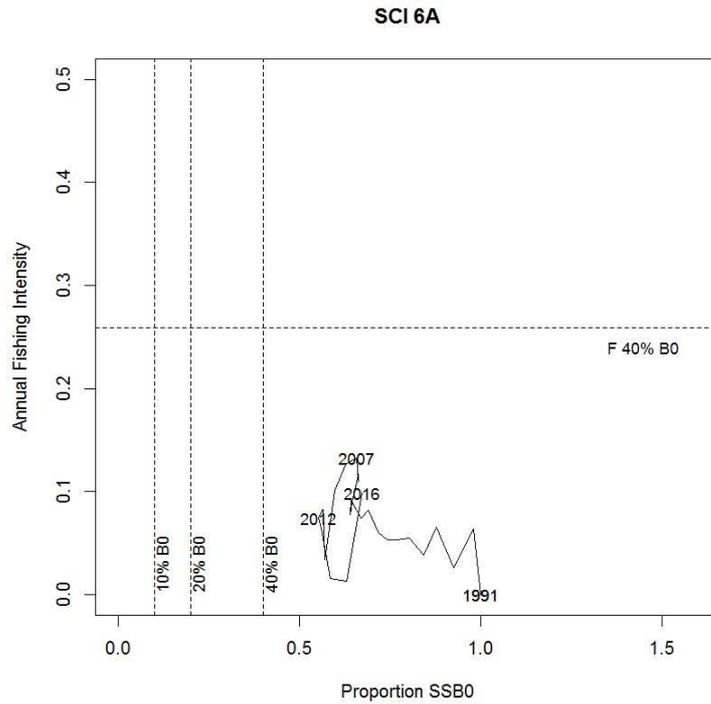
Figure 54: Trajectory of annual fishing intensity (equivalent annual F) plotted against proportion SSB$_0$ for the SCI 6A Model 1, in relation to Harvest Strategy Standard target and limit reference points.
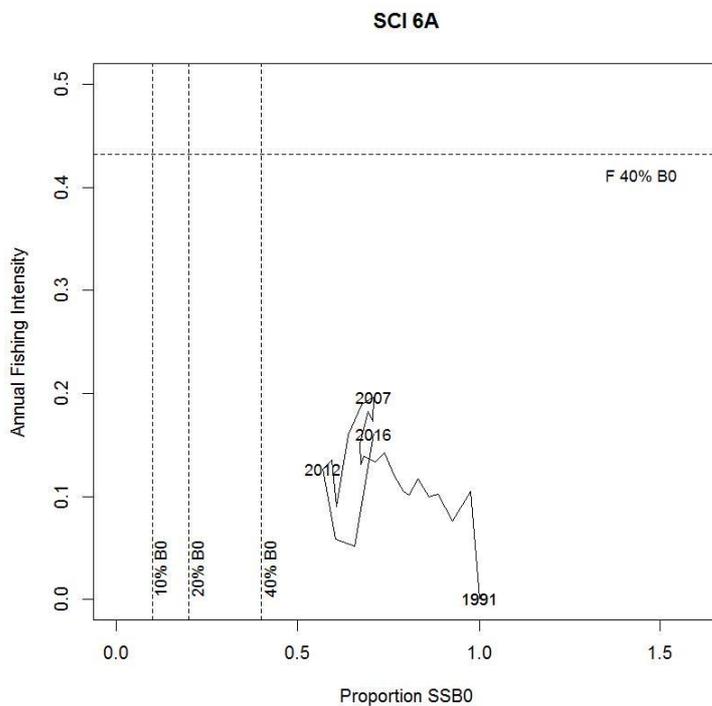
Figure 55: Trajectory of annual fishing intensity (equivalent annual F) plotted against proportion SSB$_0$ for the SCI 6A Model 3, in relation to Harvest Strategy Standard target and limit reference points.

4.6 Projections

The assessments reported SSB_0 and SSB_{2016} and used the ratio of current and projected SSB to SSB_0 as preferred indicators. Projections were conducted up to 2020 on the basis of catch scenarios proposed by MPI (current average landings of 252 t, and current TACC of 306 t) (Table 15). Projections have been conducted by randomly resampling year class strengths from the last decade estimated within the model (2005 – 2014). The probabilities of exceeding the default Harvest Strategy Standard target and limit reference points are reported (Table 15). Projected stock trajectories are shown for Models 1 and 2 (Figure 56) and Models 3 and 4 (Figure 57).

For models with a CV of 0.4 for the YCS prior, estimates of YCS_{2014} are comparable with the previous peak YCS (2002) (Models 1 and 3). Future catches at current average levels (252 tonnes) are predicted to maintain SSB at current levels, while future catches at the level of TACC (306 tonnes) are predicted to reduce the SSB relative to SSB_{2016}, but remain well above 40% SSB_0 (the most pessimistic prediction (Model 1, catches at TACC) estimating SSB_{2020} as 65% SSB_0, with 100% probability of SSB exceeding 40% SSB_0).

For models with a CV of 0.7 for the YCS prior, estimates of YCS_{2014} exceed the previous peak YCS (2002) (Models 2 and 4). Future catches at current average levels (252 tonnes) are predicted to increase SSB by 12 – 13%, while future catches at the level of TACC (306 tonnes) are predicted to increase SSB relative to SSB_{2016} by 7 – 9%. SSB is predicted to remain well above 40% SSB_0 (the most pessimistic prediction (Model 2, catches at TACC) estimating SSB_{2020} as 74% SSB_0, with 100% probability of SSB exceeding 40% SSB_0).

Table 15: SCI 6A projections. Results from MCMC runs showing B_0, B_{2016} and B_{2020} estimates at varying catch levels, and probabilities of projected spawning stock biomass exceeding the default Harvest Strategy Standard target and limit reference points.

	Model	Model 1	Model 2	Model 3	Model 4
	M	0.2	0.20	0.25	0.25
	CV YCS prior	0.4	0.7	0.4	0.7
	SSB_0	4664	4908	4464	4766
	SSB_{2016}	3175	3308	3220	3406
	SSB_{2016}/SSB_0	0.68	0.67	0.72	0.72
252 tonnes (current landings)	SSB_{2020}/SSB_0	0.68	0.77	0.72	0.80
	SSB_{2020}/SSB_{2016}	1.00	1.13	0.99	1.12
	$P\ SSB_{2020} < 10\%\ SSB_0$	0	0	0	0
	$P\ SSB_{2020} < 20\%\ SSB_0$	0	0	0	0
	$P\ SSB_{2020} > 40\%\ SSB_0$	1	1	1	1
	$P\ SSB_{2020} > SSB_{2016}$	0.51	0.78	0.48	0.72
306 tonnes (TACC)	SSB_{2020}/SSB_0	0.65	0.74	0.69	0.77
	SSB_{2020}/SSB_{2016}	0.96	1.09	0.95	1.07
	$P\ SSB_{2020} < 10\%\ SSB_0$	0	0	0	0
	$P\ SSB_{2020} < 20\%\ SSB_0$	0	0	0	0
	$P\ SSB_{2020} > 40\%\ SSB_0$	1	1	1	1
	$P\ SSB_{2020} > SSB_{2016}$	0.35	0.69	0.36	0.64
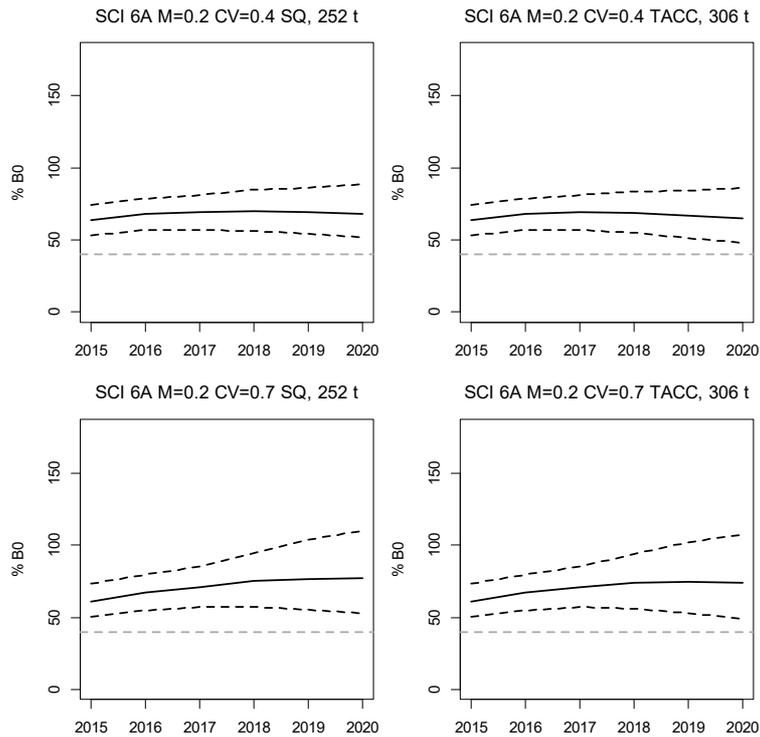
Figure 56: Projected stock trajectory (as a % of SSB₀) for SCI 6A from Model 1 (top row) and Model 2 (bottom row) for current average (left column) and TACC (right column) constant future catches. Solid black line represents median of projections, while dashed black lines represent 2.5th and 97.5th quantiles. Horizontal dashed grey line represents 40% SSB₀.
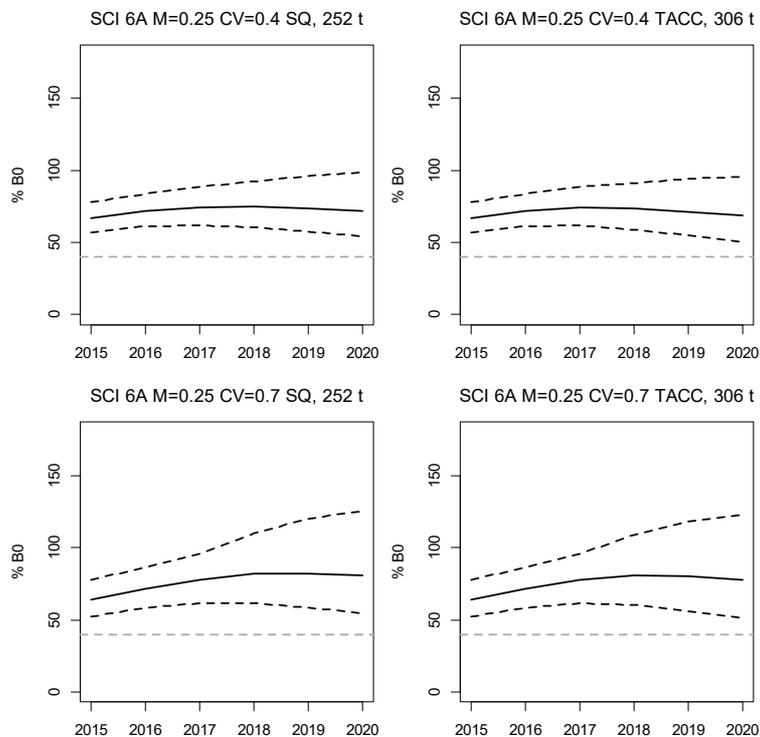
Figure 57: Projected stock trajectory (as a % of SSB₀) for SCI 6A from Model 3 (top row) and Model 4 (bottom row) for current average (left column) and TACC (right column) constant future catches. Solid black line represents median of projections, while dashed black lines represent 2.5th and 97.5th quantiles. Horizontal dashed grey line represents 40% SSB₀.

5. DISCUSSION

An assessment of the SCI 6A stock was last attempted in 2014 (Tuck 2015), and the current study has made considerable progress in developing the model further, with relevance to this and other scampi assessment models. The assessment was accepted, and this study represents the first accepted assessment for SCI 6A, and means all the main fisheries (SCI 1, 2, 3 & 6A) have accepted assessments.

Base models were developed, with M fixed at 0.2 and 0.25, and also investigating sensitivity to the CV on the YCS prior. A single annual standardised CPUE index was calculated, and along with trawl survey and photo survey data were fitted as abundance indices, with associated length frequency distributions. Projections were conducted up to 2020 on the basis of recent average and TACC future constant catch scenarios.

SSB_0 showed some sensitivity to M and the CV of the YCS prior, but overall the models were very consistent in their estimated stock trajectory and current stock status, with median estimates of SSB_{2016}/SSB_0 ranging from 67 – 72%. Diagnostics indicate that the MCMC chains for the models with qs estimated as free parameters did not converge, but models with qs estimated as nuisance parameters were considered acceptable. Overall patterns of estimated YCS were similar between models all of which estimated a series of above average YCSs in recent years, but the range over which YCS varied was sensitive to the CV on the YCS prior, with the models with the greater CV estimating the strongest YCS in the series in the final estimated year. Other data (abundance indices, length frequencies, grade composition) support an above average YCS at the end of the series, but it is unclear if there is sufficient evidence to justify choice of a model estimating such a large YCS. Projections out to 2020 suggested that SSB would remain well above 40% SSB_0 with future catches up to the TACC (the most pessimistic prediction giving a 100% probability of SSB_{2020} exceeding 40% SSB_0, and 35% probability of SSB_{2020} exceeding SSB_{2016}).

While tag recoveries have been reasonable in this fishery, the timing of the surveys mean that tagged animals (and hence recoveries) are predominantly female, and the data are quite limited (particularly for males) for estimating growth. Tagging studies are likely to be an ongoing component of surveys, and more tagging data, or other growth estimation approaches, would be beneficial.

6. ACKNOWLEDGEMENTS

7. REFERENCES

Bell, M.C.; Redant, F.; Tuck, I.D. (2006). *Nephrops* species. *In*: Phillips, B. (ed.). Lobsters: biology, management, aquaculture and fisheries, pp. 412–461. Blackwell Publishing, Oxford.

Bentley, N.; Kendrick, T.H.; Starr, P.J.; Breen, P.A. (2012). Influence plots and metrics: tools for better understanding fisheries catch-per-unit-effort standardisations. *ICES Journal of Marine Science 69*: 84–88.

Bull, B.; Dunn, A. (2002). Catch-at-age: User manual v 1.06.2002/09/12. *NIWA Internal Report 114*: 23 p.

Bull, B.; Francis, R.I.C.C.; Dunn, A.; McKenzie, A.; Gilbert, D.J.; Smith, M.H.; Bian, R. (2008). CASAL (C++ algorithmic stock assessment laboratory). *NIWA Technical Report No. 130*: 276 p.

Bull, B.; Francis, R.I.C.C.; Dunn, A.; McKenzie, A.; Gilbert, D.J.; Smith, M.H.; Bian, R.; Fu, D. (2012). CASAL (C++ algorithmic stock assessment laboratory). *NIWA Technical Report No. 135*: 280 p.

Carter, D. (2003). Inquiry into the administration and management of the scampi fishery. *Report to the Primary Production Committee No.* 226 p.

Charnov, E.L.; Berrigan, D.; Shine, R. (1983). The M/*k* ratio is the same for fish and reptiles. *American Naturalist 142*: 707–711.

Clark, W.G.; Hare, S.R. (2006). Assessment and management of Pacific halibut: data, methods, and policy. *International Pacific Halibut Commission Scientific Report No. 83*. 111 p.

Cordue, P.L. (2012). Fishing intensity metrics for use in overfishing determination. *ICES Journal of Marine Science: Journal du Conseil 69(4)*: 615-623. <http://dx.doi.org/10.1093/icesjms/fss036>

Cryer, M. (2000). A consideration of current management areas for scampi in QMAs 3, 4, 6A and 6B. *Final Research Report for Ministry of Fisheries Project MOF1999-04K No. MOF1999-04K*. 52 p.

Cryer, M.; Coburn, R. (2000). Scampi stock assessment for 1999. *New Zealand Fisheries Assessment Report 2000/7*: 61 p.

Cryer, M.; Dunn, A.; Hartill, B. (2005). Length-based population model for scampi (*Metanephrops challengeri*) in the Bay of Plenty (QMA 1). *New Zealand Fisheries Assessment Report 2005/27*: 55 p.

Cryer, M.; Stotter, D.R. (1999). Movement and growth rates of scampi inferred from tagging, Alderman Islands, western Bay of Plenty. *NIWA Technical Report No. 49*: 36 p.

Fenaughty, C. (1989). Reproduction in *Metanephrops challengeri. Unpublished Report MAF Fisheries, Wellington No.* 46 p.

Francis, R.I.C.C. (1999). The impact of correlations in standardised CPUE indices. *New Zealand Fisheries Assessment Research Document No. 99/42*. 30 p.

Francis, R.I.C.C. (2011). Data weighting in statistical fisheries stock assessment models. *Canadian Journal Fisheries and Aquatic Science 68*: 1124–1138.

Francis, R.I.C.C.; Rasmussen, S.; Fu, D.; Dunn, A. (2016). CALA: Catch-at-length and -age user manual, CALA v. *National Institute of Water & Atmospheric Research Ltd. Unpublished report.*: 92 p.

Hartill, B.; Tuck, I.D. (2010). Potential utility of scampi processor grade data as a source of length frequency data. *Final Research Report for Ministry of Fisheries Project No. SCI2007-03*. 27 p.

McCullagh, P.; Nelder, J.A. (1989). Generalised Linear Models. 2nd Ed. Chapman and Hall, London. 511 p.

Morizur, Y. (1982). Estimation de la mortalité pour quelques stocks de langoustine, *Nephrops norvegicus. ICES CM 1982/K:10*.

Pauly, D. (1980). On the interrelationships between natural mortality, growth parameters, and mean environmental temperature in 175 fish stocks. *Journal du Conseil International pour l'Exloration du Mer 39*: 175–192.

Starr, P.J. (2009). Rock lobster catch and effort data: summaries and CPUE standardisations, 1979–80 to 2007–08. *New Zealand Fisheries Assessment Report 2009/38*: 73 p.

Starr, P.J.; Breen, P.A.; Kendrick, T.H.; Haist, V. (2009). Model and data used for the 2008 stock assessment of rock lobsters (*Jasus edwardsii*) in CRA 3. *New Zealand Fisheries Assessment Report 2009/22*: 62 p.

Tuck, I.D. (2009). Characterisation of scampi fisheries and the examination of catch at length and spatial distribution of scampi in SCI 1, 2, 3, 4A and 6A. *New Zealand Fisheries Assessment Report 2009/27*: 102 p.

Tuck, I.D. (2010). Scampi burrow occupancy, burrow emergence and catchability. Final Research Report for Ministry of Fisheries research project. 2010/13: 58 p.

Tuck, I.D. (2013). Characterisation and length-based population model for scampi (*Metanephrops challengeri*) on the Mernoo Bank (SCI 3). *New Zealand Fisheries Assessment Report 2013/24*: 165 p.

Tuck, I.D. (2014). Characterisation and length-based population model for scampi (*Metanephrops challengeri*) in the Bay of Plenty (SCI 1) and Hawke Bay/Wairaraoa (SCI 2). *New Zealand Fisheries Assessment Report 2014/33*: 172 p.

Tuck, I.D. (2015). Characterisation and length-based population model for scampi (*Metanephrops challengeri*) at the Auckland Islands (SCI 6A). *New Zealand Fisheries Assessment Report 2015/21*: 164 p.

Tuck, I.D. (2016a). Characterisation and length-based assessment model for scampi (*Metanephrops challengeri*) in the Bay of Plenty (SCI 1) and Hawke Bay– Wairarapa (SCI 2). *New Zealand Fisheries Assessment Report 2016/51*: 194 p.

Tuck, I.D. (2016b). Characterisation and length-based population model for scampi (*Metanephrops challengeri*) on the Mernoo Bank (SCI 3). *New Zealand Fisheries Assessment Report 2016/55*: 221 p.

Tuck, I.D.; Atkinson, R.J.A.; Chapman, C.J. (2000). Population biology of the Norway lobster, *Nephrops norvegicus* (L.) in the Firth of Clyde, Scotland. II. Fecundity and size at onset of maturity. *ICES Journal of Marine Science 57*: 1222–1237.

Tuck, I.D.; Bian, R. (2012). Utility of grade based sampling for scampi. *Final Research Report for Ministry of Fisheries research project No. SCI200804*. 66 p.

Tuck, I.D.; Dunn, A. (2006). Length based population model for scampi (*Metanephrops challengeri*) in the Bay of Plenty (SCI 1) and Wairarapa / Hawke Bay (SCI 2). *Final Research Report for Ministry of Fisheries research project SCI2005-01 No. SCI2005-01*. 93 p.

Tuck, I.D.; Dunn, A. (2009). Length-based population model for scampi (*Metanephrops challengeri*) in the Bay of Plenty (SCI 1) and Wairarapa / Hawke Bay (SCI 2). Final Research Report for Ministry of Fisheries research project SCI2008-03. SCI2006-01 & SCI2008-03W: 30 p.

Tuck, I.D.; Dunn, A. (2012). Length-based population model for scampi (*Metanephrops challengeri*) in the Bay of Plenty (SCI 1), Wairarapa / Hawke Bay (SCI 2) and Auckland Islands (SCI 6A). *New Zealand Fisheries Assessment Report 2012/1*: 125 p.

Tuck, I.D.; Hartill, B.; Parkinson, D.; Drury, J.; Smith, M.; Armiger, H. (2009a). Estimating the abundance of scampi - Relative abundance of scampi, *Metanephrops challengeri*, from a photographic survey in SCI 6A (2009). Final Research Report for Ministry of Fisheries research project SCI2008-01. SCI2008-01: 26 p.

Tuck, I.D.; Hartill, B.; Parkinson, D.; Harper, S.; Drury, J.; Smith, M.; Armiger, H. (2009b). Estimating the abundance of scampi - Relative abundance of scampi, *Metanephrops challengeri*, from a photographic survey in SCI 1 and SCI 6A (2008). Final Research Report for Ministry of Fisheries research project SCI2008-01. SCI2007-02: 37 p.

Tuck, I.D.; Parkinson, D.; Armiger, H.; Smith, M.; Miller, A.; Rush, N.; Spong, K. (2015a). Estimating the abundance of scampi in SCI 6A (Auckland Islands) in 2013. *New Zealand Fisheries Assessment Report 2015/10*: 52 p.

Tuck, I.D.; Parkinson, D.; Armiger, H.; Smith, M.; Miller, A.; Rush, N.; Spong, K. (2017). Estimating the abundance of scampi in SCI 6A (Auckland Islands) in 2016. *New Zealand Fisheries Assessment Report 2017/06*: 40 p.

Tuck, I.D.; Parkinson, D.; Hartill, B.; Drury, J.; Smith, M.; Armiger, H. (2007). Estimating the abundance of scampi - relative abundance of scampi, *Metanephrops challengeri*, from a photographic survey in SCI 6A (2007). *Final Research Report for Ministry of Fisheries research project SCI2006-02 No. SCI2006-02*. 29 p.

Tuck, I.D.; Parsons, D.M.; Hartill, B.W.; Chiswell, S.M. (2015b). Scampi (*Metanephrops challengeri*) emergence patterns and catchability. *ICES Journal of Marine Science 72 (Supplement 1)*: i199-i210.

Vignaux, M. (1994). Catch per unit effort (CPUE) analysis of west coast South Island and Cook Strait spawning hoki fisheries, 1987–93. *New Zealand Fisheries Assessment Research Document No. 94/11*. 29 p.

Wear, R.G. (1976). Studies on the larval development of *Metanephrops challengeri* (Balss, 1914) (Decapoda, Nephropidae). *Crustaceana 30*: 113–122.

APPENDIX 1. CPUE standardisation diagnostics
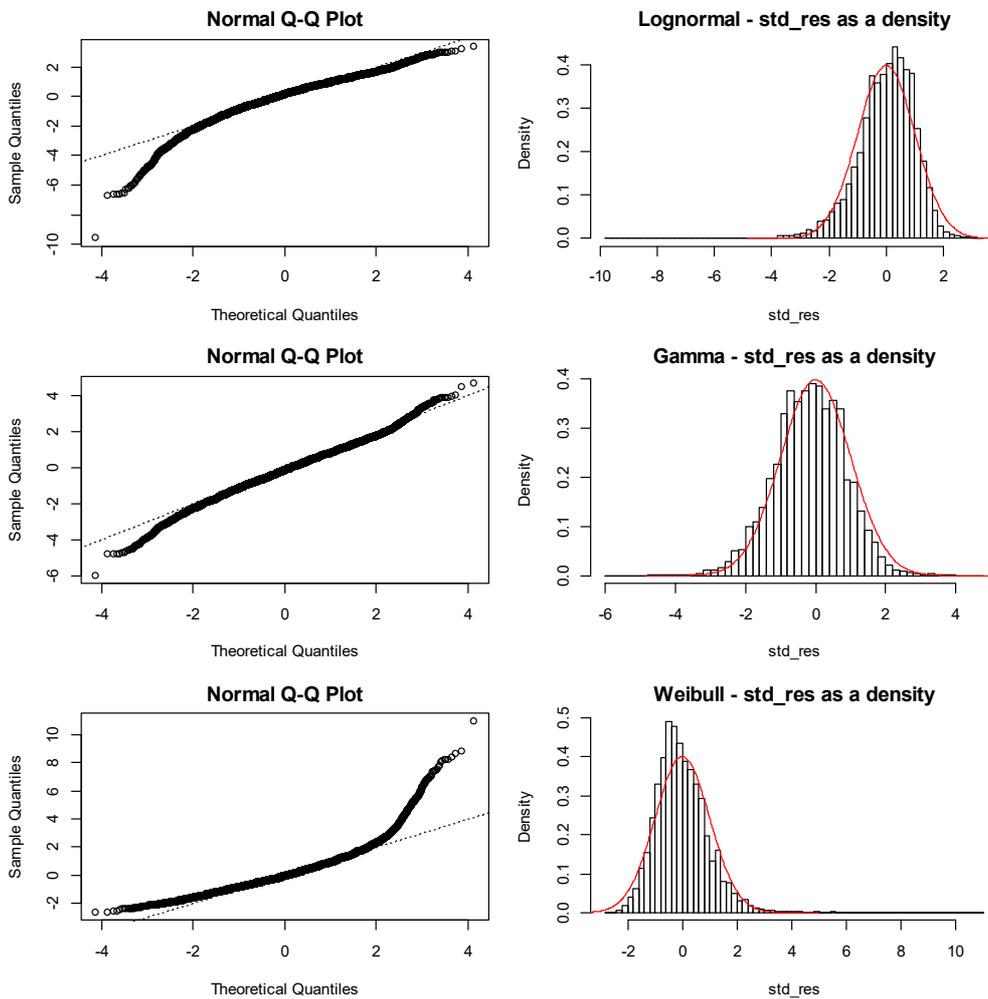
A1. 1: Plots of the distributions of standardised residuals for simple standardised CPUE models for SCI 6A with log normal (top panel), gamma (middle panel), and Weibull (bottom panel) error distributions.

Annual CPUE index
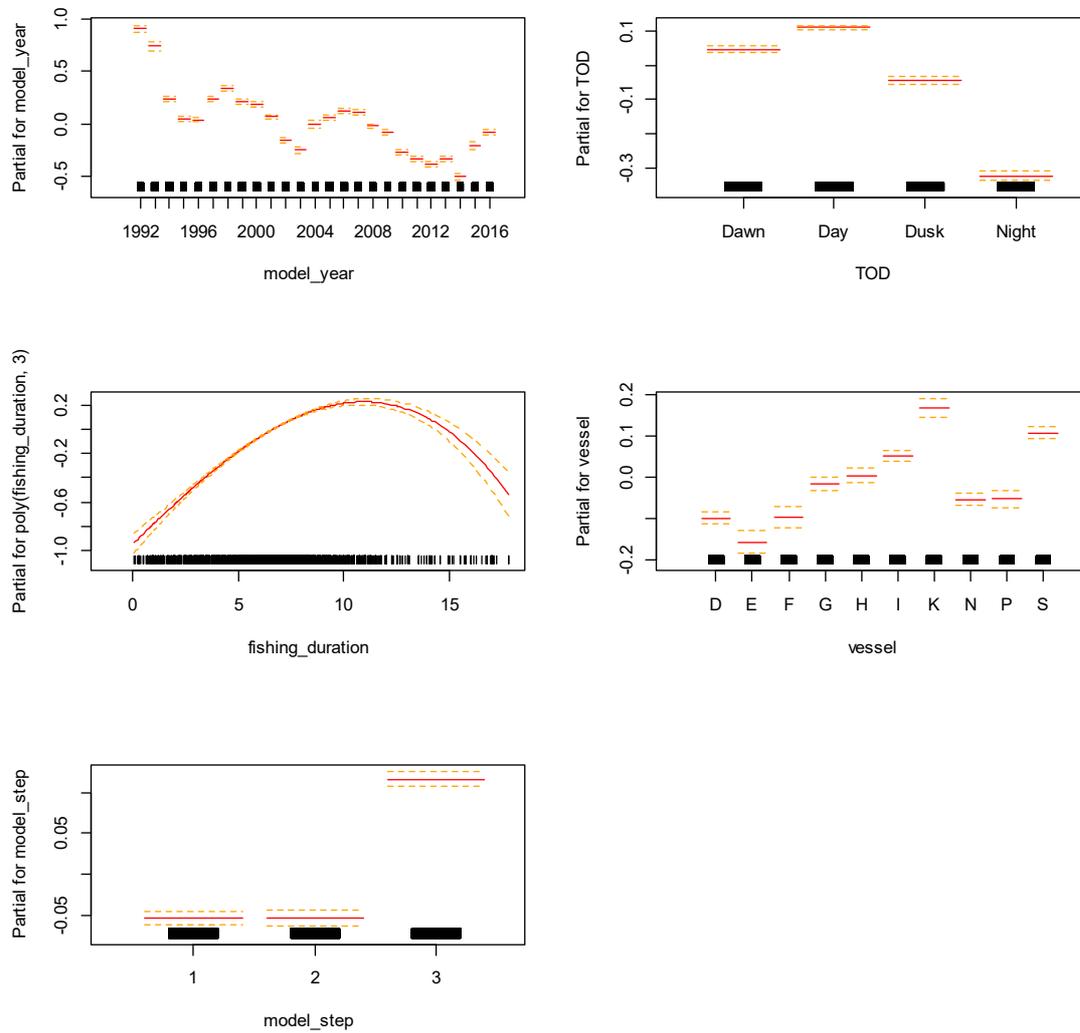
A1. 2: Termplot for final SCI 6A CPUE standardisation model.
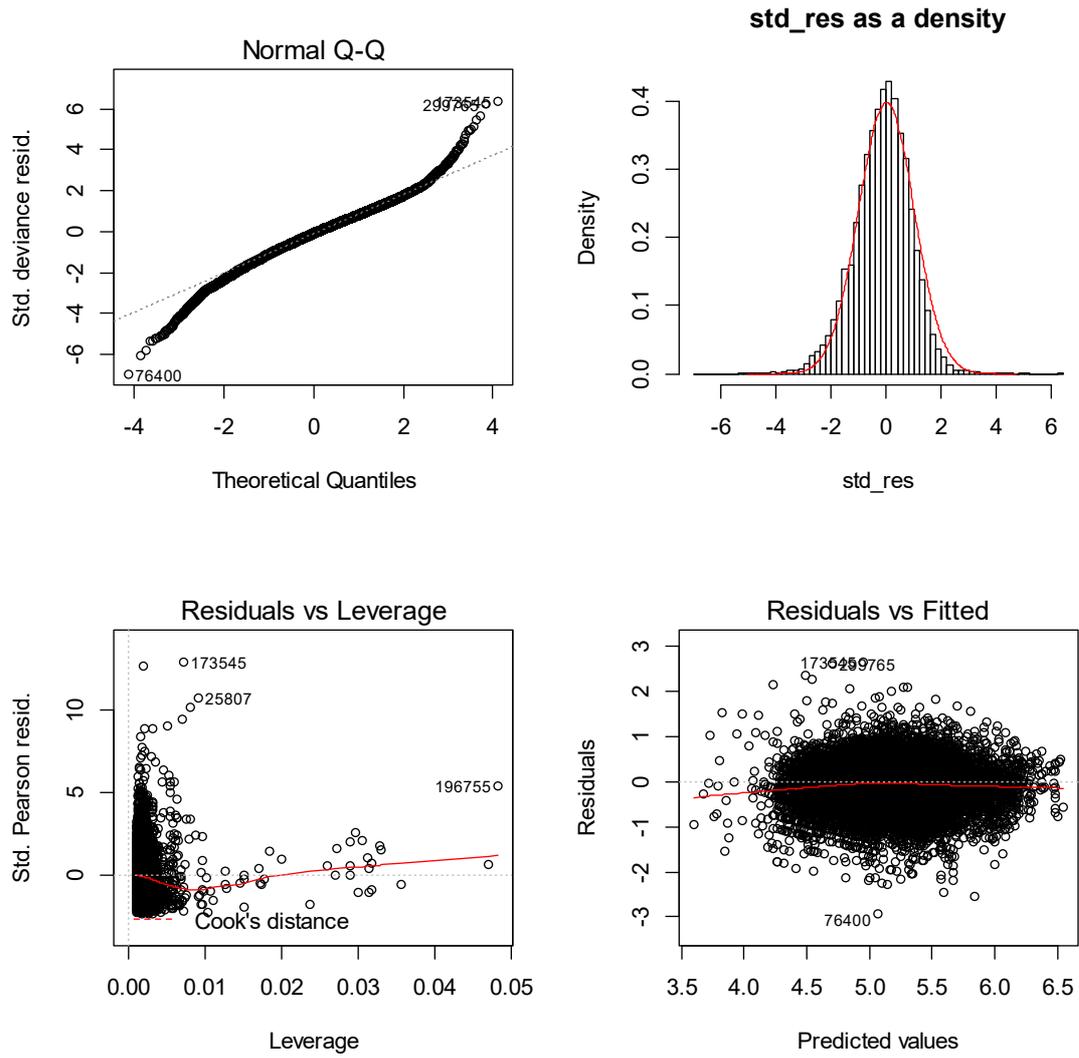
A1. 3: Diagnostic plots for final SCI 6A CPUE standardisation model.
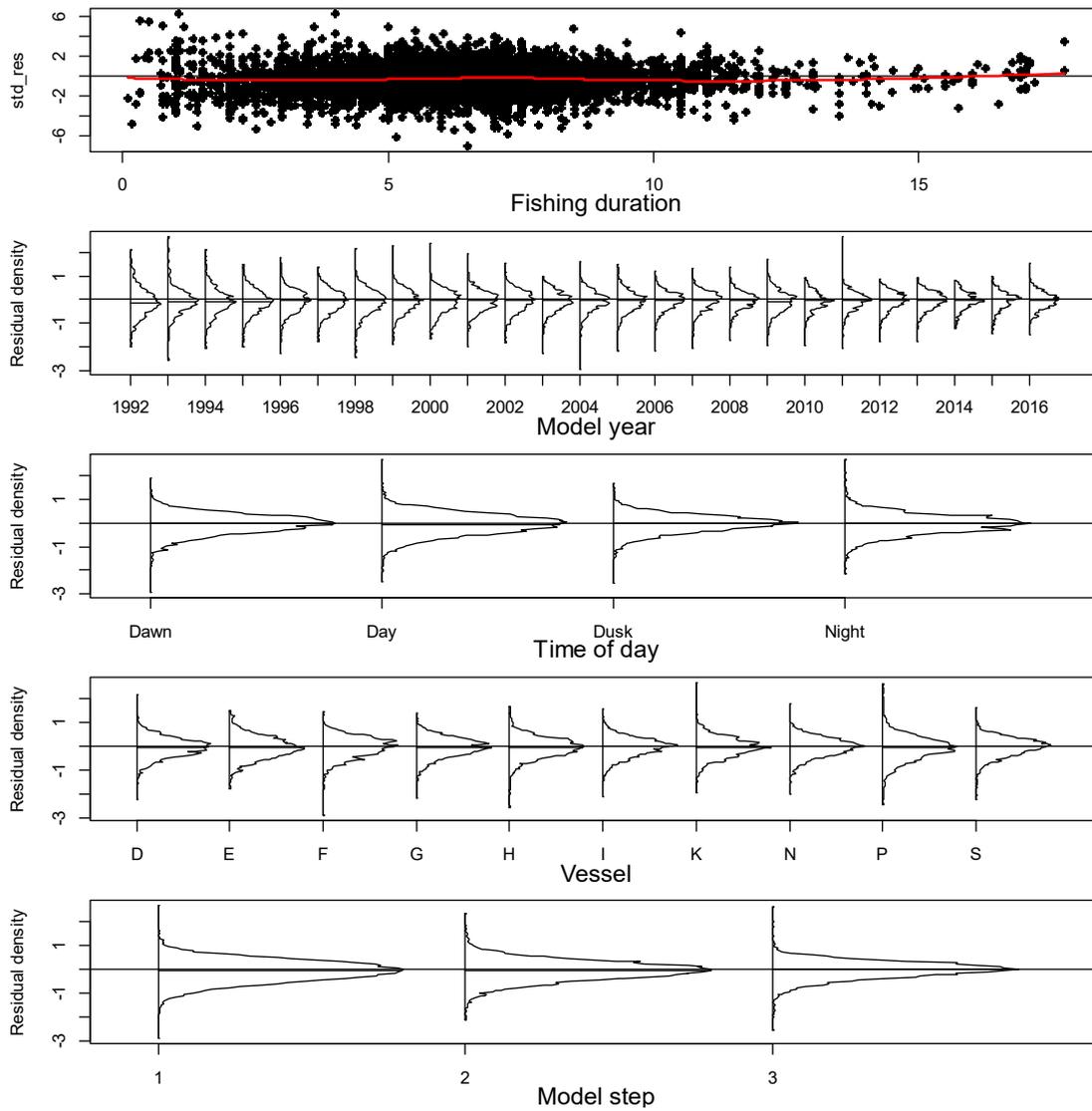
A1. 4: Distributions of residuals for final SCI 6A CPUE standardisation model.
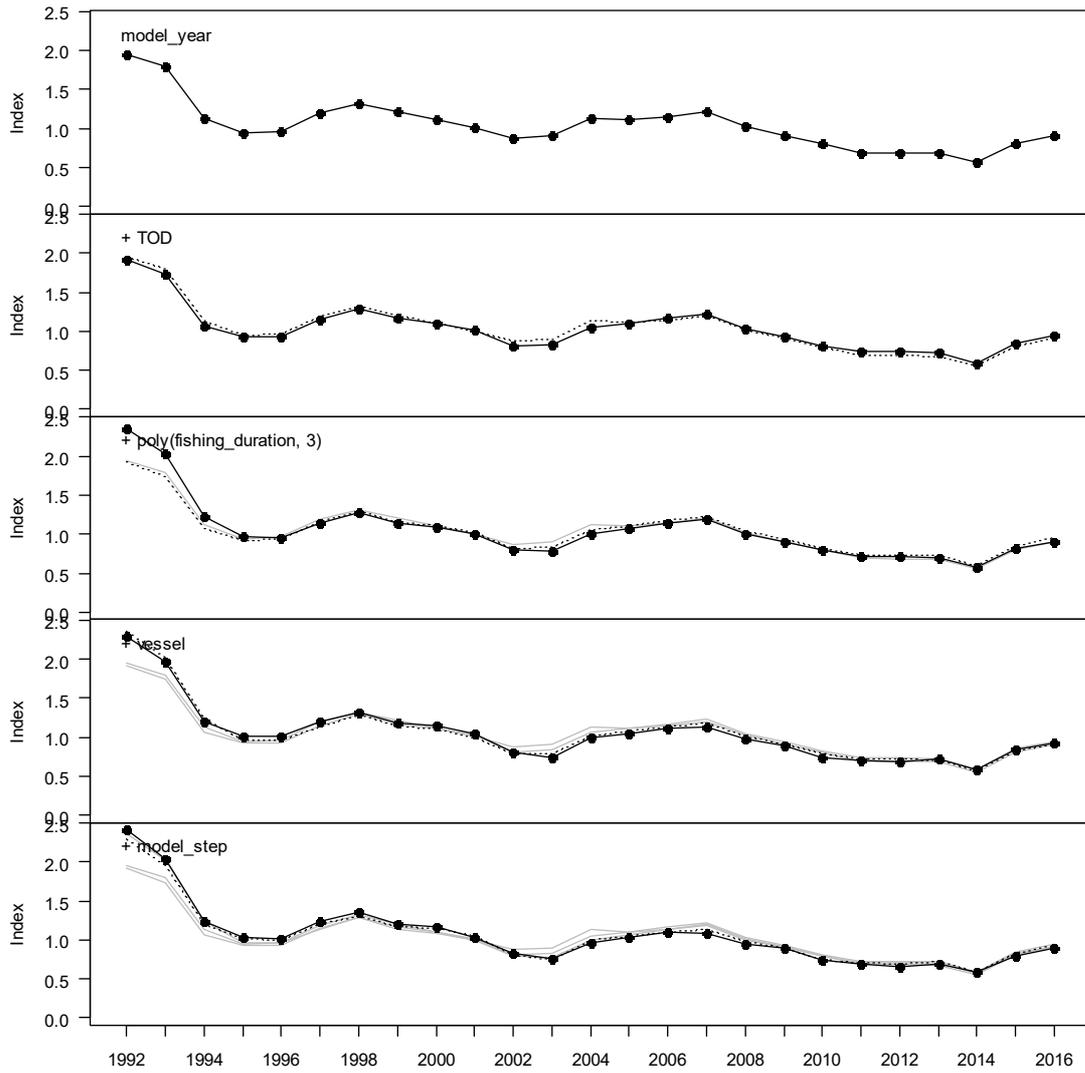
A1. 5: Step influence plot for final SCI 6A CPUE standardisation model.
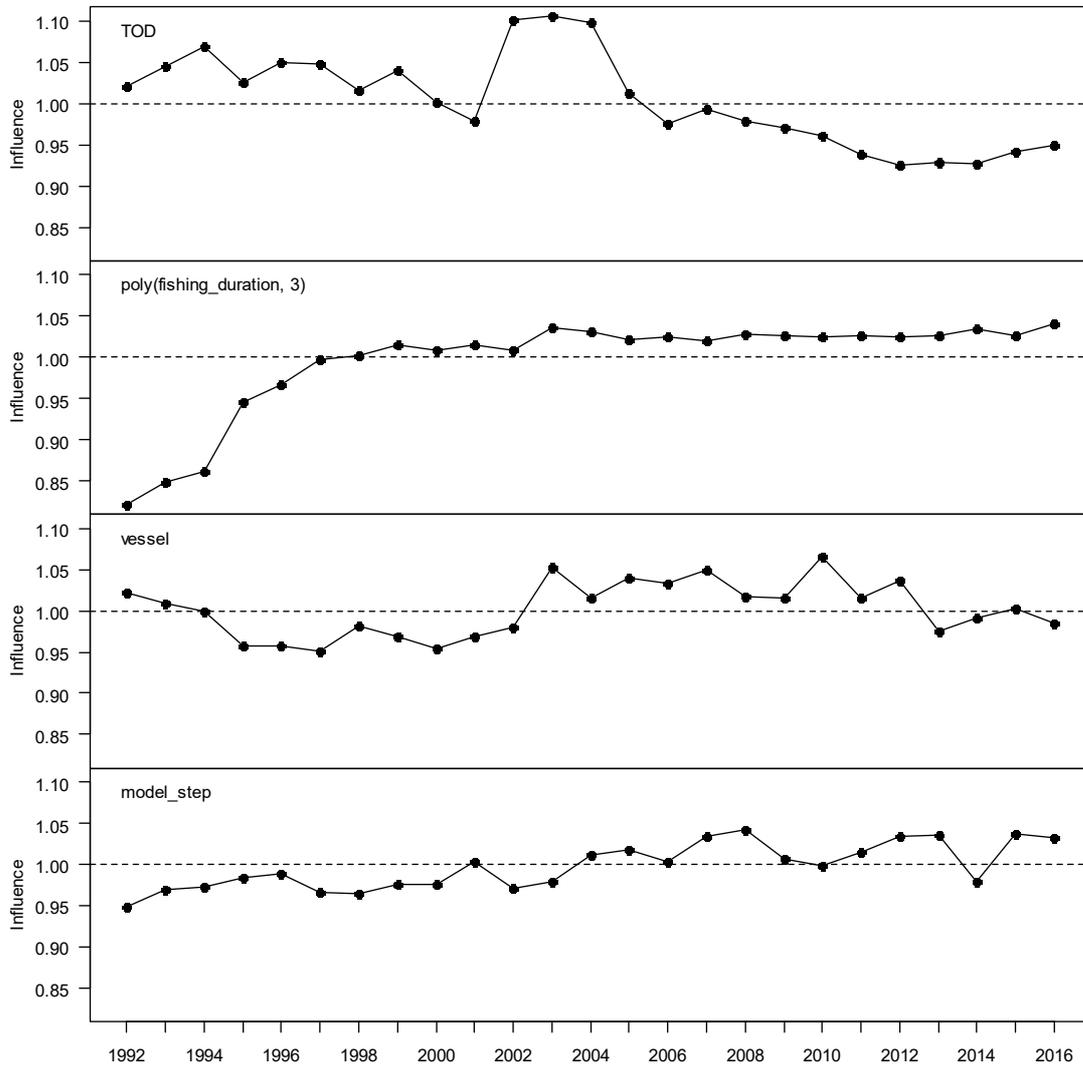
A1. 6: Year influence plots for each explanatory variable for final SCI 6A CPUE standardisation model.
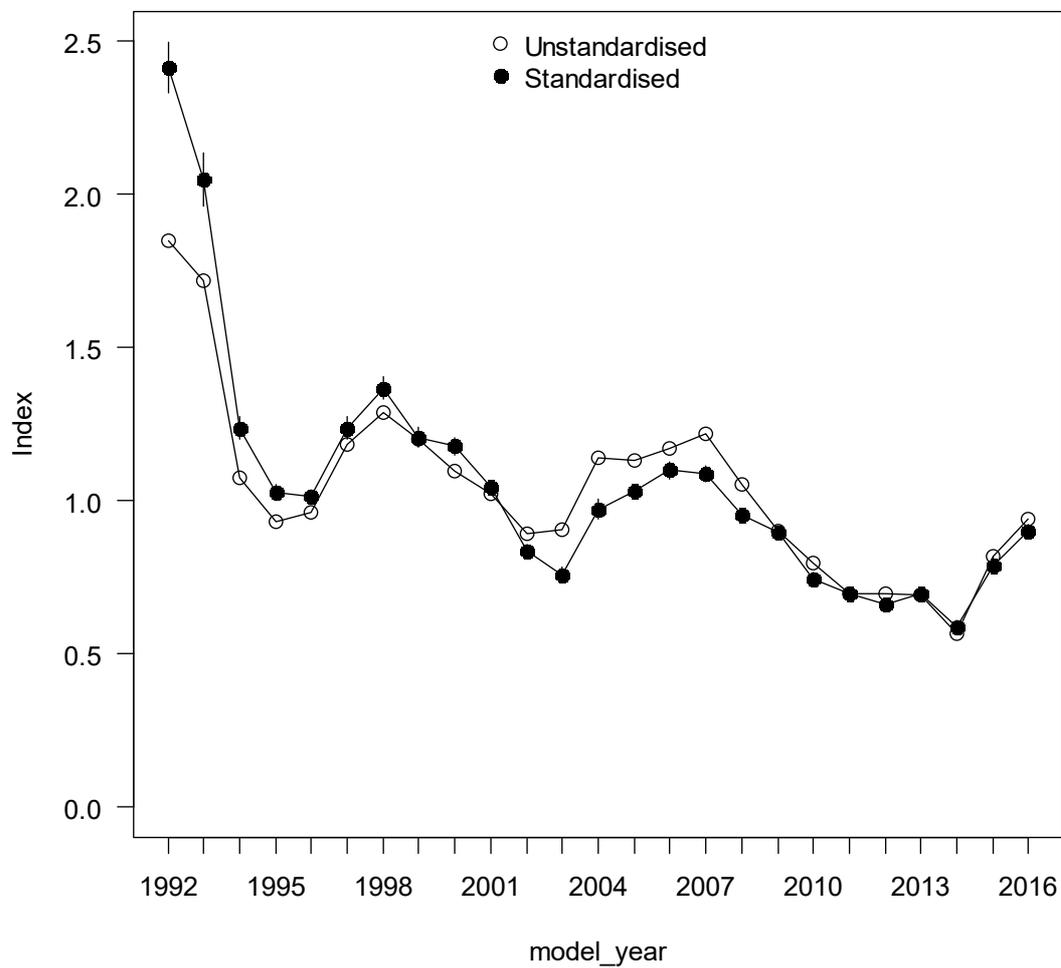
A1. 7: Plot of standardised and unstandardized CPUE indices for SCI 6A.
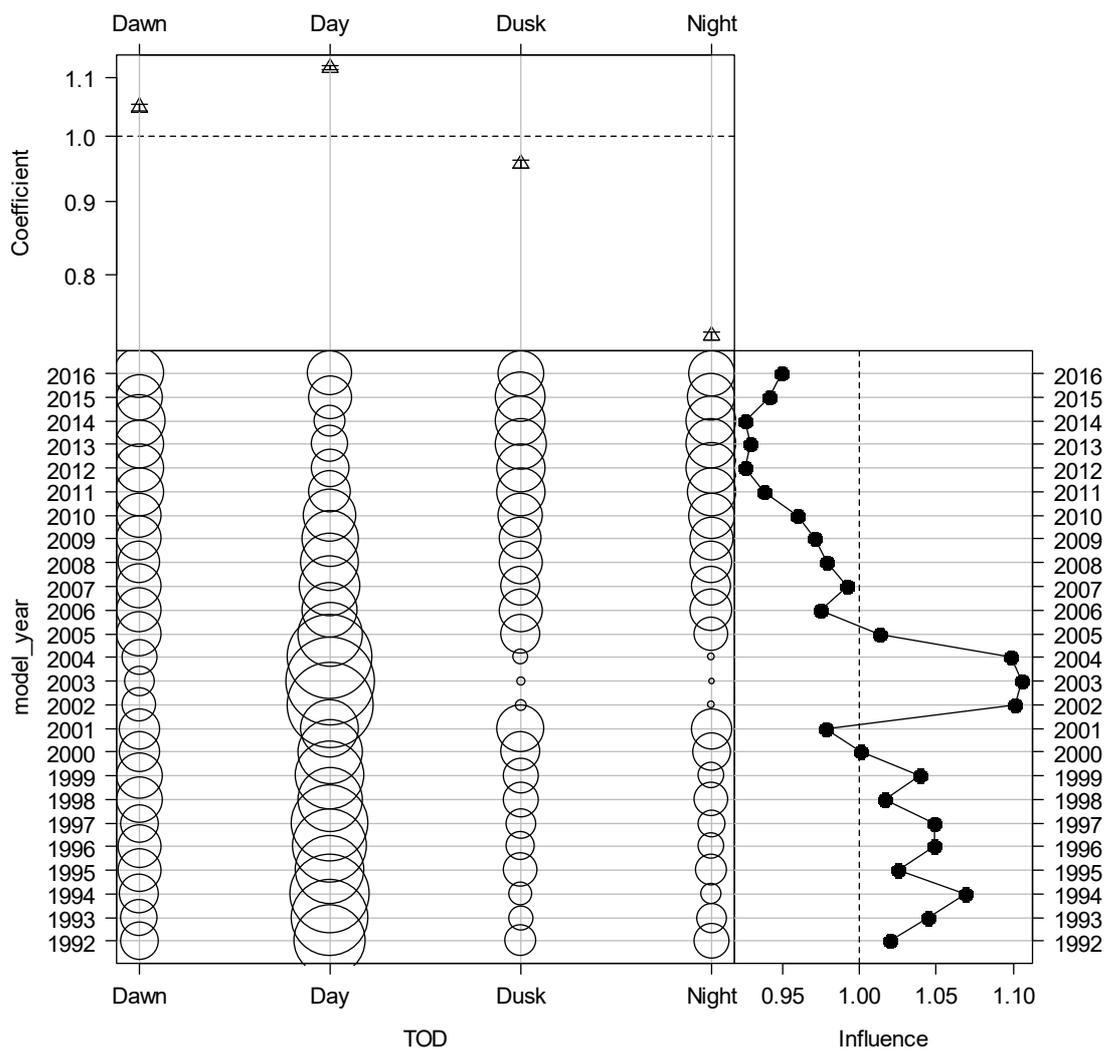
A1. 8: Coefficient-distribution influence plot for time of day for final SCI 6A CPUE standardisation model.
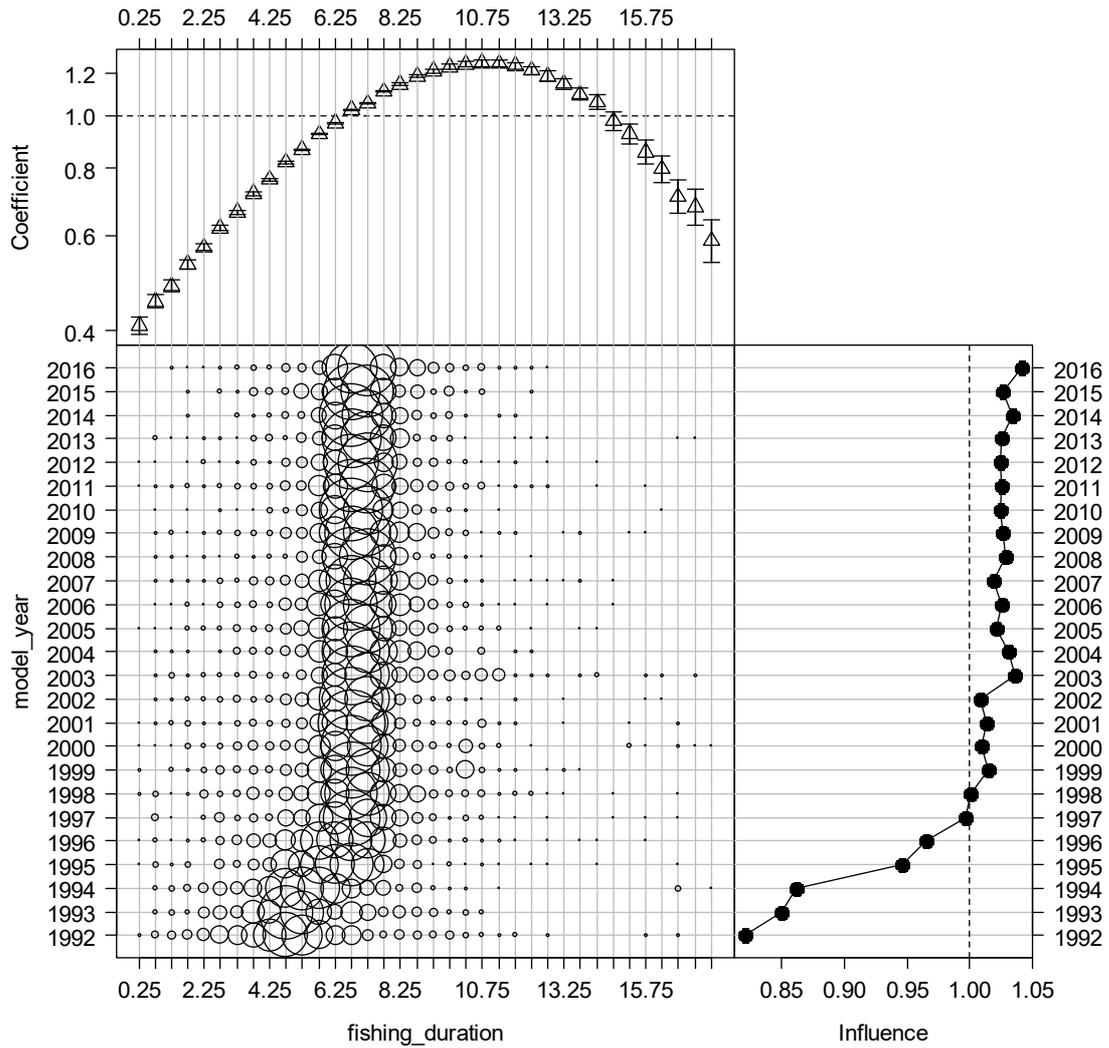
A1. 9: Coefficient-distribution influence plot for fishing duration for final SCI 6A CPUE standardisation model.
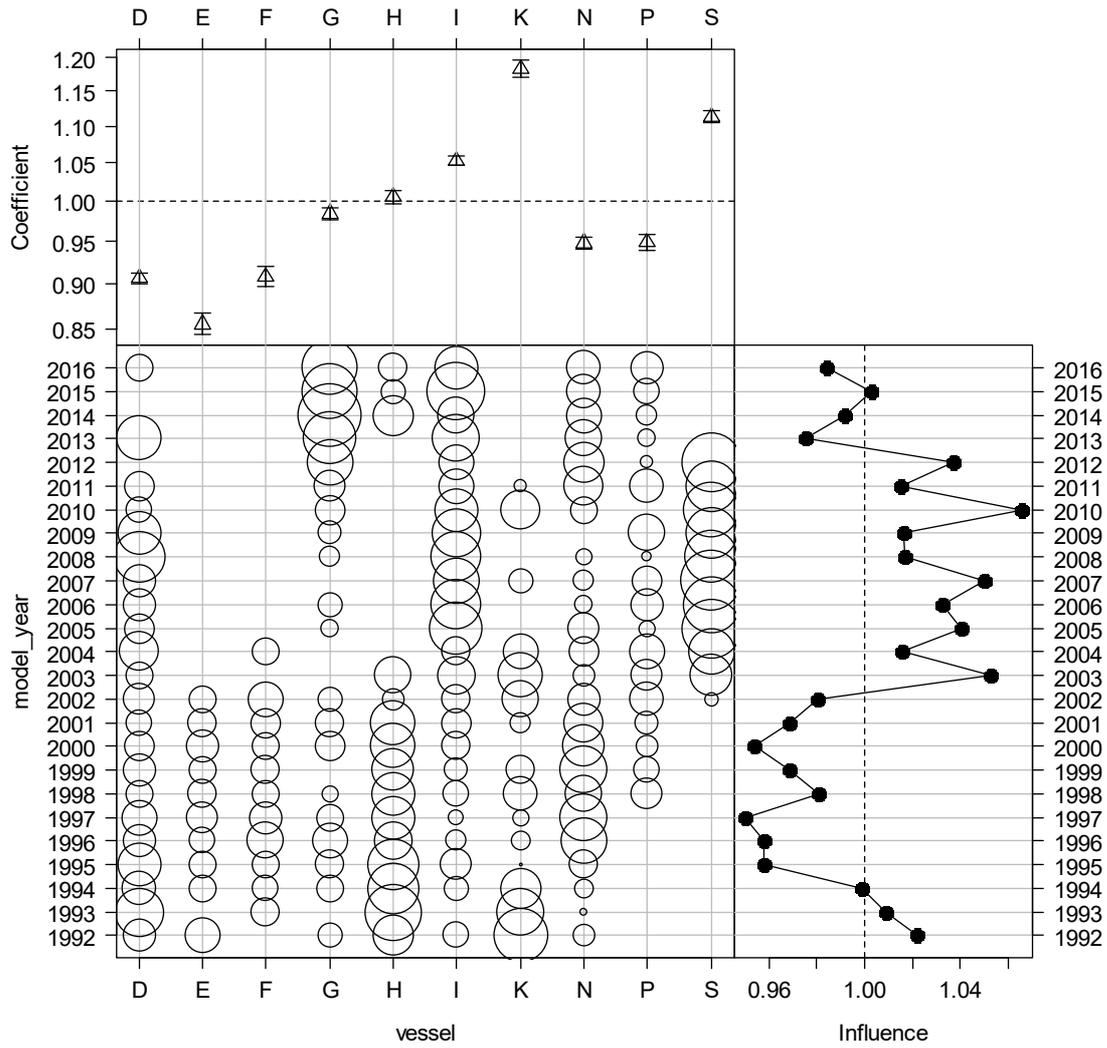
A1. 10: Coefficient-distribution influence plot for vessel for final SCI 6A CPUE standardisation model.
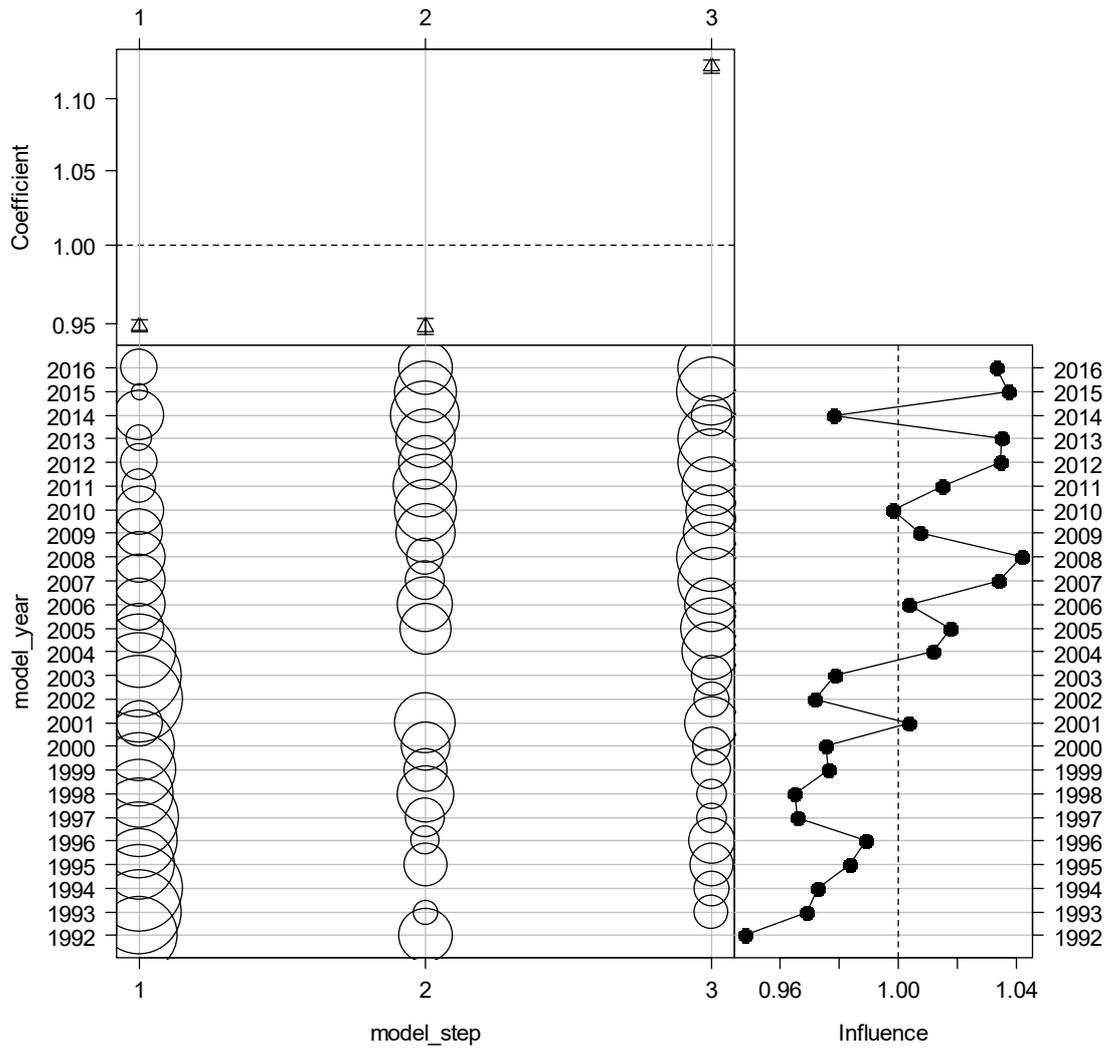
A1. 11: Coefficient-distribution influence plot for timestep for final SCI 6A CPUE standardisation model.

APPENDIX 2. Analysis of length composition data

Trawl survey length frequency
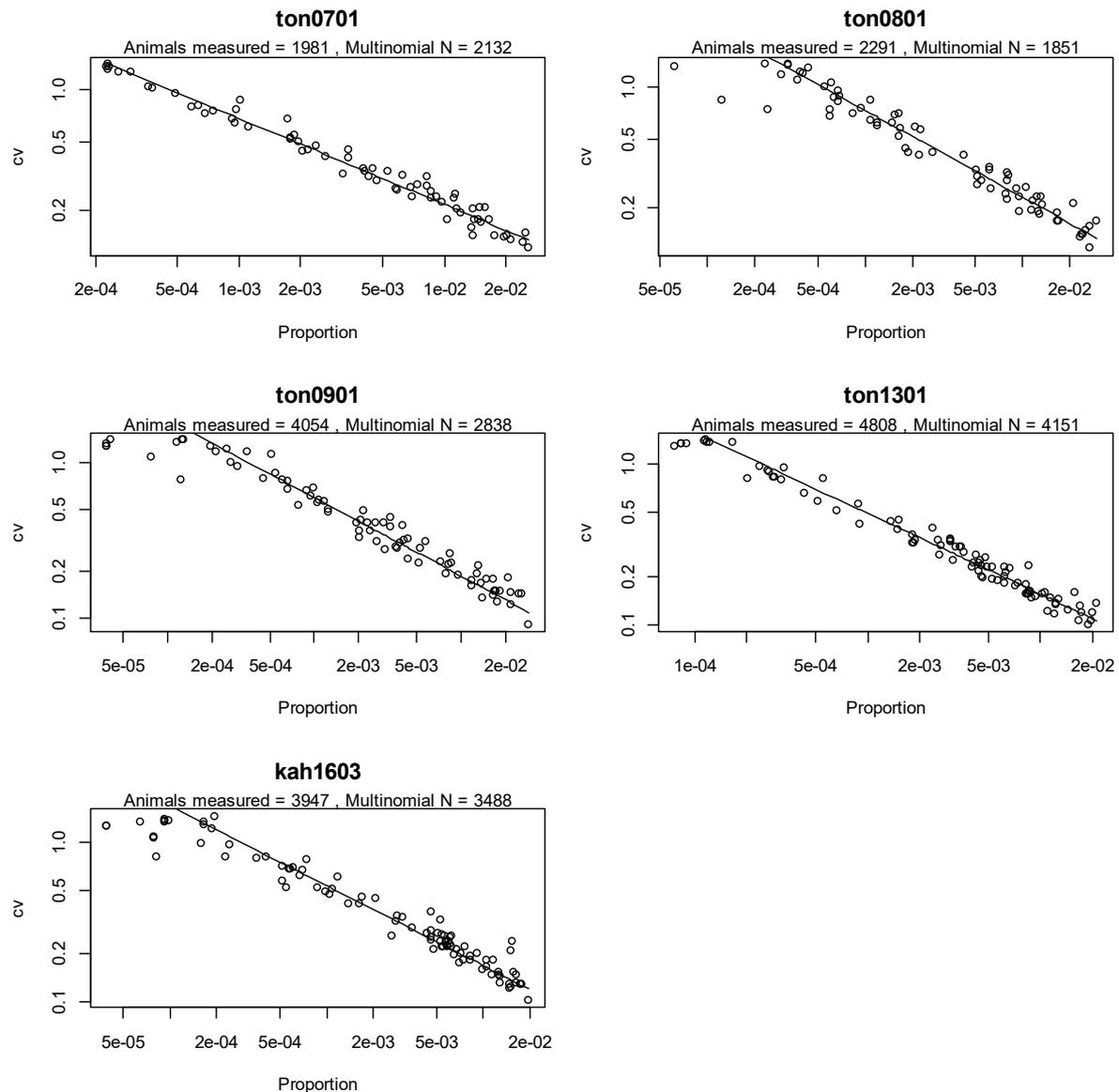
A2. 1: Observation-error CVs for the trawl survey proportions-at-length data sets. Each point represents a proportion at a specific length and sex for a given year. The diagonal line, which is the same in each panel, is added to aid comparison between panels; it shows the relationship between proportion and CV that would hold with simple multinomial sampling with sample size 500.

Observer length frequency
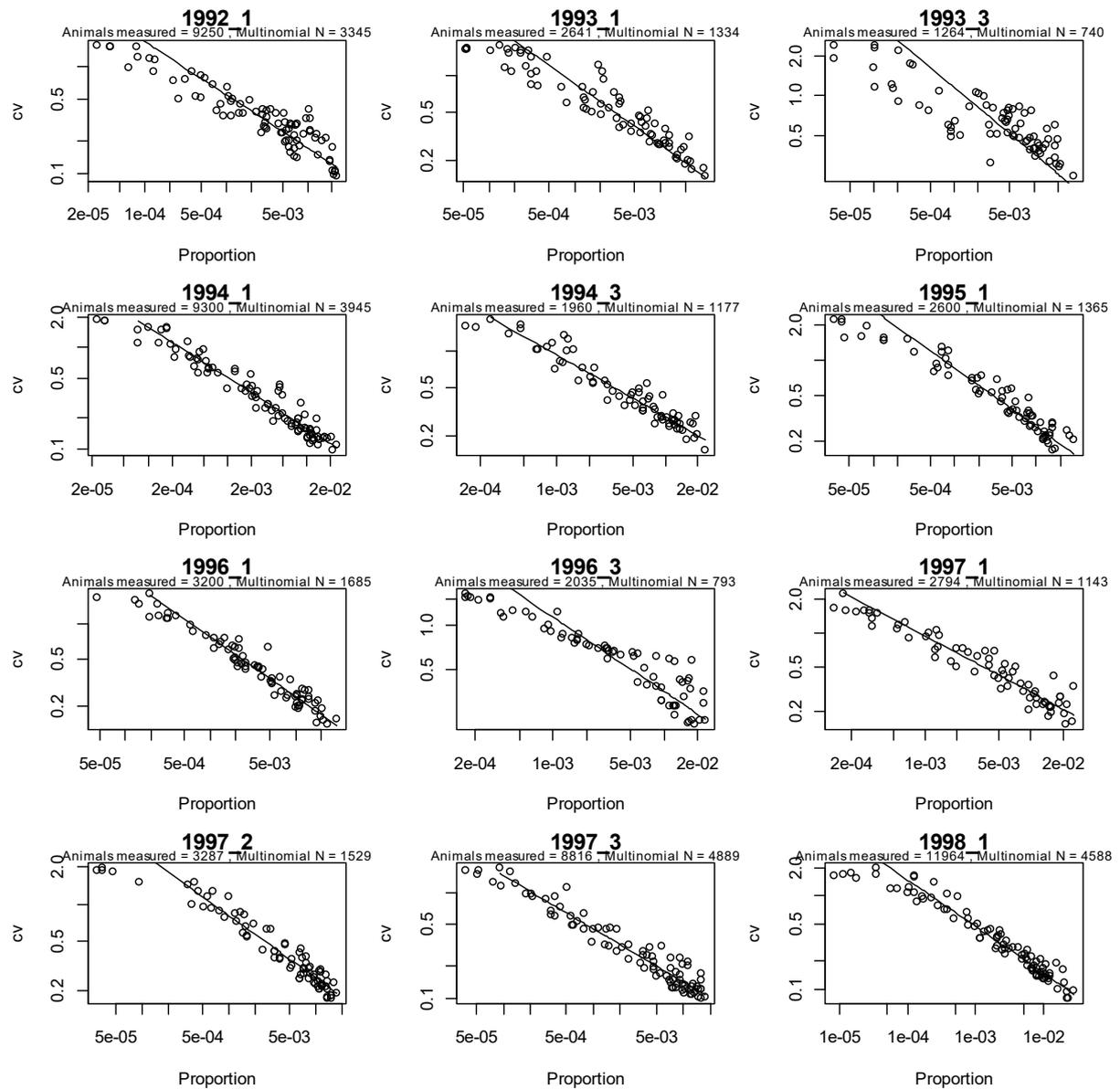
A2. 2: Observation-error CVs for the observer proportions-at-length data sets. Each point represents a proportion at a specific length and sex for a given year. The diagonal line, which is the same in each panel, is added to aid comparison between panels; it shows the relationship between proportion and CV that would hold with simple multinomial sampling with sample size 500.
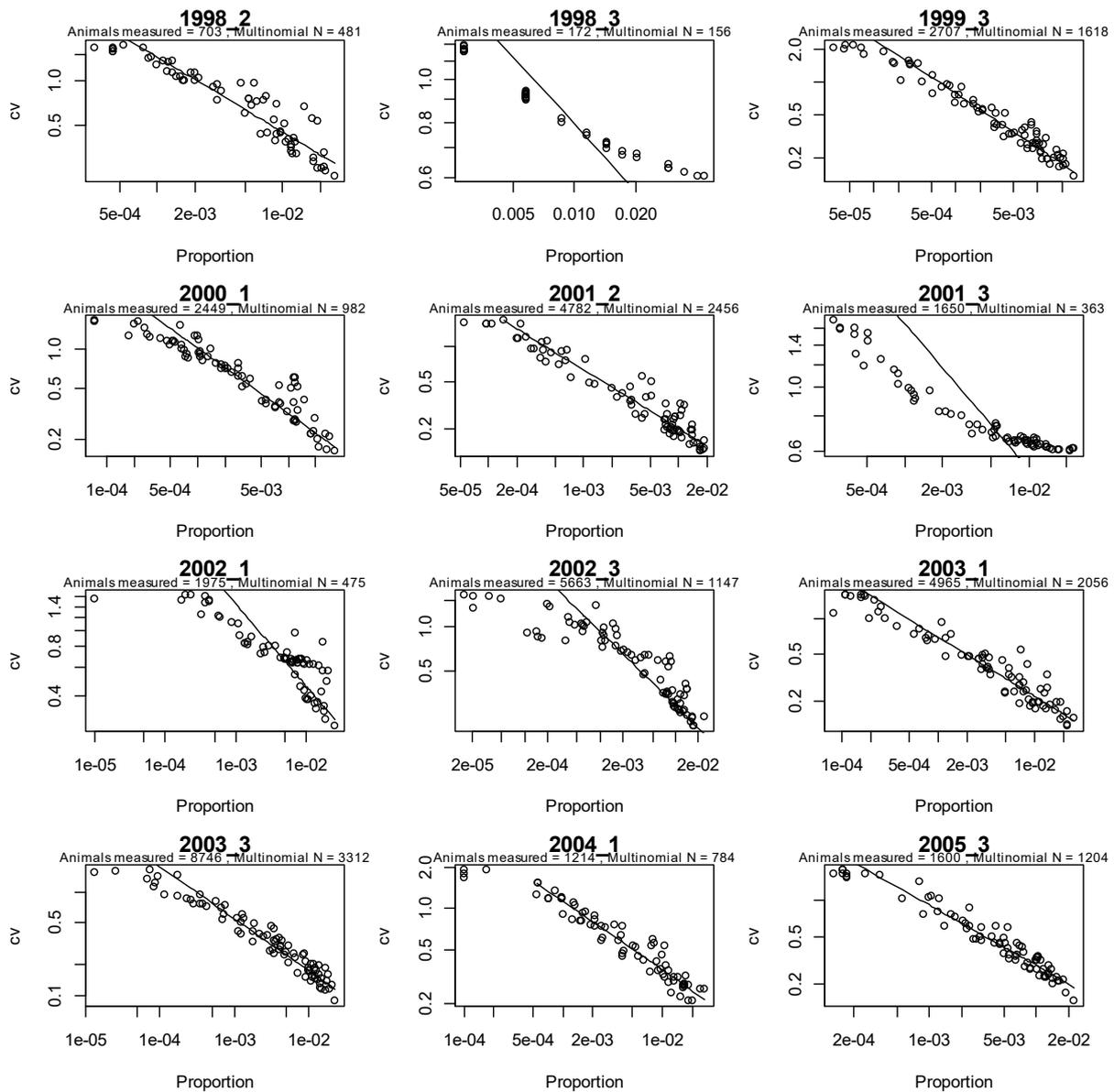
A2. 3: Observation-error CVs for the observer proportions-at-length data sets. Each point represents a proportion at a specific length and sex for a given year. The diagonal line, which is the same in each panel, is added to aid comparison between panels; it shows the relationship between proportion and CV that would hold with simple multinomial sampling with sample size 500.
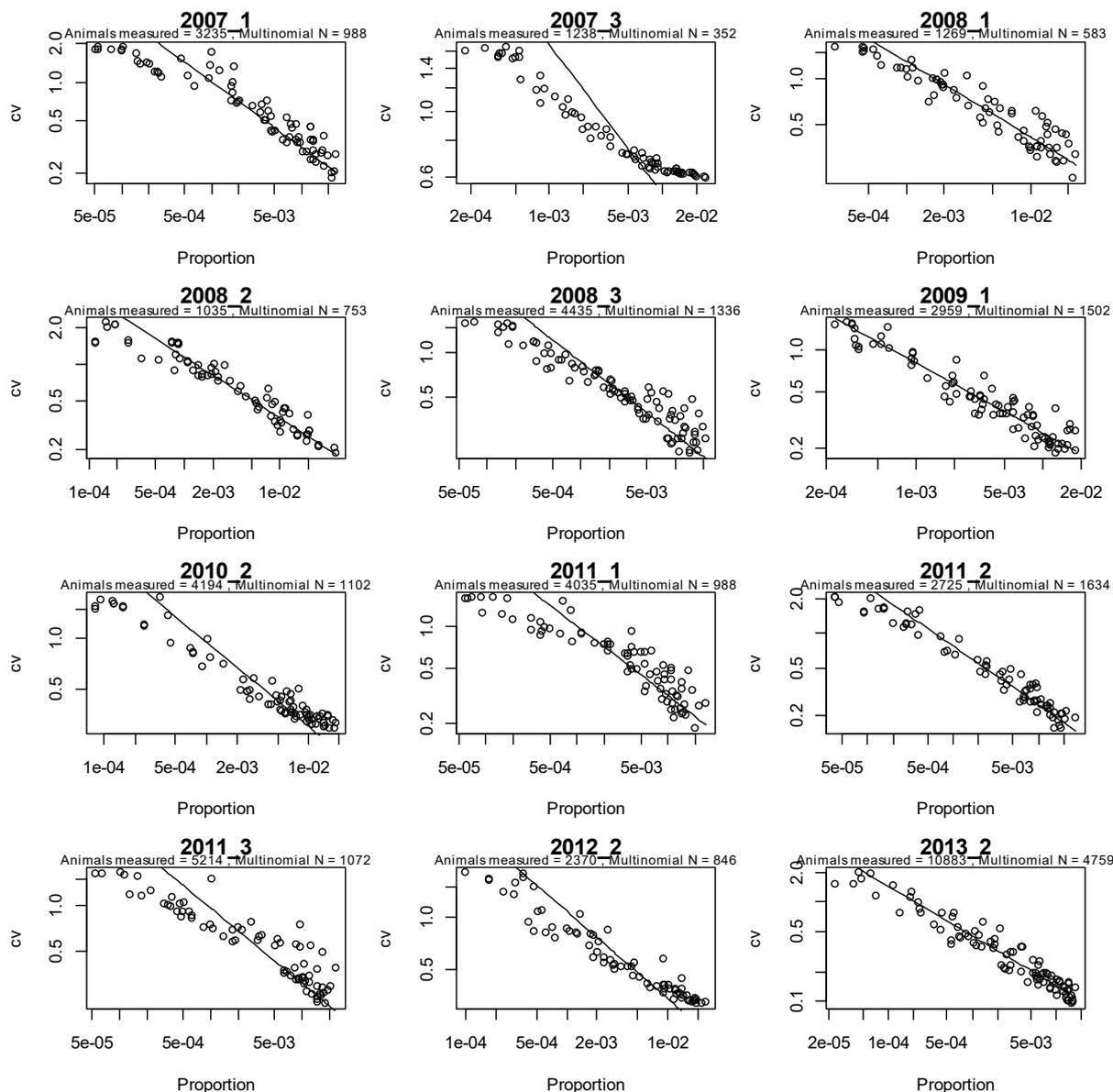
A2. 4: Observation-error CVs for the observer proportions-at-length data sets. Each point represents a proportion at a specific length and sex for a given year. The diagonal line, which is the same in each panel, is added to aid comparison between panels; it shows the relationship between proportion and CV that would hold with simple multinomial sampling with sample size 500.
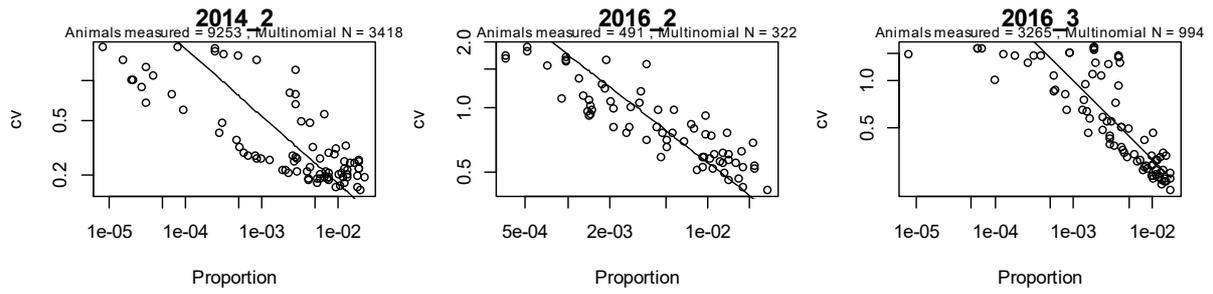
A2. 5: Observation-error CVs for the observer proportions-at-length data sets. Each point represents a proportion at a specific length and sex for a given year. The diagonal line, which is the same in each panel, is added to aid comparison between panels; it shows the relationship between proportion and CV that would hold with simple multinomial sampling with sample size 500.

Photo survey
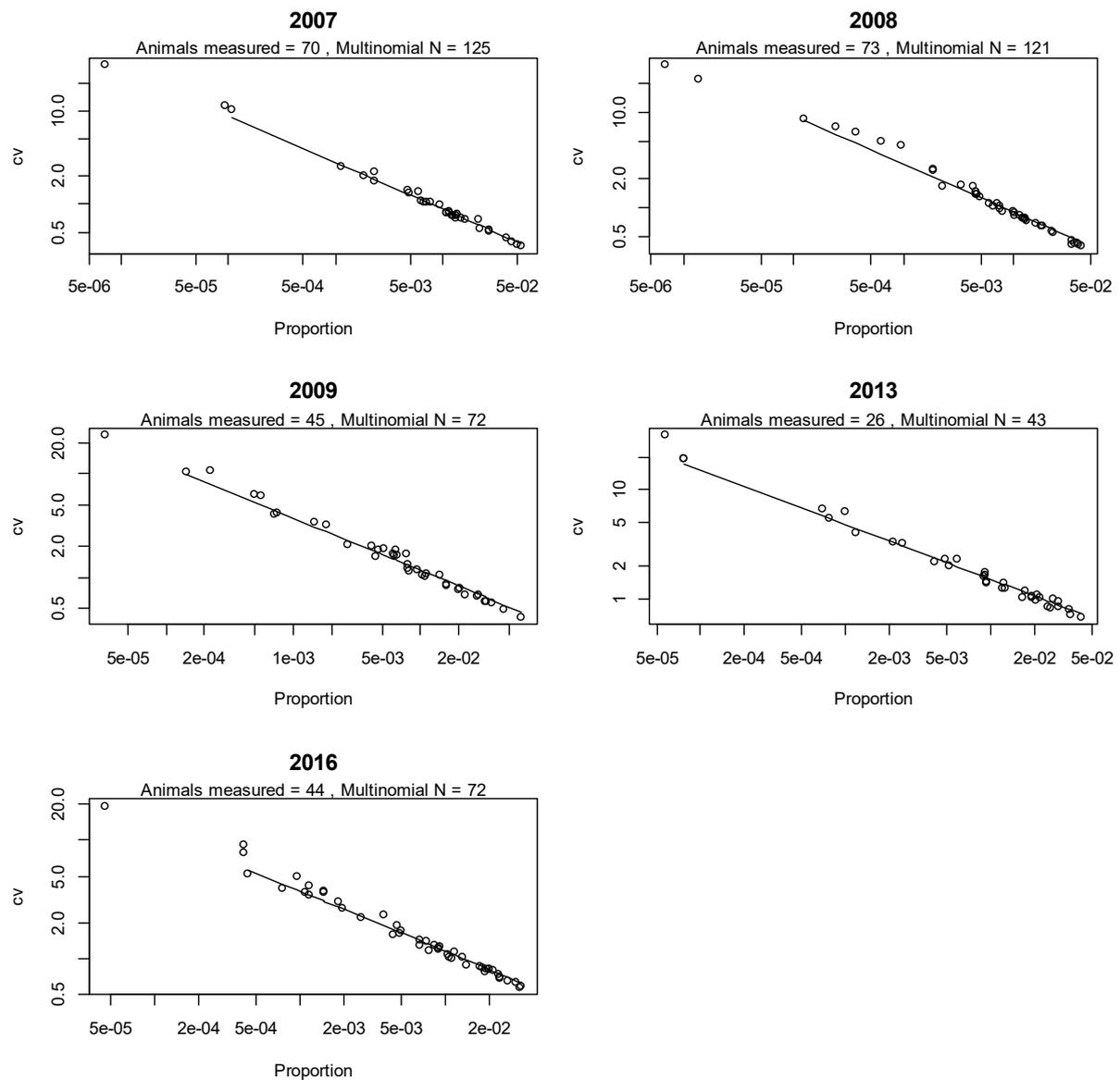
A2. 6: Observation-error CVs for the photo survey proportions-at-length data sets. Each point represents a proportion at a specific length and sex for a given year. The diagonal line, which is the same in each panel, is added to aid comparison between panels; it shows the relationship between proportion and CV that would hold with simple multinomial sampling with sample size 500.

Kaharoa scampi trawl
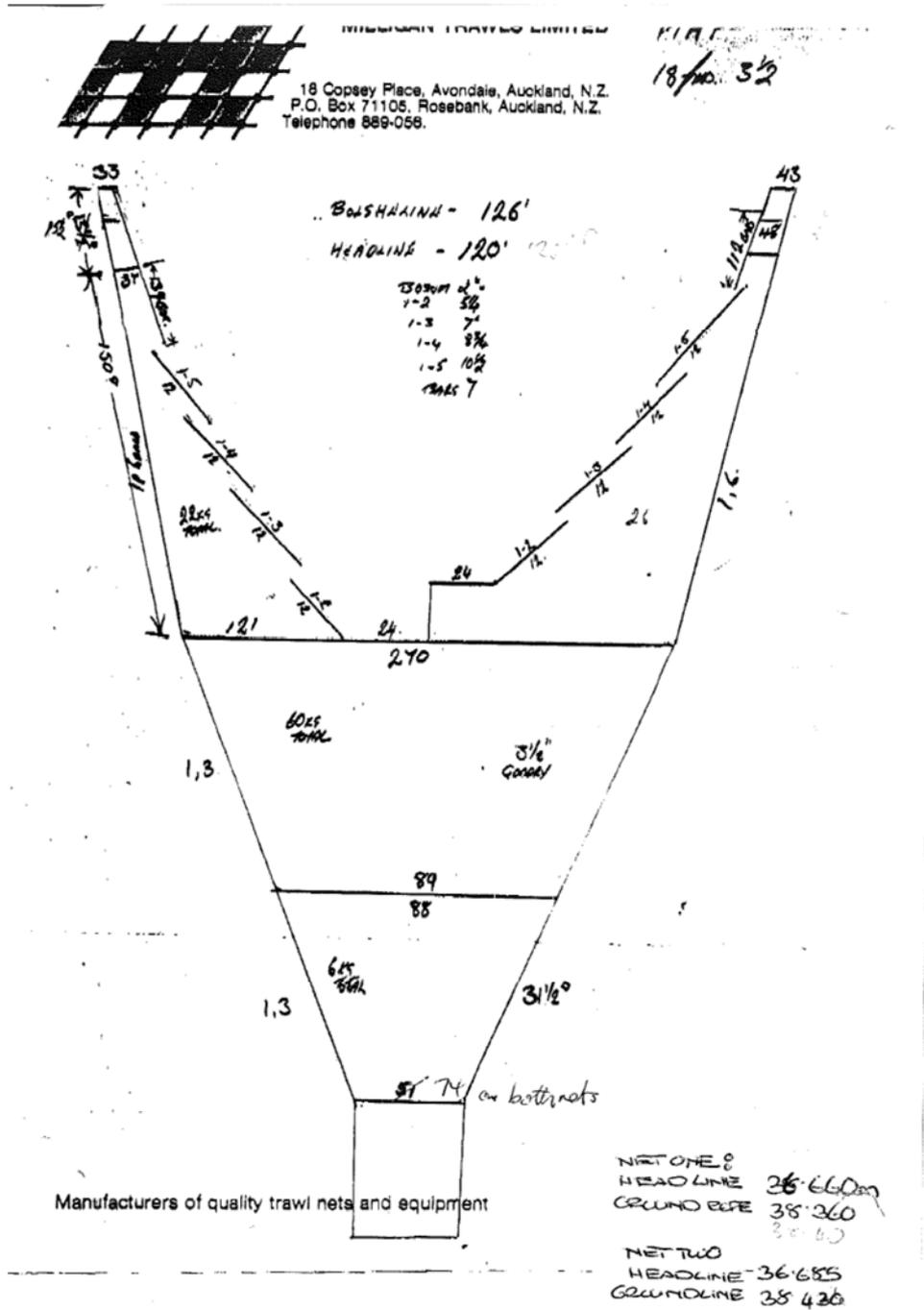
Florida Flyer type Scandi Trawl
Milligan Trawls 1992.
Headline   108' 9½"   33.18m
Bolshline   114' 11½"   35.04m
Wing Ropes   5' 6"   1.7m.

San Tongariro scampi trawl

Headline 49.77m
Footrope 49.77m 18mm rope served

REF:SAN_SCAM_01/03/05

HAMPIDJAN
30 Vickerman Street Port Nelson PO BOX 5087
TEL: +64 3 548 7942 FAX: +64 3 548 0561
www.hampidjan.co.nz

50m San Tongariro Scampi

Design: Hampidjan NZ

Sanford

San Tongariro Groundrope 49.77m

18mm 6/19RFC

Chain droppers 2 x 13mm M/L

550mm

9.38m

500mm

8.5m

490mm

4m

450mm

2m

1m

450mm

☐ Scampi weights

Distance between weights

Distance between droppers

Gear comparison between Kaharoa and San Tongariro scampi trawls (as employed during scampi surveys)

Parameter	Kaharoa	San Tongariro
Groundrope length (m)	35.04	49.77
Headline length (m)	33.18	49.77
Groundrope type	Rubber cookies	Looks like rubber cookies
Groundrope cookie diameter (mm)	65	Reported as served rope on plan but looks like rubber cookies from photographs
Groundrope (extra weights)	No	Yes
Groundrope dropper heights	5 links of 8 mm long link chain. Approx. 200 mm. Note: 1 link is in between the rubber cookies	2 × 13 mm medium link chain Aprox 100 mm
Groundrope dropper spacings	1 m apart	
Bottom contact	Video shows good contact	Extra weights on groundrope
Warps	Two warps	Single warp
Door type	Bison, Polaris. 1760 × 1200 mm. Code: 070515444	PolyIce Viking Extreme 3.9 m^2
Door weight	about 300 kg	625 kg
Bridle length	6.5–6.6 m	
Wingspread (measured)	24 m	21 m
Headline height	Approx. 1.0 m	1.5–1.8 m
Body of trawl mesh size (mm)	3.5" (88 mm) knot centres. About 80 mm actual opening. Twine is 3 mm twist	120 mm knot centres, 112.8 mm opening
Cod-end mesh size (Inside measurement.	42 mm opening or 48 mm knot centres. 3 mm twist	42 mm opening centres. 3 mm twist

APPENDIX 4. MODEL 1, M fixed at 0.20, CV on YCS prior 0.4
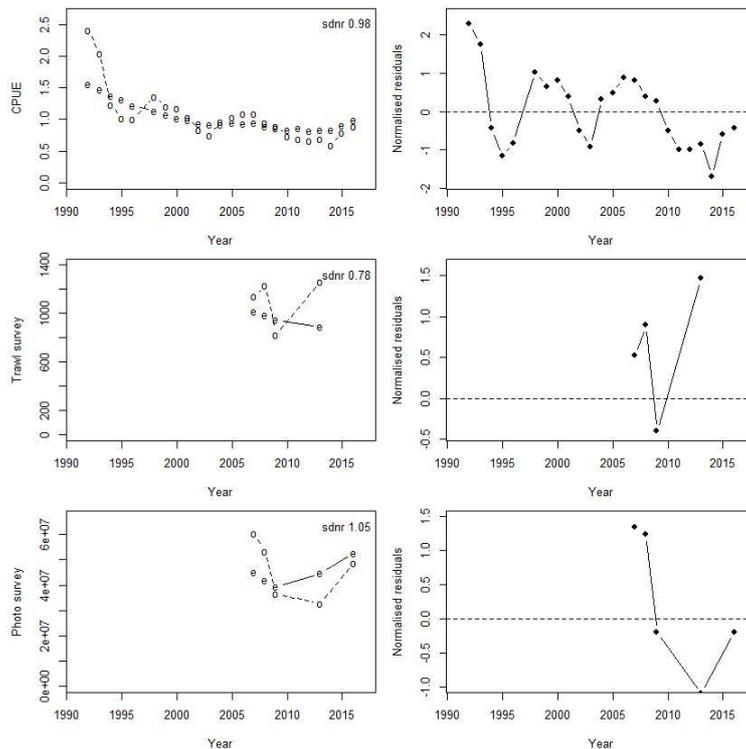
A4. 1: Fits to abundance indices (left column) and normalised residuals (right column) for standardised CPUE index (top row) trawl survey biomass index (middle row) and photo survey abundance index (bottom row) for SCI 6A Model 1.
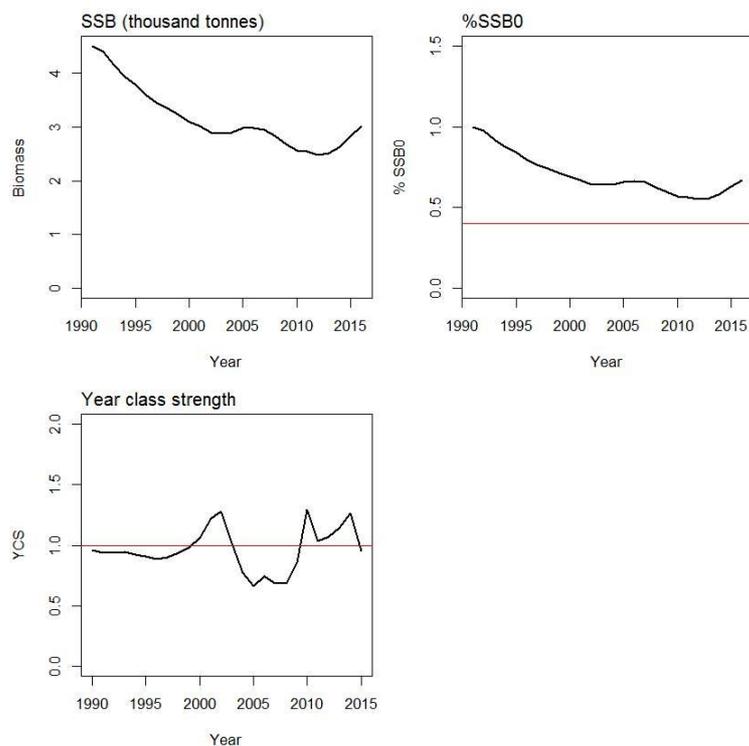
A4. 2: Spawning stock biomass trajectory (upper left), Spawning stock biomass as a percentage of SSB$_0$ (upper right), and year class strength (lower plot) for SCI 6A Model 1.
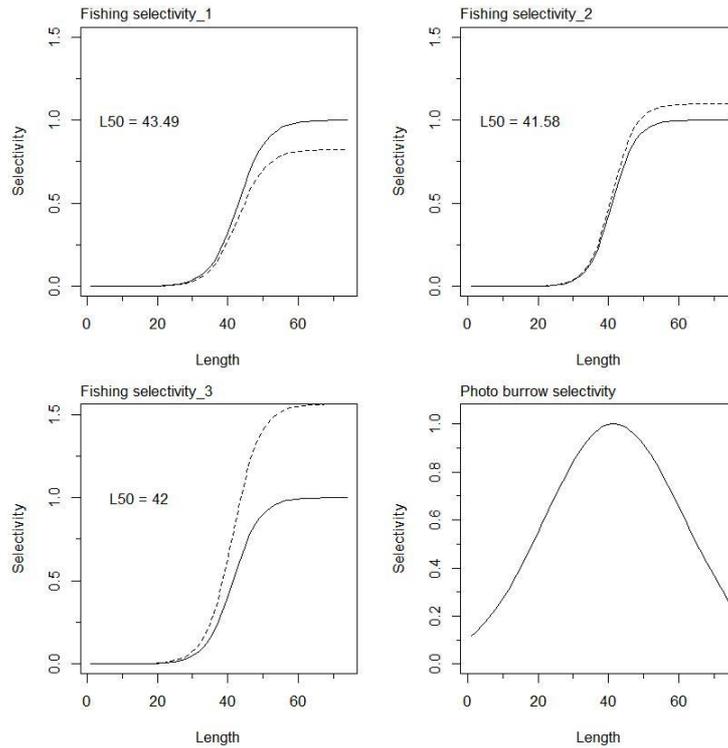
A4. 3: Fishery and photo survey selectivity curves for SCI 6A Model 1. Solid line – females, dotted line – males. The scampi photo index is not sexed, and a single selectivity applies.
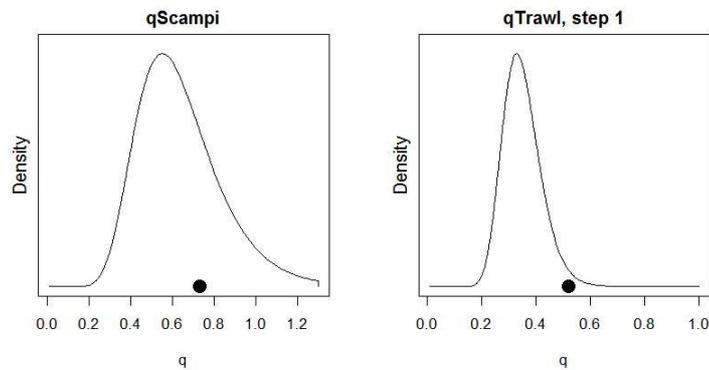
A4. 4: Catchability estimates from MPD model run for SCI 6A Model 1, plotted in relation to prior distribution.
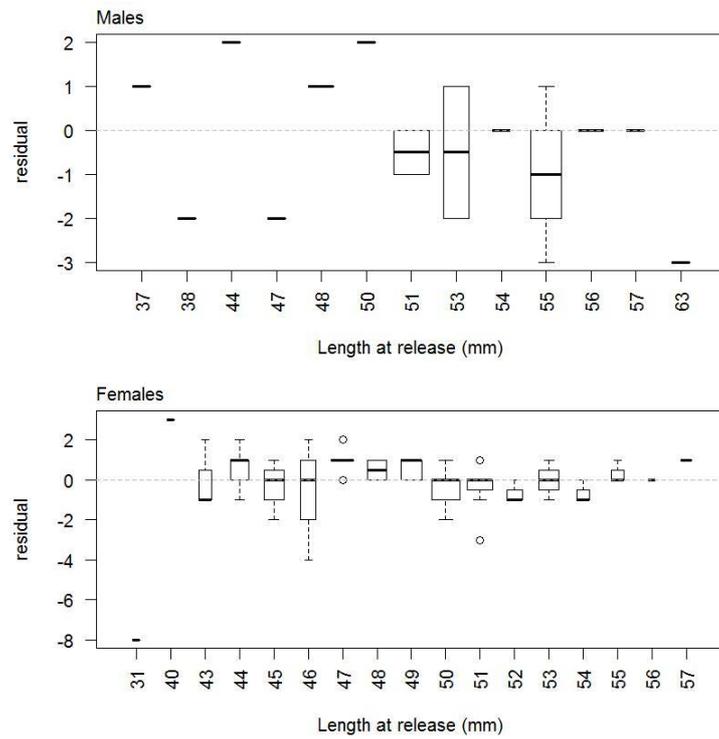
A4. 5: Box plots of residuals from the fit to growth increment by length from tag recapture data by sex for SCI 6A Model 1.
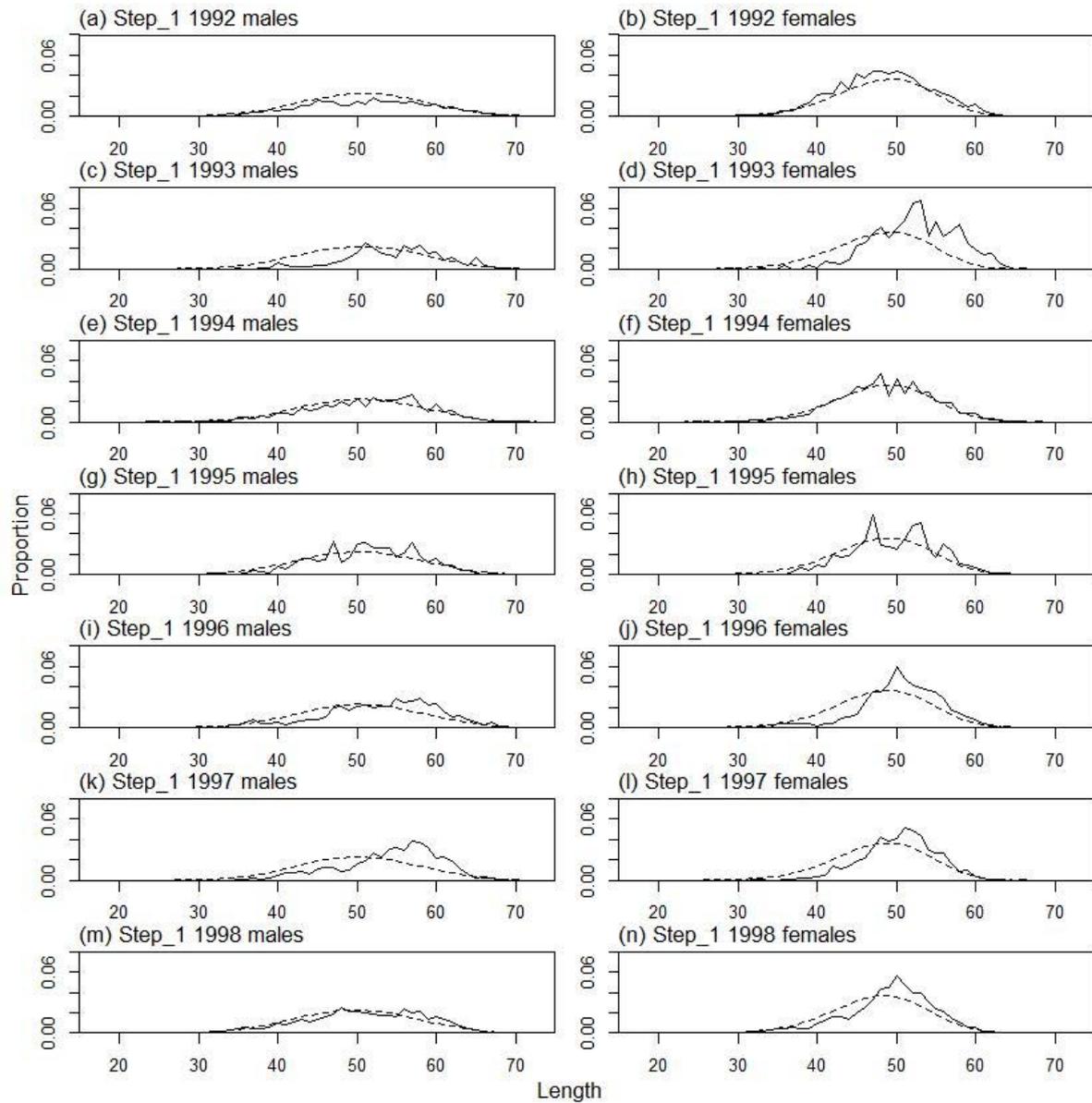
A4. 6: Observed (solid line) and fitted (dashed line) length frequency distributions for observer samples, time step 1.
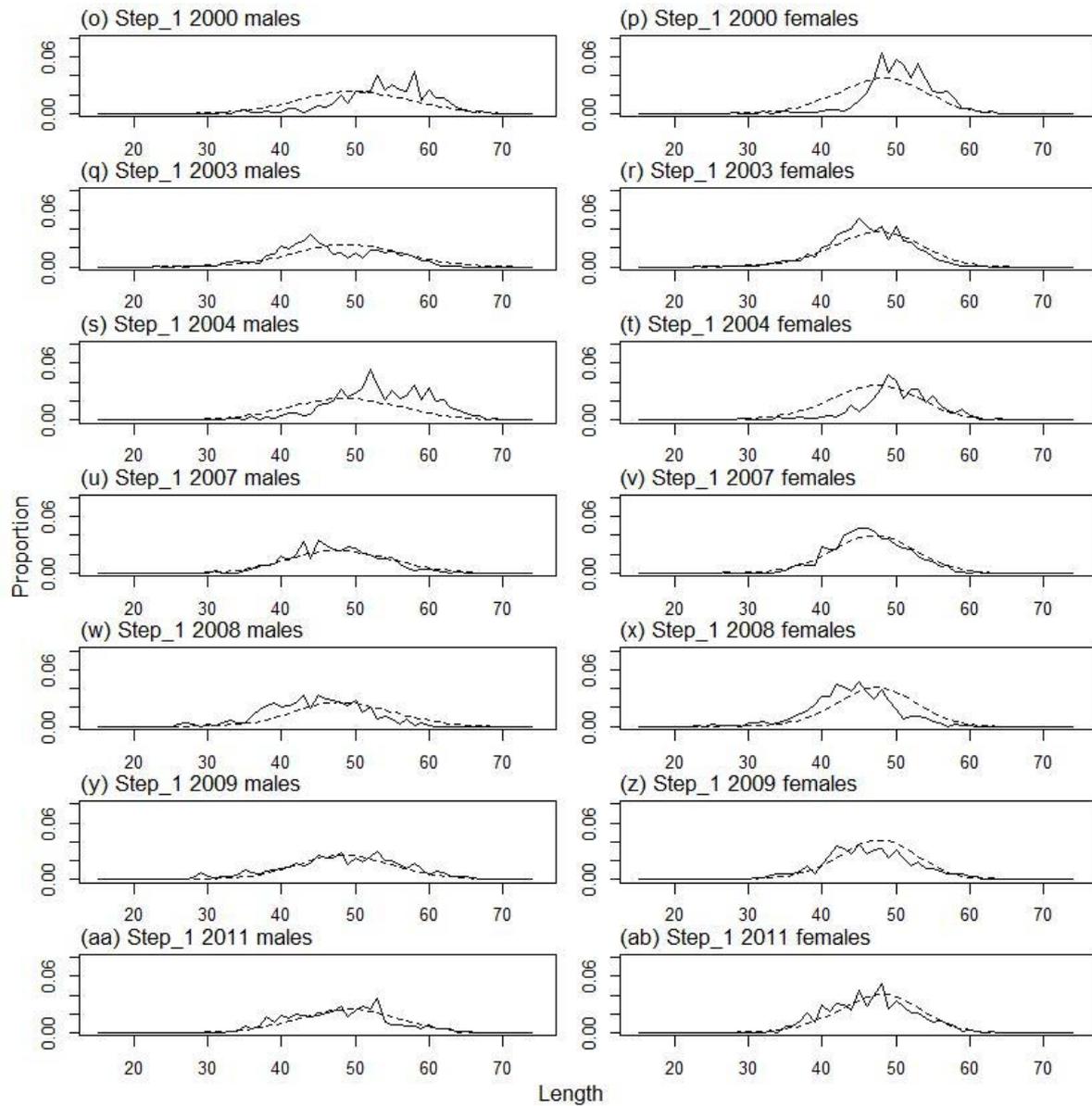
A4. 6 ctd.: Observed (solid line) and fitted (dashed line) length frequency distributions for observer samples, time step 1.
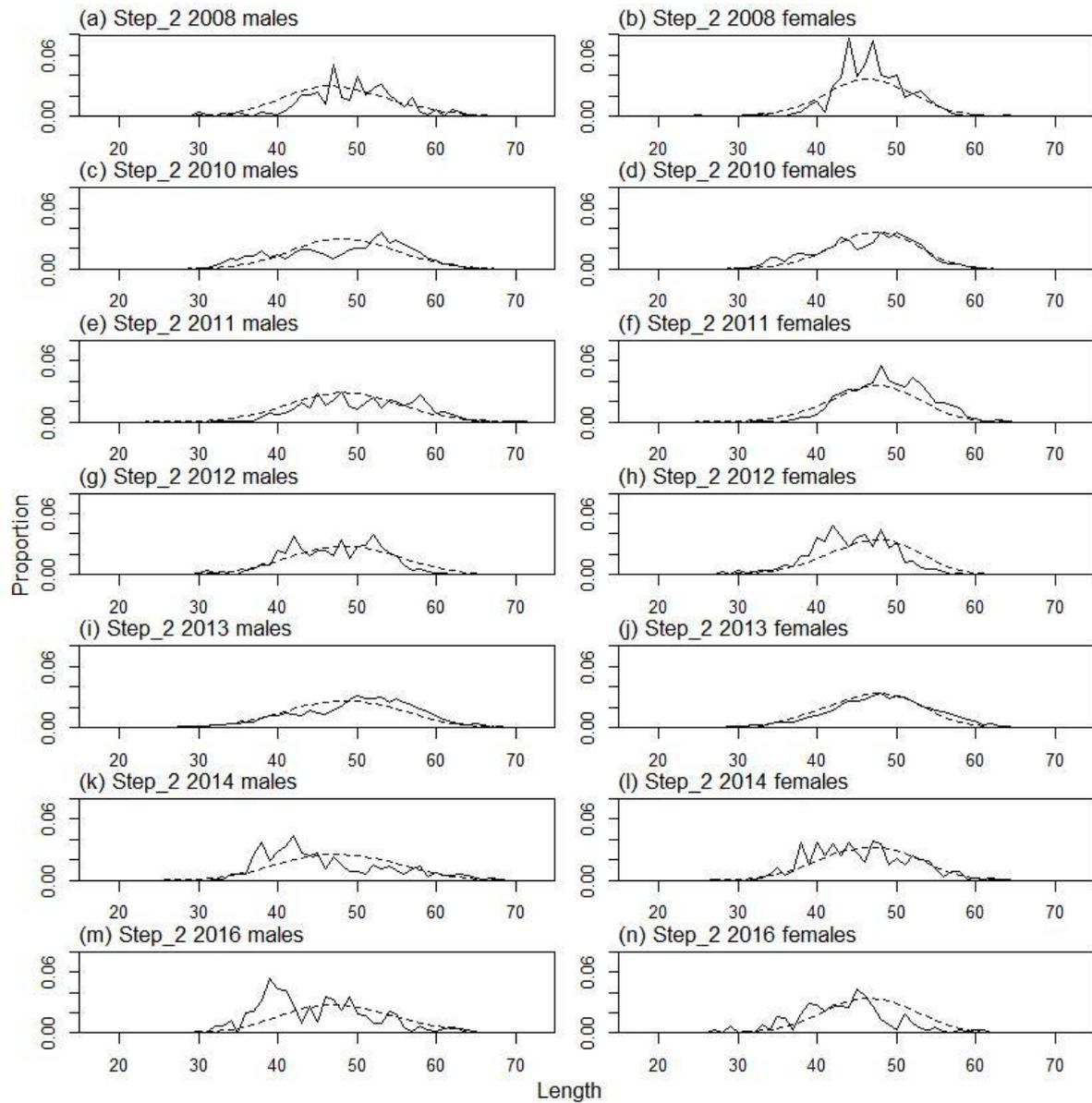
A4. 7: Observed (solid line) and fitted (dashed line) length frequency distributions for observer samples, time step 2.
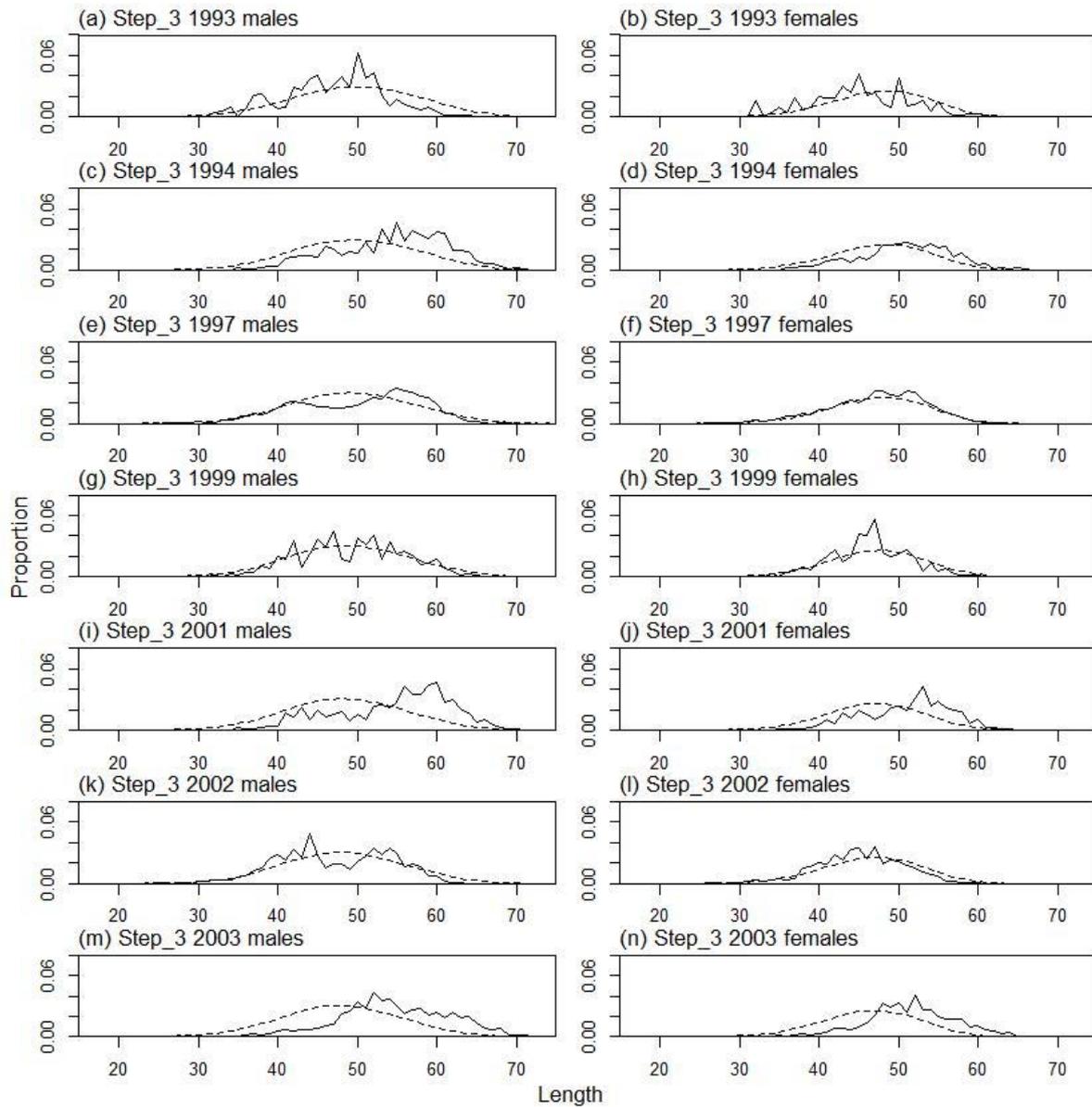
A4. 8: Observed (solid line) and fitted (dashed line) length frequency distributions for observer samples, time step 3.
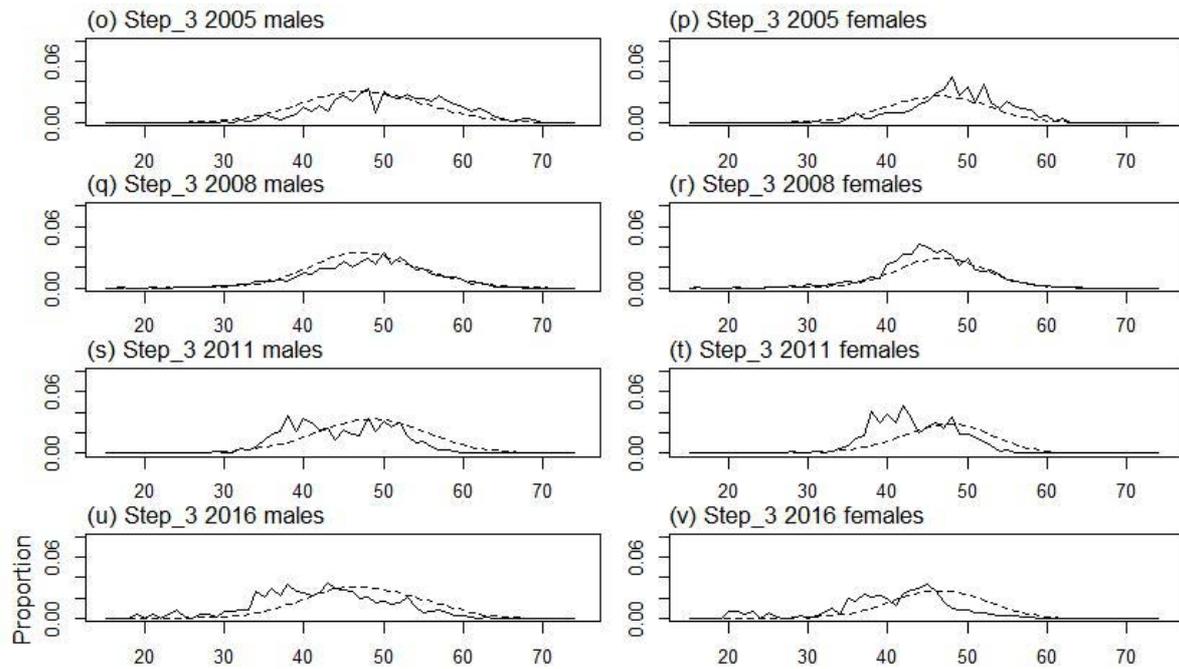
A4. 8 ctd.: Observed (solid line) and fitted (dashed line) length frequency distributions for observer samples, time step 3.

A4. 9: Numbers of scampi measured, estimated multinomial N sample size, and effective sample size used within the model for length frequency distributions for observer samples, time step 1.

	Measured	Multinomial N	Effective sample size
N_1992	9 250	3 373	25.80
N_1993	2 641	3 340	10.51
N_1994	9 300	3 924	30.03
N_1995	2 600	1 360	10.69
N_1996	3 200	1 690	13.42
N_1997	2 794	1 165	8.89
N_1998	11 964	4 863	35.60
N_2000	2 449	935	7.25
N_2002	1 975	458	3.42
N_2003	4 965	2 109	16.42
N_2004	1 214	760	6.12
N_2007	3 235	1 006	7.99
N_2008	1 269	568	4.65
N_2009	2 959	1 504	11.81
N_2011	4 035	937	7.45

A4. 10: Numbers of scampi measured, estimated multinomial N sample size, and effective sample size used within the model for length frequency distributions for observer samples, time step 2.

	Measured	Multinomial N	Effective sample size
N_1997	3 287	1 509	13.03
N_1998	703	472	4.08
N_2001	4 782	2 521	21.77
N_2008	1 035	754	6.51
N_2010	4 194	962	8.31
N_2011	2 725	1 601	13.82
N_2012	2 370	860	7.43
N_2013	10 883	4 650	40.15
N_2014	9 253	3 418	29.51
N_2016	491	322	2.78

A4. 11: Numbers of scampi measured, estimated multinomial N sample size, and effective sample size used within the model for length frequency distributions for observer samples, time step 3.

	Measured	Multinomial N	Effective sample size
N_1993	1 264	740	1.87
N_1994	1 960	1 192	3.01
N_1996	2 035	736	1.86
N_1997	8 816	5 002	12.62
N_1998	172	147	0.37
N_1999	2 707	1 575	3.97
N_2001	1 650	332	0.84
N_2002	5 663	1 184	2.99
N_2003	8 746	3 332	8.40
N_2005	1 600	1 215	3.06
N_2007	1 238	350	0.88
N_2008	4 435	1 300	3.28
N_2011	5 214	1 104	2.78
N_2016	3 265	994	2.51
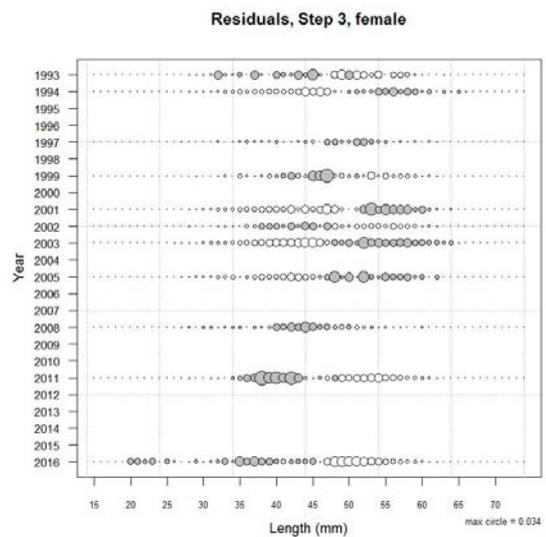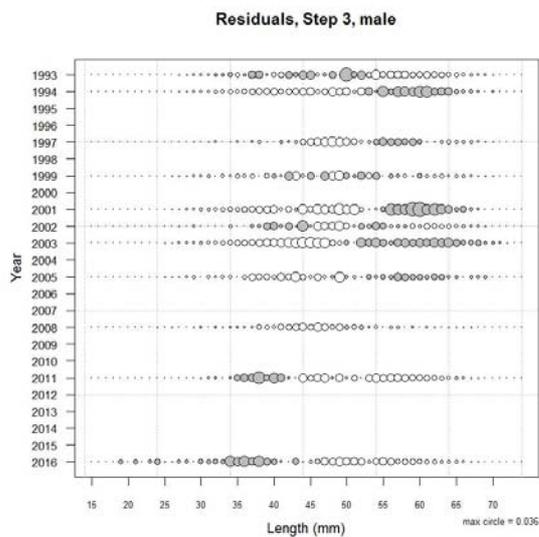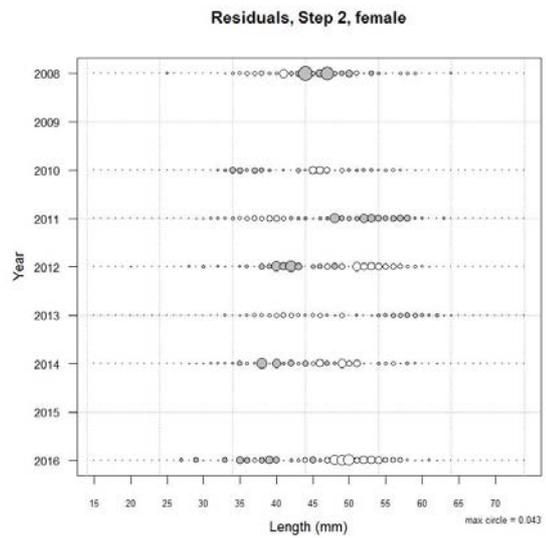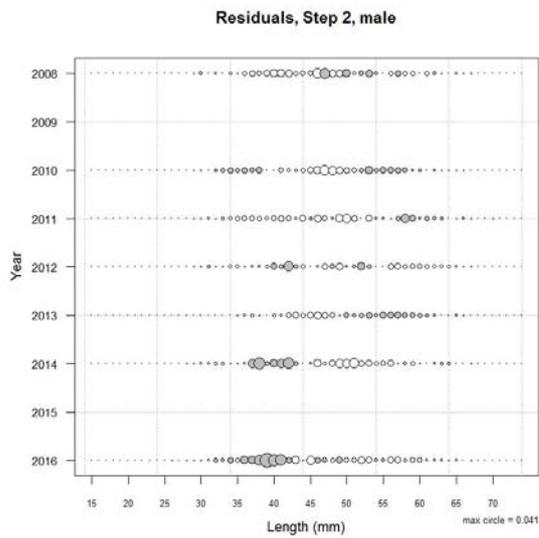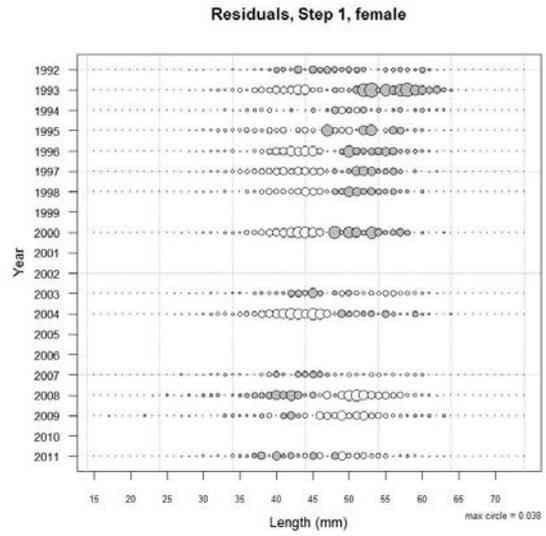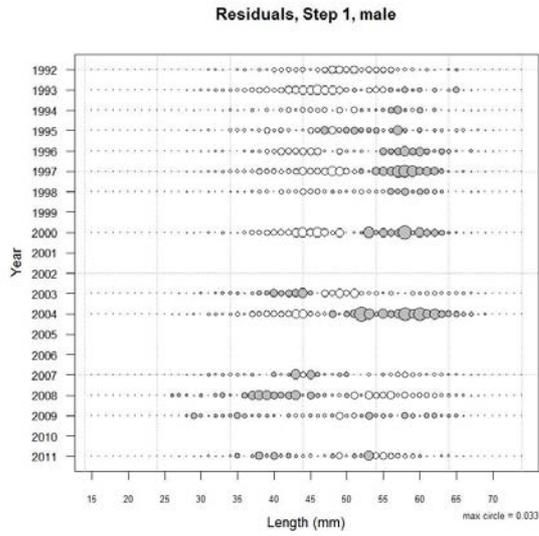
A4. 12: Bubble plots of residuals for fits to length frequency distributions for observer sampling.
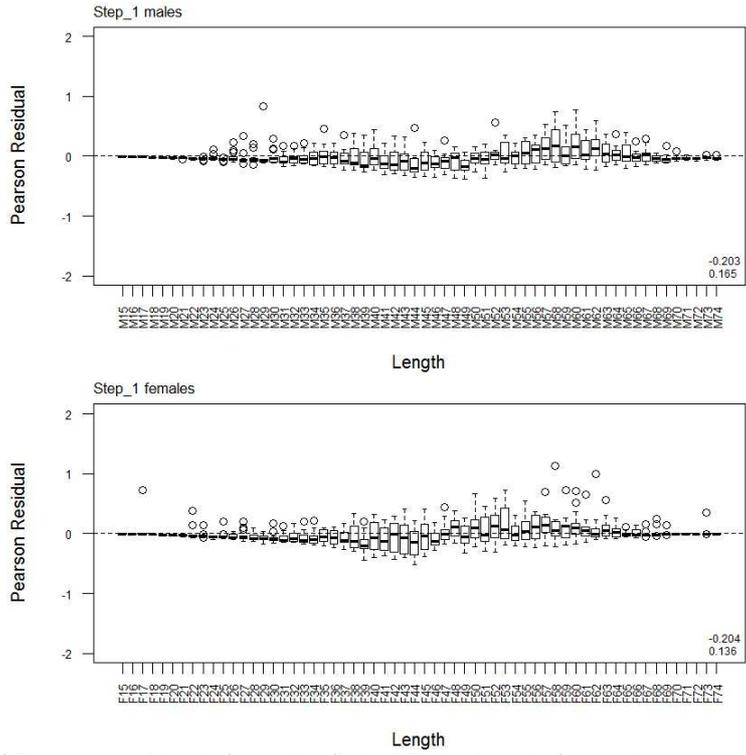
A4. 13: Box plots of Pearson residuals from the fit to LFs by length from observer sampling by sex for time step 1.
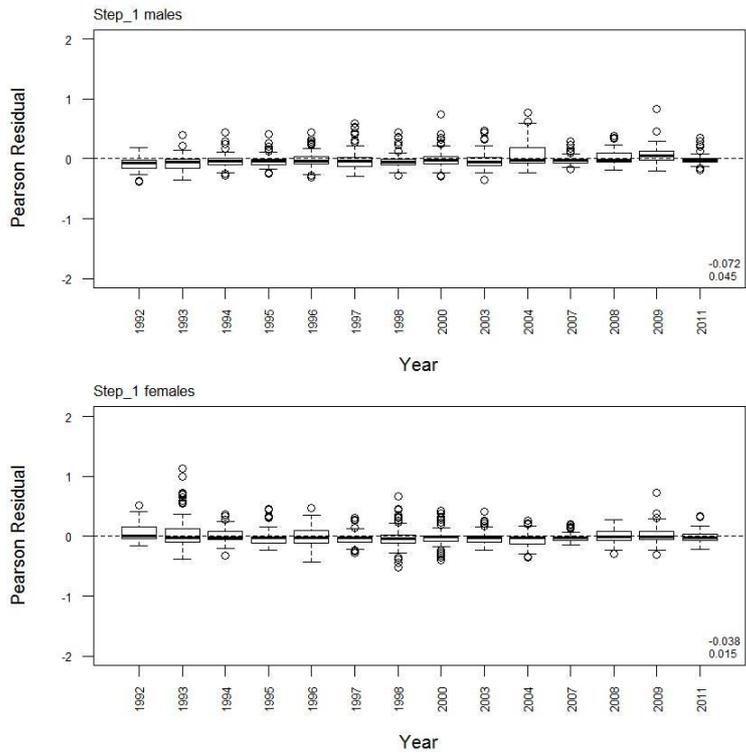
A4. 14: Box plots of Pearson residuals from the fit to LFs by year from observer sampling by sex for time step 1.
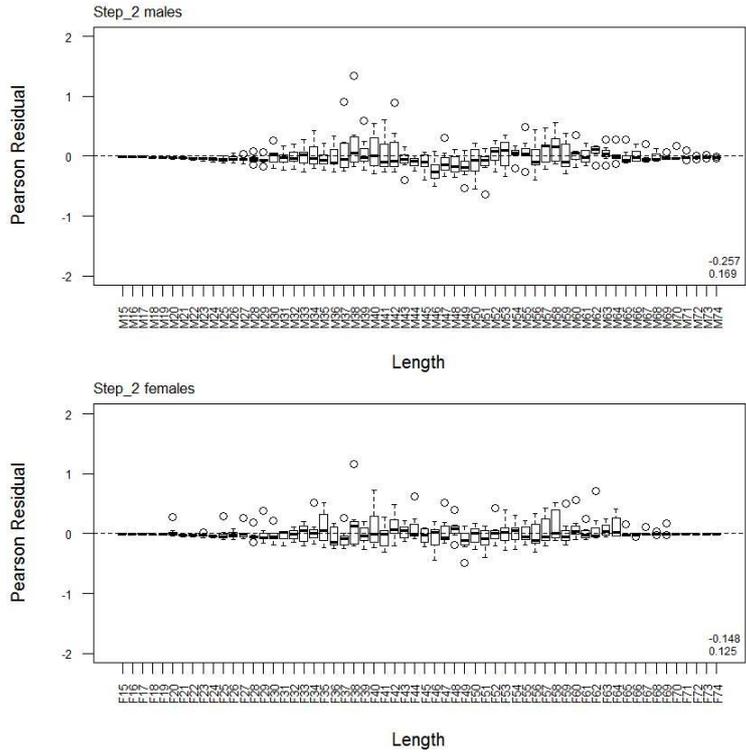
A4. 15: Box plots of Pearson residuals from the fit to LFs by length from observer sampling by sex for time step 2.
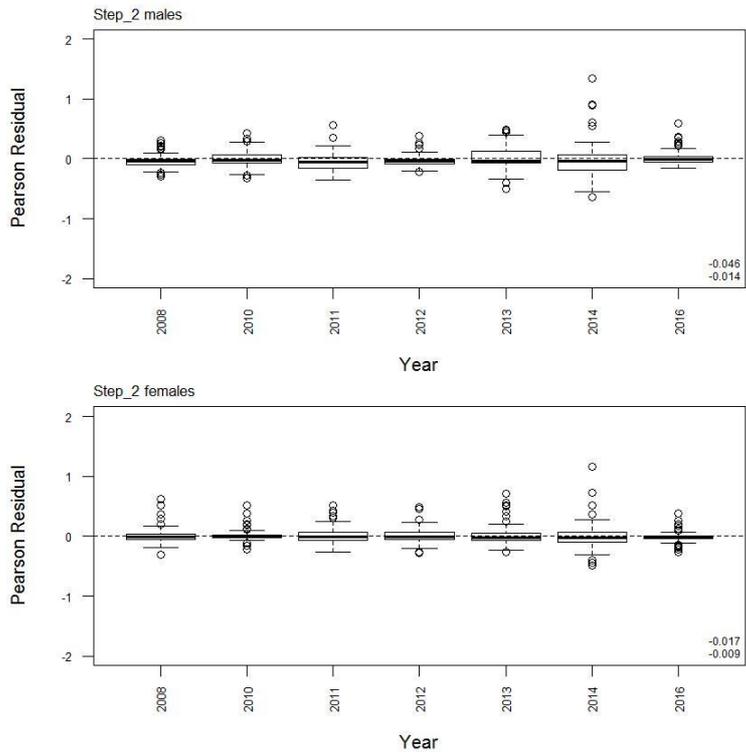
A4. 16: Box plots of Pearson residuals from the fit to LFs by year from observer sampling by sex for time step 2.
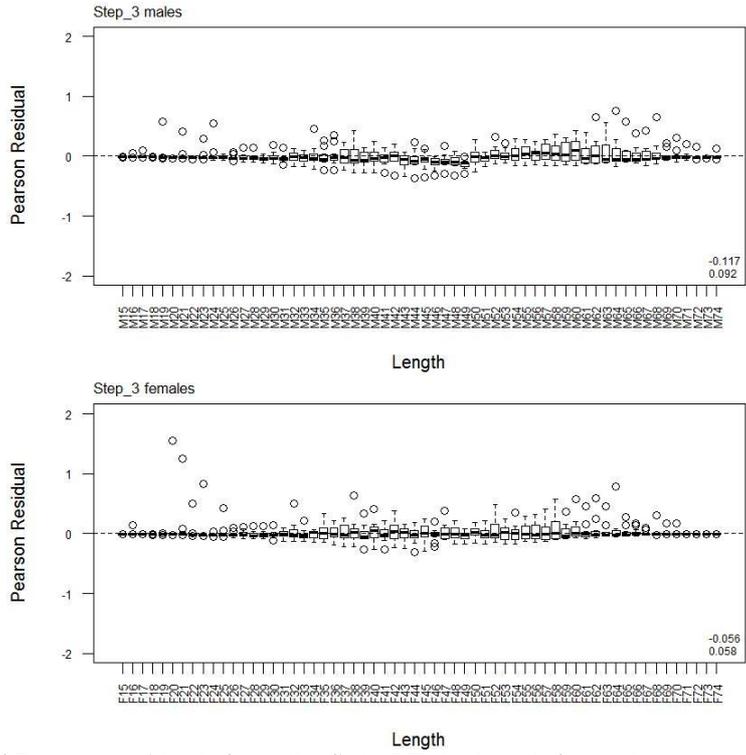
A4. 17: Box plots of Pearson residuals from the fit to LFs by length from observer sampling by sex for time step 3.
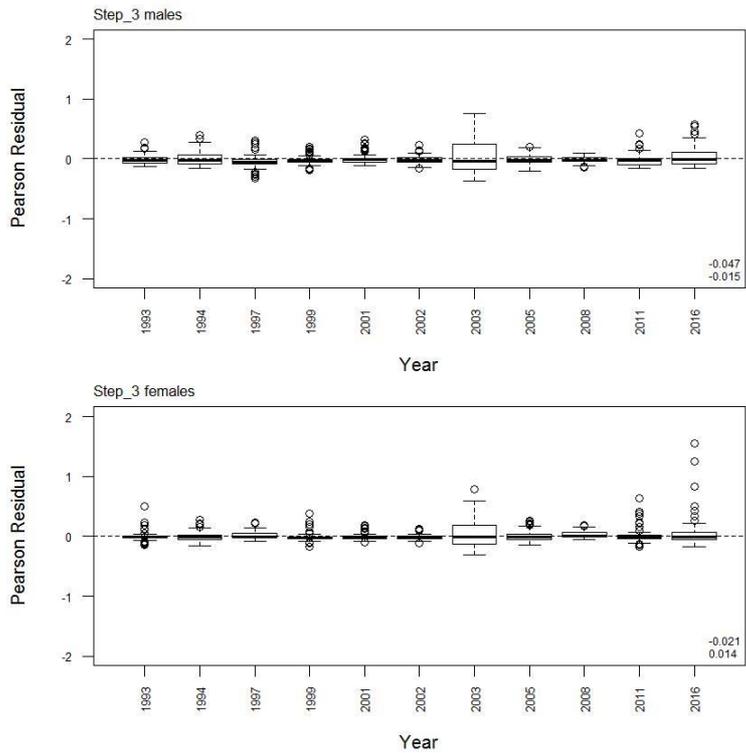
A4. 18: Box plots of Pearson residuals from the fit to LFs by year from observer sampling by sex for time step 3.
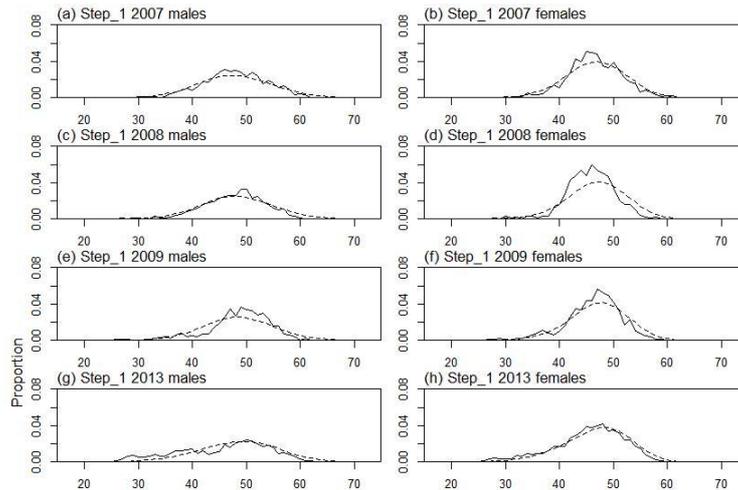
A4. 19: Observed (solid line) and fitted (dashed line) length frequency distributions for research survey samples.
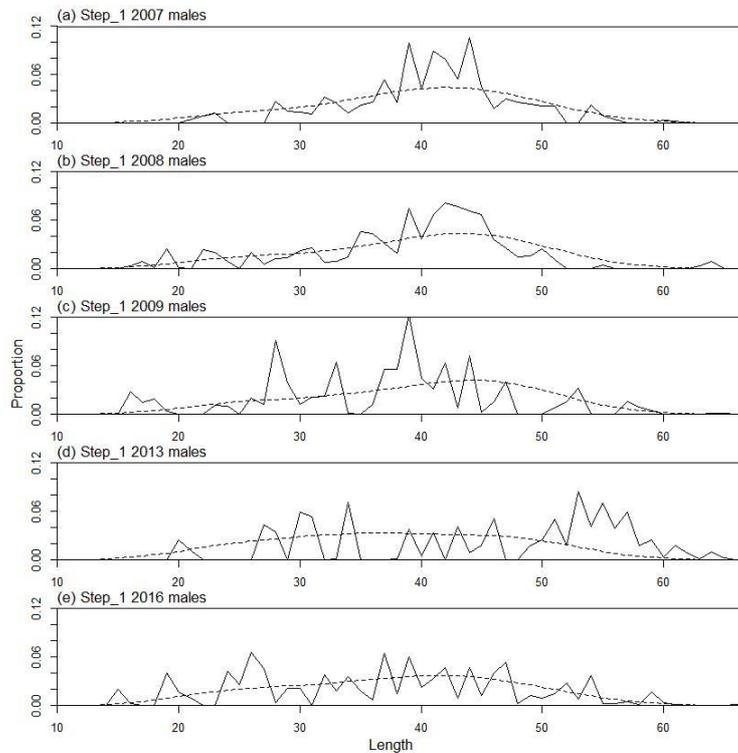
A4. 20: Observed (solid line) and fitted (dashed line) length frequency distributions for photographic survey scampi size estimation.

A4. 21: Numbers of scampi measured, estimated multinomial N sample size, and effective sample size used within the model for length frequency distributions for research survey samples.

	Measured	Multinomial N	Effective sample size
N_2007	1 981	2 127	39.21
N_2008	2 291	1 866	34.04
N_2009	4 054	2 798	52.20
N_2013	4 808	4 218	76.35

A4. 22: Numbers of scampi measured, estimated multinomial N sample size, and effective sample size used within the model for length frequency distributions for photographic survey samples.

	Measured	Multinomial N	Effective sample size
N_2007	70	125	15.40
N_2008	73	121	16.06
N_2009	45	72	9.90
N_2013	26	43	5.72
N_2016	44	72	9.68
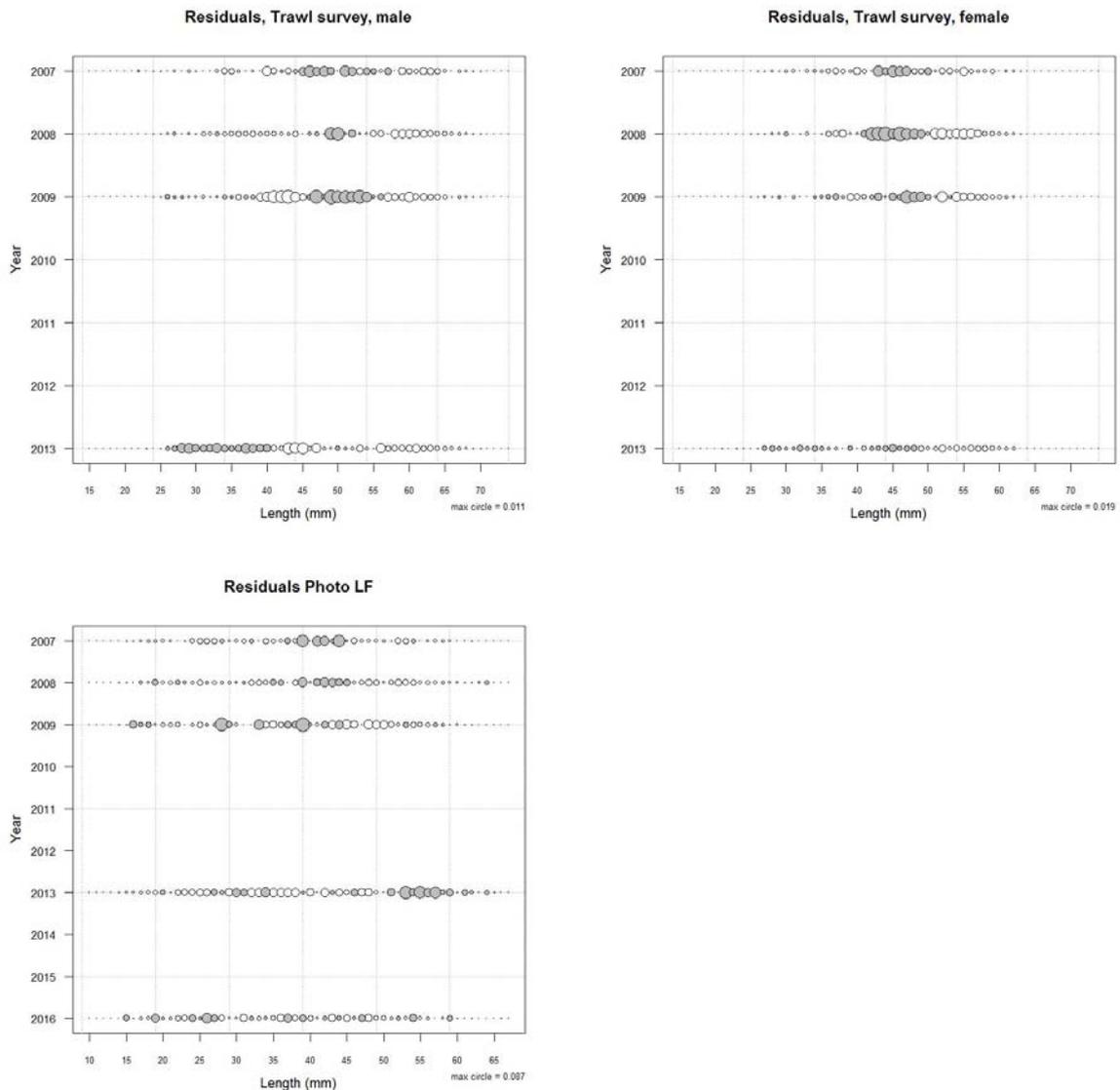
A4. 23: Bubble plots of residuals for fits to length frequency distributions for trawl survey sampling and photographic survey scampi size estimation.
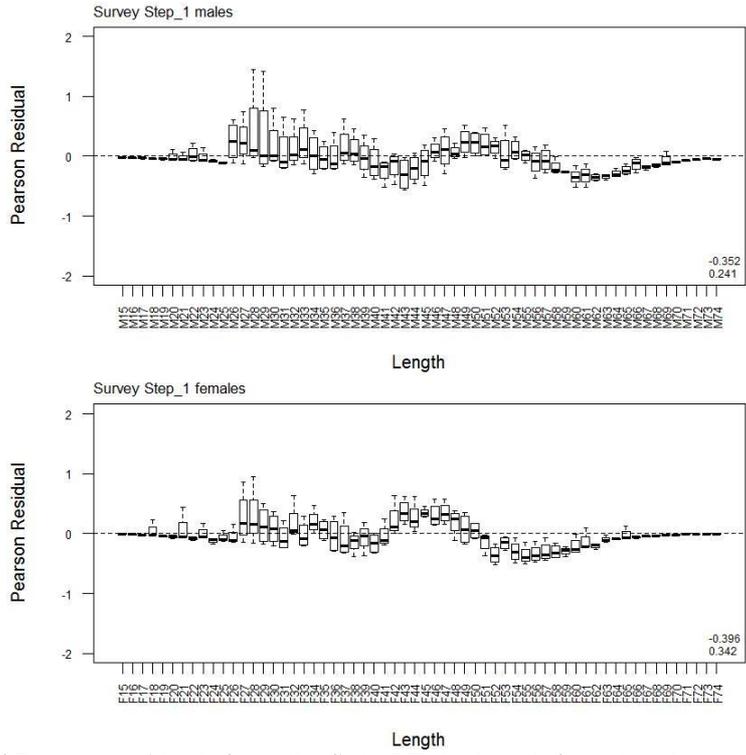
A4. 24: Box plots of Pearson residuals from the fit to LFs by length from trawl survey sampling by sex for time step 1.
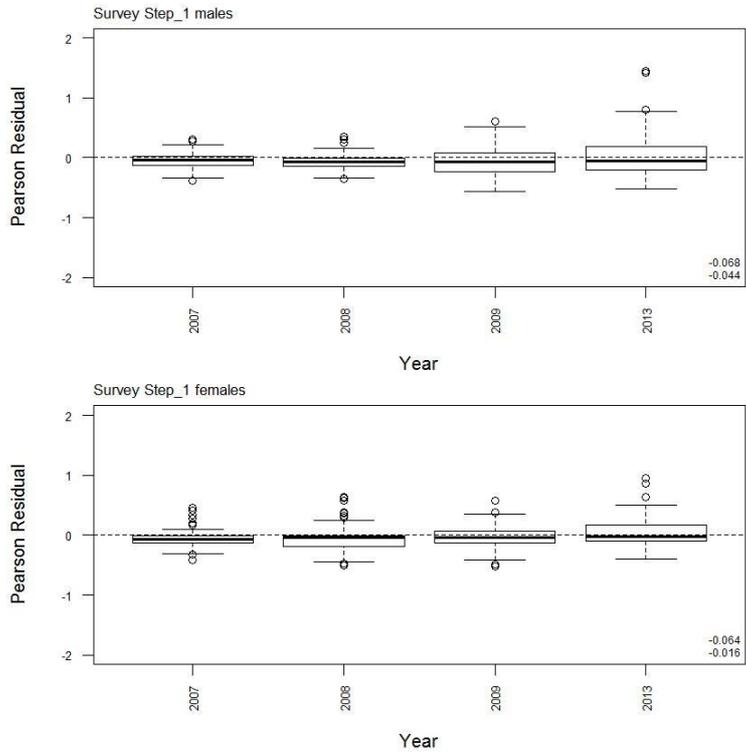
A4. 25: Box plots of Pearson residuals from the fit to LFs by year from trawl survey sampling by sex for time step 1.
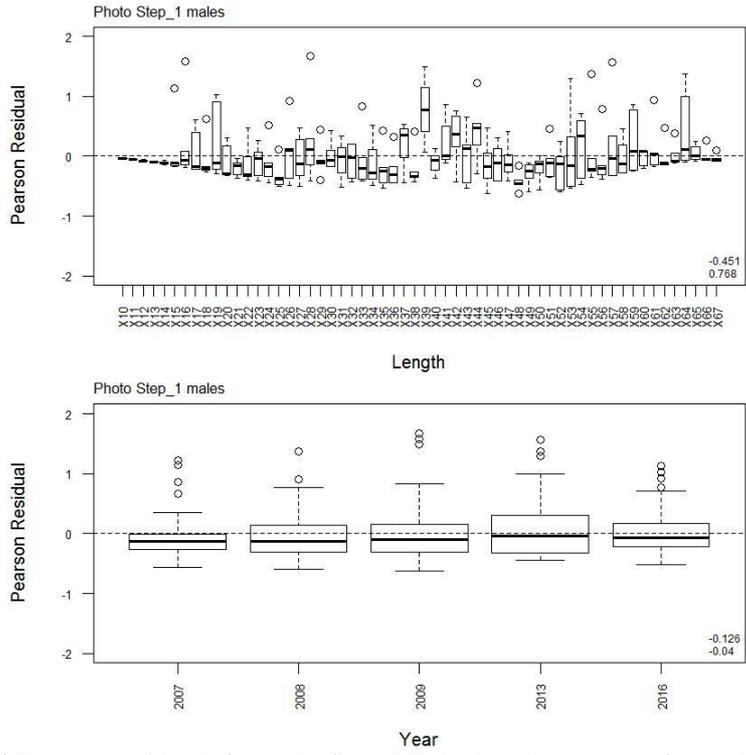
A4. 26: Box plots of Pearson residuals from the fit to LFs by length and year from photo survey sampling for time step 1.
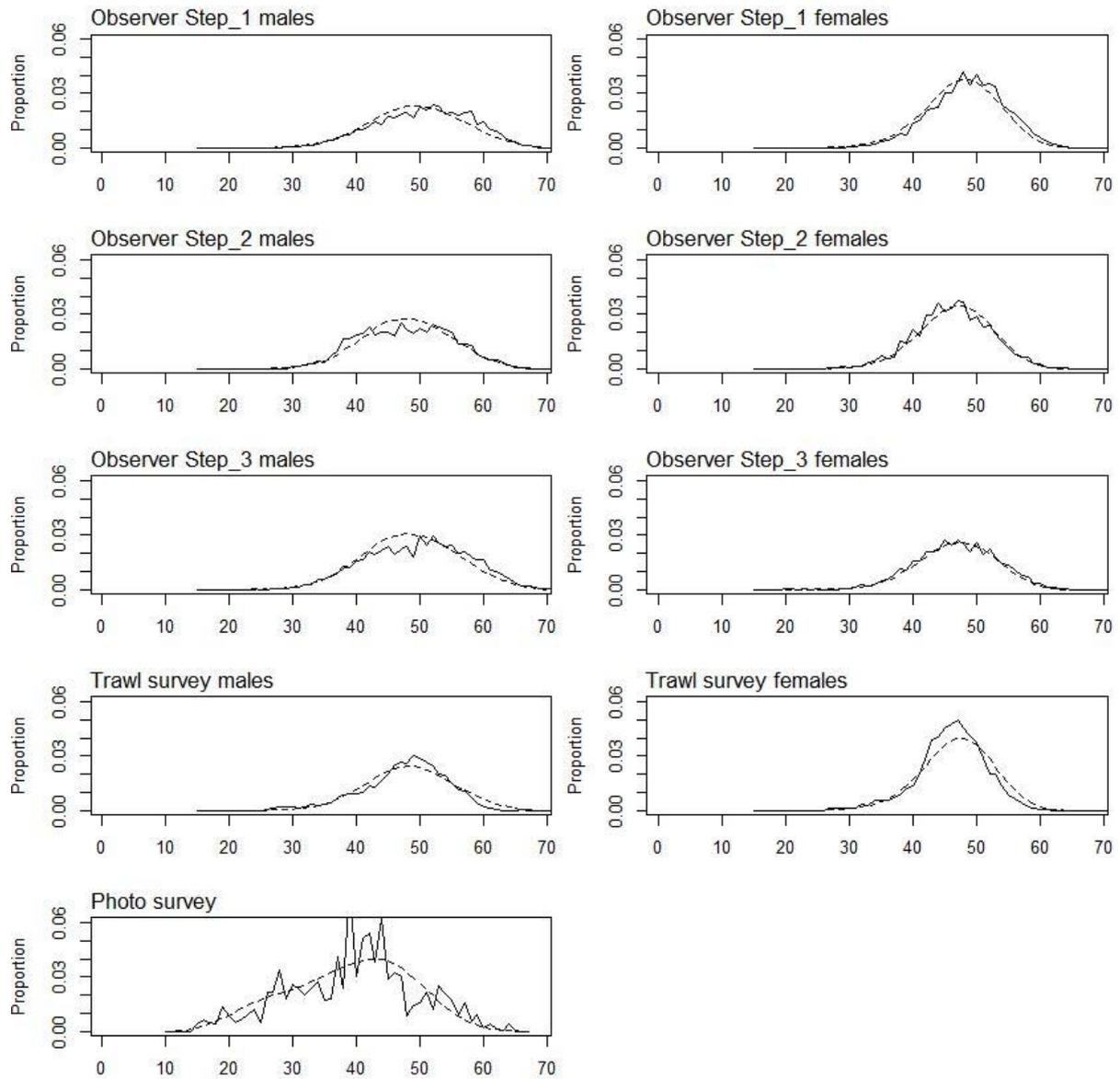
A4. 27: Average observed (solid line) and fitted (dashed line) length frequency distributions for observer and survey samples.
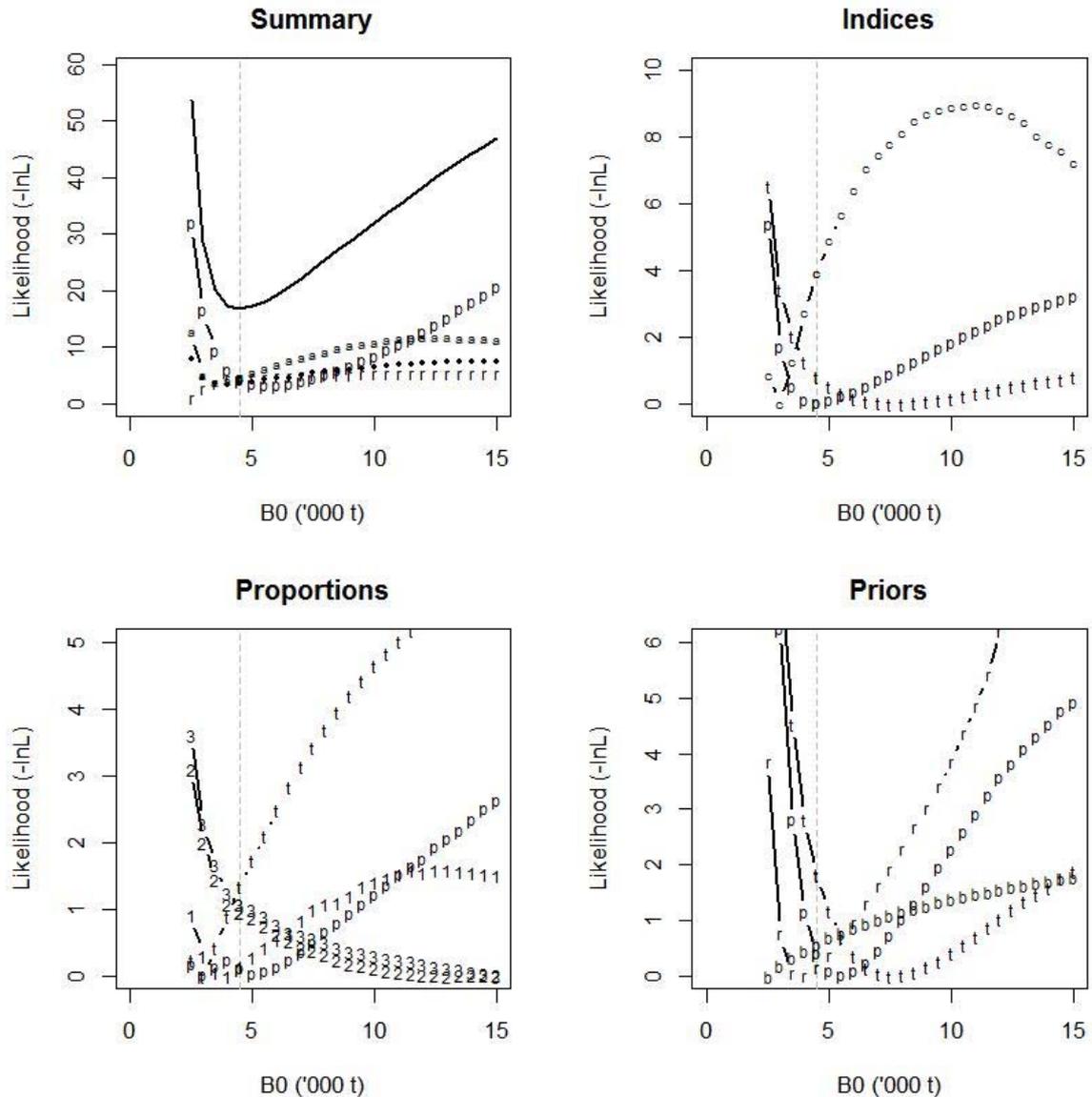
A4. 28: Likelihood profiles for SCI 6A Model 1 when B$_0$ is fixed in the model. Figures show profiles for main priors (top left, p – priors, a - abundance indices, • – proportions at length, r – recapture data), abundance indices (top right, t - trawl survey, c - CPUE, p – photo survey), proportion at length data (bottom left, a-trawl, 1 – observer time step 1, 2 – observer time step 2, 3 – observer time step 3, p - photo) and priors (bottom right, b- B$_0$, YCS - r, p- *q-Photo*, t – *q-Trawl*). Vertical dashed line represents MPD.
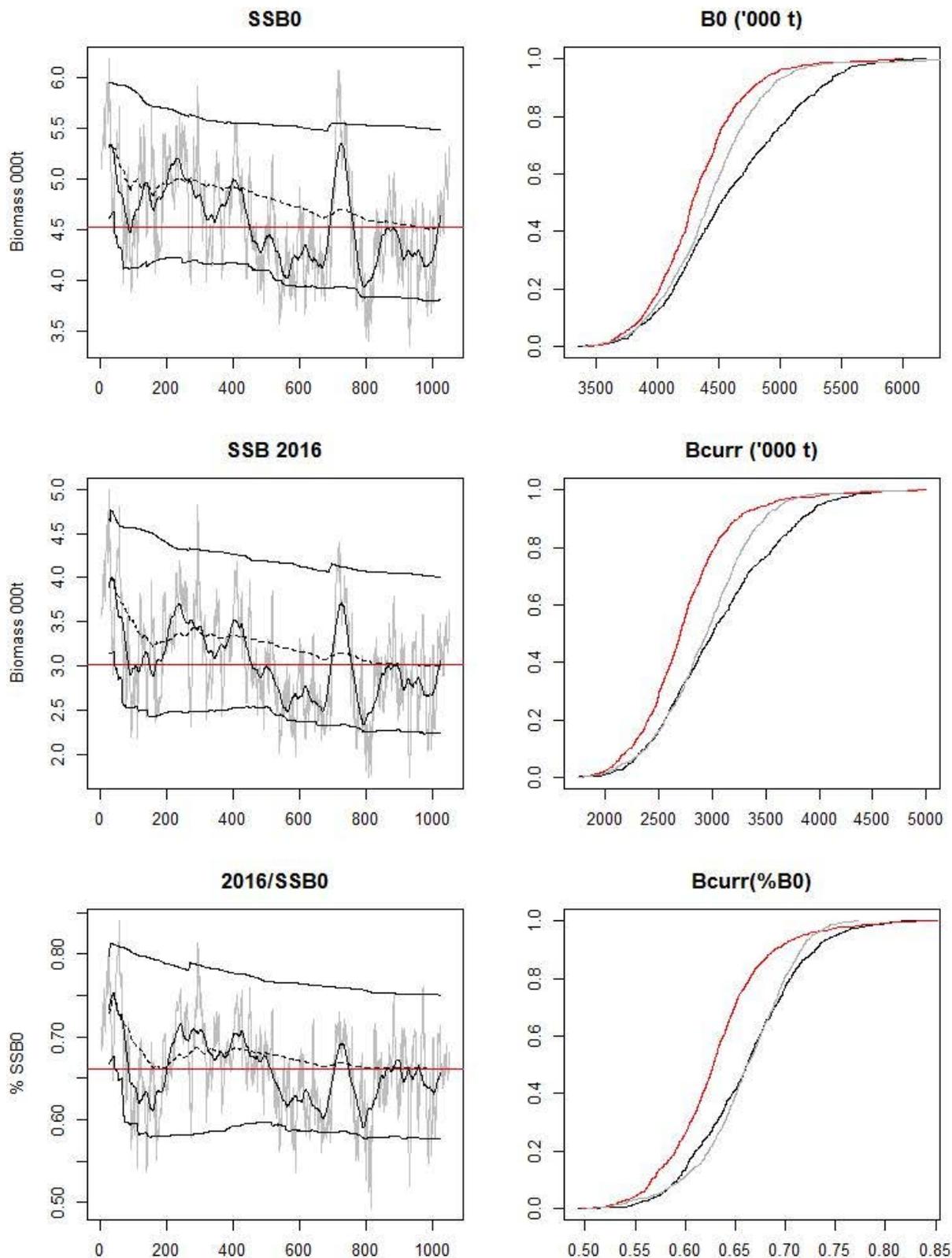
A4. 29: MCMC traces for SSB$_0$, SSB$_{2016}$, and SSB$_{2016}$/SSB$_0$ terms for SCI 6A Model 1 (free q) (trace – grey line, cumulative moving median –dashed black line, moving average and cumulative moving 2.5%, 97.5% quantiles – solid black lines, overall median – solid red line, left plots), along with cumulative frequency distributions for three independent MCMC chains (shown as red, grey and black lines, right plots).
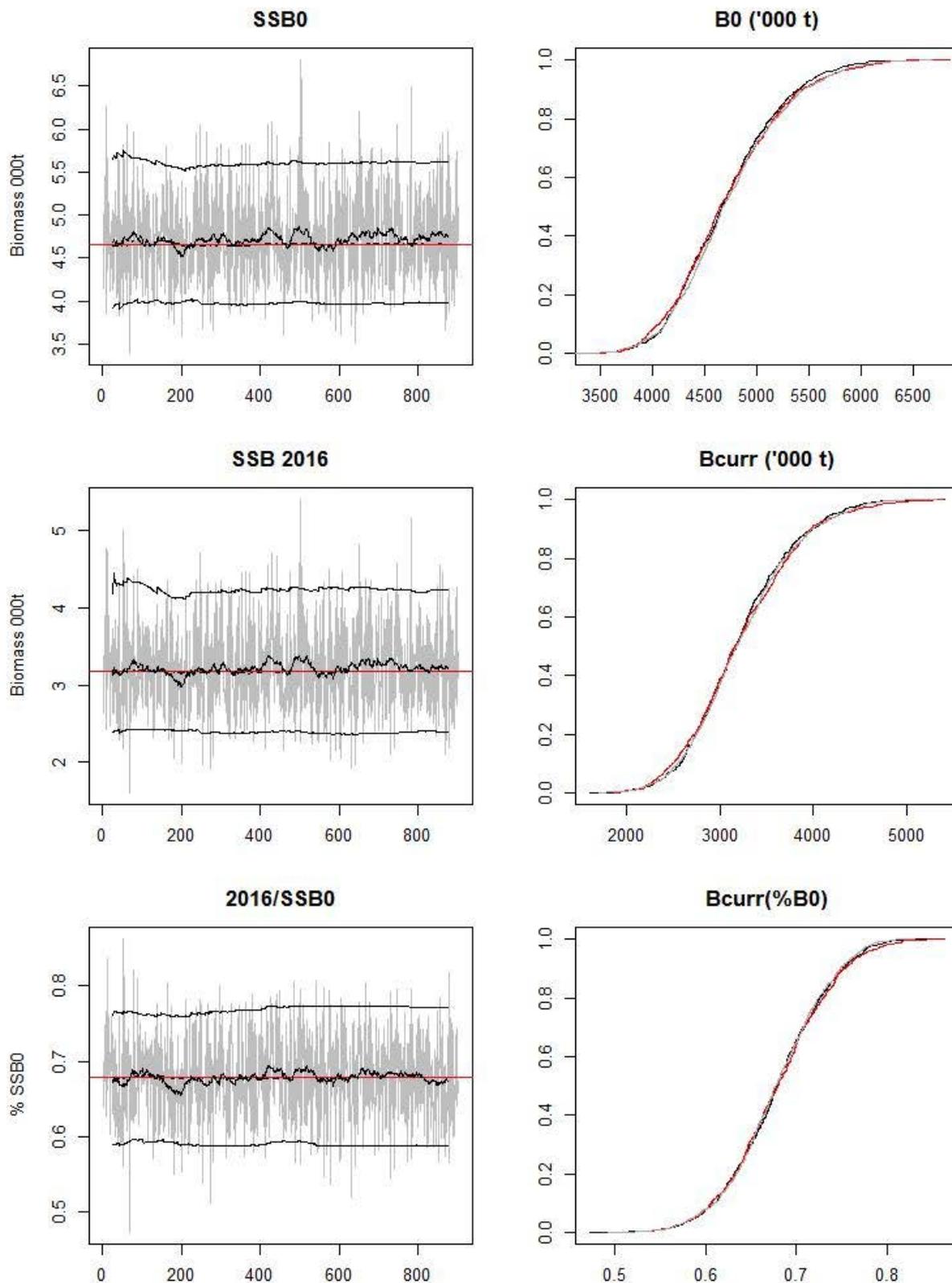
A4. 30: MCMC traces for SSB$_0$, SSB$_{2016}$, and SSB$_{2016}$/SSB$_0$ terms for SCI 6A Model 1 (nuisance q)(trace – grey line, cumulative moving median –dashed black line, moving average and cumulative moving 2.5%, 97.5% quantiles – solid black lines, overall median – solid red line, left plots), along with cumulative frequency distributions for three independent MCMC chains (shown as red, grey and black lines, right plots).
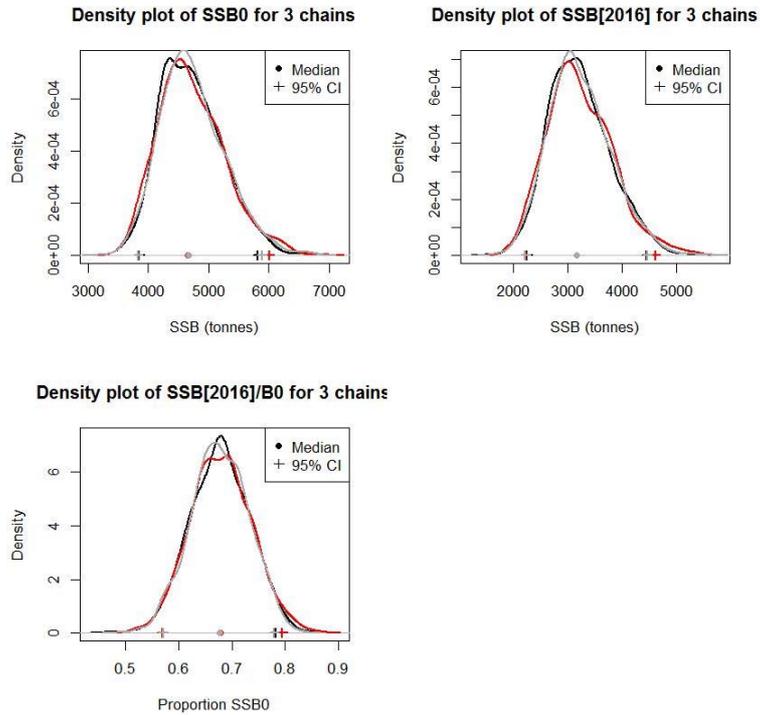
A4. 31: Density plots for SSB$_0$, SSB$_{2016}$, and SSB$_{2016}$/SSB$_0$ terms for SCI 6A Model 1 for three independent MCMC chains, with median and 95% confidence intervals.
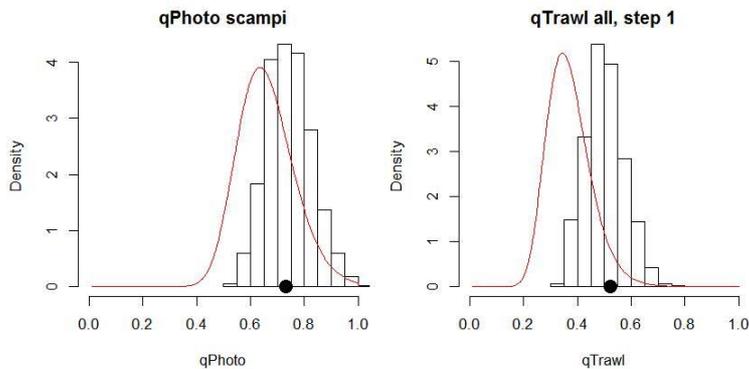
A4. 32: Marginal posterior distributions (histograms), MPD estimates (solid symbols) and distributions of priors (lines) for catchability terms.
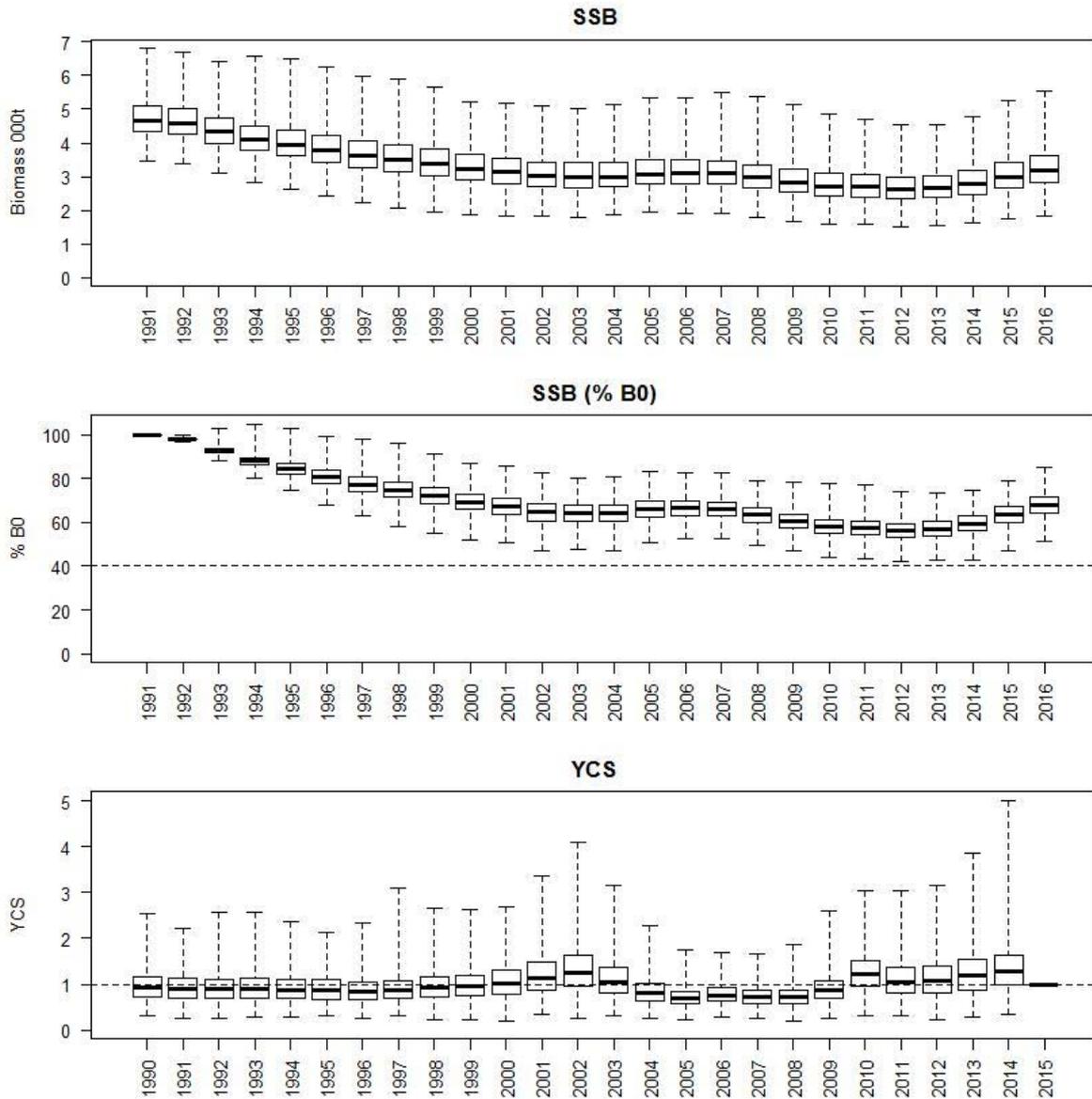
A4. 33: Posterior trajectory of SSB, SSB_{2016}/SSB_0 and YCS.

APPENDIX 5. MODEL 2, M fixed at 0.20, CV on YCS prior 0.7
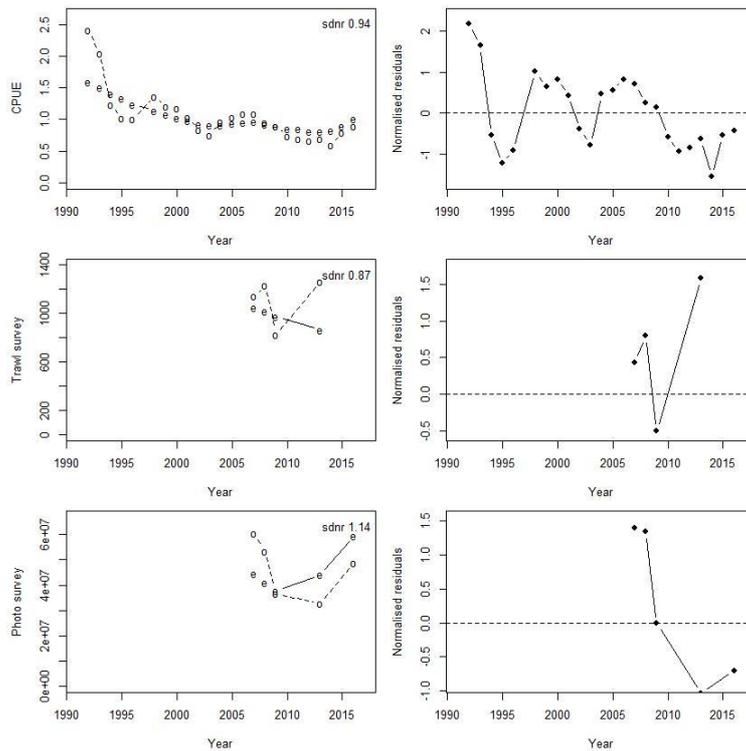
A5. 1: Fits to abundance indices (left column) and normalised residuals (right column) for standardised CPUE index (top row) trawl survey biomass index (middle row) and photo survey abundance index (bottom row) for SCI 6A Model 2.
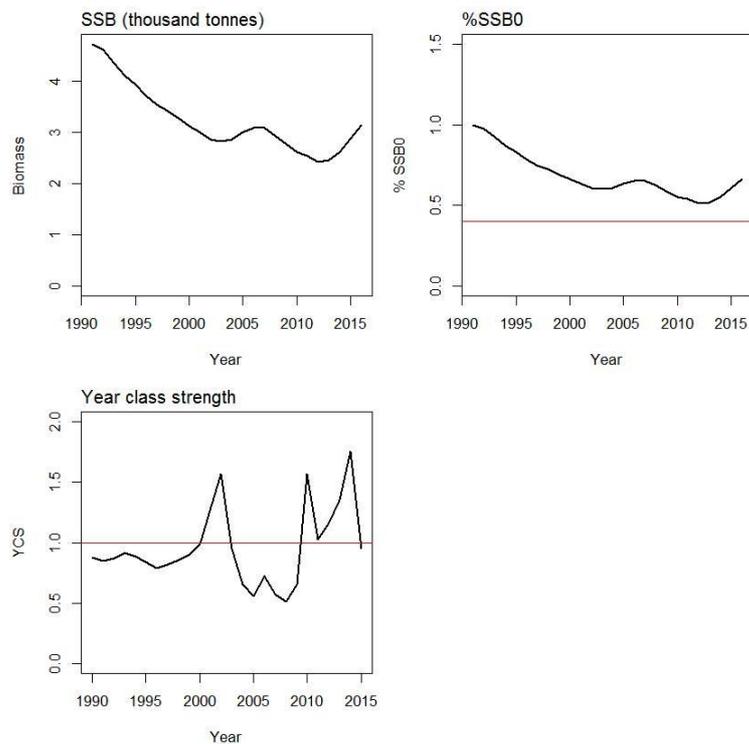
A5. 2: Spawning stock biomass trajectory (upper left), Spawning stock biomass as a percentage of SSB₀ (upper right), and year class strength (lower plot) for SCI 6A Model 2.
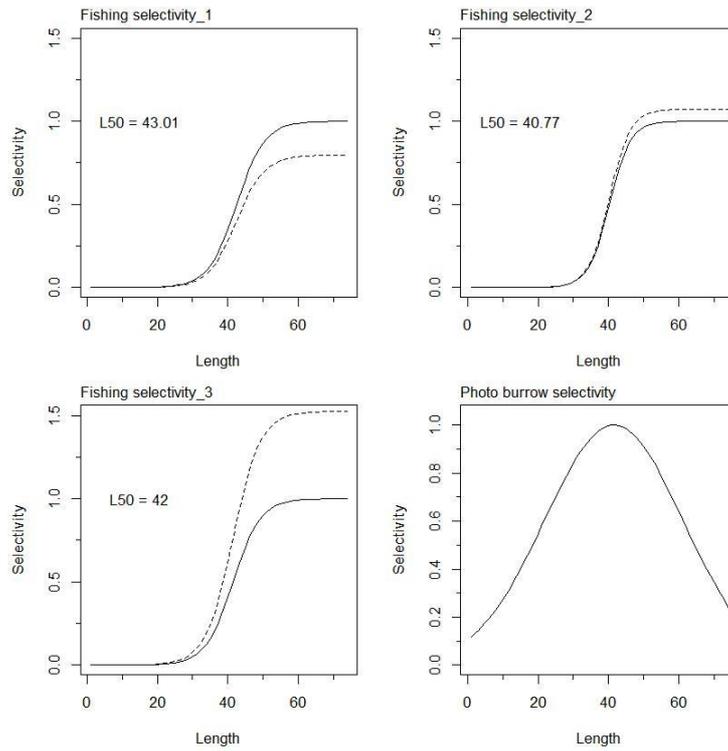
A5. 3: Fishery and photo survey selectivity curves for SCI 6A Model 2. Solid line – females, dotted line – males. The scampi photo index is not sexed, and a single selectivity applies.
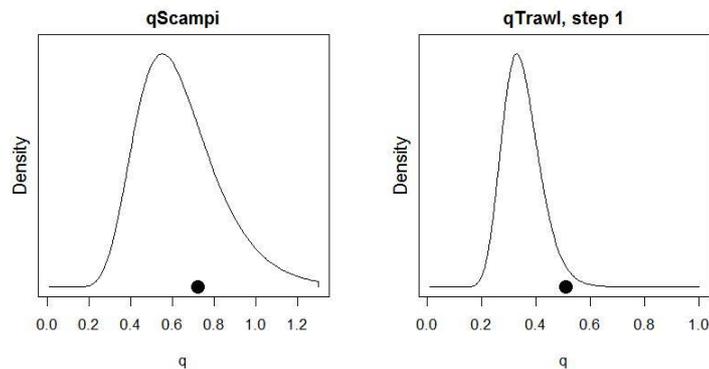
A5. 4: Catchability estimates from MPD model run for SCI 6A Model 2, plotted in relation to prior distribution.
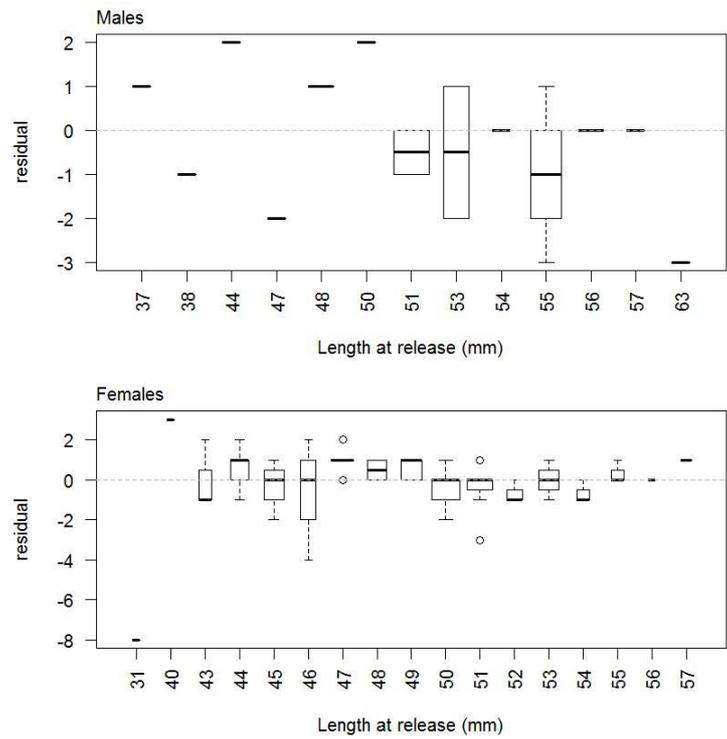
A5. 5: Box plots of residuals from the fit to growth increment by length from tag recapture data by sex.
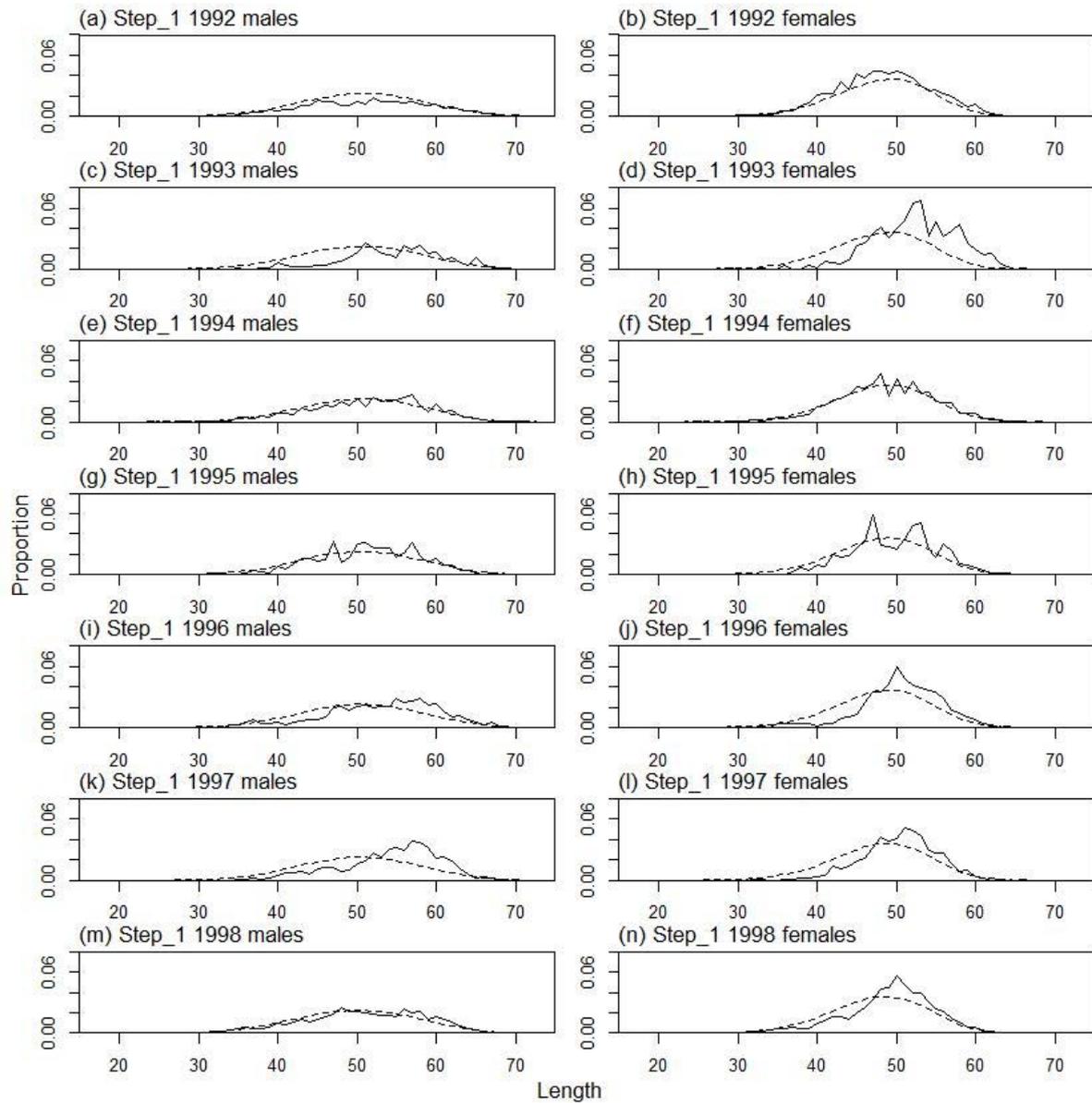
A5. 6: Observed (solid line) and fitted (dashed line) length frequency distributions for observer samples, time step 1.
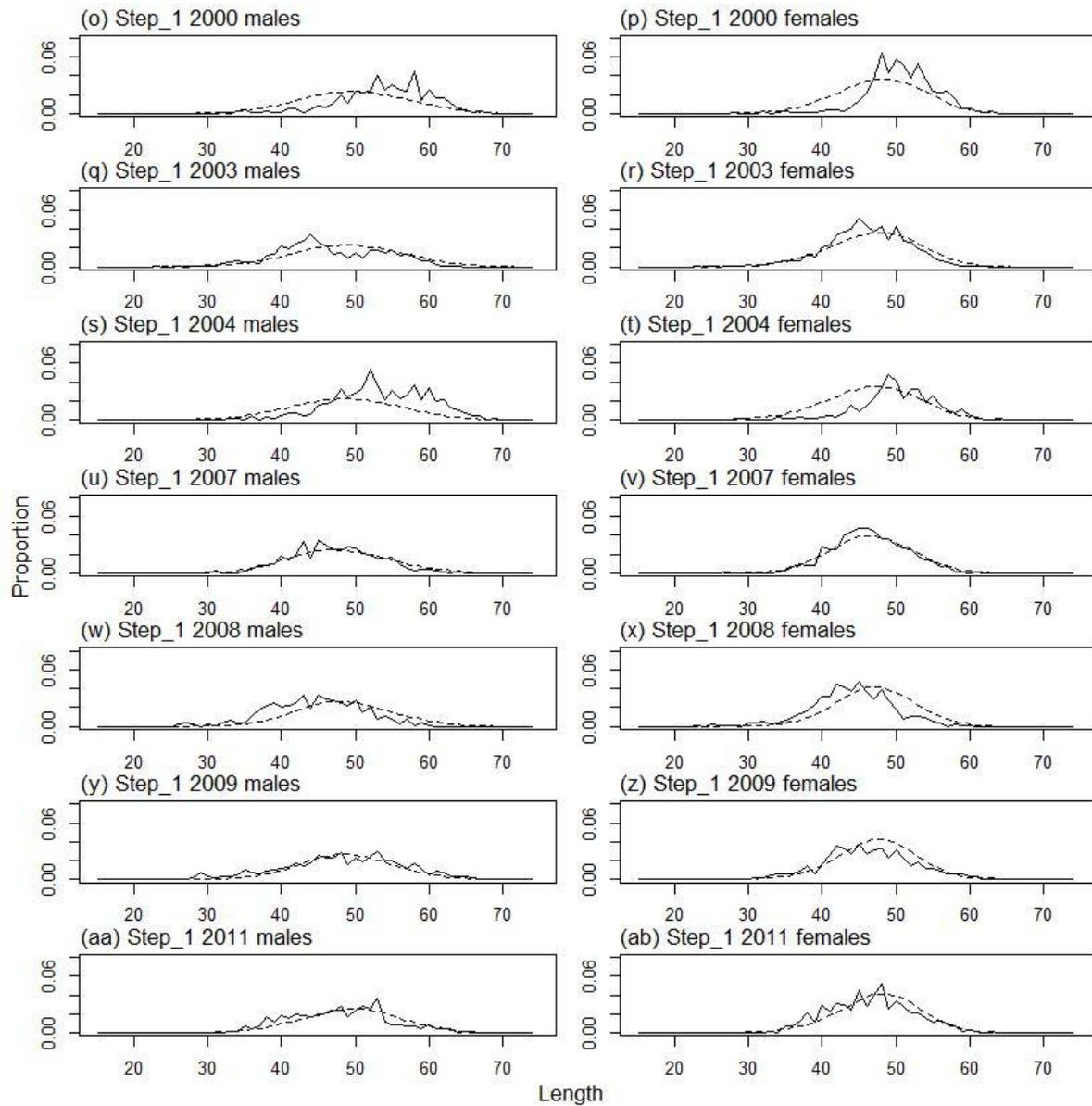
A5. 6 ctd.: Observed (solid line) and fitted (dashed line) length frequency distributions for observer samples, time step 1.
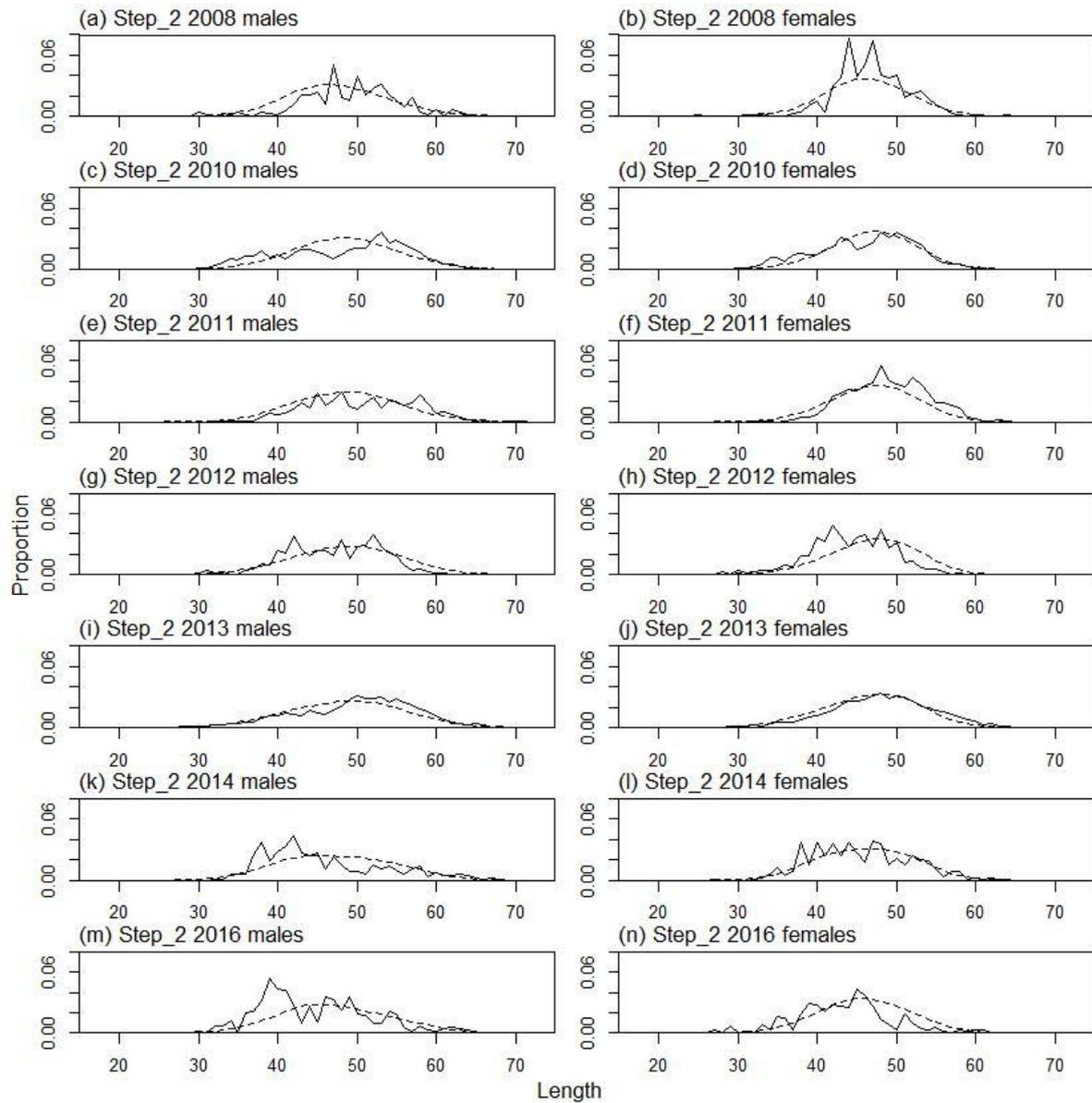
**A5. 7: Observed (solid line) and fitted (dashed line) length frequency distributions for observer samples, time step 2.**
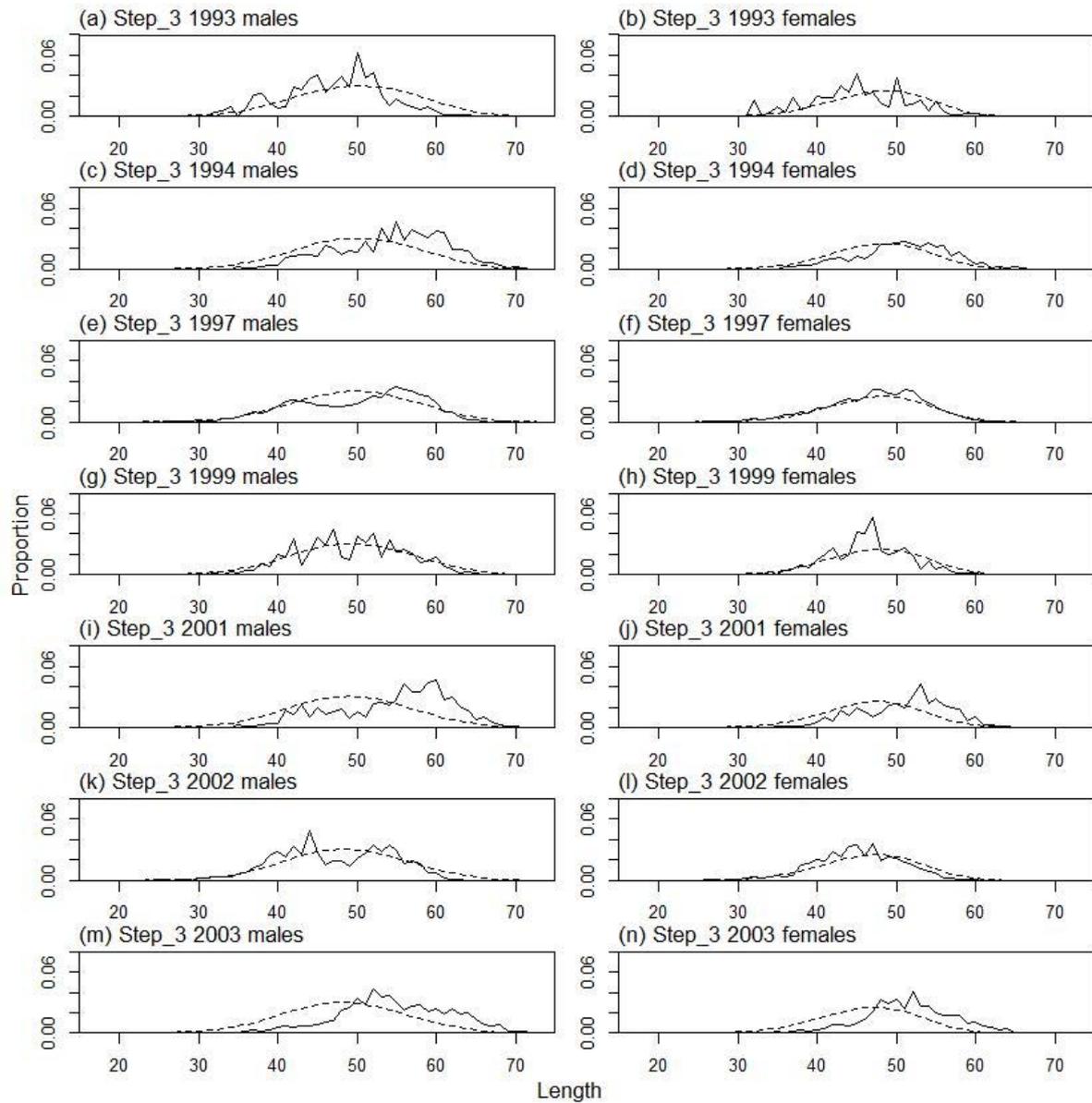
A5. 8: Observed (solid line) and fitted (dashed line) length frequency distributions for observer samples, time step 3.
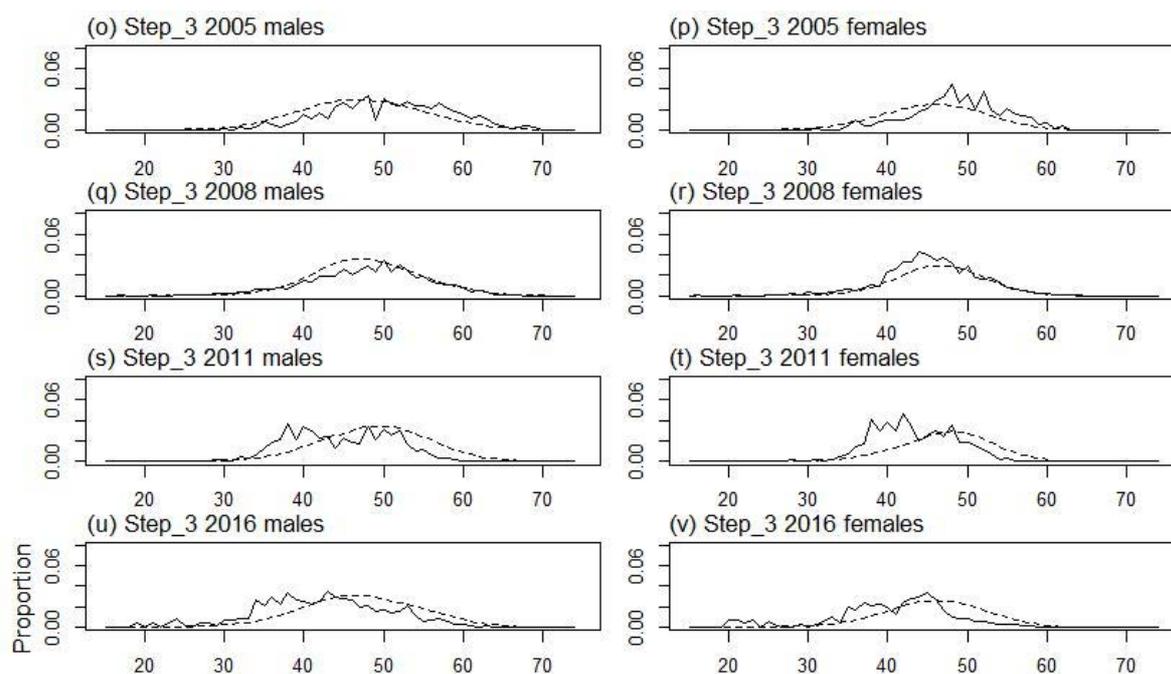
A5. 8 ctd.: Observed (solid line) and fitted (dashed line) length frequency distributions for observer samples, time step 3.

A5. 9: Numbers of scampi measured, estimated multinomial N sample size, and effective sample size used within the model for length frequency distributions for observer samples, time step 1.

	Measured	Multinomial N	Effective sample size
N_1992	9 250	3 373	25.81
N_1993	2 641	3 340	10.51
N_1994	9 300	3 924	30.04
N_1995	2 600	1 360	10.69
N_1996	3 200	1 690	13.42
N_1997	2 794	1 165	8.89
N_1998	11 964	4 863	35.61
N_2000	2 449	935	7.26
N_2002	1 975	458	3.42
N_2003	4 965	2 109	16.43
N_2004	1 214	760	6.12
N_2007	3 235	1 006	7.99
N_2008	1 269	568	4.66
N_2009	2 959	1 504	11.82
N_2011	4 035	937	7.45

A5. 10: Numbers of scampi measured, estimated multinomial N sample size, and effective sample size used within the model for length frequency distributions for observer samples, time step 2.

	Measured	Multinomial N	Effective sample size
N_1997	3 287	1 509	14.39
N_1998	703	472	4.50
N_2001	4 782	2 521	24.04
N_2008	1 035	754	7.19
N_2010	4 194	962	9.18
N_2011	2 725	1 601	15.27
N_2012	2 370	860	8.20
N_2013	10 883	4 650	44.35
N_2014	9 253	3 418	32.60
N_2016	491	322	3.07

A5. 11: Numbers of scampi measured, estimated multinomial N sample size, and effective sample size used within the model for length frequency distributions for observer samples, time step 3.

	Measured	Multinomial N	Effective sample size
N_1993	1 264	740	1.95
N_1994	1 960	1 192	3.14
N_1996	2 035	736	1.94
N_1997	8 816	5 002	13.17
N_1998	172	147	0.39
N_1999	2 707	1 575	4.15
N_2001	1 650	332	0.87
N_2002	5 663	1 184	3.12
N_2003	8 746	3 332	8.78
N_2005	1 600	1 215	3.20
N_2007	1 238	350	0.92
N_2008	4 435	1 300	3.42
N_2011	5 214	1 104	2.91
N_2016	3 265	994	2.62
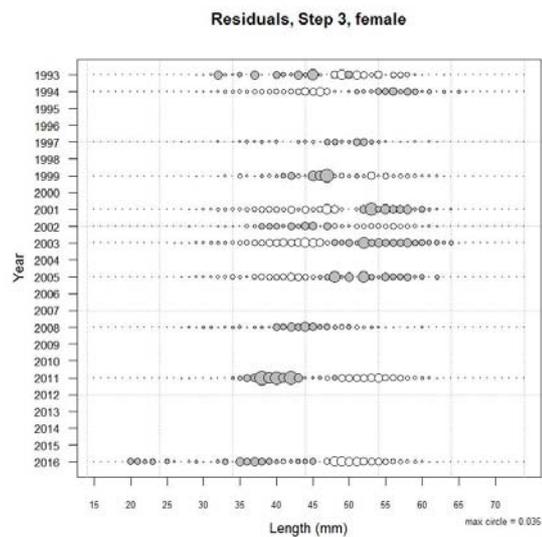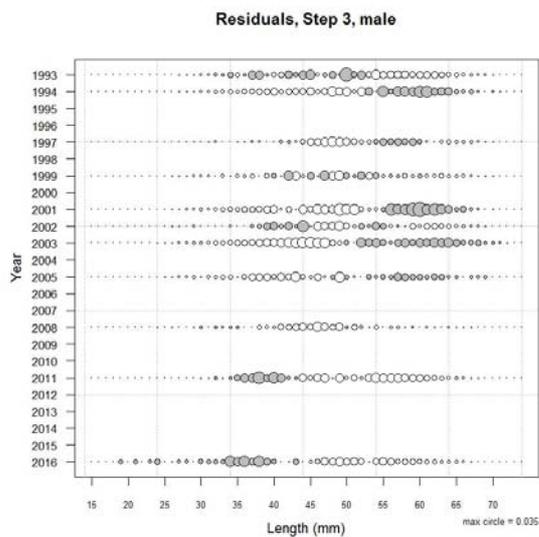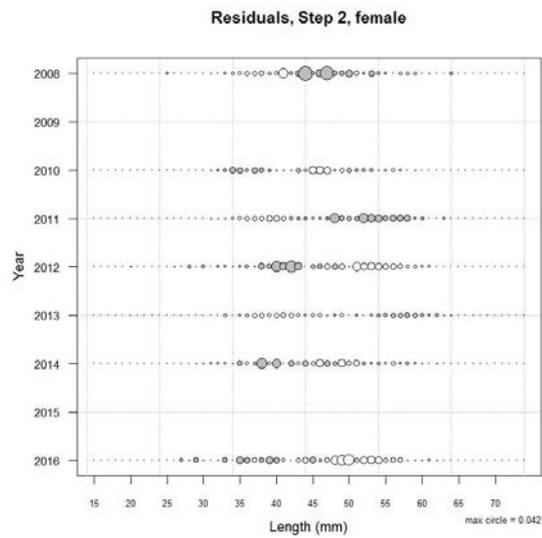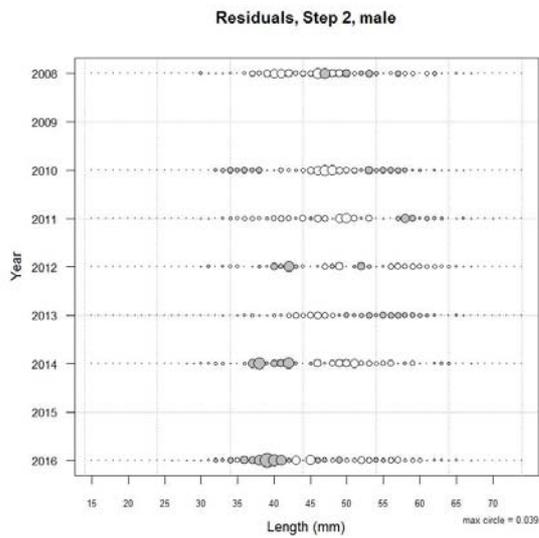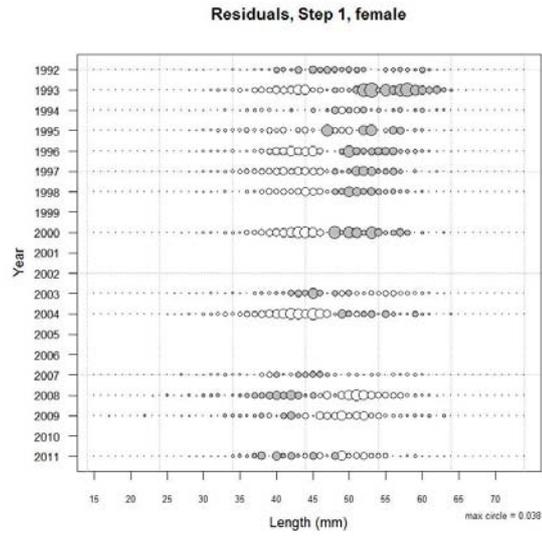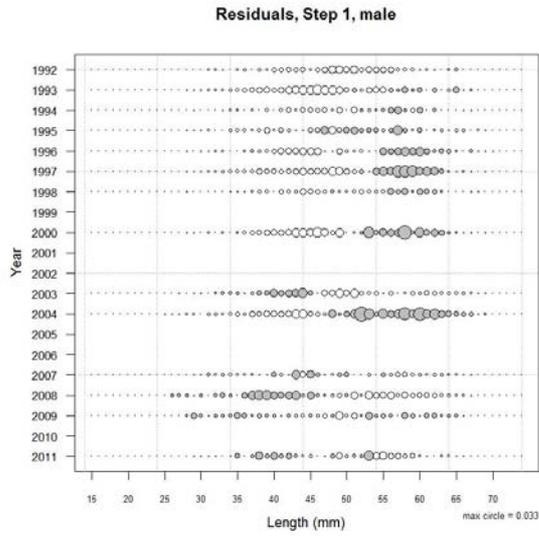
A5. 12: Bubble plots of residuals for fits to length frequency distributions for observer sampling.
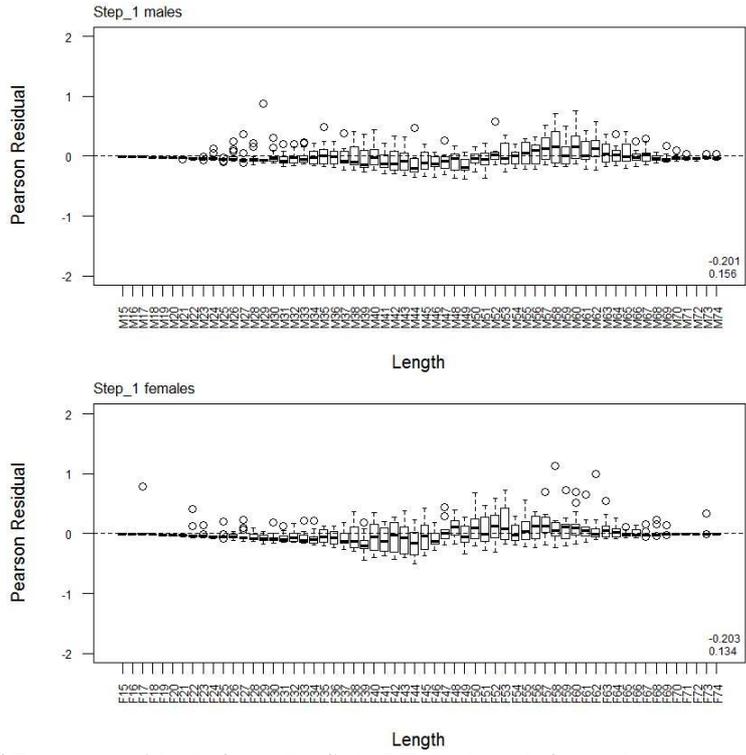
A5. 13: Box plots of Pearson residuals from the fit to LFs by length from observer sampling by sex for time step 1.
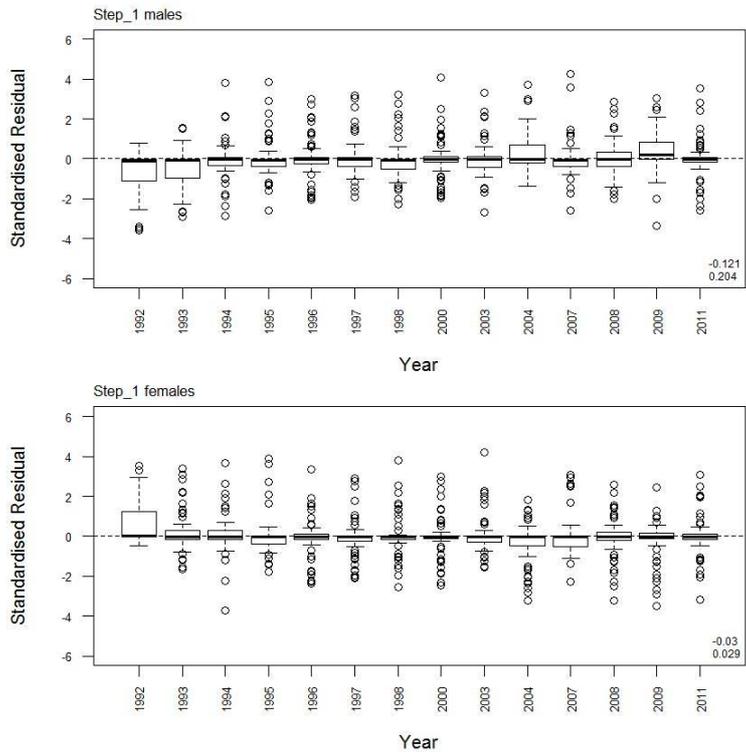

A5. 14: Box plots of Pearson residuals from the fit to LFs by year from observer sampling by sex for time step 1.
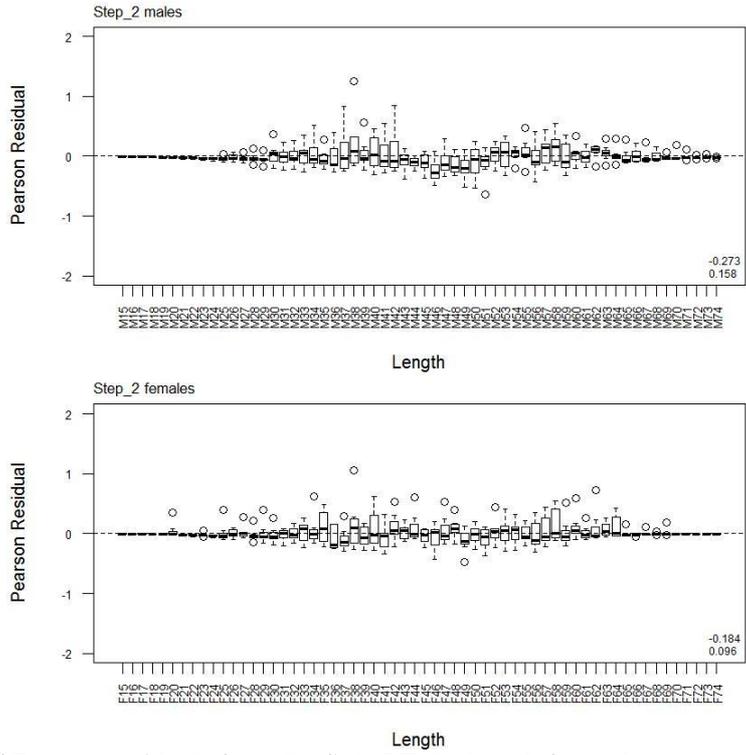
A5. 15: Box plots of Pearson residuals from the fit to LFs by length from observer sampling by sex for time step 2.
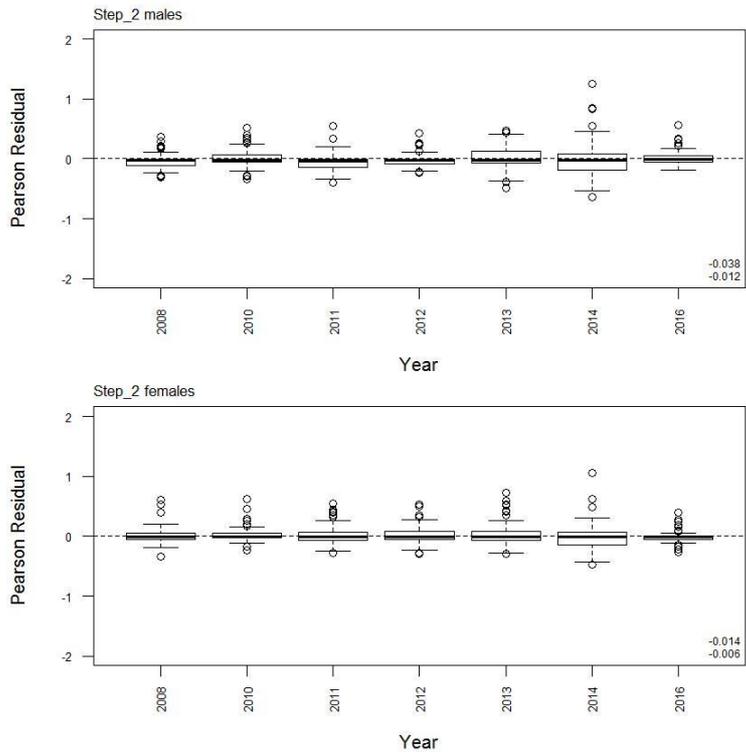
A5. 16: Box plots of Pearson residuals from the fit to LFs by year from observer sampling by sex for time step 2.
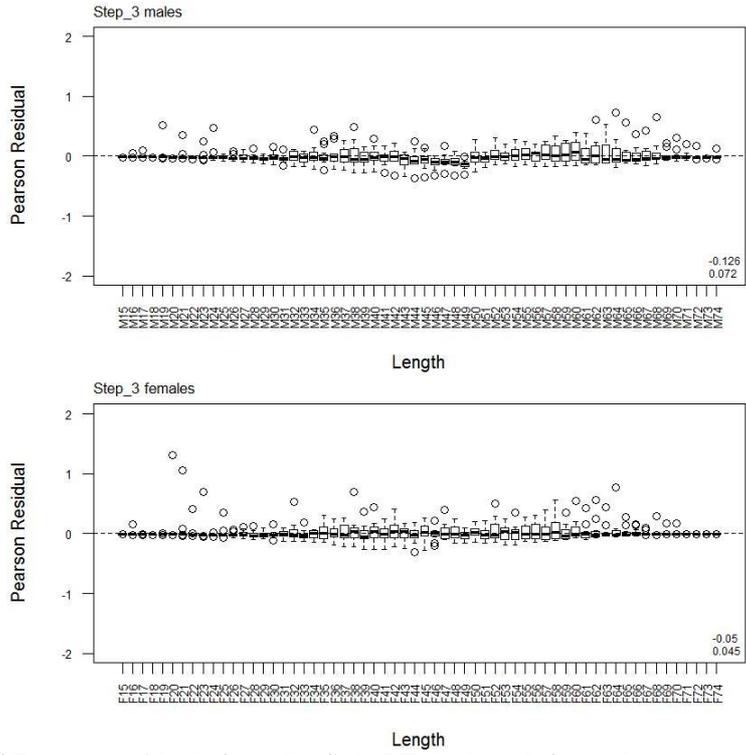
A5. 17: Box plots of Pearson residuals from the fit to LFs by length from observer sampling by sex for time step 3.
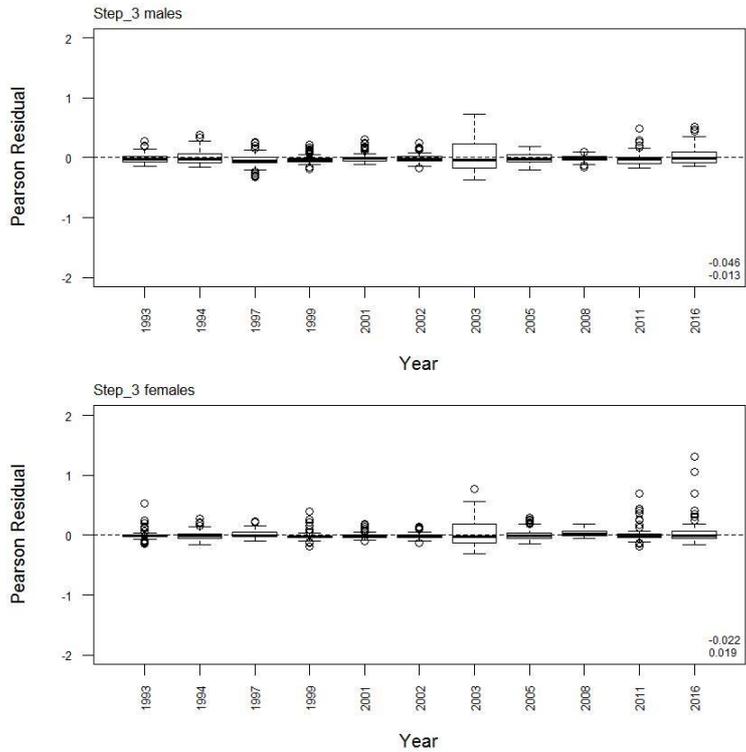
A5. 18: Box plots of Pearson residuals from the fit to LFs by year from observer sampling by sex for time step 3.
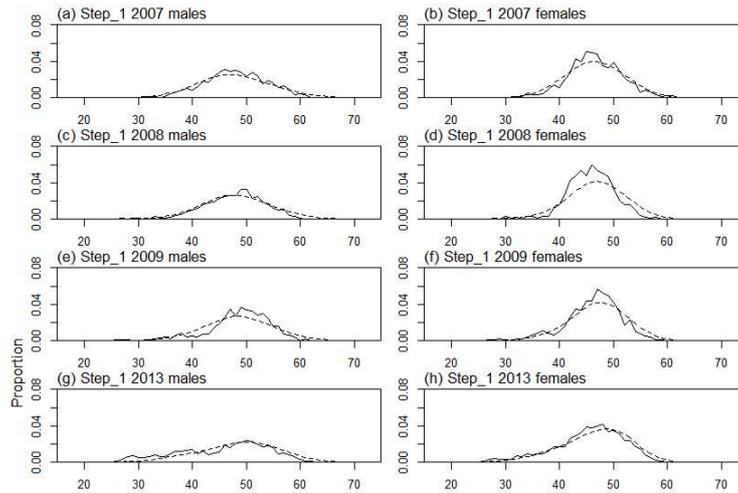
A5. 19: Observed (solid line) and fitted (dashed line) length frequency distributions for research survey samples.
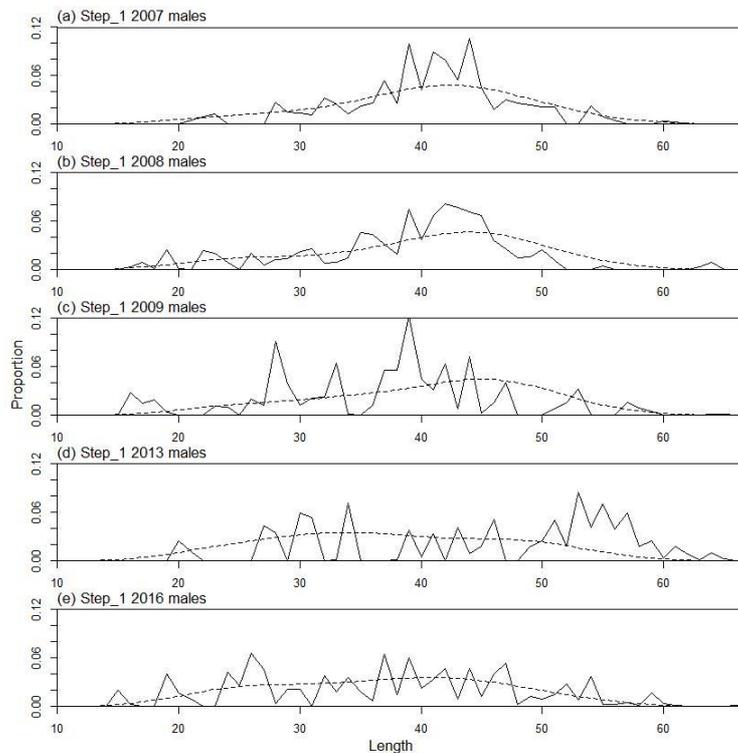
A5. 20: Observed (solid line) and fitted (dashed line) length frequency distributions for photographic survey scampi size estimation.

A5. 21: Numbers of scampi measured, estimated multinomial N sample size, and effective sample size used within the model for length frequency distributions for research survey samples.

	Measured	Multinomial N	Effective sample size
N_2007	1 981	2 127	39.96
N_2008	2 291	1 866	34.69
N_2009	4 054	2 798	53.19
N_2013	4 808	4 218	77.80

A5. 22: Numbers of scampi measured, estimated multinomial N sample size, and effective sample size used within the model for length frequency distributions for photographic survey samples.

	Measured	Multinomial N	Effective sample size
N_2007	70	125	12.86
N_2008	73	121	13.42
N_2009	45	72	8.27
N_2013	26	43	4.78
N_2016	44	72	8.09
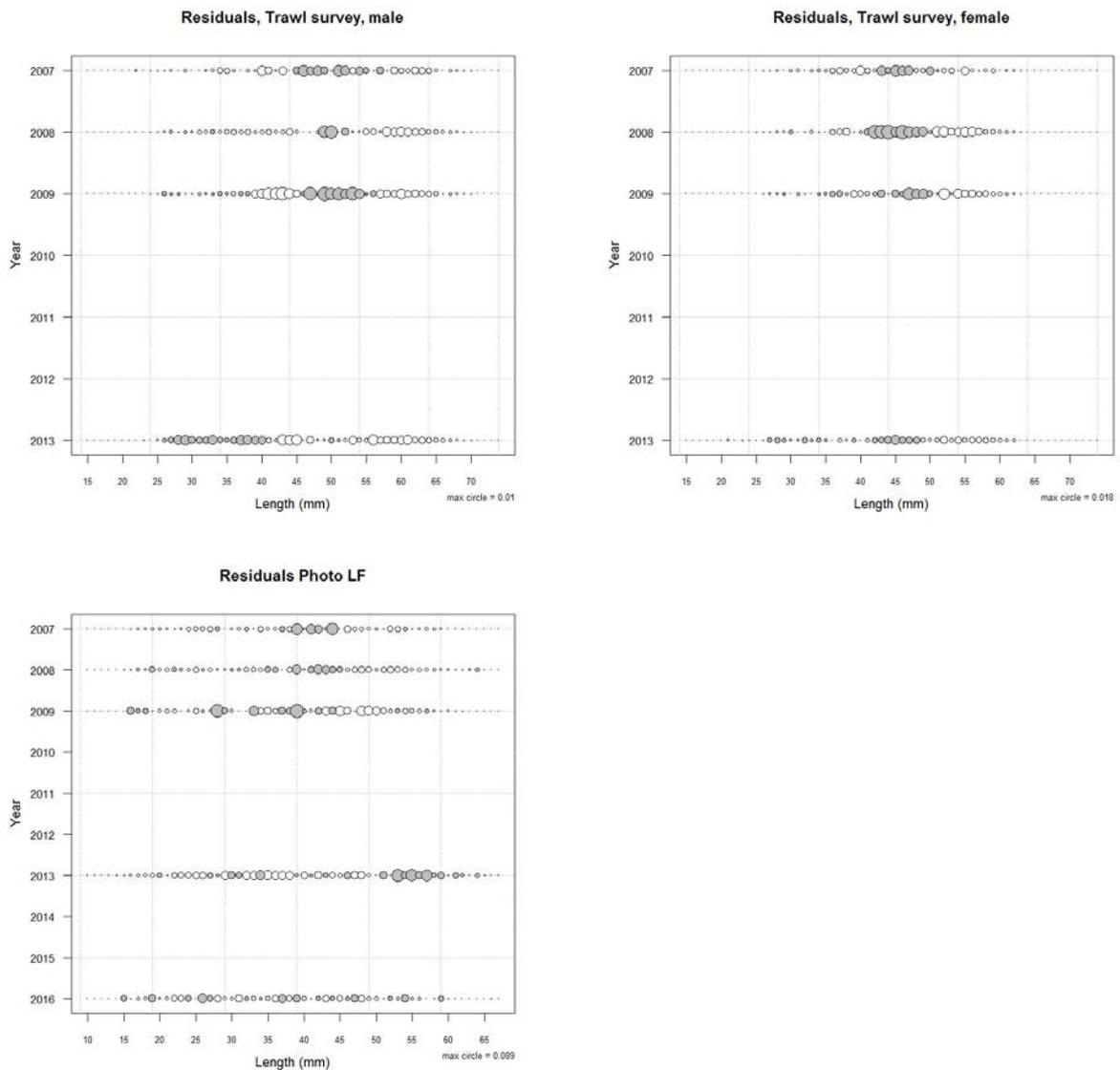
A5. 23: Bubble plots of residuals for fits to length frequency distributions for trawl survey sampling and photographic survey scampi size estimation.
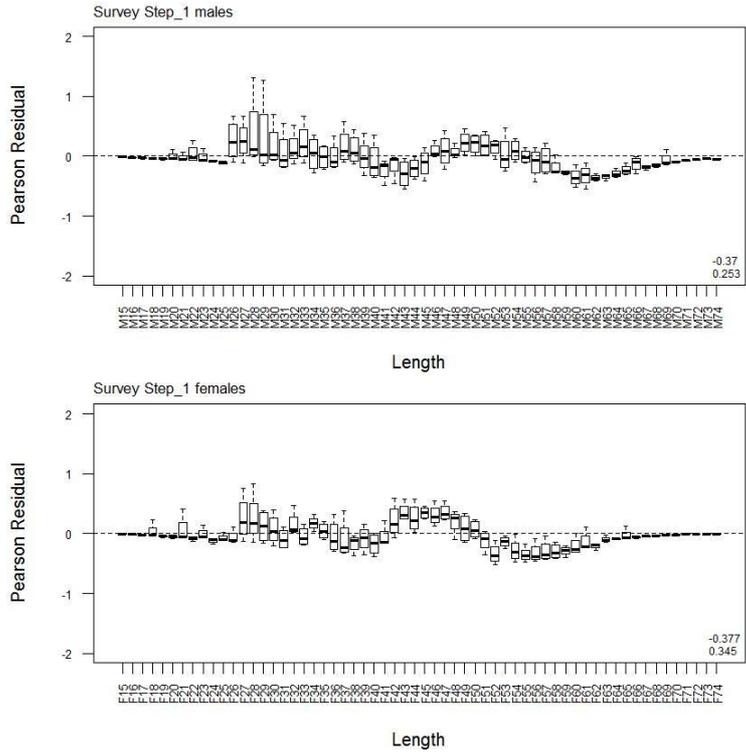
A5. 24: Box plots of Pearson residuals from the fit to LFs by length from trawl survey sampling by sex for time step 1.
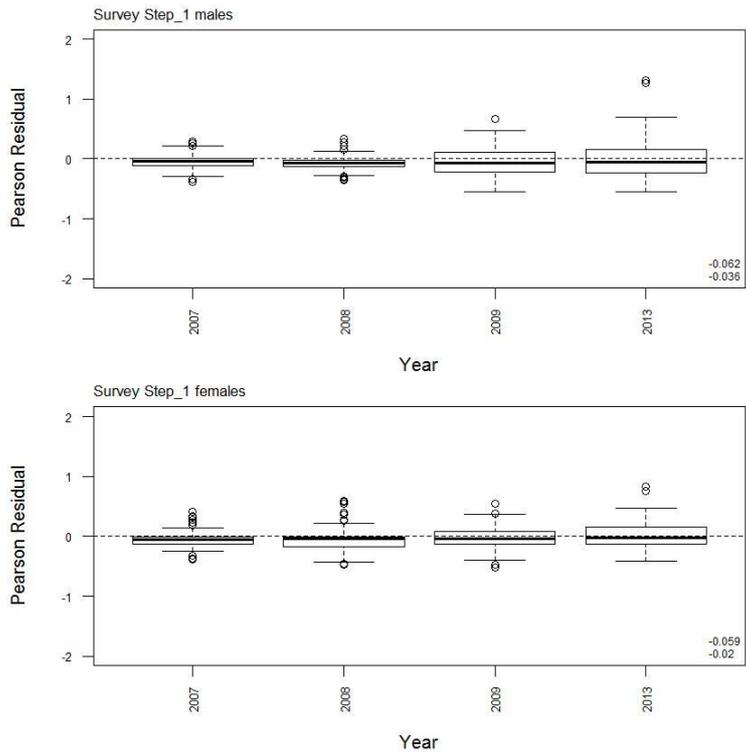
A5. 25: Box plots of Pearson residuals from the fit to LFs by year from trawl survey sampling by sex for time step 1.
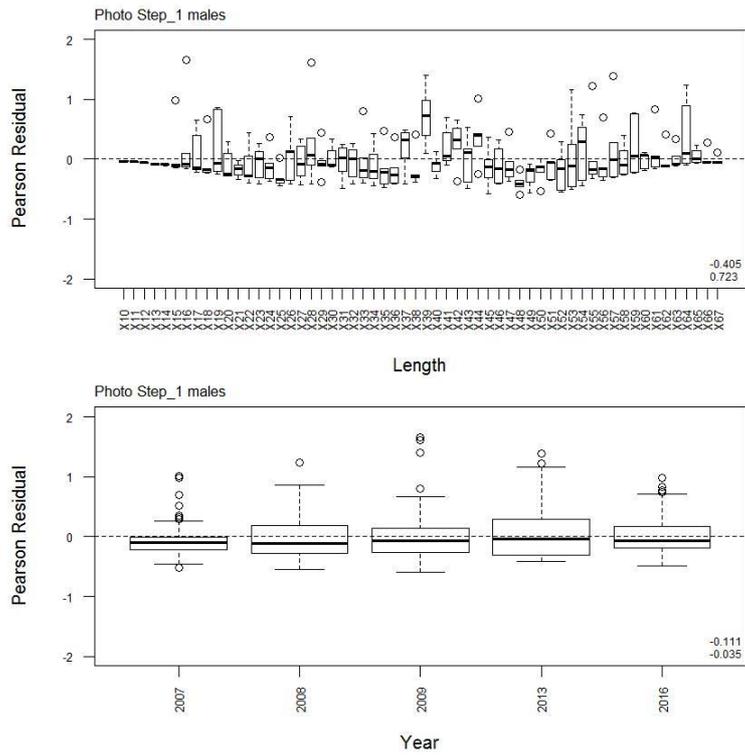
A5. 26: Box plots of Pearson residuals from the fit to LFs by length and year from photo survey sampling for time step 1.
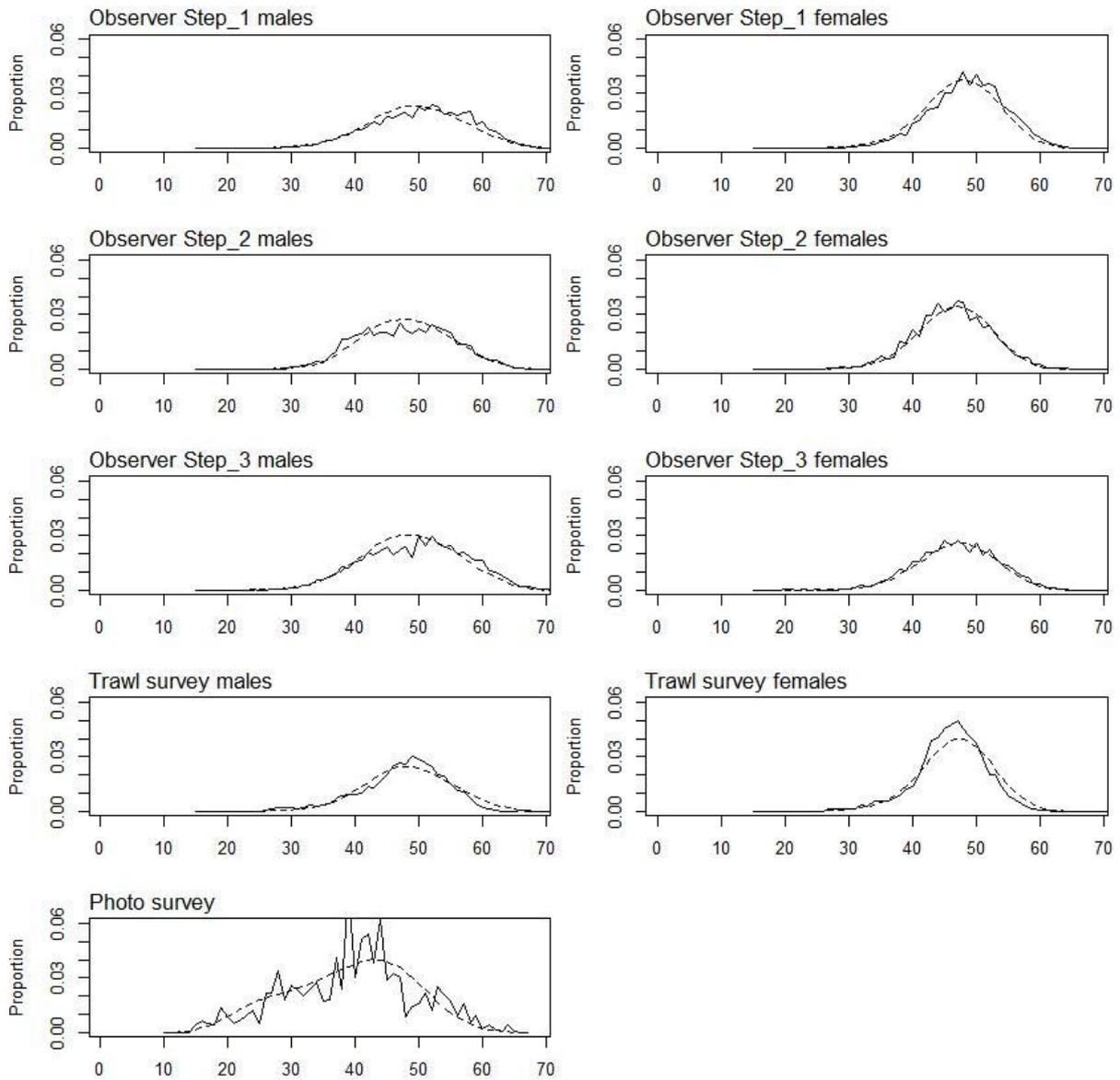
A5. 27: Average observed (solid line) and fitted (dashed line) length frequency distributions for observer and survey samples.
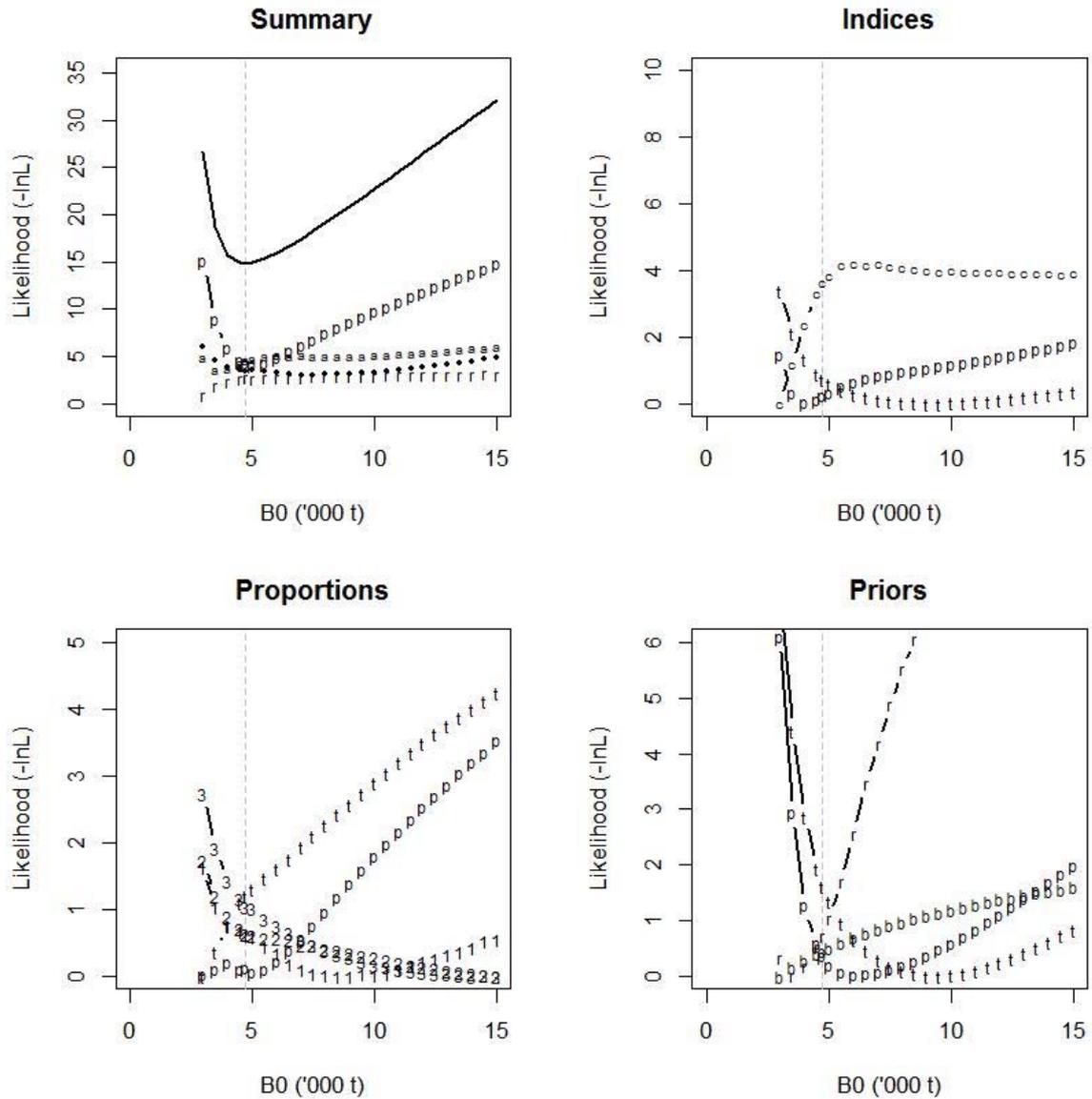
A5. 28: Likelihood profiles for SCI 6A Model 2 when B$_0$ is fixed in the model. Figures show profiles for main priors (top left, p – priors, a - abundance indices, • – proportions at length, r – recapture data), abundance indices (top right, t - trawl survey, c - CPUE, p – photo survey), proportion at length data (bottom left, a-trawl, 1 – observer time step 1, 2 – observer time step 2, 3 – observer time step 3, p - photo) and priors (bottom right, b- B$_0$, YCS - r, p- *q-Photo***, t –** *q-Trawl***). Vertical dashed line represents MPD.**
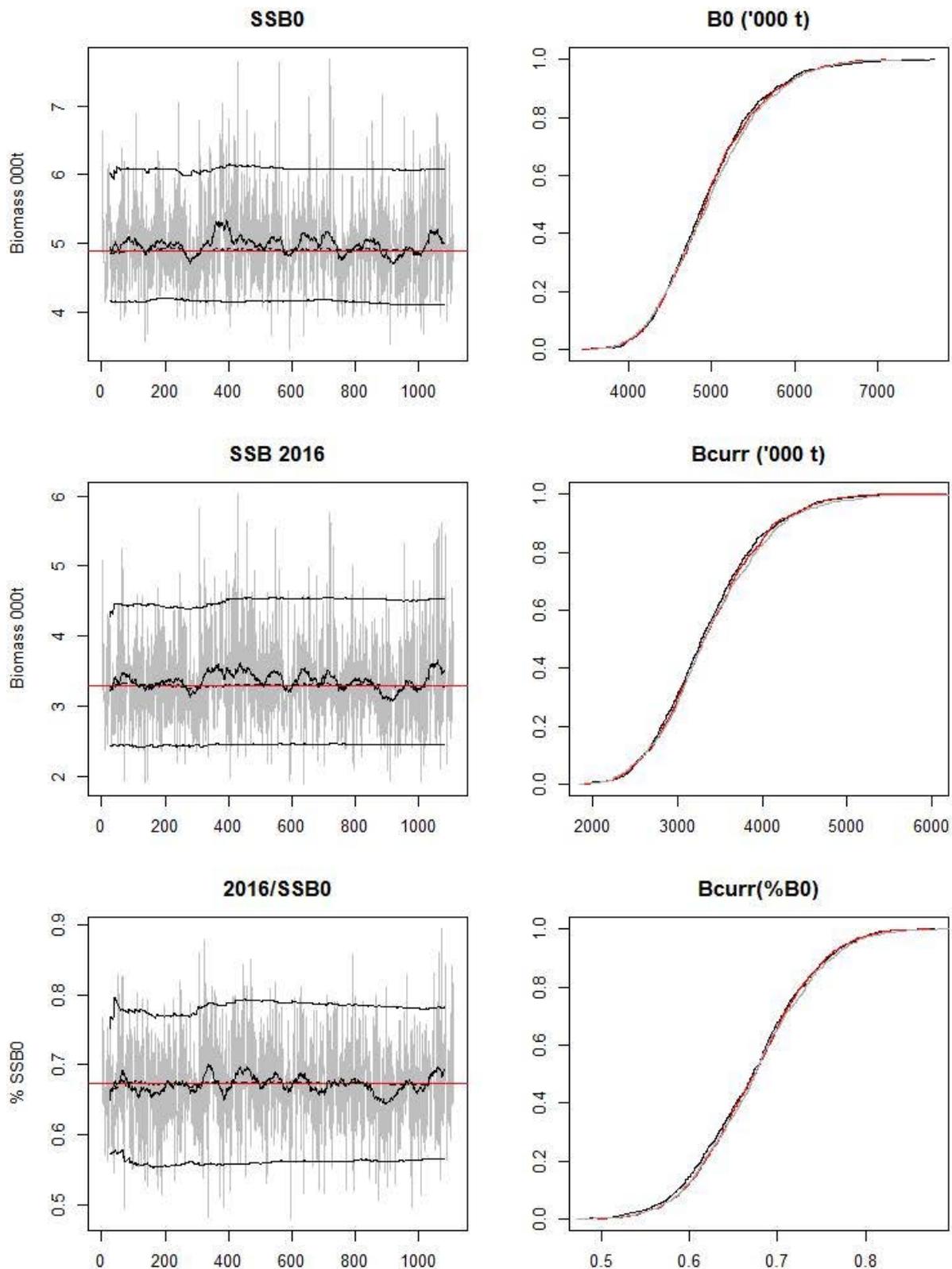
A5. 29: MCMC traces for SSB$_0$, SSB$_{2016}$, and SSB$_{2016}$/SSB$_0$ terms for SCI 6A Model 2 (trace – grey line, cumulative moving median –dashed black line, moving average and cumulative moving 2.5%, 97.5% quantiles – solid black lines, overall median – solid red line, left plots), along with cumulative frequency distributions for three independent MCMC chains (shown as red, grey and black lines, right plots).
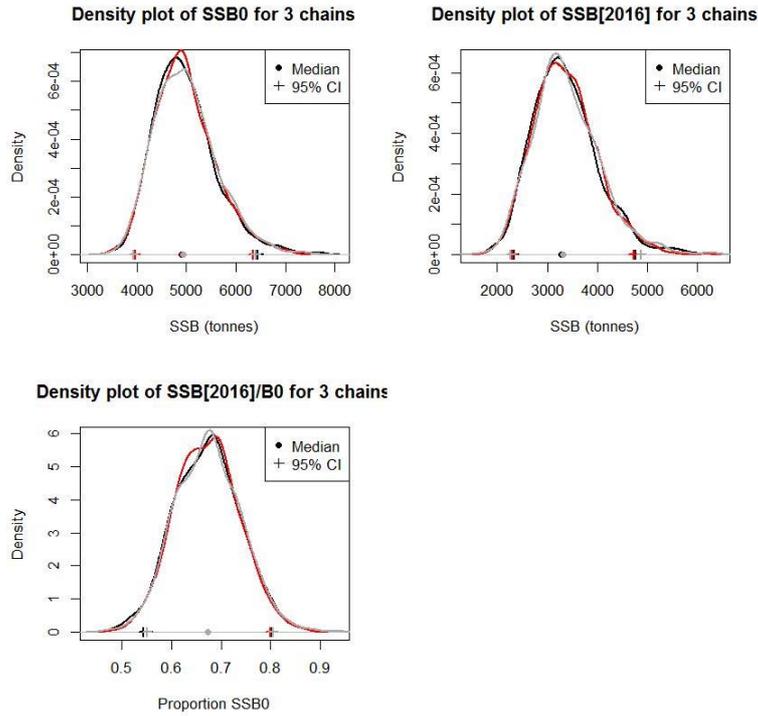
A5. 30: Density plots for SSB_0, SSB_{2016}, and SSB_{2016}/SSB_0 terms for SCI 6A Model 2 for three independent MCMC chains, with median and 95% confidence intervals.
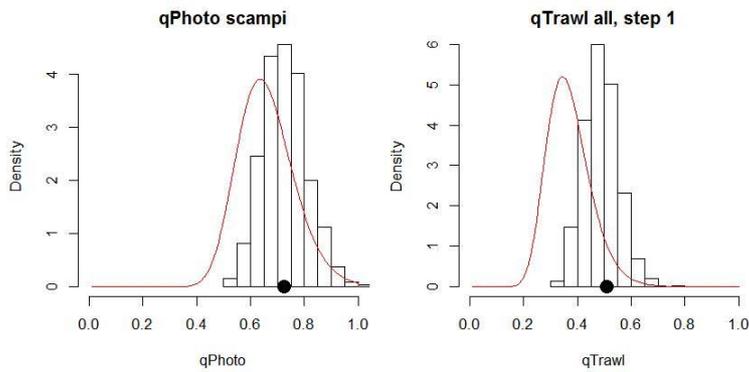
A5. 31: Marginal posterior distributions (histograms), MPD estimates (solid symbols) and distributions of priors (lines) for catchability terms.
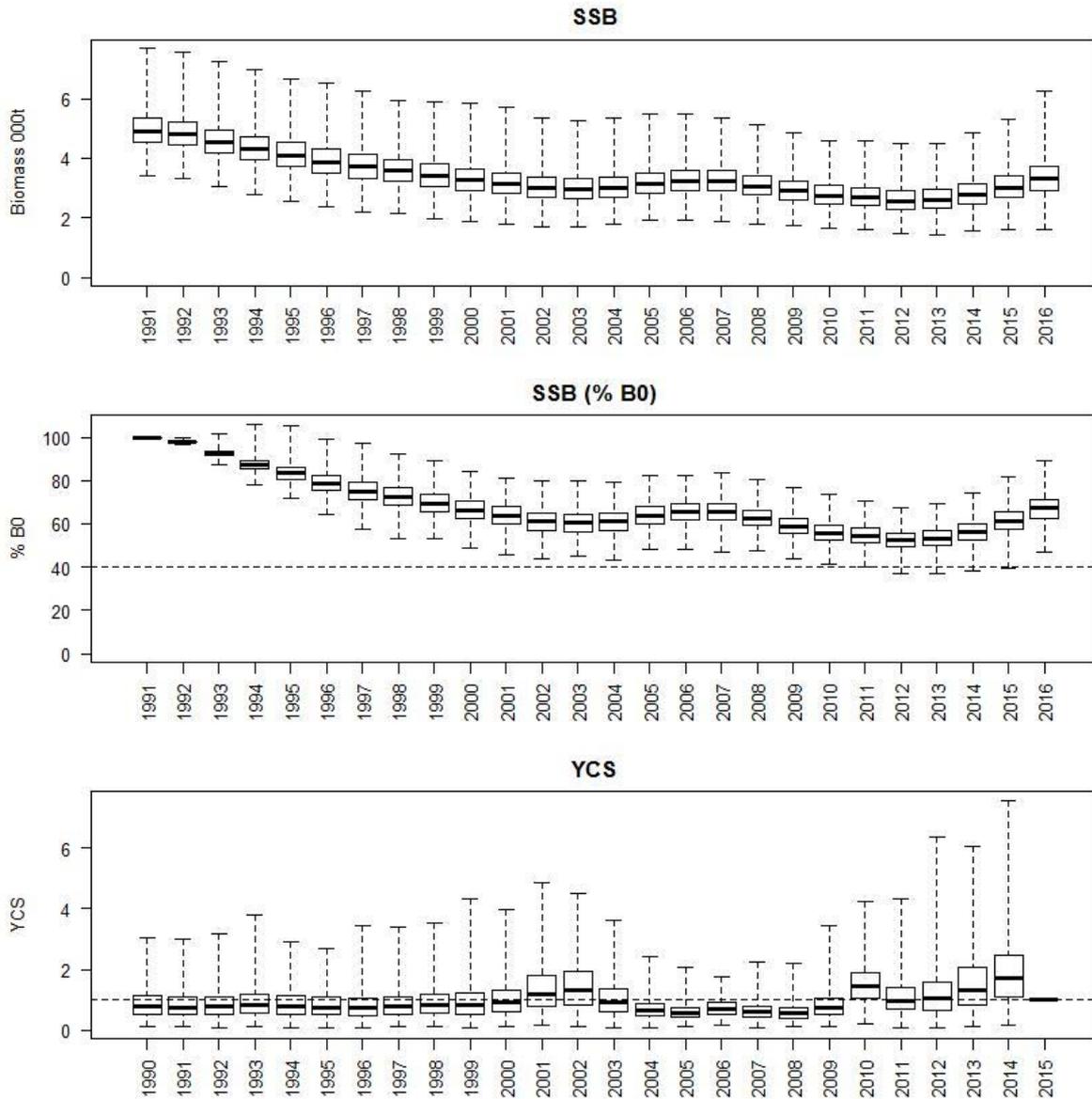
A5. 32: Posterior trajectory of SSB, SSB_{2016}/SSB_0 and YCS.

APPENDIX 6. MODEL 3, M fixed at 0.25, CV on YCS prior 0.4
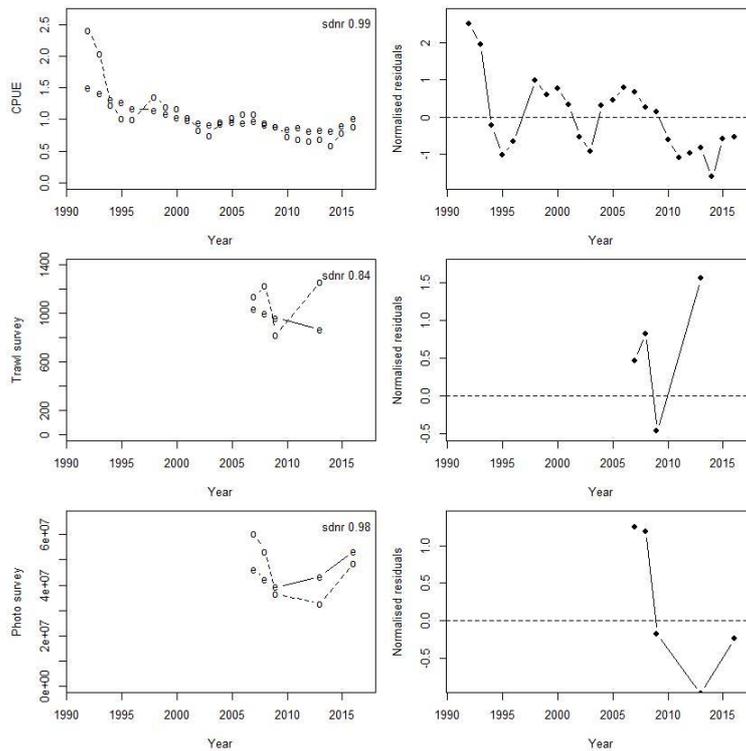
A6. 1: Fits to abundance indices (left column) and normalised residuals (right column) for standardised CPUE index (top row) trawl survey biomass index (middle row) and photo survey abundance index (bottom row) for SCI 6A Model 3.
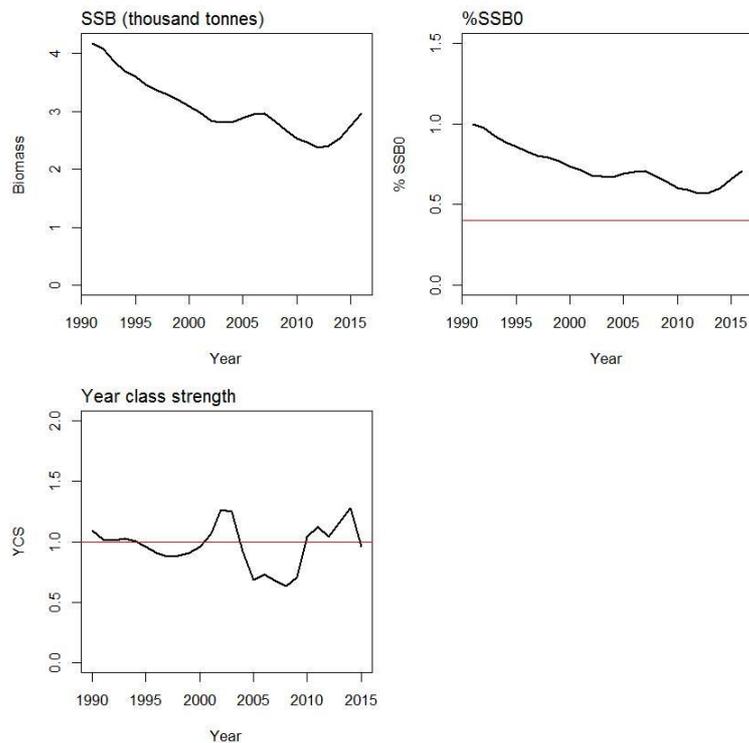
A6. 2: Spawning stock biomass trajectory (upper left), Spawning stock biomass as a percentage of SSB$_0$ (upper right), and year class strength (lower plot) for SCI 6A Model 3.
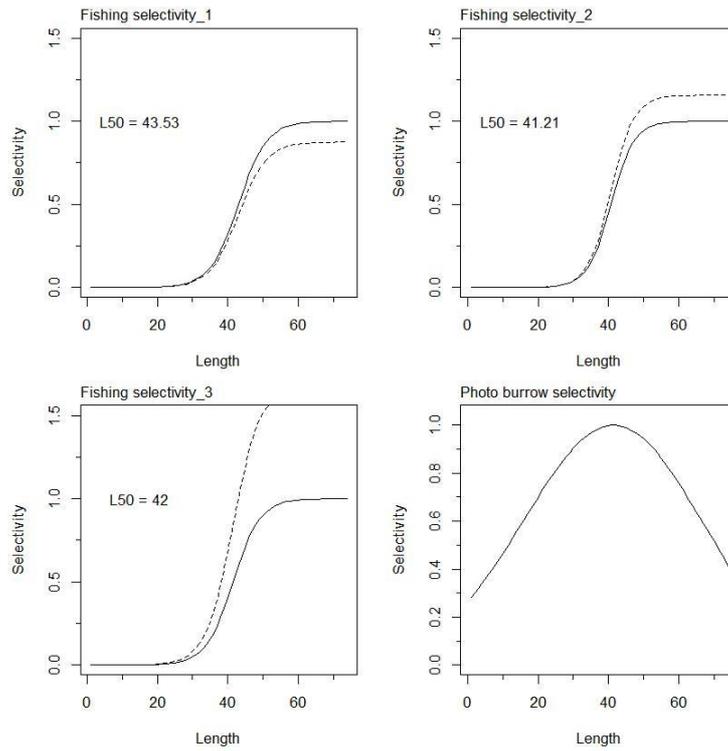
A6. 3: Fishery and photo survey selectivity curves for SCI 6A Model 3. Solid line – females, dotted line – males. The scampi photo index is not sexed, and a single selectivity applies.
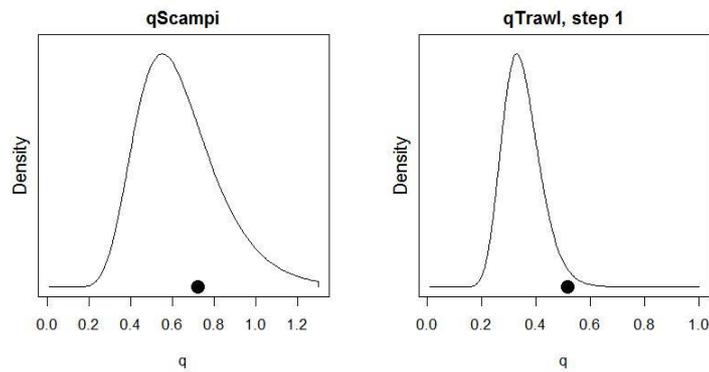
A6. 4: Catchability estimates from MPD model run for SCI 6A Model 3, plotted in relation to prior distribution.
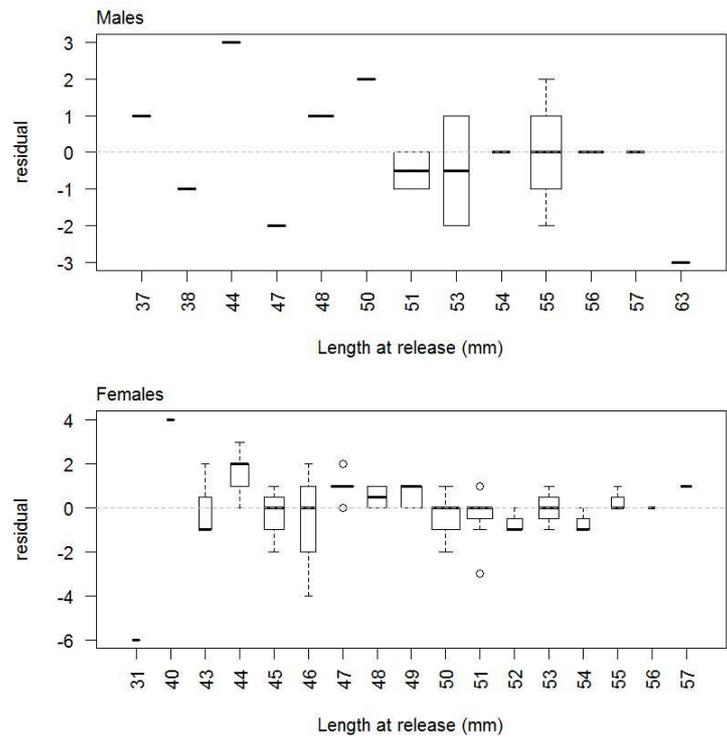
A6. 5: Box plots of residuals from the fit to growth increment by length from tag recapture data by sex.
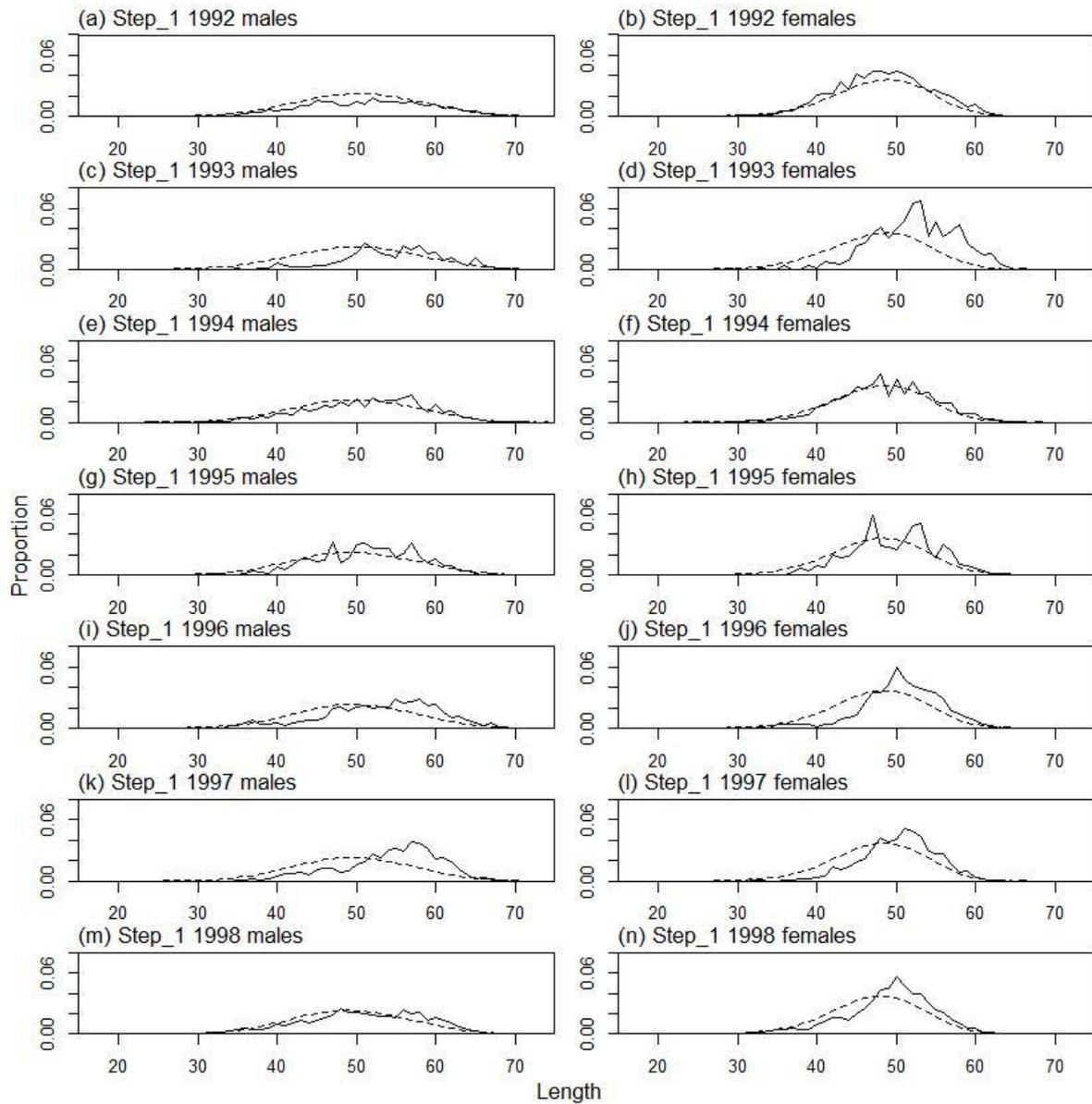
A6. 6: Observed (solid line) and fitted (dashed line) length frequency distributions for observer samples, time step 1.
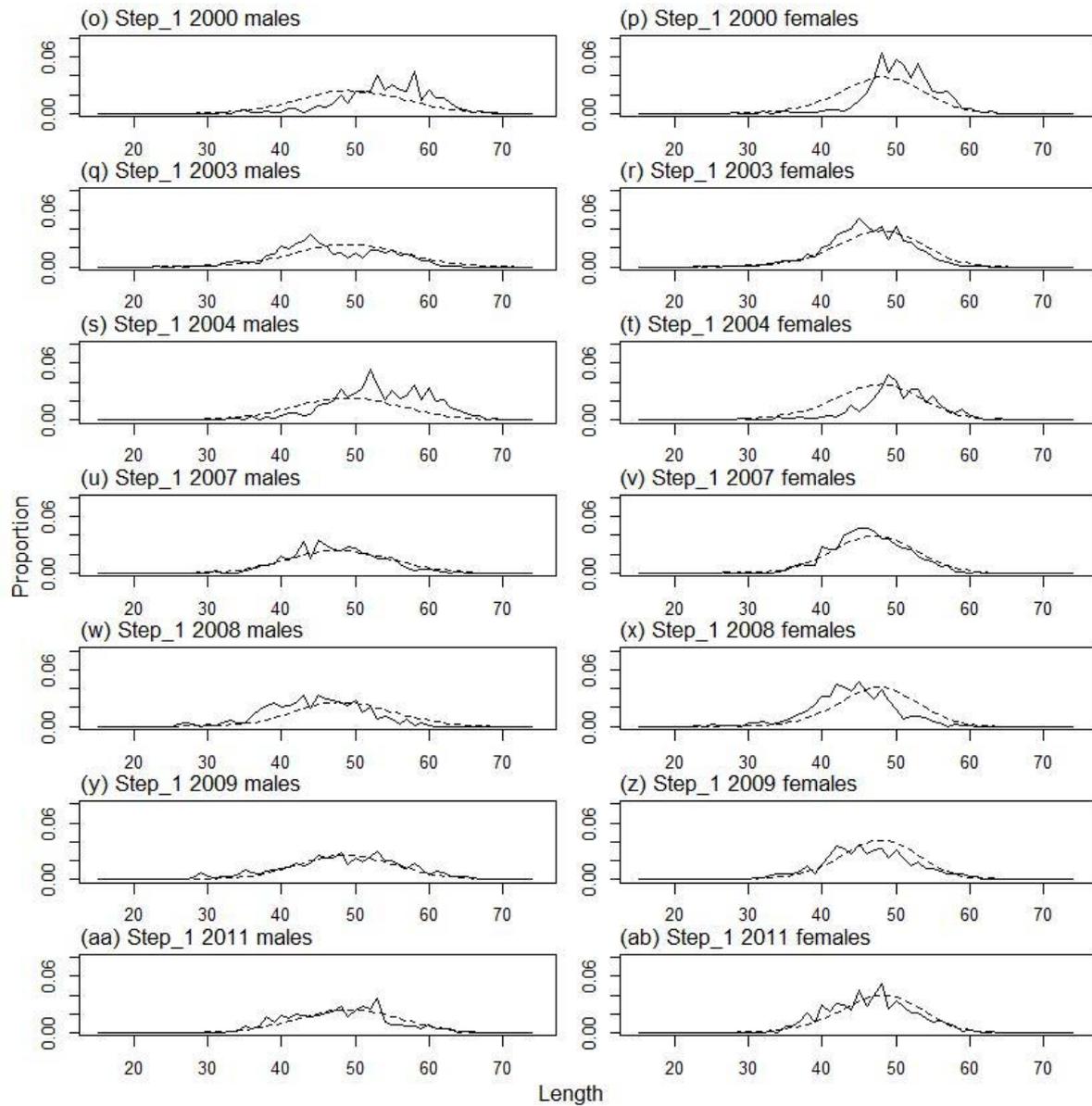
A6. 6 ctd.: Observed (solid line) and fitted (dashed line) length frequency distributions for observer samples, time step 1.
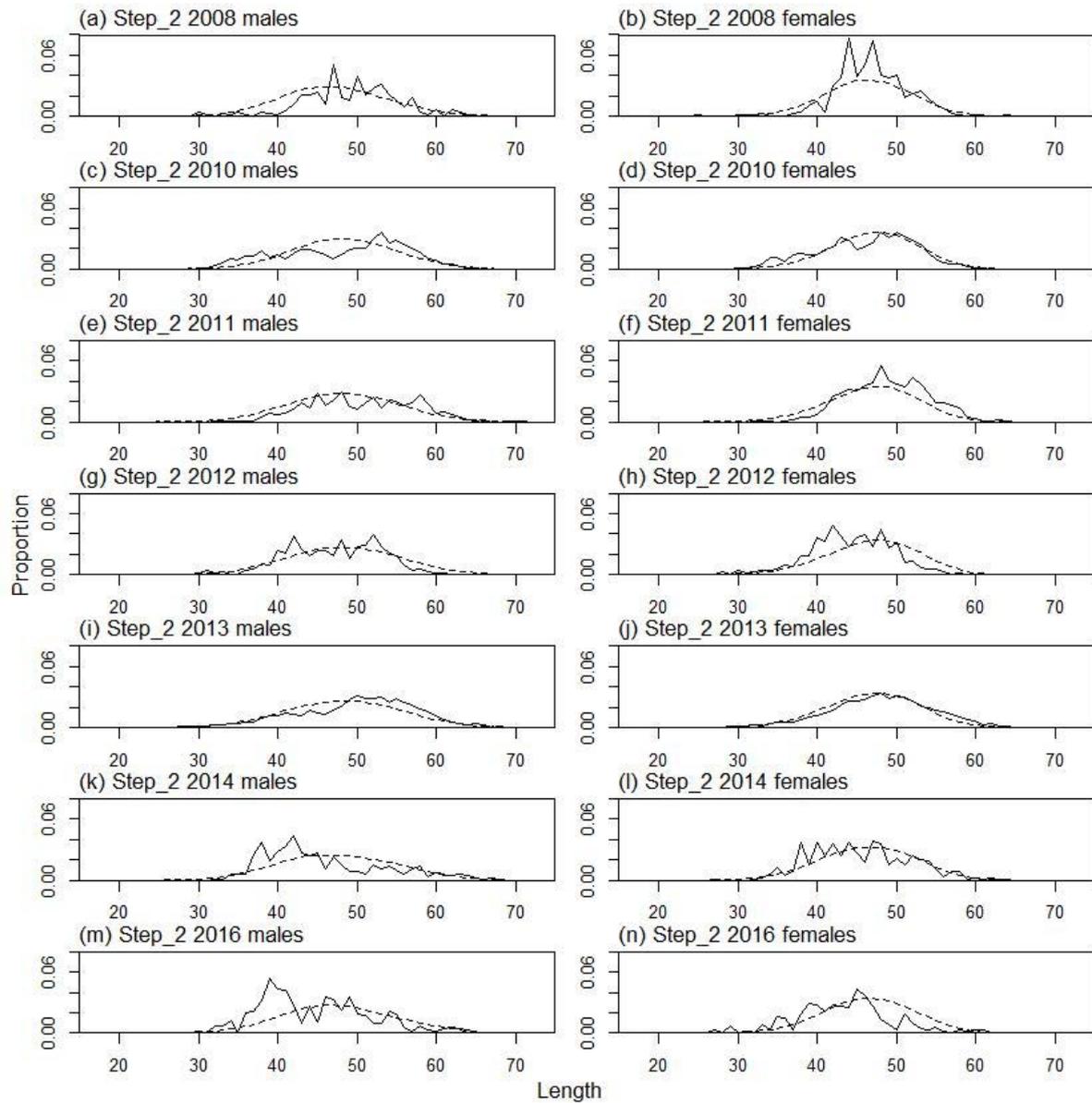
A6. 7: Observed (solid line) and fitted (dashed line) length frequency distributions for observer samples, time step 2.
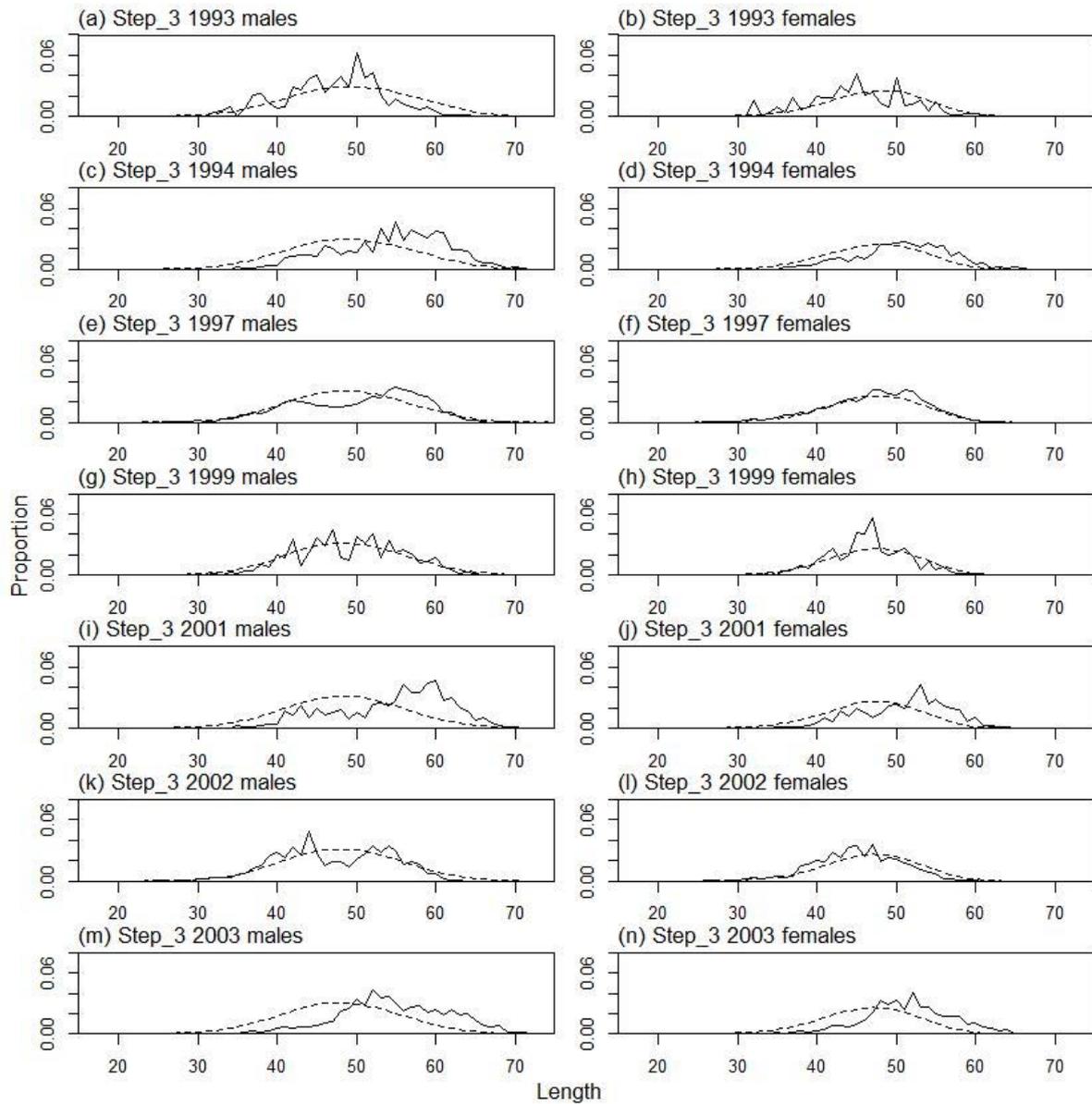
A6. 8: Observed (solid line) and fitted (dashed line) length frequency distributions for observer samples, time step 3.
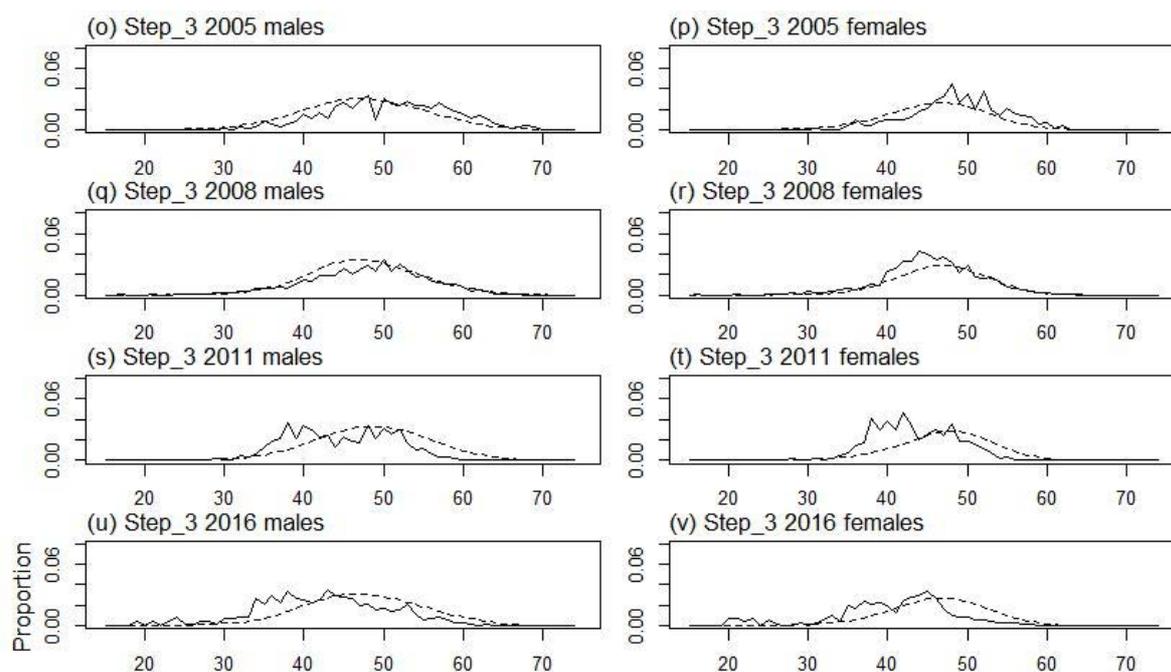
A6. 8 ctd.: Observed (solid line) and fitted (dashed line) length frequency distributions for observer samples, time step 3.

A6. 9: Numbers of scampi measured, estimated multinomial N sample size, and effective sample size used within the model for length frequency distributions for observer samples, time step 1.

	Measured	Multinomial N	Effective sample size
N_1992	9 250	3 373	21.40
N_1993	2 641	3 340	8.71
N_1994	9 300	3 924	24.91
N_1995	2 600	1 360	8.86
N_1996	3 200	1 690	11.13
N_1997	2 794	1 165	7.37
N_1998	11 964	4 863	29.52
N_2000	2 449	935	6.02
N_2002	1 975	458	2.83
N_2003	4 965	2 109	13.62
N_2004	1 214	760	5.08
N_2007	3 235	1 006	6.62
N_2008	1 269	568	3.86
N_2009	2 959	1 504	9.80
N_2011	4 035	937	6.18

A6. 10: Numbers of scampi measured, estimated multinomial N sample size, and effective sample size used within the model for length frequency distributions for observer samples, time step 2.

	Measured	Multinomial N	Effective sample size
N_1997	3 287	1 509	14.01
N_1998	703	472	4.38
N_2001	4 782	2 521	23.41
N_2008	1 035	754	7.00
N_2010	4 194	962	8.93
N_2011	2 725	1 601	14.87
N_2012	2 370	860	7.99
N_2013	10 883	4 650	43.19
N_2014	9 253	3 418	31.74
N_2016	491	322	2.99

A6. 11: Numbers of scampi measured, estimated multinomial N sample size, and effective sample size used within the model for length frequency distributions for observer samples, time step 3.

	Measured	Multinomial N	Effective sample size
N_1993	1 264	740	1.83
N_1994	1 960	1 192	2.95
N_1996	2 035	736	1.82
N_1997	8 816	5 002	12.40
N_1998	172	147	0.36
N_1999	2 707	1 575	3.90
N_2001	1 650	332	0.82
N_2002	5 663	1 184	2.93
N_2003	8 746	3 332	8.26
N_2005	1 600	1 215	3.01
N_2007	1 238	350	0.87
N_2008	4 435	1 300	3.22
N_2011	5 214	1 104	2.74
N_2016	3 265	994	2.46
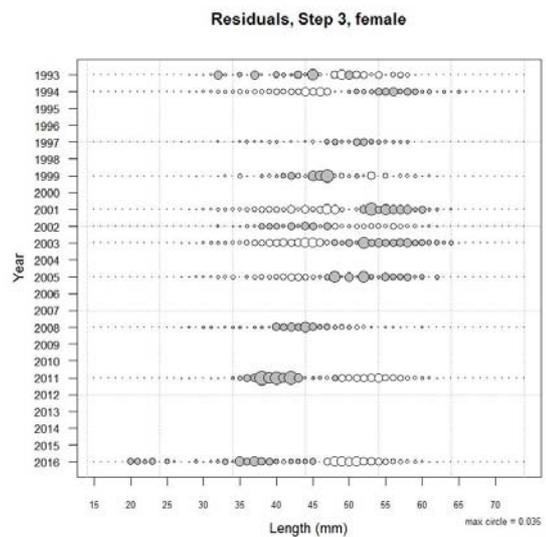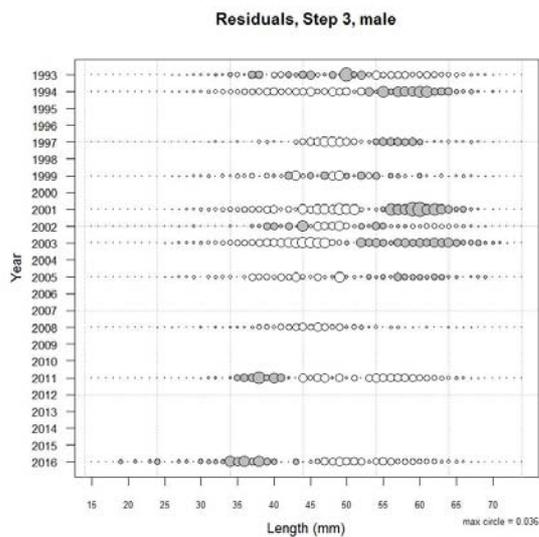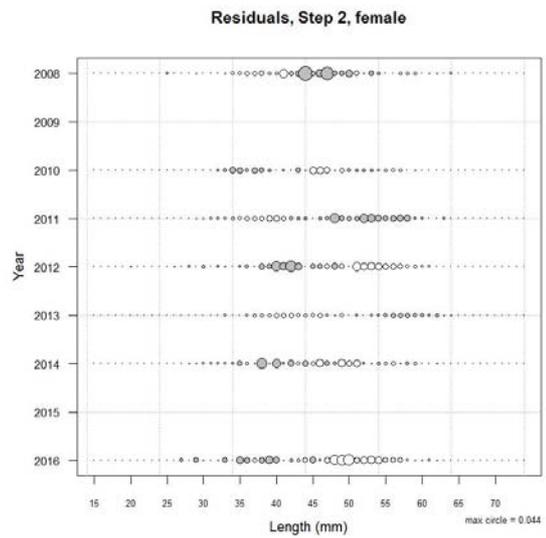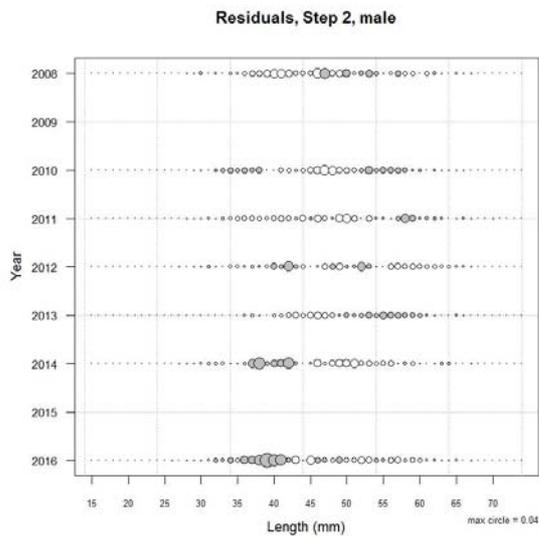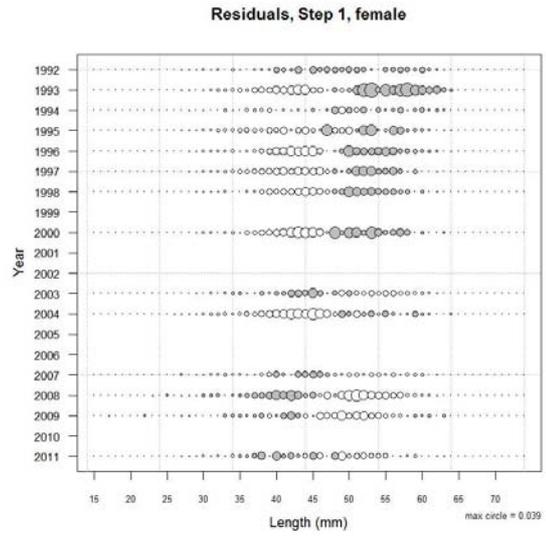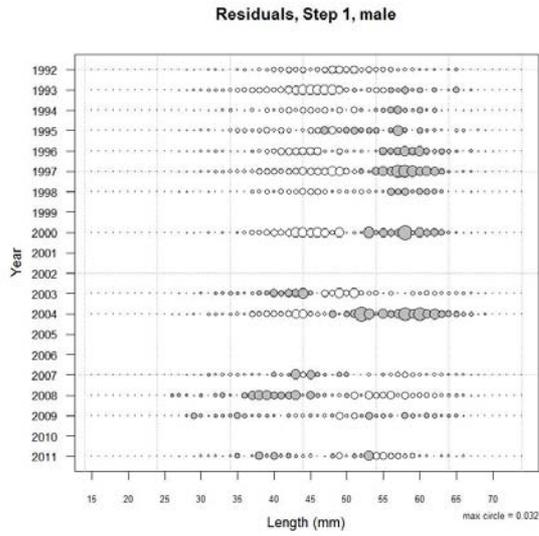
A6. 12: Bubble plots of residuals for fits to length frequency distributions for observer sampling.
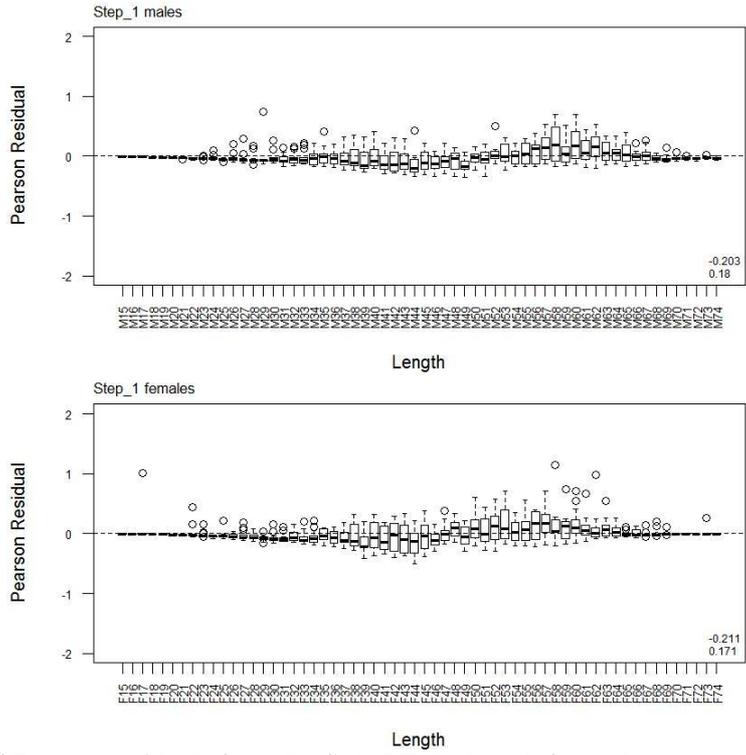
A6. 13: Box plots of Pearson residuals from the fit to LFs by length from observer sampling by sex for time step 1.
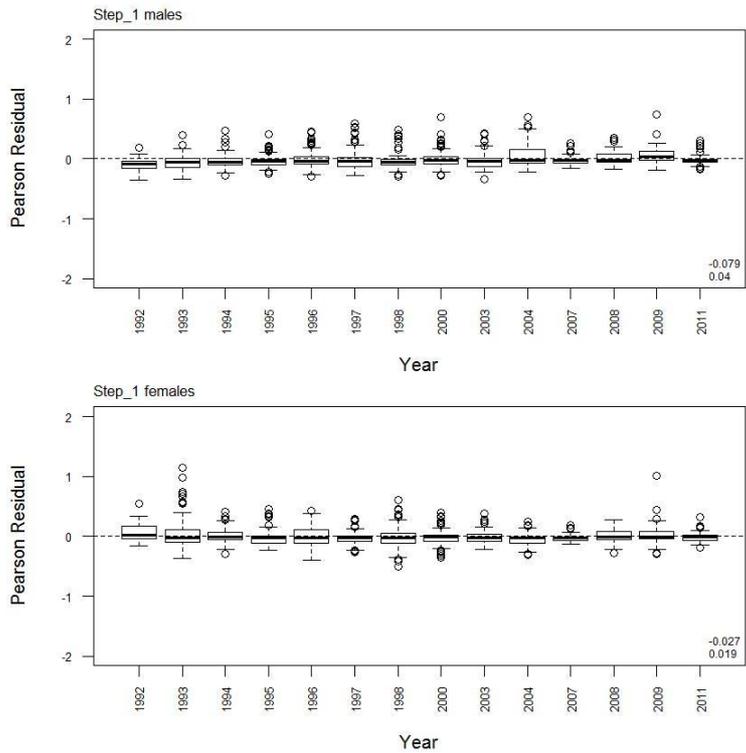
A6. 14: Box plots of Pearson residuals from the fit to LFs by year from observer sampling by sex for time step 1.
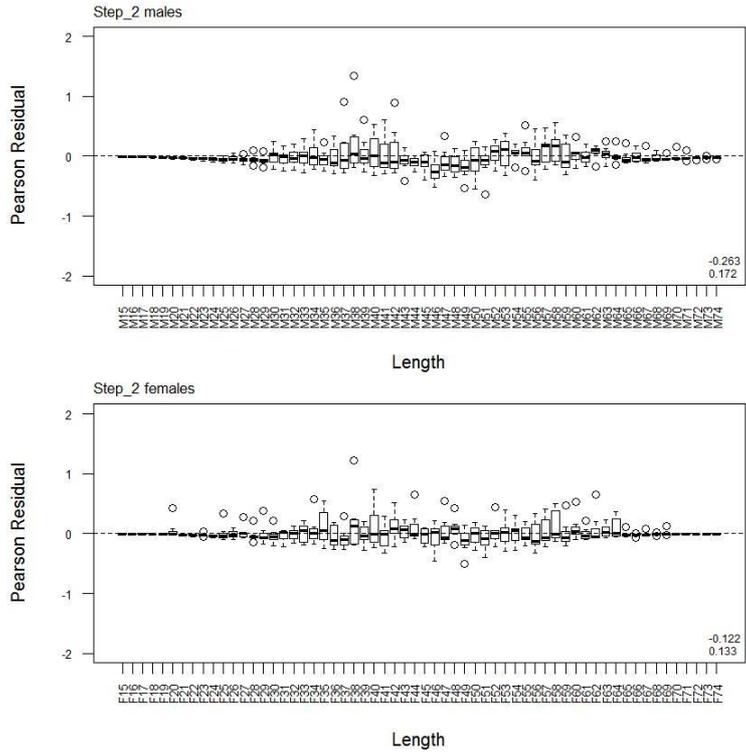
A6. 15: Box plots of Pearson residuals from the fit to LFs by length from observer sampling by sex for time step 2.
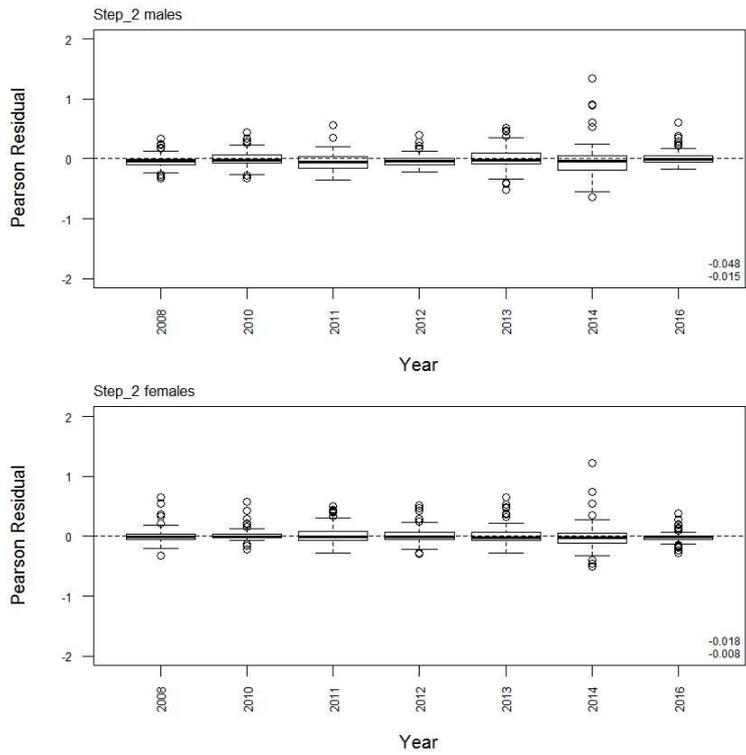

A6. 16: Box plots of Pearson residuals from the fit to LFs by year from observer sampling by sex for time step 2.
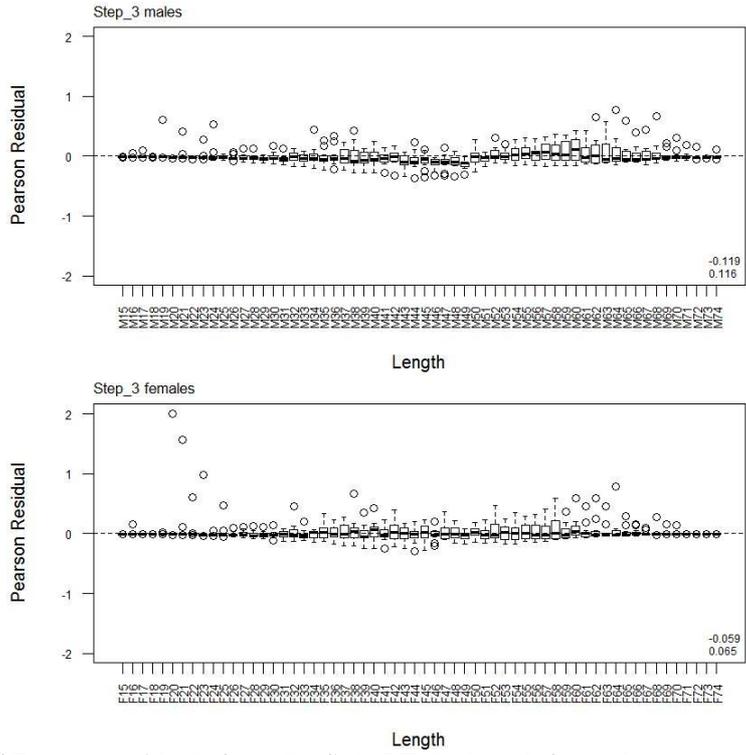
A6. 17: Box plots of Pearson residuals from the fit to LFs by length from observer sampling by sex for time step 3.
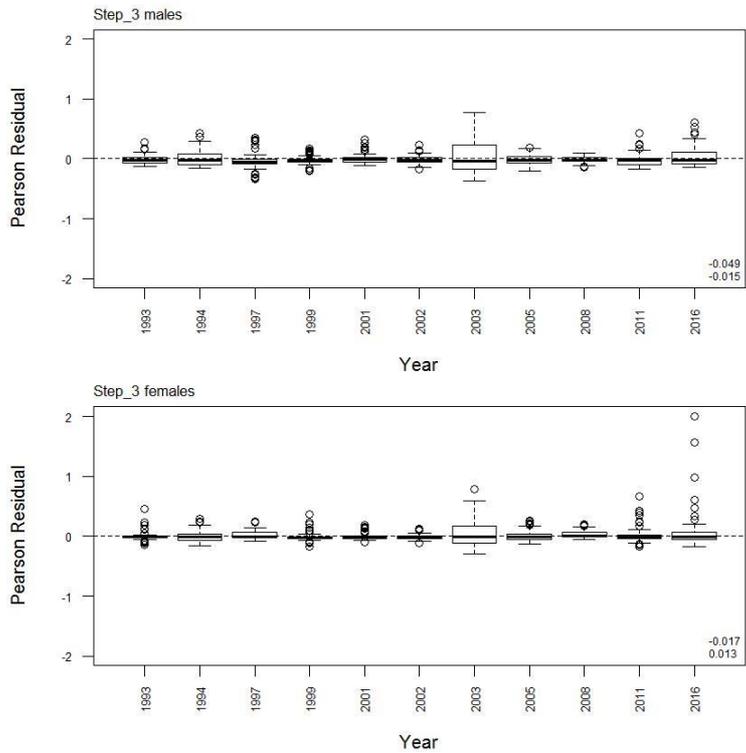
A6. 18: Box plots of Pearson residuals from the fit to LFs by year from observer sampling by sex for time step 3.
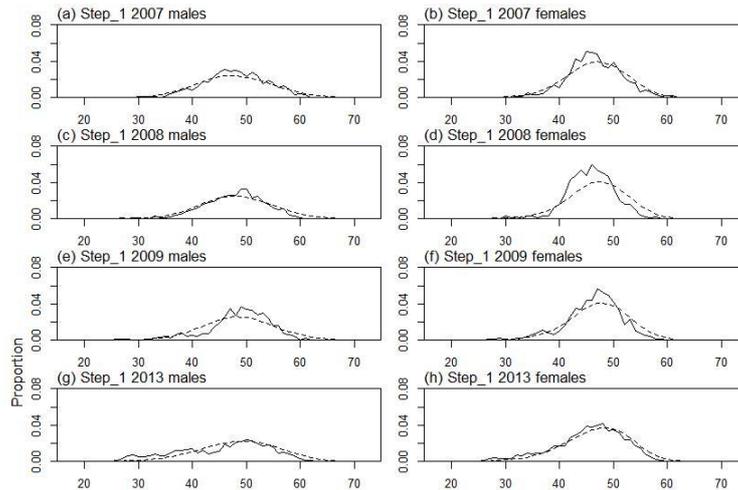
A6. 19: Average observed (solid line) and fitted (dashed line) length frequency distributions for observer samples.
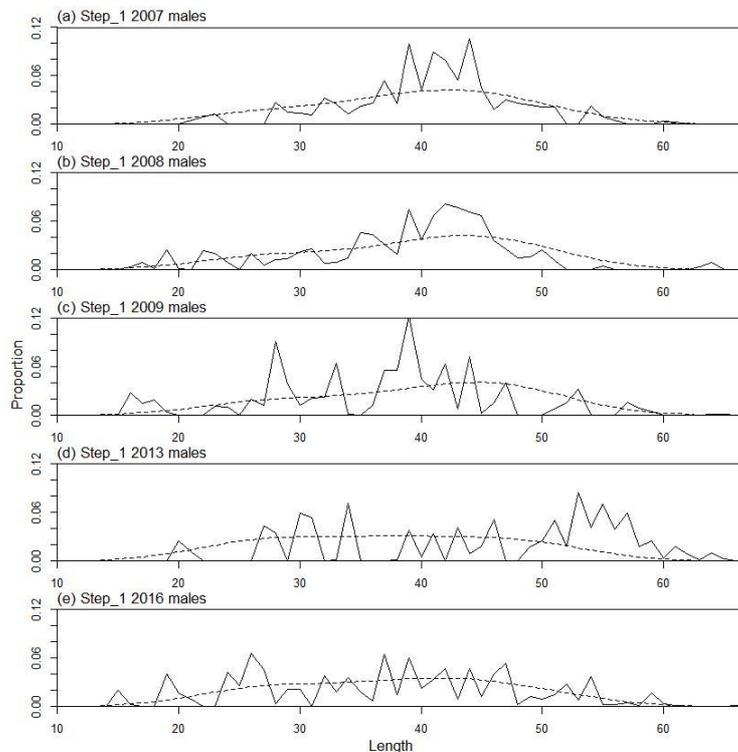
A6. 20: Observed (solid line) and fitted (dashed line) length frequency distributions for photographic survey scampi size estimation.

A6. 21: Numbers of scampi measured, estimated multinomial N sample size, and effective sample size used within the model for length frequency distributions for research survey samples.

	Measured	Multinomial N	Effective sample size
N_2007	1 981	2 127	35.29
N_2008	2 291	1 866	30.64
N_2009	4 054	2 798	46.97
N_2013	4 808	4 218	68.71

A6. 22: Numbers of scampi measured, estimated multinomial N sample size, and effective sample size used within the model for length frequency distributions for photographic survey samples.

	Measured	Multinomial N	Effective sample size
N_2007	70	125	15.52
N_2008	73	121	16.18
N_2009	45	72	9.97
N_2013	26	43	5.76
N_2016	44	72	9.75
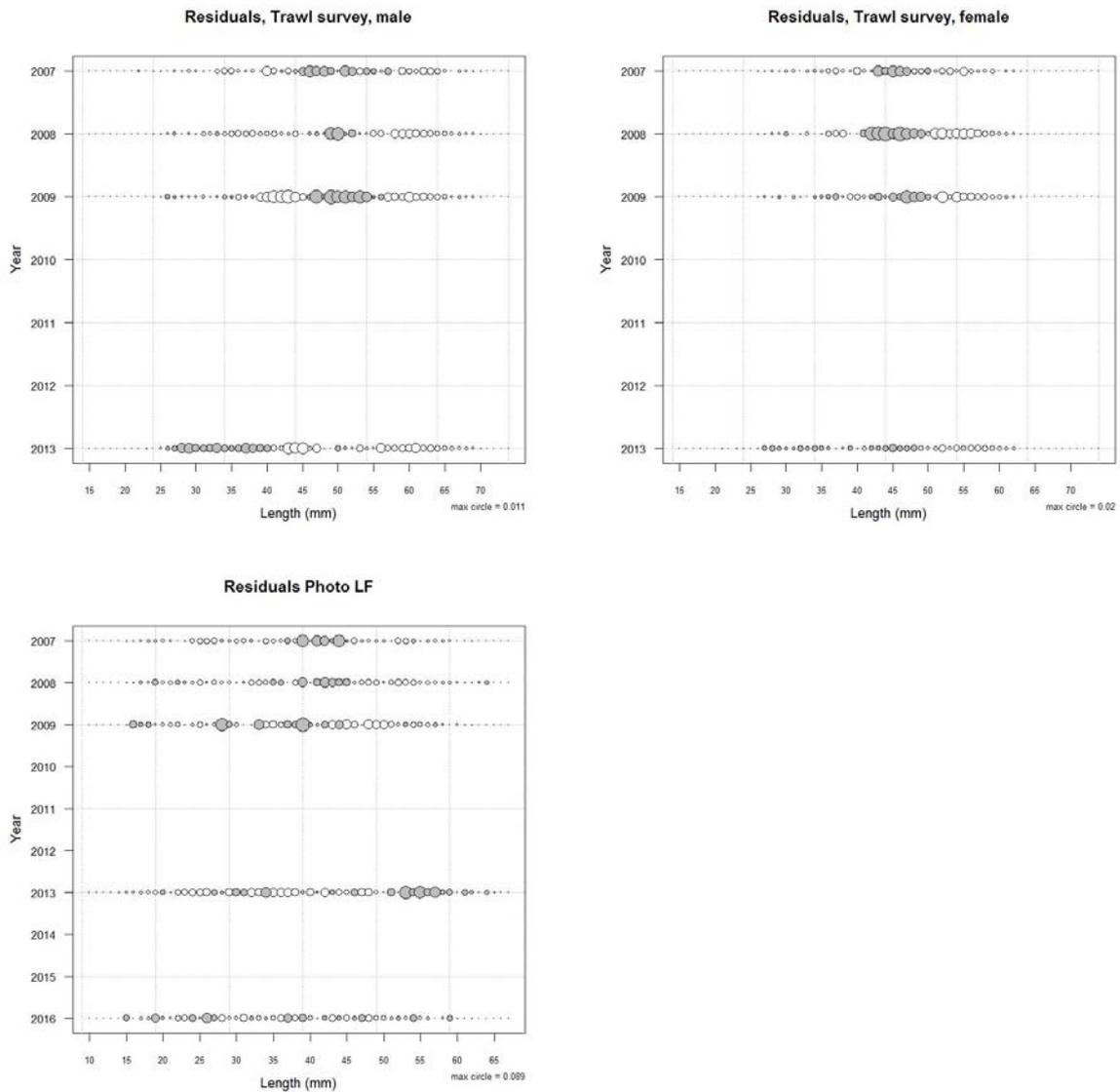
A6. 23: Bubble plots of residuals for fits to length frequency distributions for trawl survey sampling and photographic survey scampi size estimation.
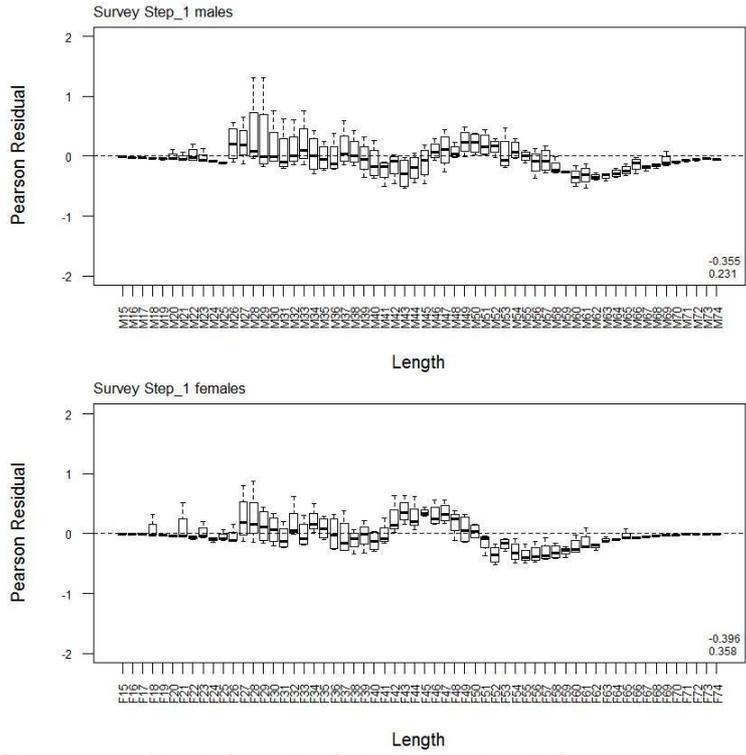
A6. 24: Box plots of Pearson residuals from the fit to LFs by length from trawl survey sampling by sex for time step 1.
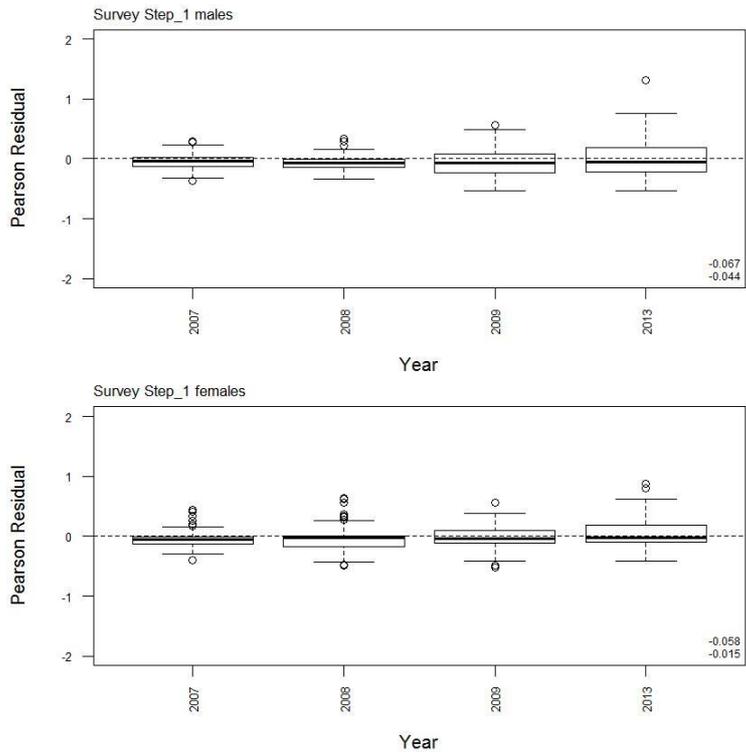
A6. 25: Box plots of Pearson residuals from the fit to LFs by year from trawl survey sampling by sex for time step 1.
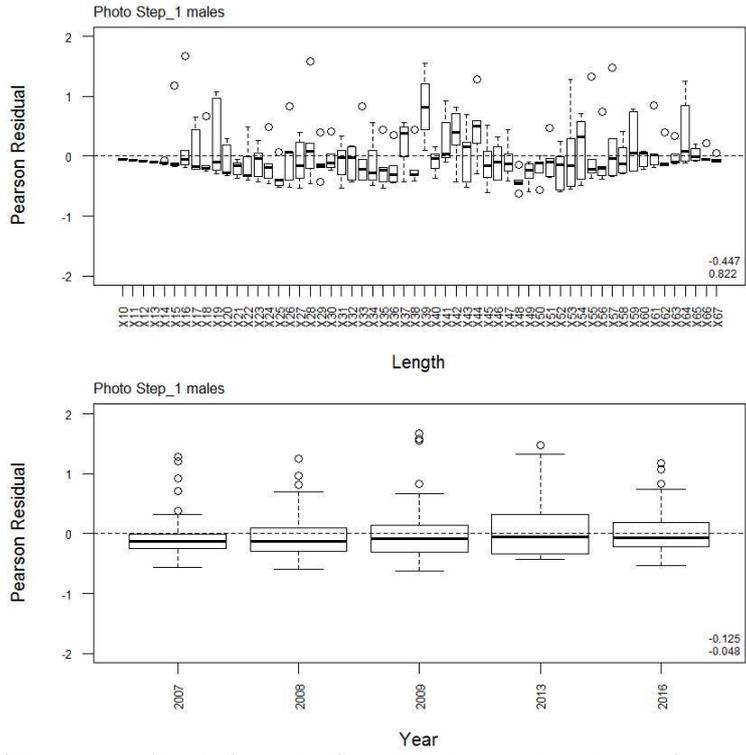
A6. 26: Box plots of Pearson residuals from the fit to LFs by length and year from photo survey sampling for time step 1.
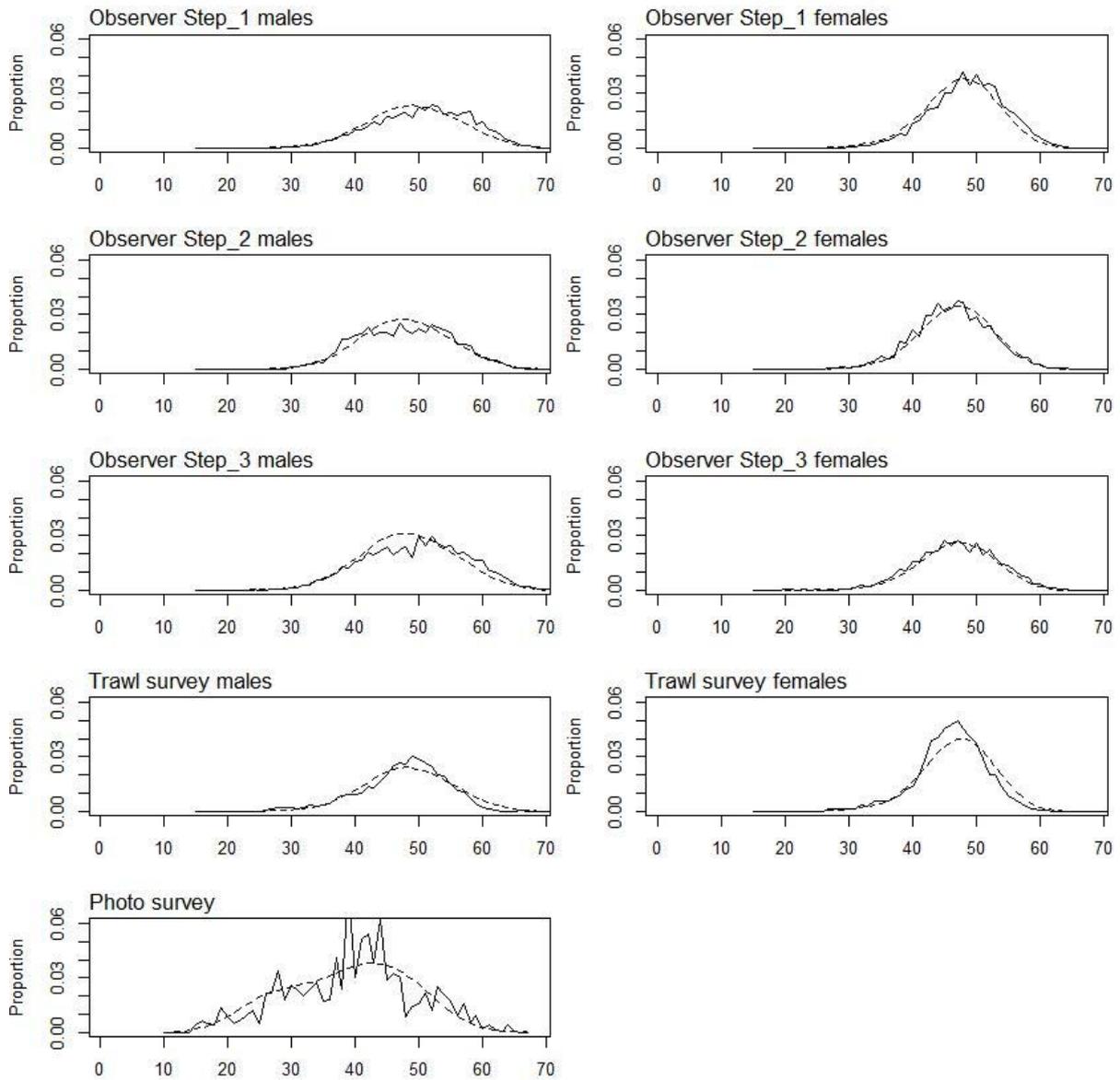
A6. 27: Average observed (solid line) and fitted (dashed line) length frequency distributions for trawl survey sampling and photographic survey scampi size estimation.
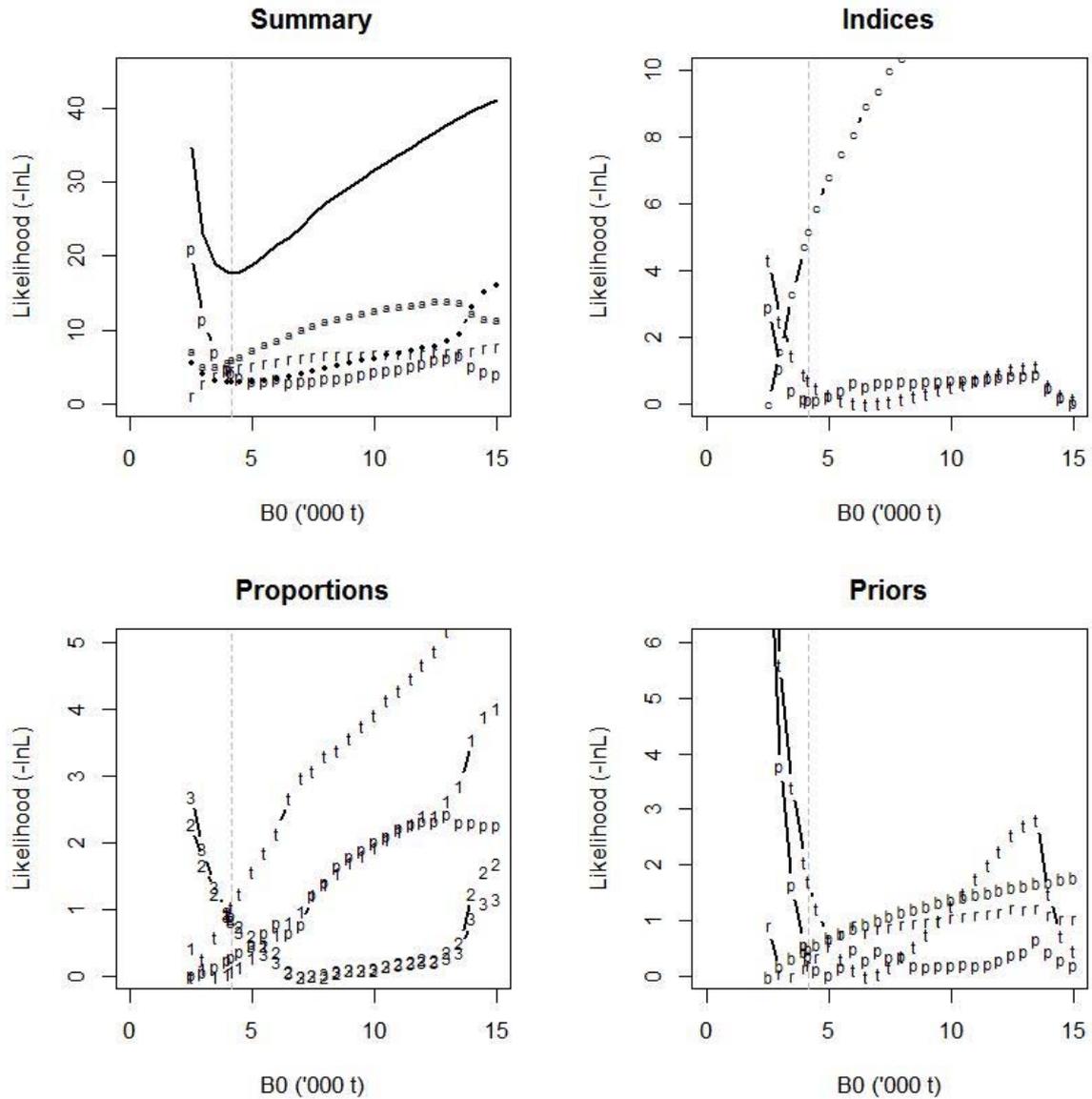
A6. 28: Likelihood profiles for SCI 6A Model 3 when B₀ is fixed in the model. Figures show profiles for main priors (top left, p – priors, a - abundance indices, • – proportions at length, r – recapture data), abundance indices (top right, t - trawl survey, c - CPUE, p – photo survey), proportion at length data (bottom left, a-trawl, 1 – observer time step 1, 2 – observer time step 2, 3 – observer time step 3, p - photo) and priors (bottom right, b- B₀, YCS - r, p- *q-Photo***, t –** *q-Trawl***). Vertical dashed line represents MPD.**
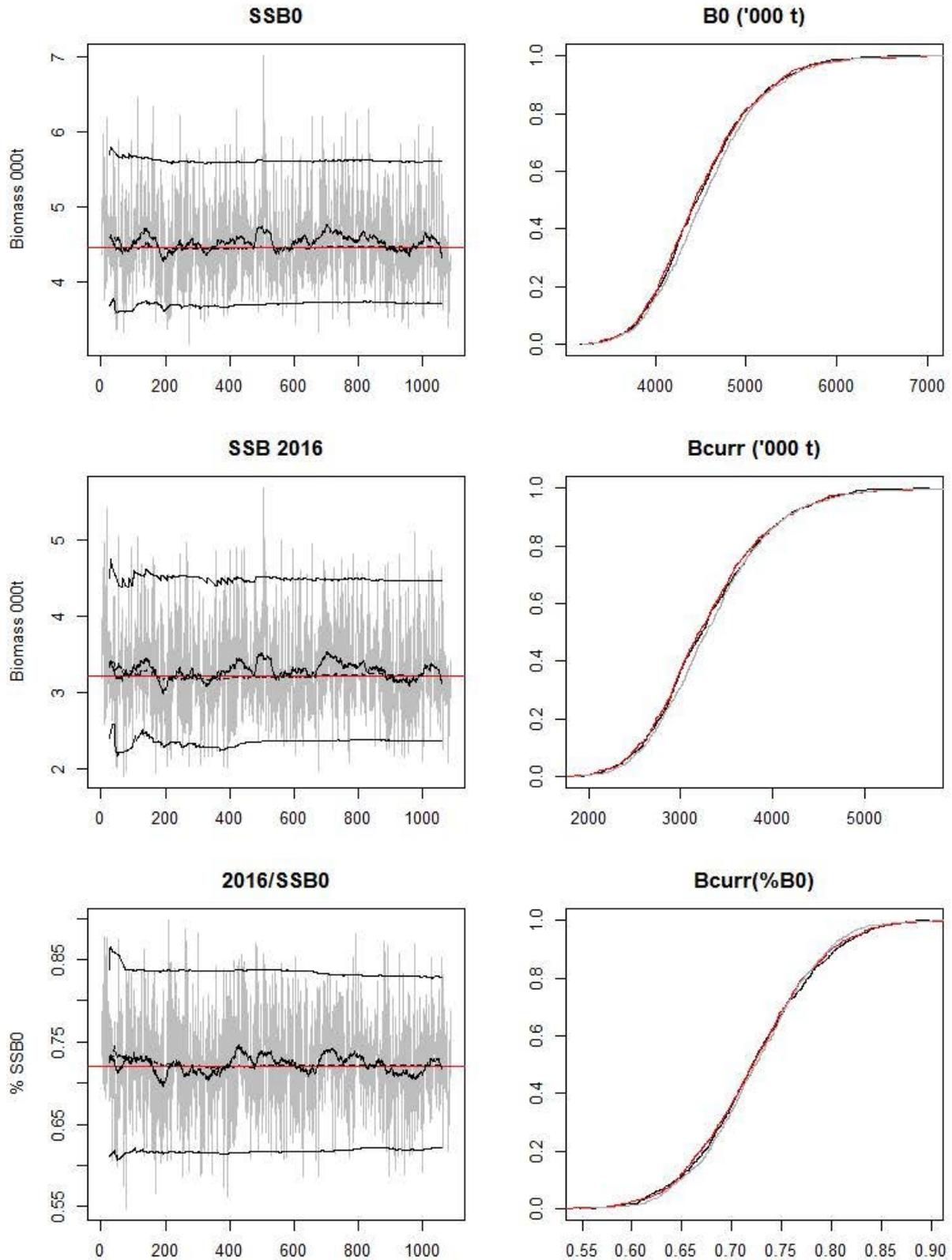
A6. 29: MCMC traces for SSB$_0$, SSB$_{2016}$, and SSB$_{2016}$/SSB$_0$ terms for SCI 6A Model 3 (trace – grey line, cumulative moving median –dashed black line, moving average and cumulative moving 2.5%, 97.5% quantiles – solid black lines, overall median – solid red line, left plots), along with cumulative frequency distributions for three independent MCMC chains (shown as red, grey and black lines, right plots).
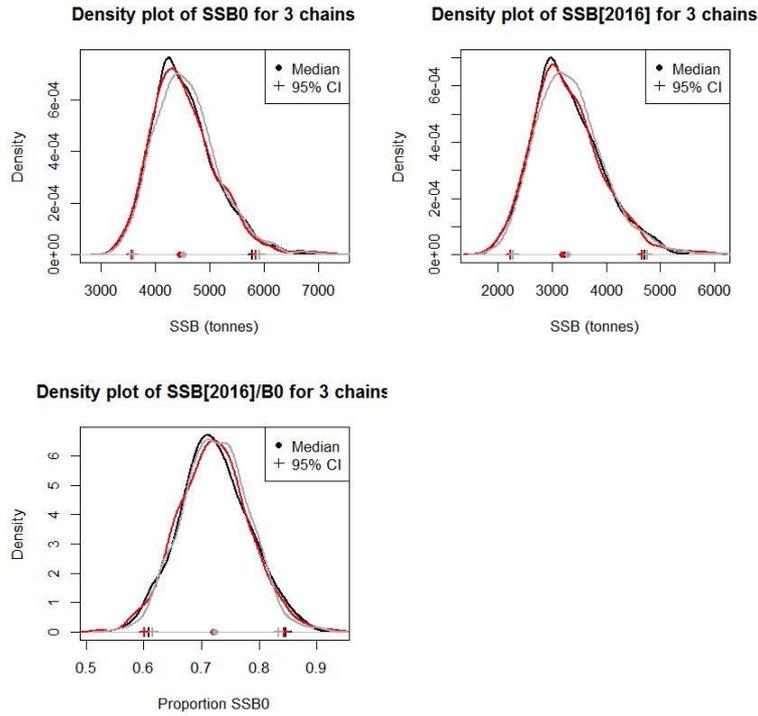
A6. 30: Density plots for SSB$_0$, SSB$_{2016}$, and SSB$_{2016}$/SSB$_0$ terms for SCI 6A Model 3 for three independent MCMC chains, with median and 95% confidence intervals.
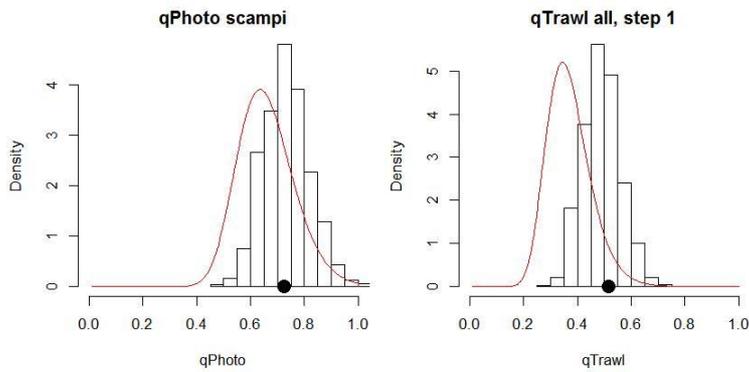
A6. 31: Marginal posterior distributions (histograms), MPD estimates (solid symbols) and distributions of priors (lines) for catchability terms.
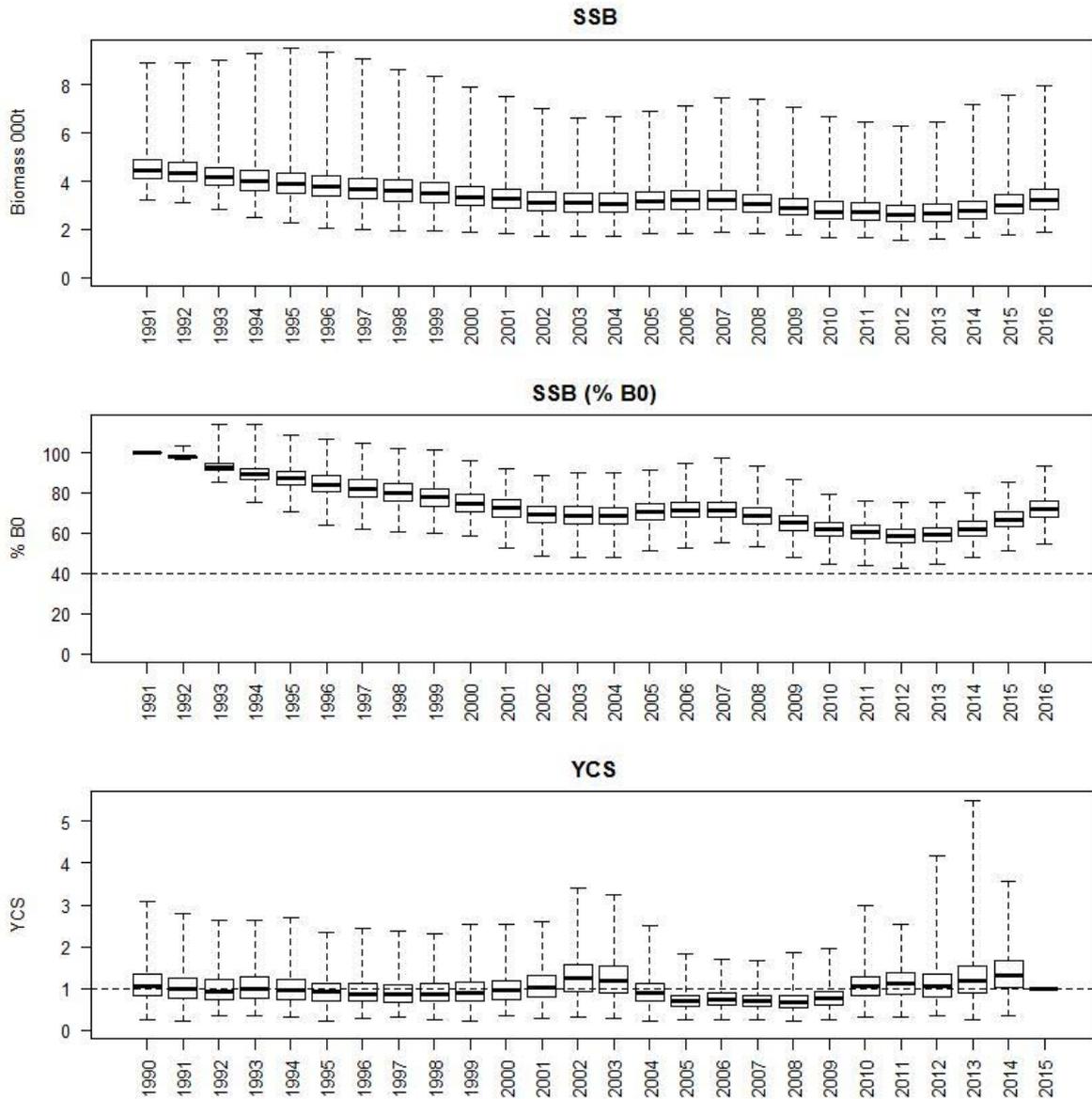
A6. 32: Posterior trajectory of SSB, SSB_{2016}/SSB_0 and YCS.

APPENDIX 7. MODEL 4, M fixed at 0.25, CV on YCS prior 0.7
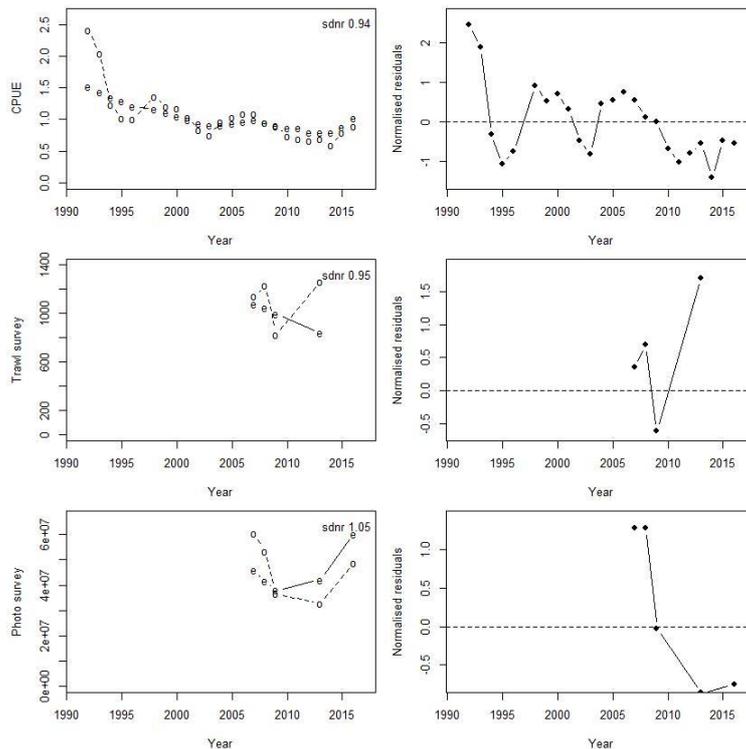
A7. 1: Fits to abundance indices (left column) and normalised residuals (right column) for standardised CPUE index (top row) trawl survey biomass index (middle row) and photo survey abundance index (bottom row) for SCI 6A Model 4.
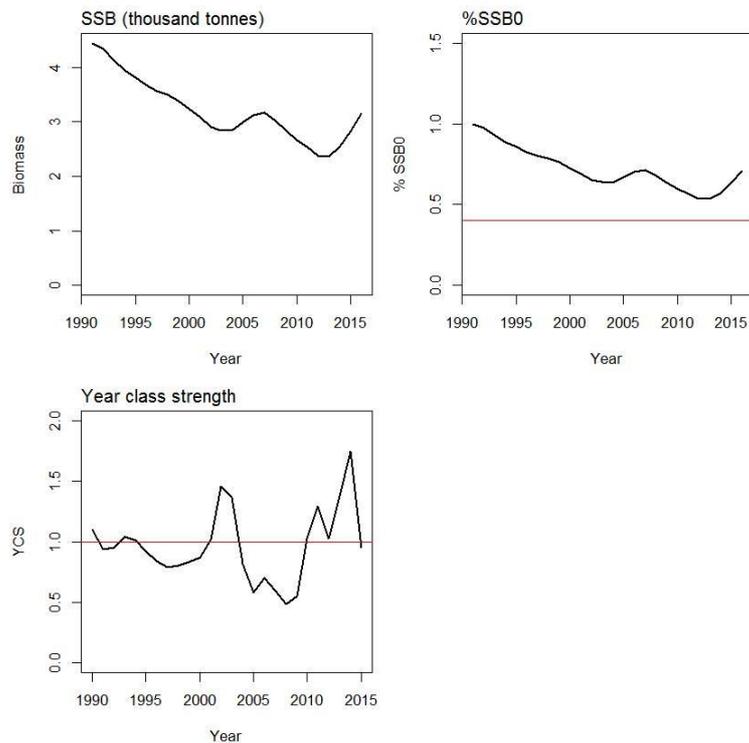
A7. 2: Spawning stock biomass trajectory (upper left), Spawning stock biomass as a percentage of SSB₀ (upper right), and year class strength (lower plot) for SCI 6A Model 4.
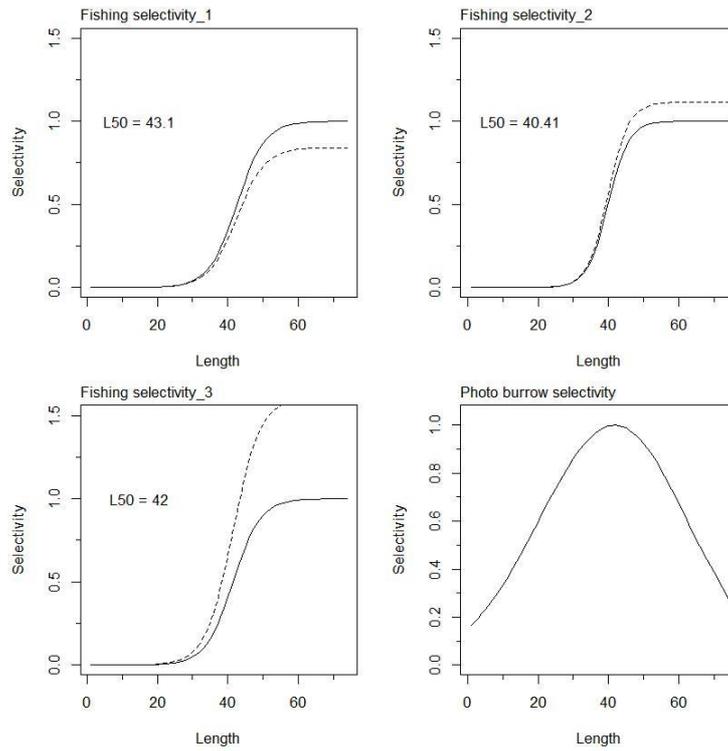
A7. 3: Fishery and photo survey selectivity curves for SCI 6A Model 4. Solid line – females, dotted line – males. The scampi photo index is not sexed, and a single selectivity applies.
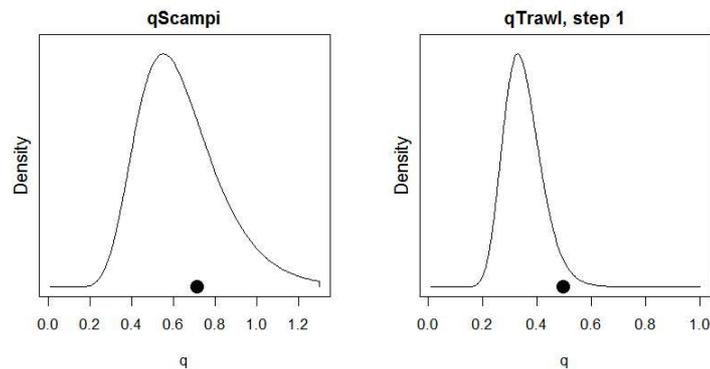
A7. 4: Catchability estimates from MPD model run for SCI 6A Model 4, plotted in relation to prior distribution.
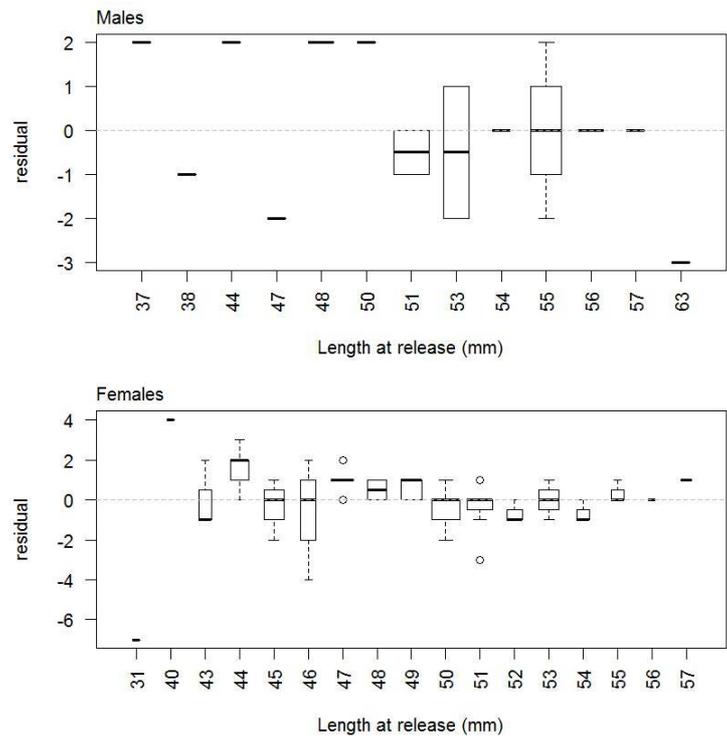
A7. 5: Box plots of residuals from the fit to growth increment by length from tag recapture data by sex.
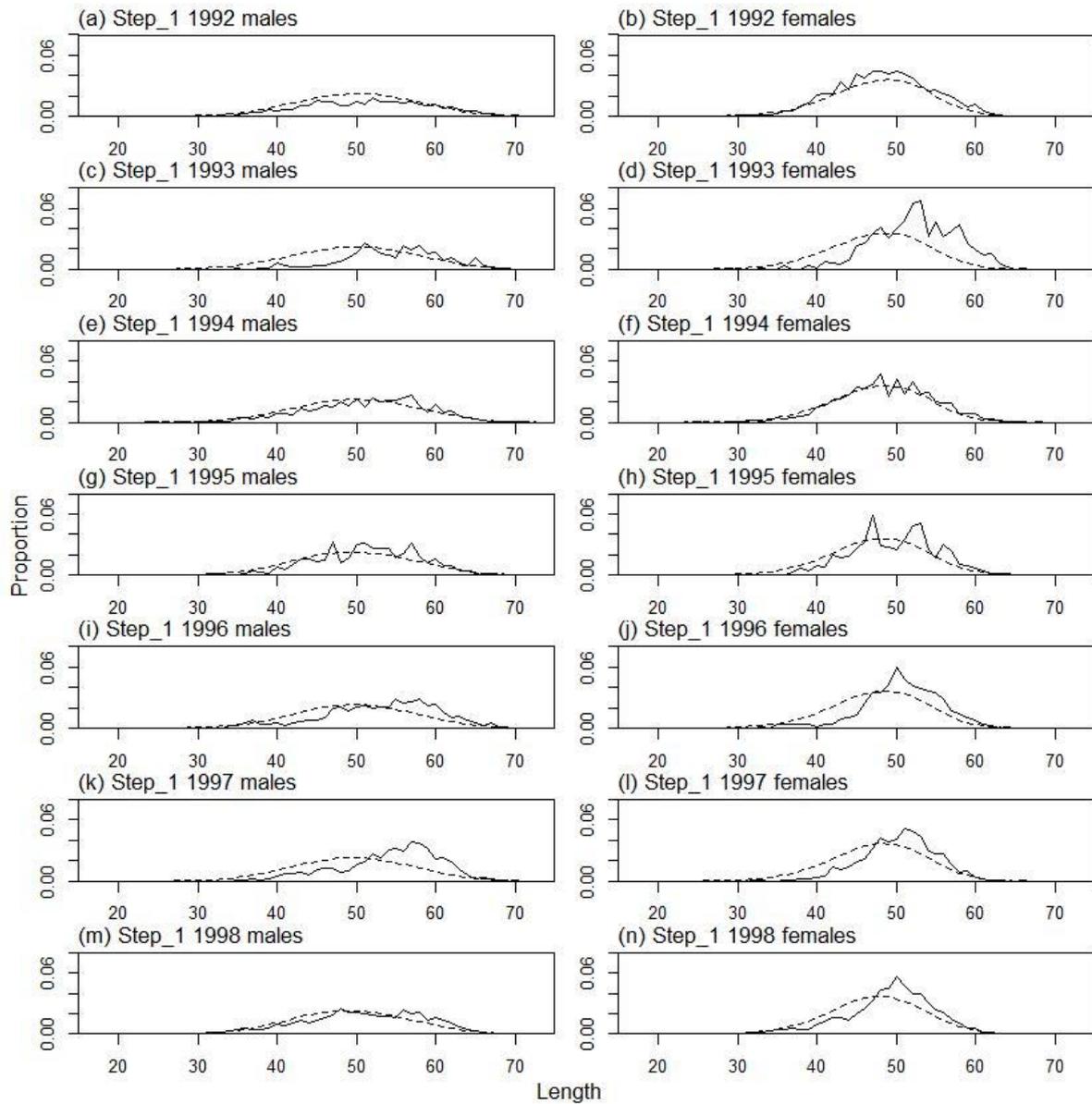
A7. 6: Observed (solid line) and fitted (dashed line) length frequency distributions for observer samples, time step 1.
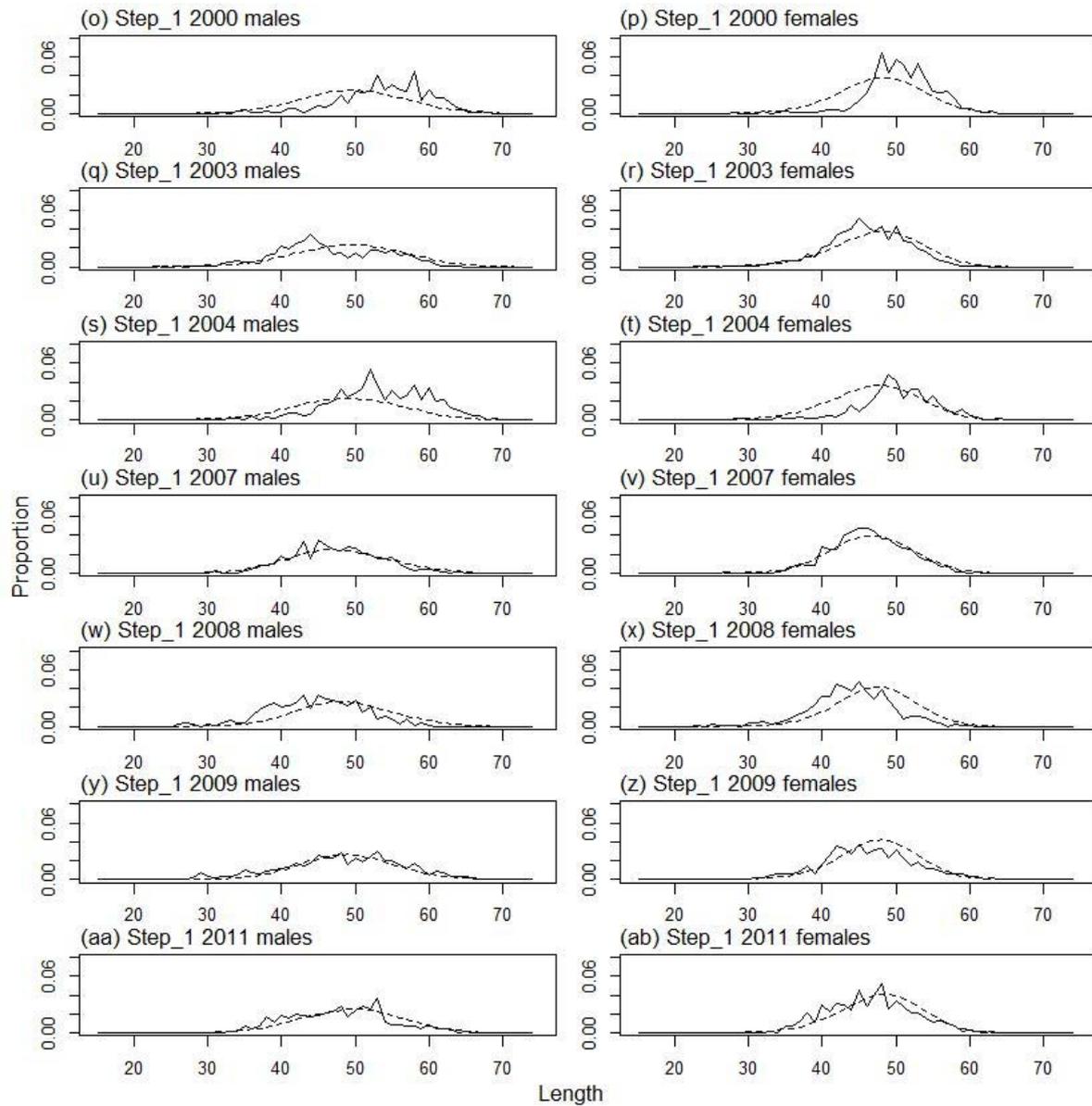
A7. 6 ctd.: Observed (solid line) and fitted (dashed line) length frequency distributions for observer samples, time step 1.
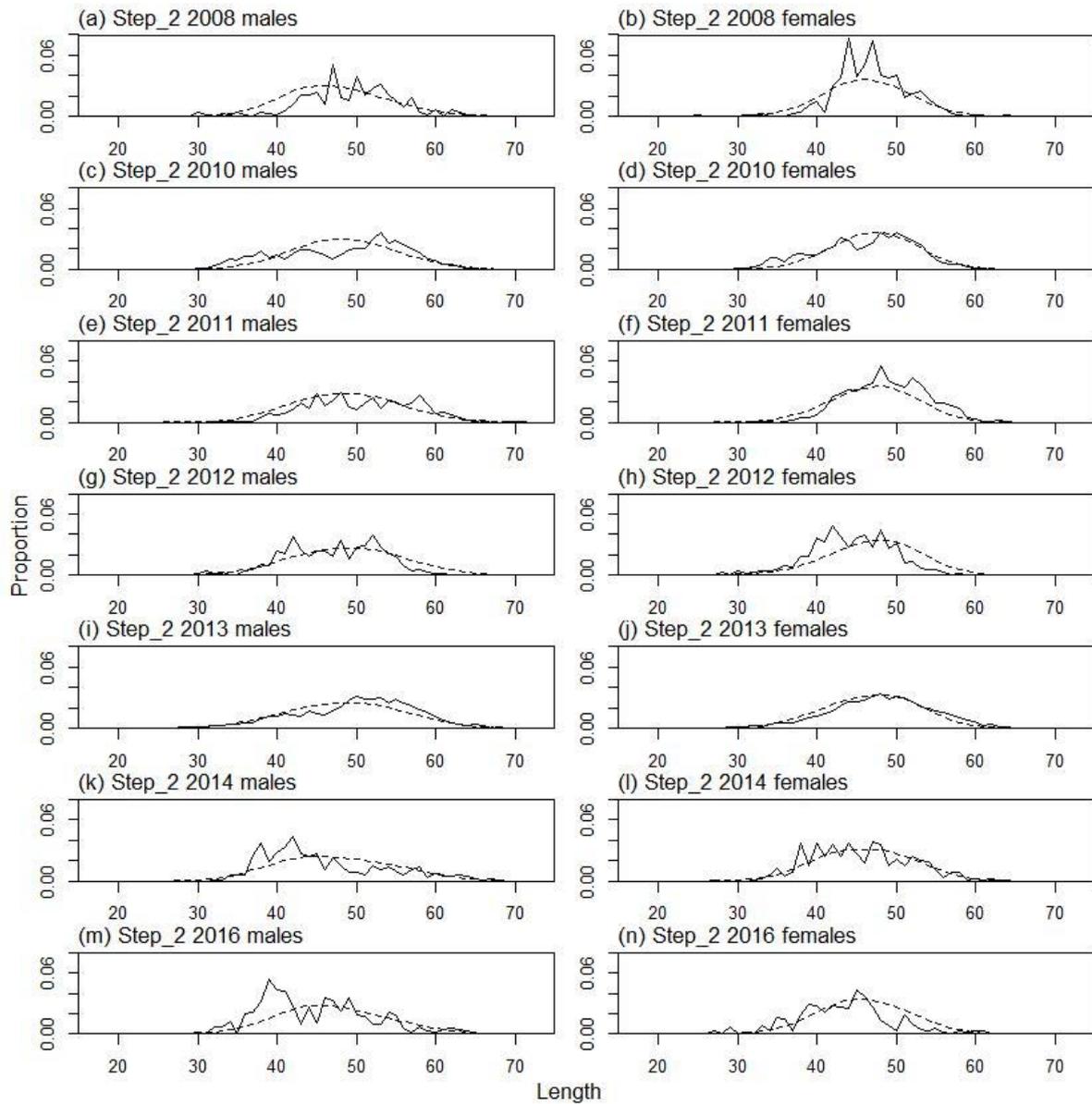
A7. 7: Observed (solid line) and fitted (dashed line) length frequency distributions for observer samples, time step 2.
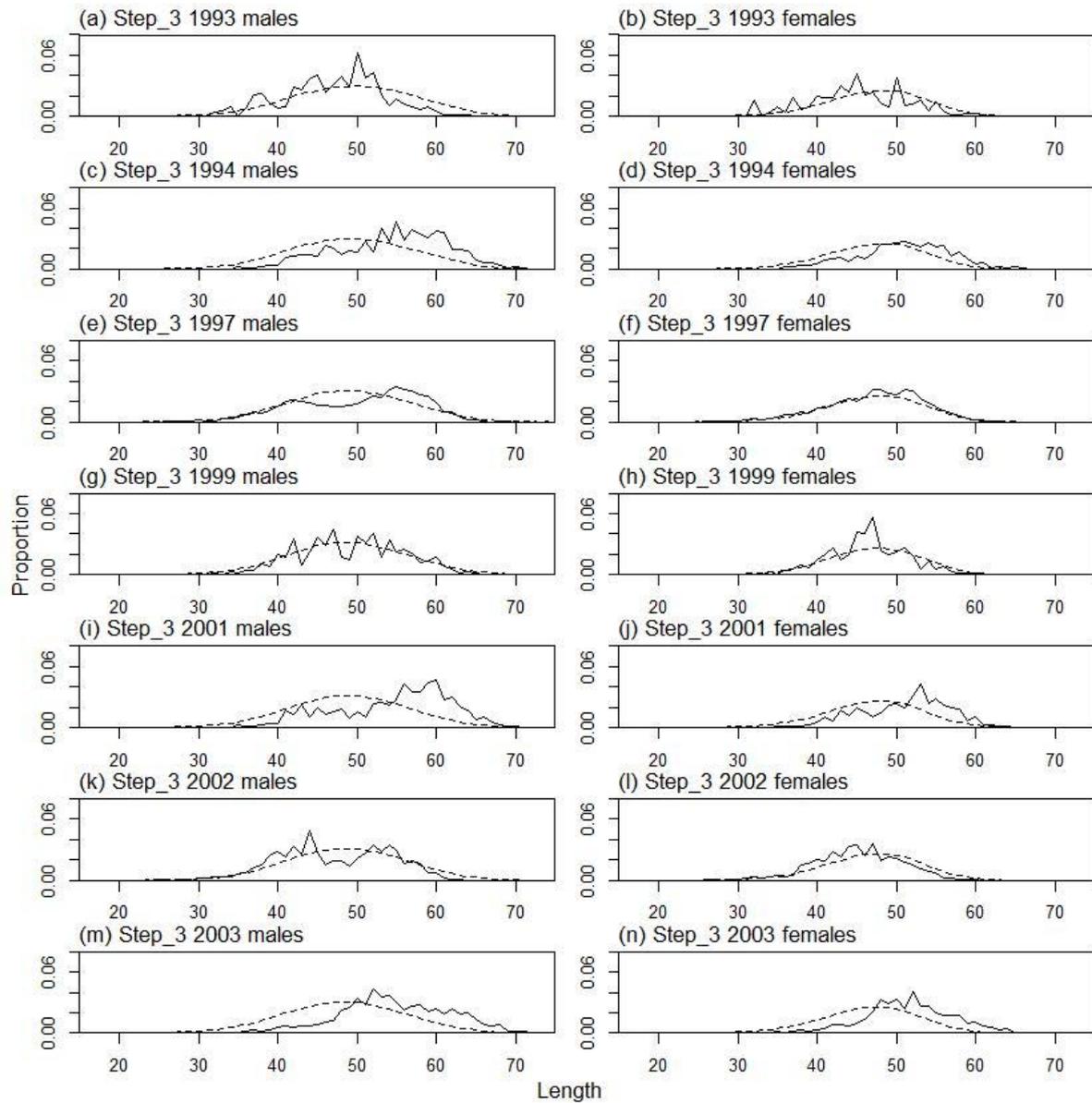
A7. 8: Observed (solid line) and fitted (dashed line) length frequency distributions for observer samples, time step 3.
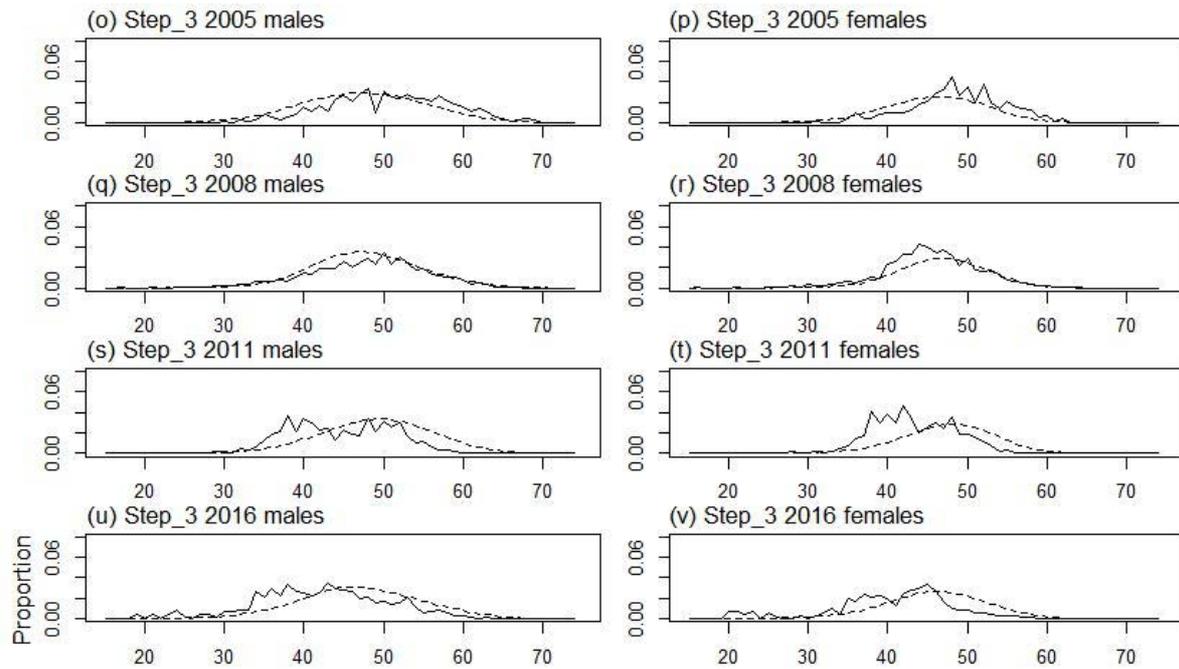
A7. 8 ctd.: Observed (solid line) and fitted (dashed line) length frequency distributions for observer samples, time step 3.

A7. 9: Numbers of scampi measured, estimated multinomial N sample size, and effective sample size used within the model for length frequency distributions for observer samples, time step 1.

	Measured	Multinomial N	Effective sample size
N_1992	9 250	3 373	20.72
N_1993	2 641	3 340	8.44
N_1994	9 300	3 924	24.11
N_1995	2 600	1 360	8.58
N_1996	3 200	1 690	10.78
N_1997	2 794	1 165	7.14
N_1998	11 964	4 863	28.58
N_2000	2 449	935	5.82
N_2002	1 975	458	2.74
N_2003	4 965	2 109	13.19
N_2004	1 214	760	4.91
N_2007	3 235	1 006	6.41
N_2008	1 269	568	3.74
N_2009	2 959	1 504	9.49
N_2011	4 035	937	5.98

A7. 10: Numbers of scampi measured, estimated multinomial N sample size, and effective sample size used within the model for length frequency distributions for observer samples, time step 2.

	Measured	Multinomial N	Effective sample size
N_1997	3 287	1 509	16.12
N_1998	703	472	5.04
N_2001	4 782	2 521	26.92
N_2008	1 035	754	8.05
N_2010	4 194	962	10.27
N_2011	2 725	1 601	17.10
N_2012	2 370	860	9.18
N_2013	10 883	4 650	49.66
N_2014	9 253	3 418	36.50
N_2016	491	322	3.44

A7. 11: Numbers of scampi measured, estimated multinomial N sample size, and effective sample size used within the model for length frequency distributions for observer samples, time step 3.

|	Measured	Multinomial N	Effective sample size
N_1993	1 264	740	1.93
N_1994	1 960	1 192	3.11
N_1996	2 035	736	1.92
N_1997	8 816	5 002	13.06
N_1998	172	147	0.38
N_1999	2 707	1 575	4.11
N_2001	1 650	332	0.87
N_2002	5 663	1 184	3.09
N_2003	8 746	3 332	8.70
N_2005	1 600	1 215	3.17
N_2007	1 238	350	0.91
N_2008	4 435	1 300	3.39
N_2011	5 214	1 104	2.88
N_2016	3 265	994	2.60
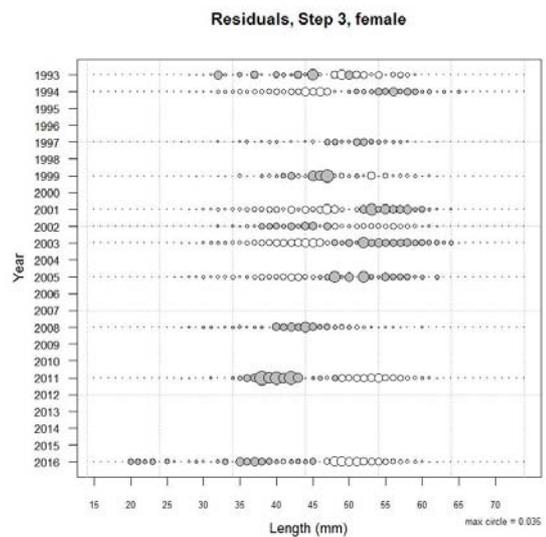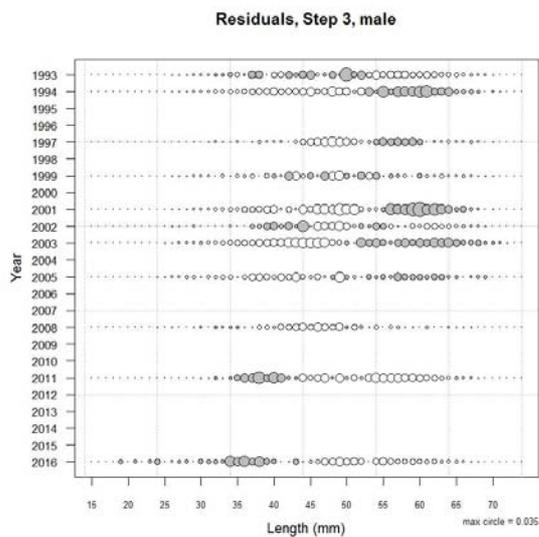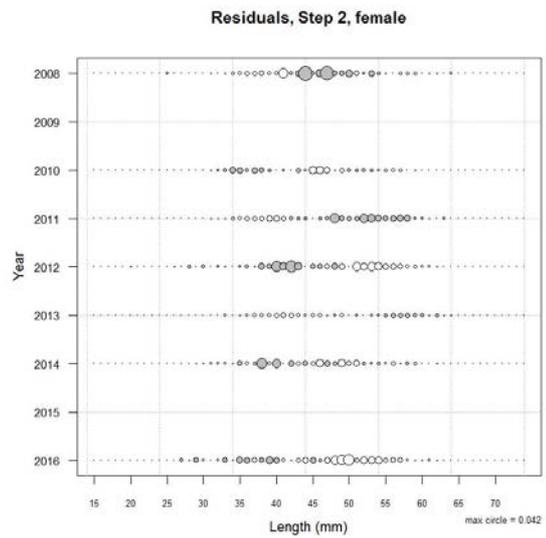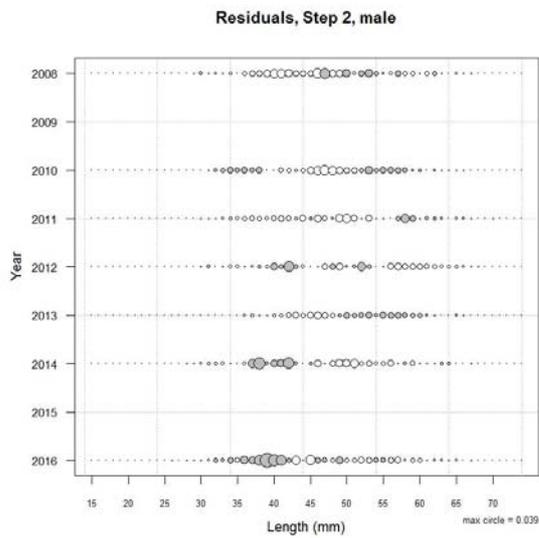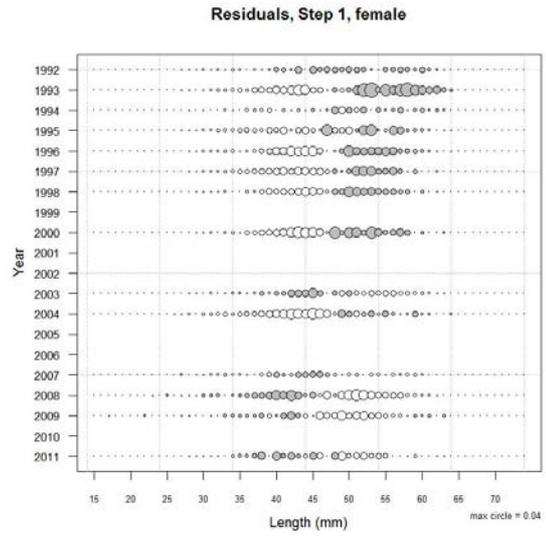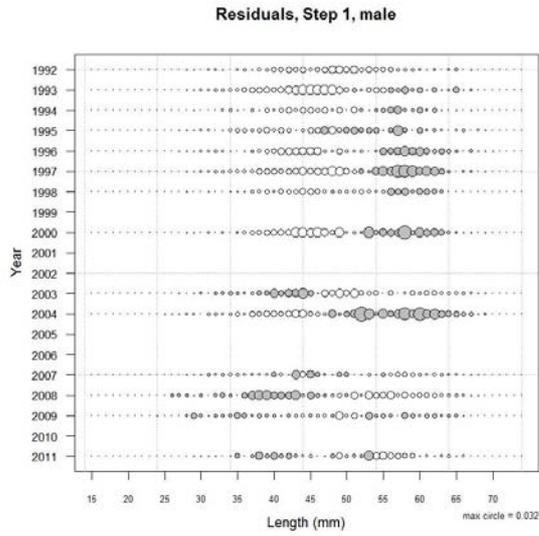
**A7. 12: Bubble plots of residuals for fits to length frequency distributions for observer sampling.**
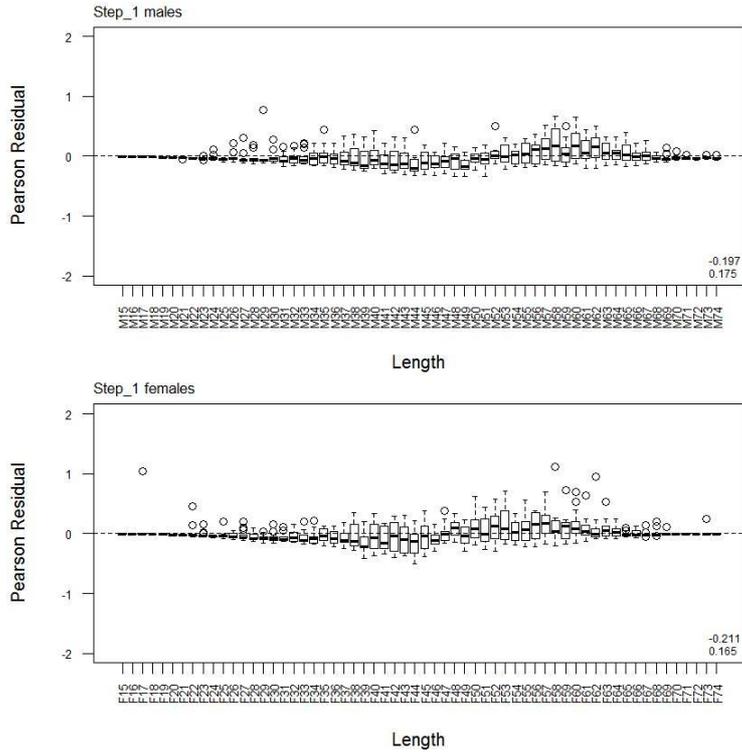
A7. 13: Box plots of Pearson residuals from the fit to LFs by length from observer sampling by sex for time step 1.
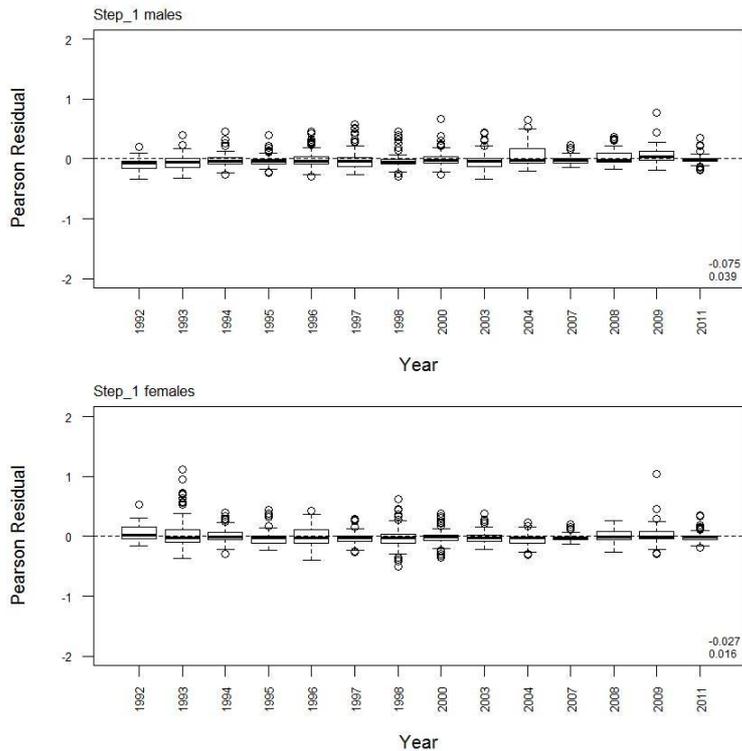

A7. 14: Box plots of Pearson residuals from the fit to LFs by year from observer sampling by sex for time step 1.
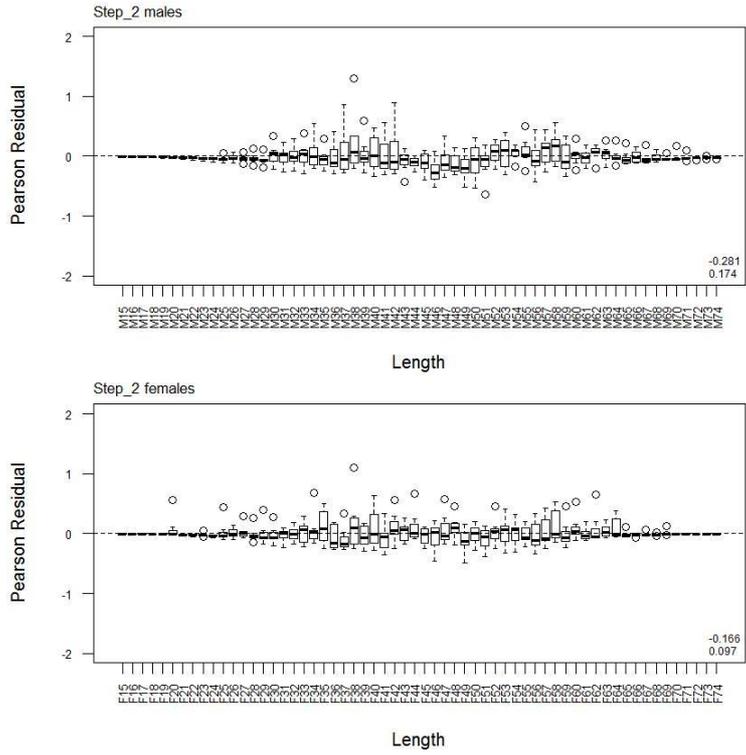
A7. 15: Box plots of Pearson residuals from the fit to LFs by length from observer sampling by sex for time step 2.
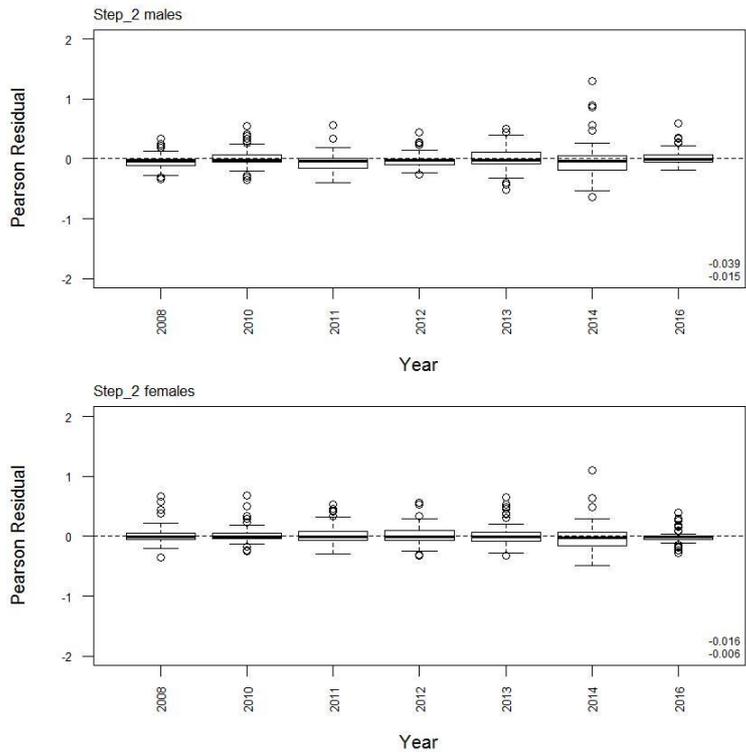
A7. 16: Box plots of Pearson residuals from the fit to LFs by year from observer sampling by sex for time step 2.
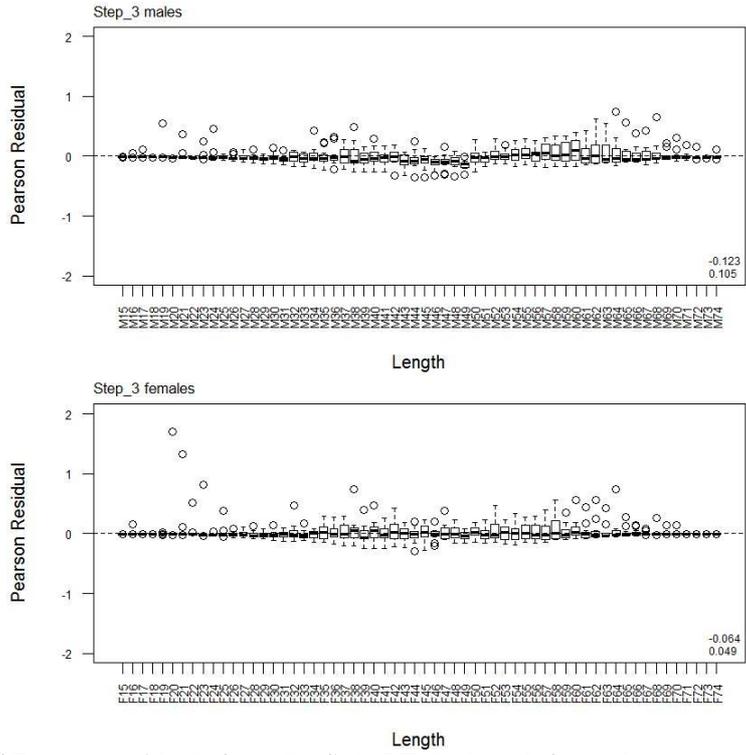
A7. 17: Box plots of Pearson residuals from the fit to LFs by length from observer sampling by sex for time step 3.
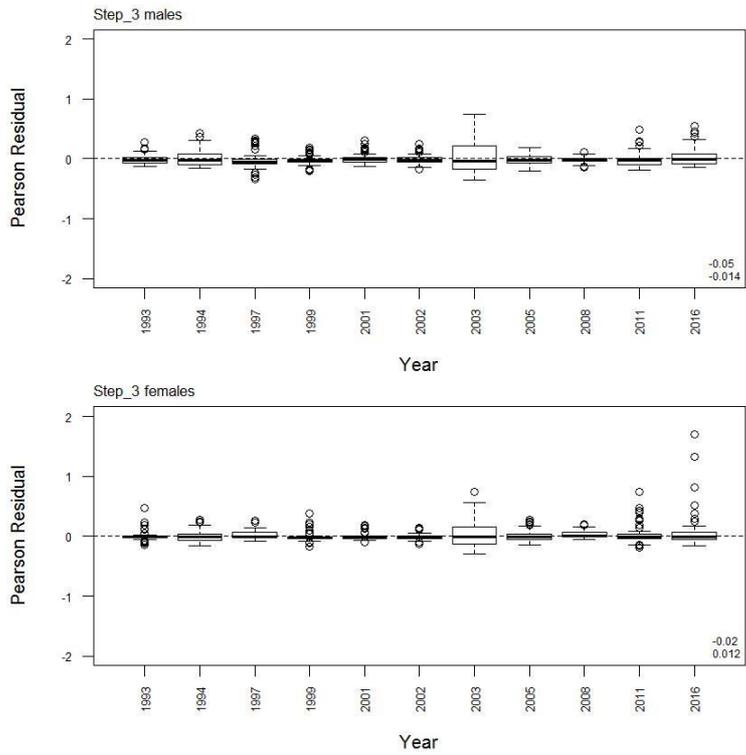
A7. 18: Box plots of Pearson residuals from the fit to LFs by year from observer sampling by sex for time step 3.
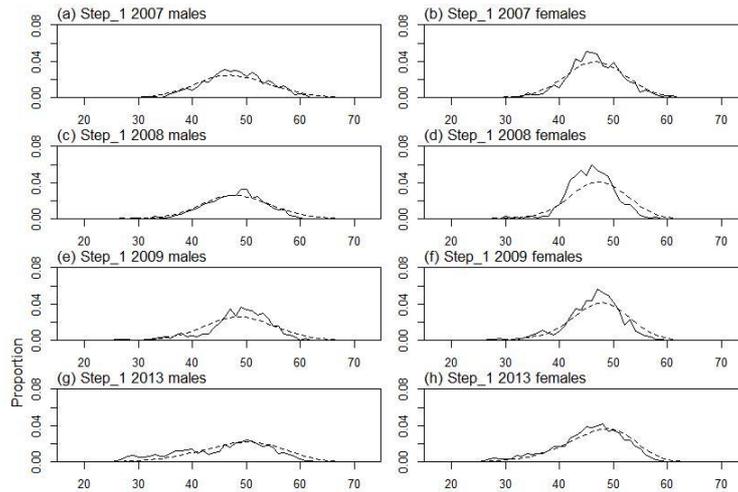
A7. 19: Average observed (solid line) and fitted (dashed line) length frequency distributions for observer samples.
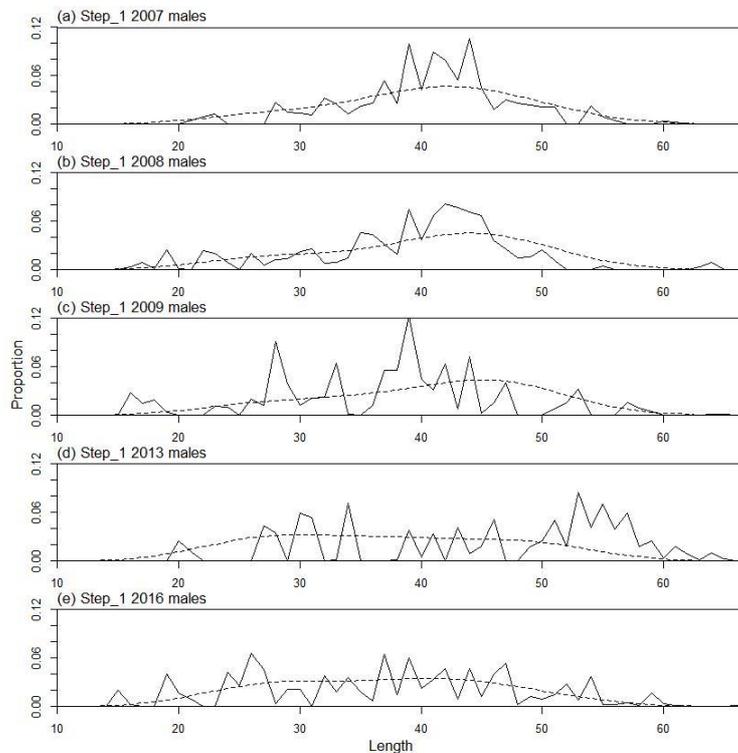
A7. 20: Observed (solid line) and fitted (dashed line) length frequency distributions for photographic survey scampi size estimation.

A7. 21: Numbers of scampi measured, estimated multinomial N sample size, and effective sample size used within the model for length frequency distributions for research survey samples.

	Measured	Multinomial N	Effective sample size
N_2007	1 981	2 127	33.40
N_2008	2 291	1 866	29.00
N_2009	4 054	2 798	44.47
N_2013	4 808	4 218	65.04

A7. 22: Numbers of scampi measured, estimated multinomial N sample size, and effective sample size used within the model for length frequency distributions for photographic survey samples.

	Measured	Multinomial N	Effective sample size
N_2007	70	125	12.14
N_2008	73	121	12.67
N_2009	45	72	7.81
N_2013	26	43	4.51
N_2016	44	72	7.63
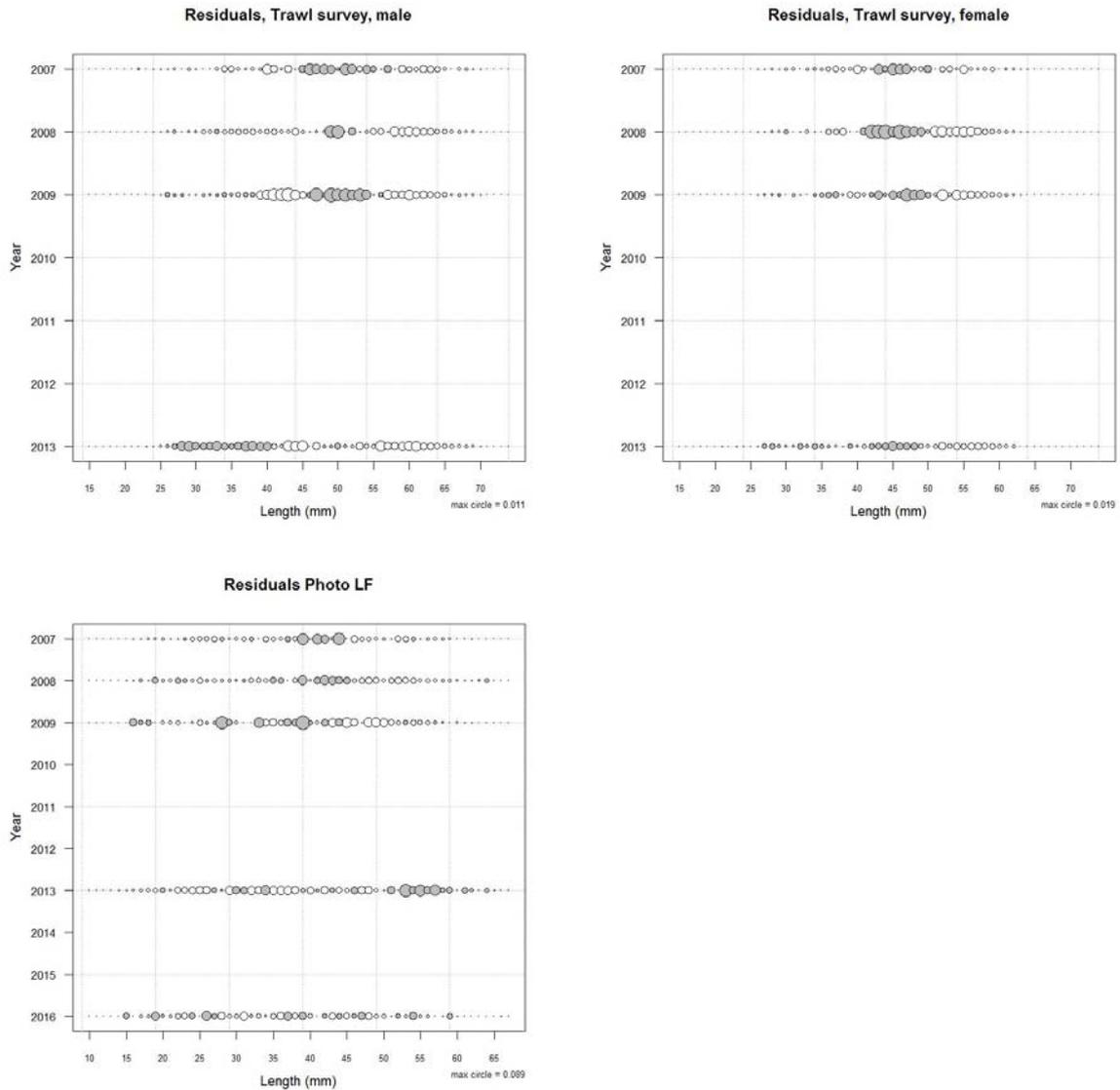
A7. 23: Bubble plots of residuals for fits to length frequency distributions for trawl survey sampling and photographic survey scampi size estimation.
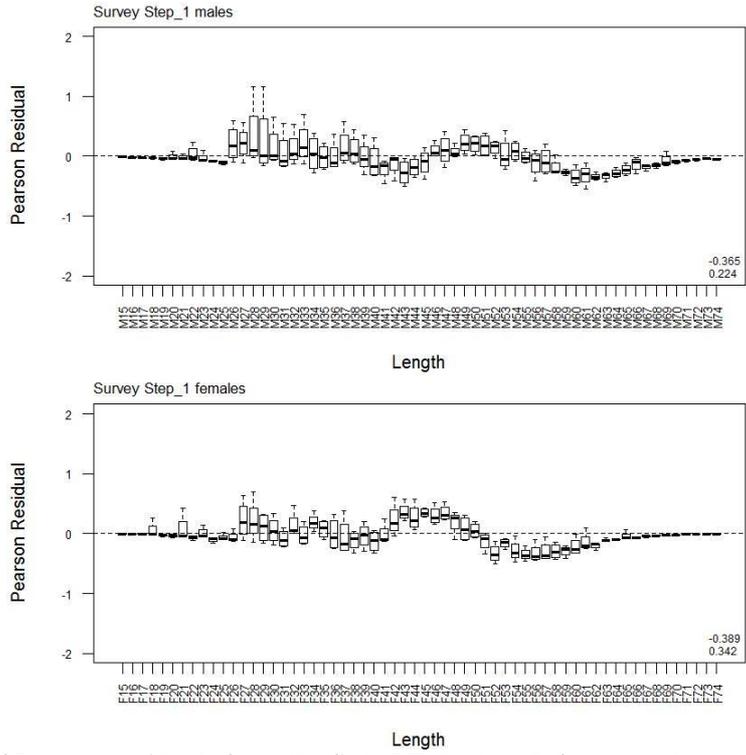
A7. 24: Box plots of Pearson residuals from the fit to LFs by length from trawl survey sampling by sex for time step 1.
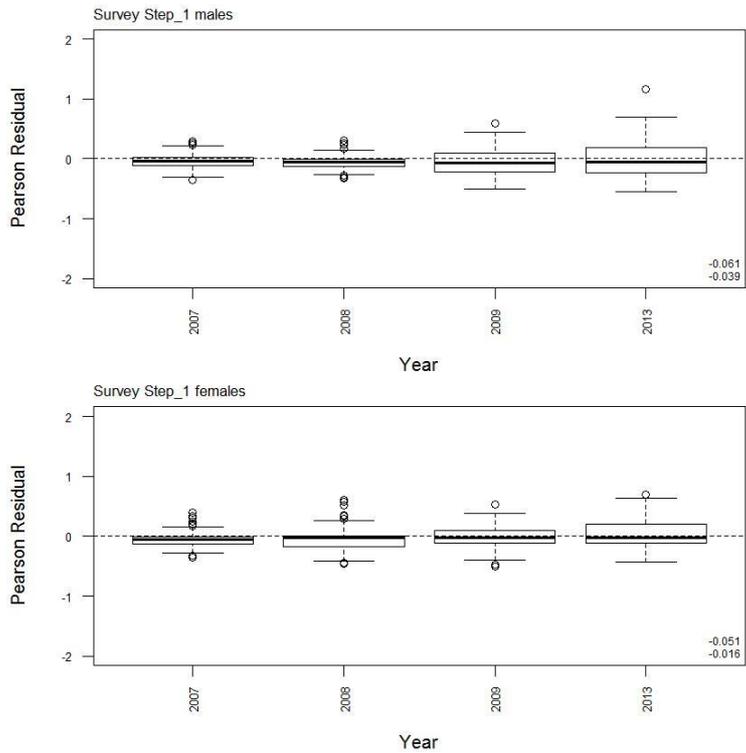

A7. 25: Box plots of Pearson residuals from the fit to LFs by year from trawl survey sampling by sex for time step 1.
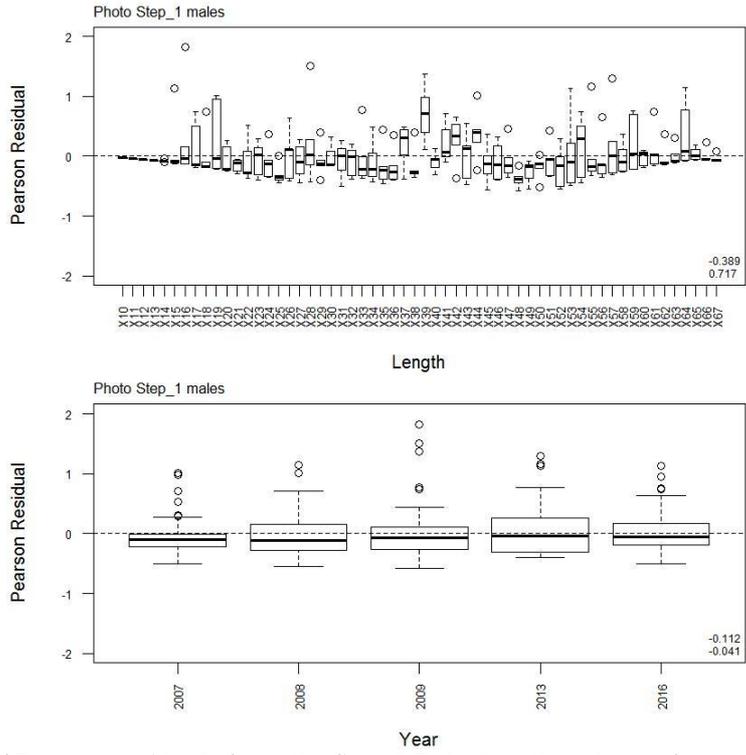
A7. 26: Box plots of Pearson residuals from the fit to LFs by length and year from photo survey sampling for time step 1.
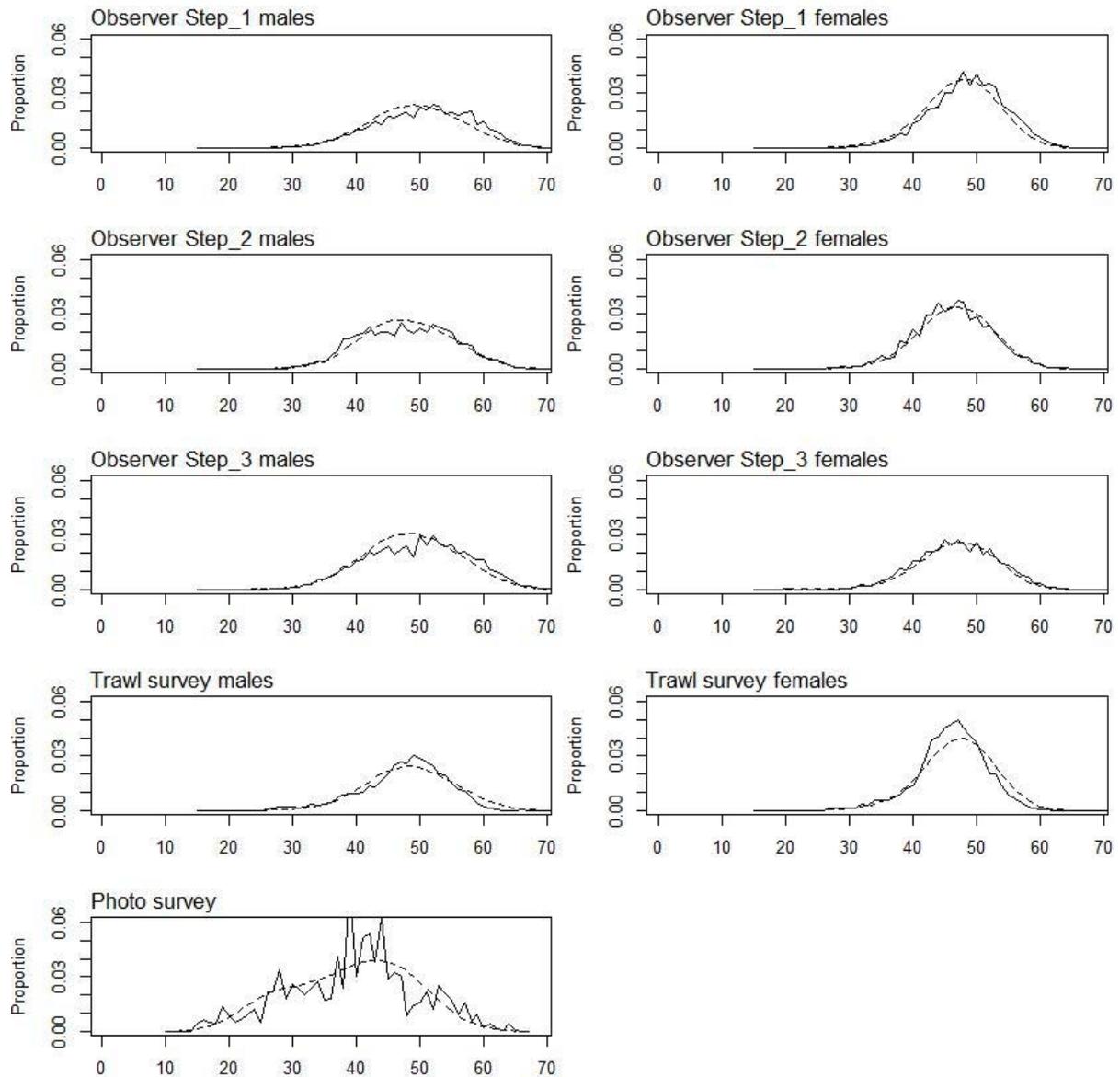
A7. 27: Average observed (solid line) and fitted (dashed line) length frequency distributions for trawl survey sampling and photographic survey scampi size estimation.
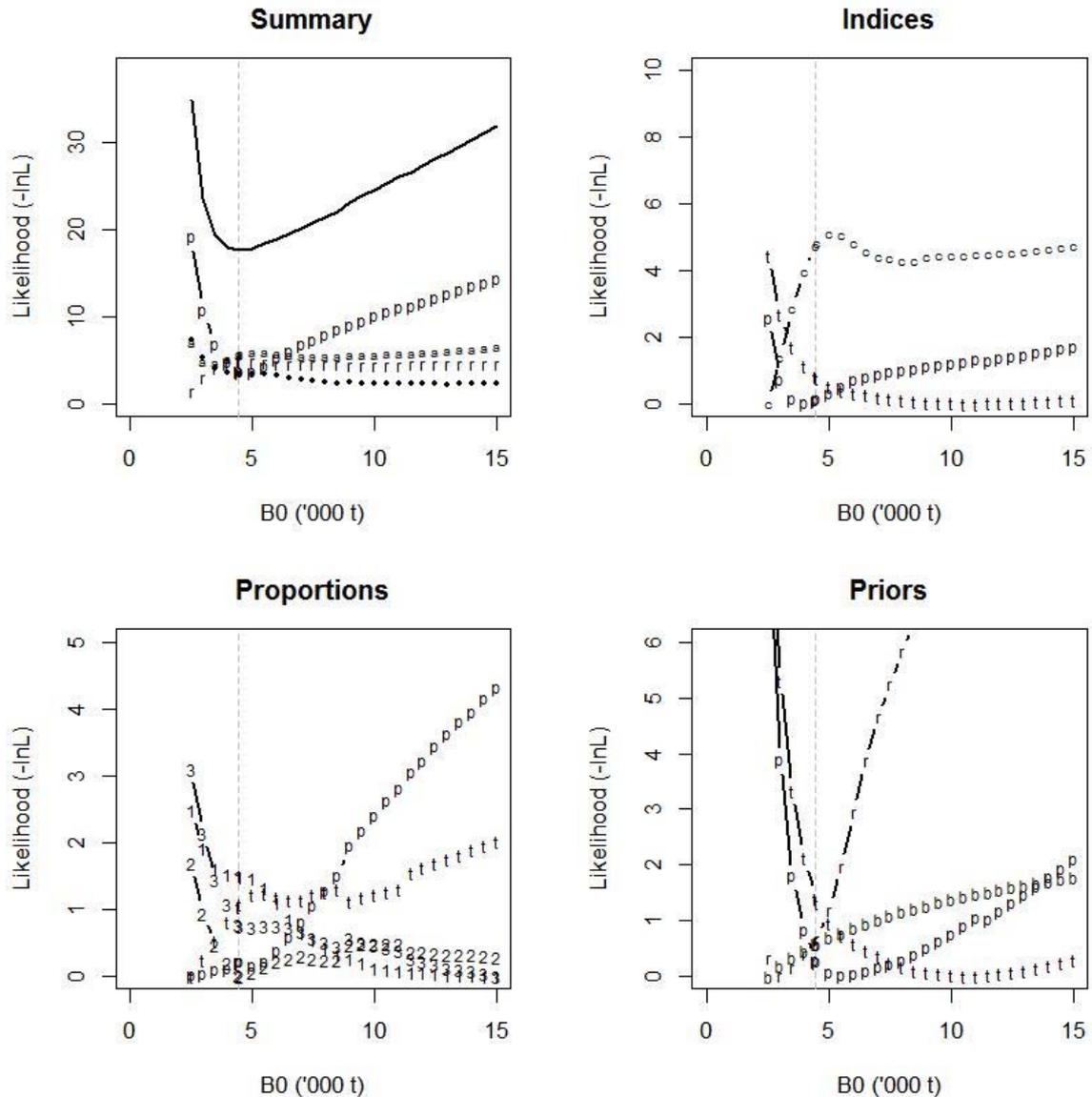
A7. 28: Likelihood profiles for SCI 6A Model 4 when B₀ is fixed in the model. Figures show profiles for main priors (top left, p – priors, a - abundance indices, ● – proportions at length, r – recapture data), abundance indices (top right, t - trawl survey, c - CPUE, p – photo survey), proportion at length data (bottom left, a-trawl, 1 – observer time step 1, 2 – observer time step 2, 3 – observer time step 3, p - photo) and priors (bottom right, b- B₀, YCS - r, p- *q-Photo*, t – *q-Trawl*). Vertical dashed line represents MPD.
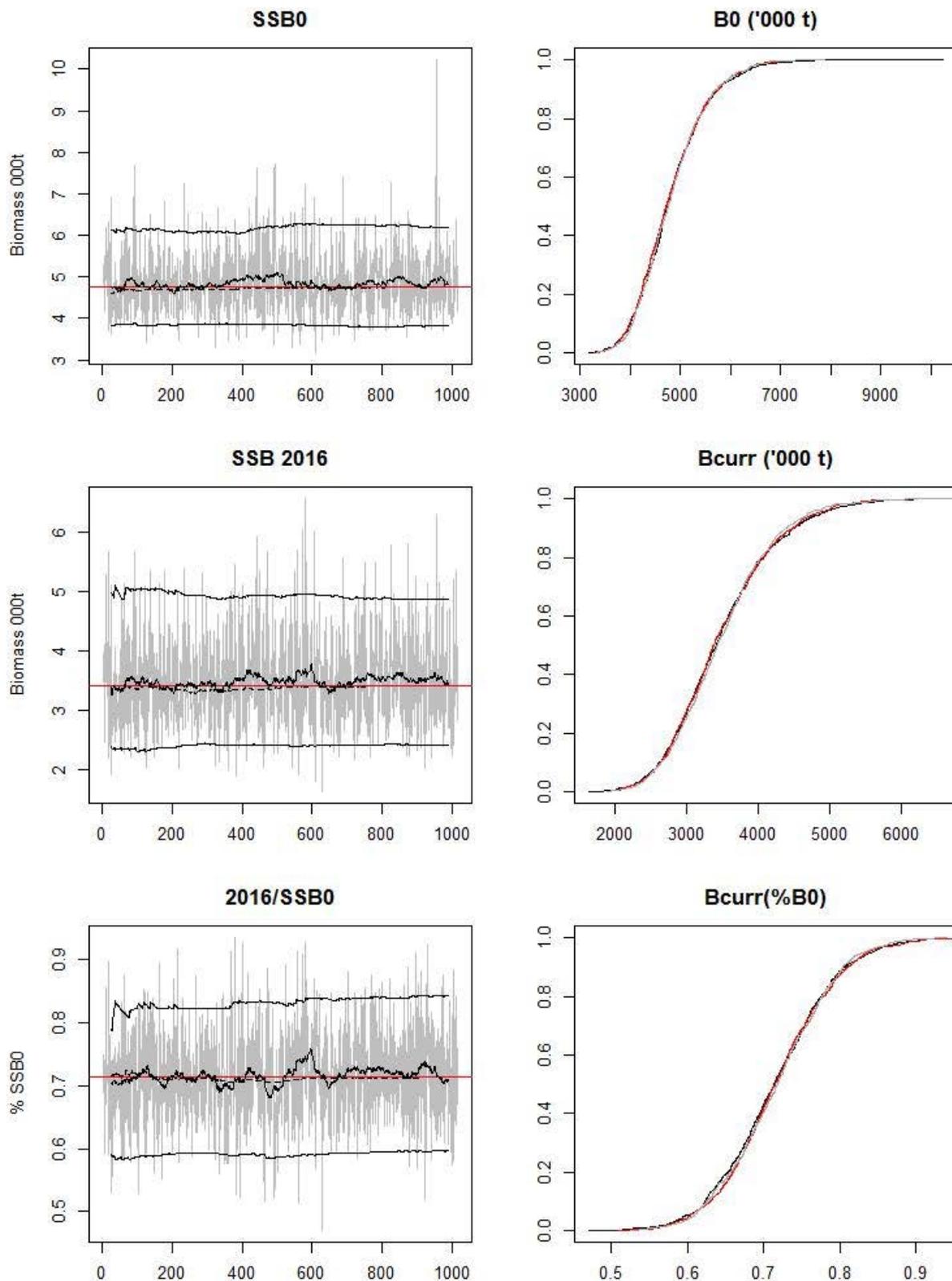
A7. 29: MCMC traces for SSB$_0$, SSB$_{2016}$, and SSB$_{2016}$/SSB$_0$ terms for SCI 6A Model 4 (trace – grey line, cumulative moving median –dashed black line, moving average and cumulative moving 2.5%, 97.5% quantiles – solid black lines, overall median – solid red line, left plots), along with cumulative frequency distributions for three independent MCMC chains (shown as red, grey and black lines, right plots).
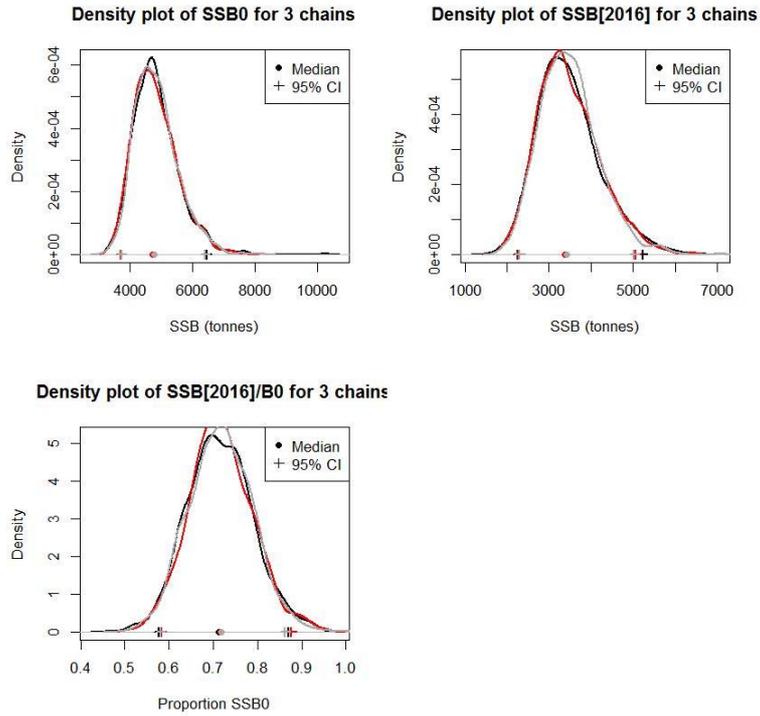
A7. 30: Density plots for SSB$_0$, SSB$_{2016}$, and SSB$_{2016}$/SSB$_0$ terms for SCI 6A Model 4 for three independent MCMC chains, with median and 95% confidence intervals.
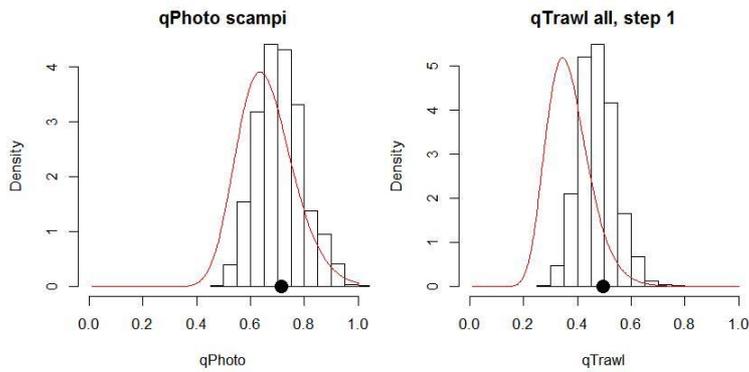
A7. 31: Marginal posterior distributions (histograms), MPD estimates (solid symbols) and distributions of priors (lines) for catchability terms.

A7. 32: Posterior trajectory of SSB, SSB_{2016}/SSB_0 and YCS.